Lenzinger Berichte, 82 (2003) 1-5

SUSTAINABLE DEVELOPMENT AT LENZING

Dr. Franz Raninger

Member of the Managing Board
Lenzing AG
A-4840 Lenzing
Phone: +43 (0) 7672/701-2184
Fax: +43 (0) 7672/918-2184
E-mail: f.raninger@lenzing.com

Lenzing Milestones for the Environment

Innovative technologies and significant investments have made Lenzing the biggest, cleanest and most diversified manufacturer of man-made cellulosic fibers.

1979 : Elimination of elementary chlorine for pulp bleaching (ECF)
1983 : Recovery of acetic acid and furfural
1992 : Pulp bleaching with ozone (TCF)
1992 : Introduction of TCF fibers
1992 : 200 million euros investment program finalized to clean up pulp and viscose fibers production
1997 : Separation of xylose from spent liquor by Danisco
1997 : Start-up of Lyocell production at Heiligenkreuz

Sustainability is "a development which meets the needs of the present without compromising the ability of future generations to meet their own needs." [1]

With this widely-used definition by Gro Harlem Brundtland, the concept of sustainability reached further public recognition in 1987, after marine biologist Rachel Carson launched the American and global environmental movements with her best-selling book *Silent Spring* in 1962 and the Club of Rome had published its report *Limits to Growth* in 1972. Further highlights followed: In 1992, the Summit Conference on Environment in Rio de Janeiro, and, in 1997, the World Climate Conference in Kyoto. With the World Summit on Sustainable Development in Johannesburg in 2002, the topic of sustainability became a priority issue in headlines throughout the world.

The essential element of this concept is the consideration that a balance has to be reached between economic performance, ecological awareness and social values. For industry, this means that targets such as growth, productivity, innovation and sustainable earnings are counterbalanced by values such as the careful use of resources, the reduction of emissions and life cycle considerations, as well as by social standards such as safety, health and a sustainable human-resources policy.

Lenzing AG is committed to the principle of sustainability, as its production processes are based on the use of wood, a renewable raw material. With its high environmental, economic and social standards, the company is the world leader in the pulp and cellulosic fiber industry.

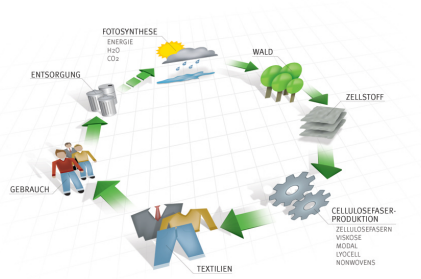

Figure 1. Life cycle of cellulose fibers

Cellulosic fibers are based on cellulose, the natural polymer, which is abundantly available with a global stock of 700 billion tons and readily biodegradable. 40 billion tons per year go through the biological cycle of biosynthesis and biodegradation. Only less than 0.5% (0.19 bill. tons) of the annually generated cellulose is used for pulp, paper and fiber production.

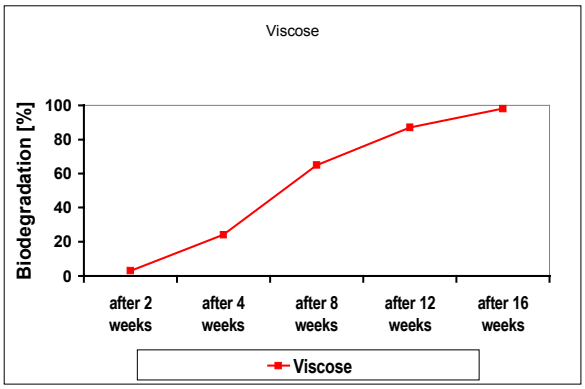

Figure 2. Soil bacteria decompose cellulose fibers within 3-4 months, thus closing the natural carbon cycle.

Wood from Sustainable Forests

The concept of sustainability originated in forestry. The principle of sustainable forestry in Central Europe was first mentioned in 1713, in the *Handbook of Forestry by* C. v. Carlowitz. A forestry law dating back to 1852 regulates felling and reforestation and spelled out specific rules for protective forests. Today, statutory regulations in all Central European countries include biological diversity and the ability to reproduce naturally.

The forests in Europe are expanding. In Austria, a classical woodland country, the expansion amounts to approximately 30 million solid cubic meters per year, and only two thirds of this quantity are actually harvested. All wood used by Lenzing comes from Austria and the surrounding countries.

In Lenzing, beech wood is processed into chemical pulp, which in turn is the raw material for our fiber production. Throughout the fully integrated production chain, the process chemicals are recovered.

100% Wood Utilization by Lenzing

Approximately 40% of the wood substance is extracted in the form of cellulose and processed into pulp. From the remaining cooking liquor, valuable by-products, such as acetic acid, furfural and xylose, are extracted. Process chemicals are recycled and re-used. The surplus energy generated in this process is used for our fiber production (2.68 GJ surplus thermal energy per ton of wood correspond to the thermal value of 69 kg fuel oil per ton). By using state-of-the-art environmental technologies, emissions into air and water are kept at a minimum.

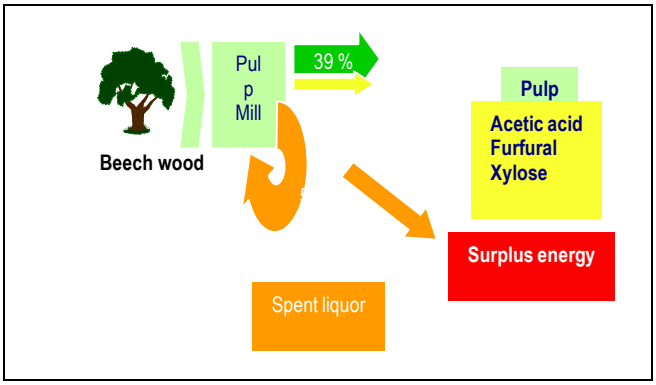

Figure 3. Extraction of by-products and recycling of purified condensate.

Flue-Gas Recovery

The sulphurous flue gases coming from the pulp and fiber processes are recycled, using different technologies. The odorous waste-gas flows, generated in the viscose process, are partly recycled and partly converted into sulfuric acid, which is needed for the preparation of the spin bath. The process chemical CS_2 is recovered by condensation and adsorption and re-used in the viscose process. Less concentrated odorous gases from the pulp and fiber production are used as combustion air in the energy boilers.

Fuel for Energy Production

77% of the fuel needed at the Lenzing site for its energy production are based on renewable resources (biogenic fuels and residual

materials), so that the resulting CO_2 emissions do not contribute to the greenhouse effect. The surplus energy, produced by the pulp mill, is used in the fiber production process.

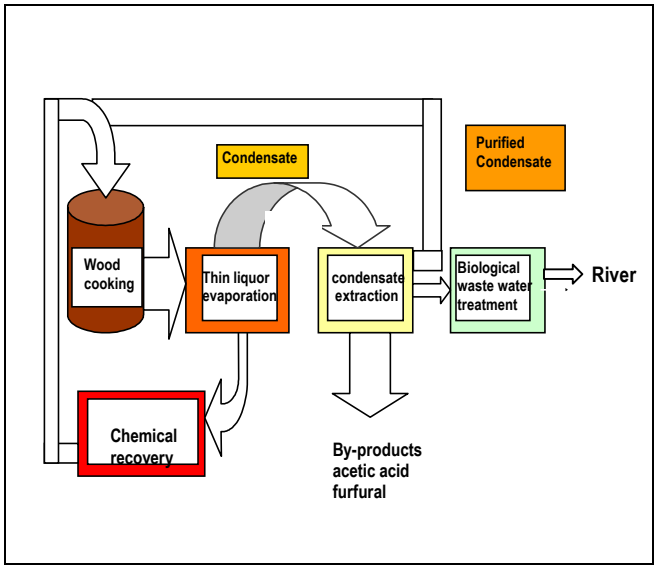

Figure 4. Extraction of by-products and recycling of purified condensate.

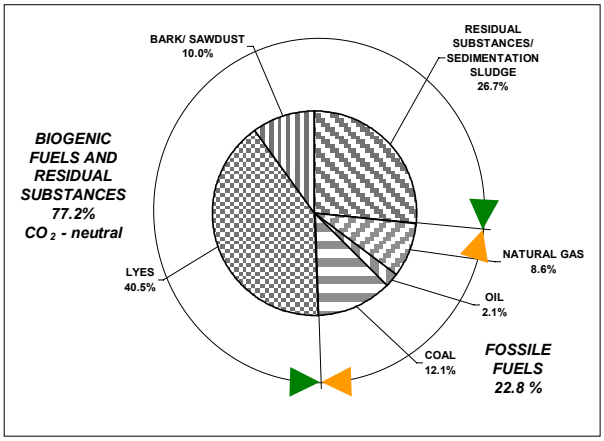

Figure 5. Lenzing AG: Fuel mix at Lenzing AG (incl. RVL)

Effective Waste-Water Treatment

Lenzing spends 100,000 euros per day to operate its environmental protection plants, in order to keep up the highest environmental standards in the industry.

Water is important for the production of pulp and viscose. Environmentally friendly processes, the recycling of process chemicals and the effective treatment of waste water, together with consistent efforts to reduce the use of fresh water are the means to reach this standard. Environmental protection that is integrated in the production process is given priority over end-of-pipe technologies, such as waste-water treatment.

The first construction stage of Lenzing's two-stage biological waste-water treatment plant was put into operation in 1987, the second stage was completed in 1991. Ever since, waste-water emissions have been drastically reduced.

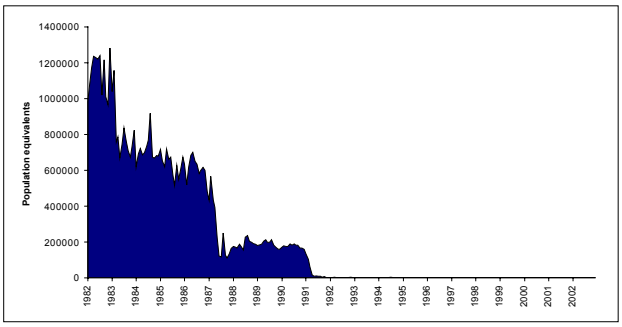

Figure 6. Population equivalents for monthly waste-water values (based on BOD 5).

Prizes and Environmental Labels Awarded to Lenzing

With the development of the Lyocell technology, a production process that is particularly compatible with the environment, Lenzing has set a milestone in its environmental performance. In 2000, Lenzing received the European Award for the Environment for this technology.

Lenzing fibers carry the "European Eco-Label", which is granted to products that meet all European environmental criteria, such as low organo-chlorine limits (Lenzing is a pioneer regarding the totally chlorine-free TCF bleaching process), low limits for air-borne, as well as water-borne emissions and requirements for the biodegradability of chemicals used in the process.

The Lenzing site was certified according to the ISO 140001 standard in July 2003.

The Social Dimension of Sustainability

A well-trained, motivated staff and a good working climate result in low personnel fluctuation: On average, staff members stay with the Lenzing Group for approximately 17 years.

On the workshop floor, as well as at Lenzing's in-house training center, apprentices are being trained for occupations, such as chemical process technology, chemical laboratory technology, mechanical engineering, process control, etc. All staff members have a wide range of options for broadening their qualifications in many different fields. Multi-disciplinary development programs and management and leadership seminars are offered to employees showing a high potential for personal development.

Health and safety are top corporate priorities. The successful program "Easy to Reach 100%" with the goal of complying 100% with all safety regulations was nominated for the State Award of the Federal Ministry of the Economy and Labor.

In addition to offering routine medical check-ups, Lenzing AG organizes "Health Days" for staff members. The goal is to improve the level of awareness in the fields of health and nutrition among the participating employees. Programs such as health gymnastics, seminars to give up smoking and a number of similar campaigns are offered regularly.

In addition to a performance-oriented remuneration, Lenzing staff members also share in the success of the company. Furthermore, staff members benefit from many options in structuring their working hours, such as part-time work, different options of shift work or flexible working hours.

In 2002, almost 500 staff members actively contributed their suggestions for improvements to Lenzing's "Ideas Exchange". The resulting savings for Lenzing AG amounted to EUR 1.5 mill.

Team work was introduced consistently in fiber production processes. The success is reflected in excellent working results (quality, productivity) and in improved communication that leads to smoother and more efficient routines at work.

Sustainability and Economic Success

It is only through sustainable economic success that we can build the foundations for assuming environmental and social responsibility. According to the concept of sustainability, long-term considerations are given priority over short-term, non-sustainable profits.

The Lenzing Group, which is strategically positioned as a globally leading manufacturer of cellulose fibers for the textile and nonwovens industry, is the only manufacturer worldwide that unites under one roof all three generations of man-made cellulose fibers – Viscose, Modal and Lyocell.

The Lenzing Group has a very solid economic basis that ensures satisfactory earnings, even when market conditions are less favorable. Lenzing has demonstrated that it is possible to manufacture products for the world market – also in a classical "high-wage country" like Austria and when complying with the highest environmental standards. A prerequisite for that is leadership in technology, a very rigid cost management, consistency in improving productivity, as well as to be clearly guided by customer requirements when developing new products.

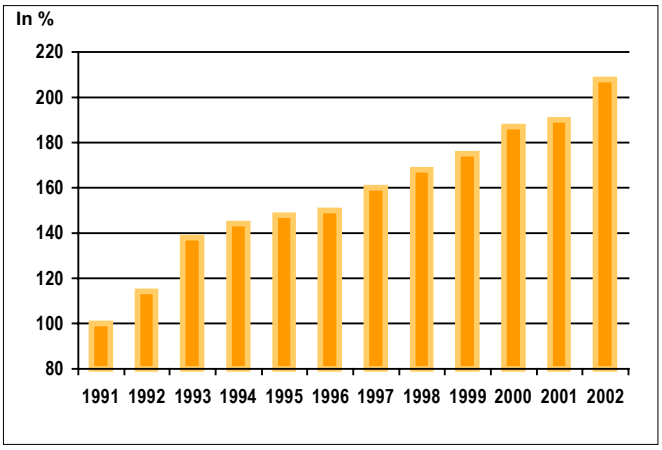

Figure 7. Since 1991 productivity has more than doubled.

Lenzing has succeeded in becoming less dependent on the fiber cycle by focusing on special fibers and nonwovens products, a strategy that will be further continued in the future.

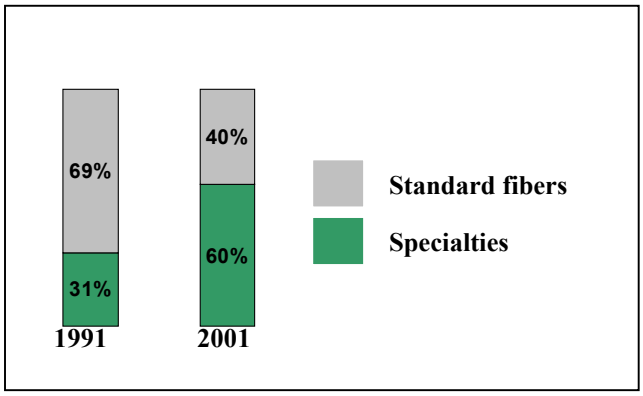

Figure 8. Strong growth with specialty fibers.

With its long-standing experience in the industry, Lenzing is clearly the leader in technology. An efficient Applications Technology Department provides strong customer support. Specialists with know-how of the entire textile chain (spinning, weaving and knitting, dyeing and finishing, nonwovens) and of the state-of-the-art plant equipment provide competence and reliable support for the entire value chain.

Research and development are essential elements for our strategic position as world leader in cellulose fiber technology. The annual expenditure amounts to approximately 2% of sales (2002: EUR 13.3 mill). R&D provides the company with the expertise needed for innovative projects, such as expertise in wood, cellulose and textile chemistry, pulp and fiber technology, as well as the requisite analytical methods and environmental technology. Priority is given to the development of innovative fibers, process optimizations, improvement of quality and the securing of an environmentally friendly production.

In the area of research and development there is close cooperation with Lenzing AG customers. Major results also derive from a series of longer-term co-operations with industrial partners and university research institutions. Furthermore, Lenzing's R & D participates in different EU projects and other cooperation establishments: The better utilization of wood is at the center of attention of the partnership with the center of competence K + WOOD "Holzverbundwerkstoffe und Holzchemie" (Wood Chemistry and Wood Compound Materials). The "Christian Doppler-Labor für Zellstoffreaktivität" (CD Laboratory for Pulp Reactivity) in Vienna works on new analytical methods and a better understanding of the chemistry of the process. The "Christian Doppler-Labor für die Chemie zellulosischer Fasern und Textilien" (CD Laboratory for the chemistry of cellulose fibers and textiles) in Dornbirn, Austria, focuses on the better understanding of fiber properties from the fiber production to the finished textile product.

New Innovative Fibers

Lyocell: For textiles and nonwovens
Lyocell Fill: New filling fiber for quilts and pillows. Currently in a market introduction stage.
Viscostar: High absorbent fiber for, e.g., tampons. The commercialization stage is at its beginning.
Rainbow: Innovative viscose fiber for blends with polyester. Suitable for the single-bath dyeing of textiles. Currently in the development stage.

Reference:

[1] Gro Harlem Brundtland: World Commission Report on Development, 1987.

Lenzinger Berichte, 82 (2003) 6-11

DIE ENTWICKLUNG DES WELTFASERMARKTES IN DEN LETZTEN 20 JAHREN IM VERGLEICH STAPELFASER ZU FILAMENT

Bachinger Josef

Lenzing AG, A-4860 Lenzing, Austria
e-mail: j.bachinger@lenzing.com

Einleitung

Die Jahrtausendwende stellte insofern einen Meilenstein dar, als nun bereits mehr als 100 Jahre vergangen sind, seit erstmals Chemiefasern am Textilmarkt Eingang gefunden haben. Die Chemiefaserproduktion ist seit 1970 stark, um das Vierfache auf heute fast 34 Millionen Tonnen weltweit, angestiegen. Chemiefasern, allen voran Polyesterfasern, haben heute mengenmäßig Baumwolle, als bedeutendste Naturfaser, den Spitzenrang abgenommen. In den letzten beiden Jahren fiel das Chemiefaserwachstum allerdings nur sehr bescheiden aus, trotz Rekordproduktionsmengen in China.

Betrachtet man die wirtschaftliche Entwicklung in den letzten Jahren, so sticht besonders das Jahr 2000 positiv hervor. Die Weltwirtschaft befand sich damals in einer Hochkonjunktur, die Chemiefaserproduktion stieg um 6 % an und die Textilindustrie Asiens konnte im Export mit 2-stelligen Zuwachsraten aufwarten. Mittlerweile hat sich die Stimmungslage gedreht, bereits seit 3 Jahren lahmt die Weltwirtschaft und man hofft auf einen baldigen Aufschwung. Obwohl die Aussichten auch für dieses Jahr nicht gut sind und erst im Verlauf des nächsten Jahres mit einer Besserung gerechnet wird, bin ich optimistisch, was die weitere Entwicklung der Chemiefaser- und Textilindustrie betrifft. Langfristig betrachtet sind Höhen und Tiefen in der Branche beinahe normal, das Wachstum wird sich weltweit fortsetzen.

Innerhalb der Faser- bzw. Chemiefaserindustrie gab es in den letzten 20 Jahren eine Reihe von bedeutenden Veränderungen, auf die ich in den nachfolgenden Ausführungen näher eingehen werde.

Historische Entwicklung des Faseraufkommens

Noch vor einer Generation wurde der Bekleidungs- und sonstige Faserbedarf fast ausschließlich mit Naturfasern wie Baumwolle, Wolle und Leinen abgedeckt. Heute hat sich das Bild grundsätzlich geändert, das weltweite Faseraufkommen wird zu mehr als 60 % von Chemiefasern bestimmt (Abb.1).

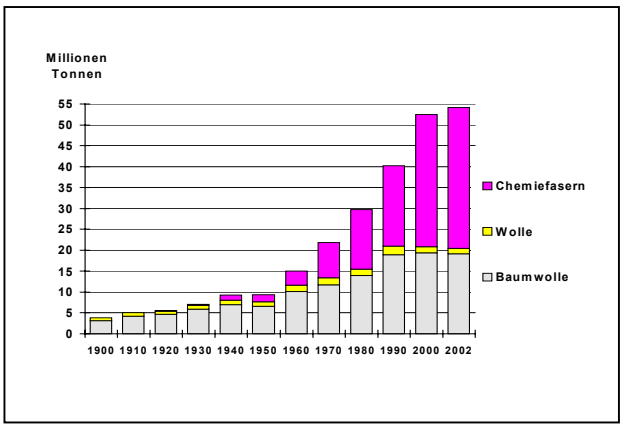

Abb. 1. Weltproduktion Fasern

Die Verarbeitung von Baumwolle und Wolle ist mit der Erfindung der Textilmaschinen zu Beginn des 20. Jahrhunderts stark angestiegen. Vorallem Baumwolle war zu dieser Zeit knapp und teuer und mußte in Westeuropa importiert werden, was die Entwicklung der Chemiefasern begünstigt hat. Trotz des starken Anstiegs der Chemiefasern in den letzten 20 bis 30 Jahren ist Baumwolle mit 20 Millionen Tonnen auch heute noch zumindest in der Kurzstapelspinnerei die dominierende Faser. Allerdings stagniert das Baumwollaufkommen in den letzten 10 Jahren mehr oder weniger und es ist zu erwarten, daß

das Wachstum auch im nächsten Jahrzent nur moderat ausfallen wird. Gründe für diese Entwicklung sind u.a. Arealbeschränkungen in großen Anbauländern wie China, Konkurrenz im Anbau zu anderen Agrarprodukten, Kürzung der Subventionen und eine starke Zunahme vorallem der Polyesterfaserproduktion. Ein Anstieg der Baumwollproduktion ist künftig nur durch eine Steigerung im Flächenertrag möglich. Der Anbau von genetisch veränderter Baumwolle kann dazu beitragen den Flächenertrag zu erhöhen, es ist aber nicht sicher, ob sich deren Anbau in allen großen Ernteländern wesentlich durchsetzen wird.
Das Wollaufkommen erreichte Anfang der 90-er Jahre den höchsten Stand mit ca. 2 Millionen Tonnen weltweit. Allerdings stiegen damals auch die weltweiten Lagerbestände stark an, bedingt vorallem durch den Verbrauchsrückgang in Osteuropa. Die Folge waren sinkende Preise und eine schwere Krise in der Wollindustrie. Seither ist die Wollproduktion um ein Drittel gefallen, vorallem in Australien haben viele Farmer aufgegeben. Verschärft wurde die Lage zwischenzeitlich noch durch den Nachfragerückgang in China während der Asienkrise 1997 und 1998. Das Wollaufkommen dürfte auch in den nächsten Jahren niedrig bleiben und damit das Preisniveau hoch halten. Wolle wird damit immer mehr zur sogenannten „Luxusfaser“.

Die Entwicklung der Chemiefasern beginnt Ende des 19. Jahrhunderts mit der Produktion von Zellulosefasern nach dem Viskoseverfahren (Abb. 2).

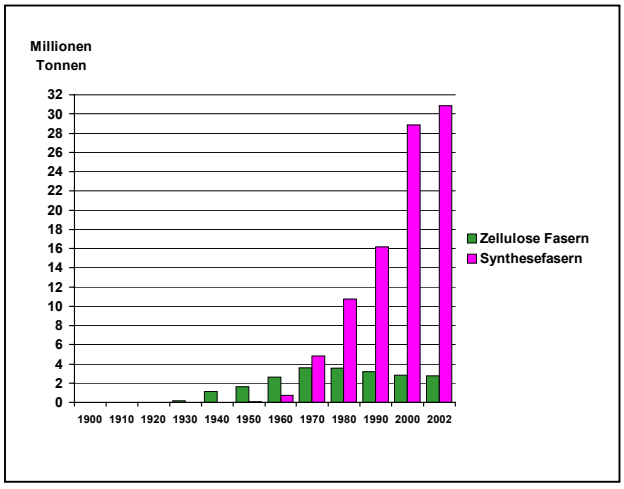

Abb. 2. Weltproduktion Chemiefasern

Am Beginn der Entwicklung waren hauptsächlich Viskosefilamente vetreten, die Stapelfaserproduktion erfolgte um 1920. In diese Zeit fällt auch die Entwicklung von Zellulosefasern nach dem Azetatverfahren. Die Zellulosefaserproduktion hatte ihren Höhepunkt Anfang der 70- er Jahre erreicht, seither stagniert die Produktion bzw. ist je nach Faserart mehr oder weniger stark rückläufig. Ein Hauptgrund für diese Entwicklung ist in der starken Konkurrenz durch die Synthesefasern zu sehen.
Viskosestapelfasern stellen heute mit 1,6 Millionen Tonnen den überwiegend größten Anteil am Zellulosefaseraufkommen dar (Abb.3).

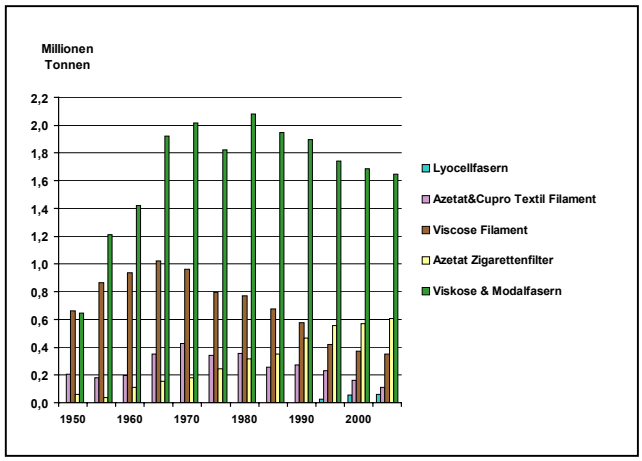

Abb. 3. Weltproduktion Zellulosefasern

In den letzten 20 Jahren hat sich die Zahl der Hersteller und die Kapazität um ein Drittel reduziert, vorallem in Osteuropa wurden aufgrund der politischen Veränderungen Anfang 1990 viele Werke geschlossen. Der Produktionsrückgang in Osteuropa wurde allerdings durch die Zunahme des Verbrauchs in Asien mehr als kompensiert. Einen starken Rückgang gab es in den letzten Jahren bei textilen und hochfesten Viskosefilamenten. Dieser Rückgang ist hauptsächlich auf die starke Konkurrenz von Polyesterfilament zurückzuführen. Gleiches gilt auch für Azetatfilamente, welche hauptsächlich zu Futterstoffen und modischer Damenoberbekleidung verarbeitet werden. Azetat Kabel wird ausschließlich für Zigarettenfilter eingesetzt. Die weltweite Produktion ist auf ca. 600.000 Tonnen angestiegen, vorallem in Osteuropa und China wächst die Nachfrage nach Filterzigaretten. Dagegen ist der Verbrauch in den klassischen Industrieländern nicht zuletzt aufgrund

staatlicher Regulierungen stagnierend bzw. rückläufig. Die kommerzielle Produktion von Lyocellfasern geht auf das Jahr 1992 zurück. Es handelt sich hier um eine völlig neue Generation von Zellulosefasern nach dem sog. „Solvent spun“ Verfahren, welches sich durch seine besonders umweltfreundliche Herstellungstechnologie auszeichnet. Lyocellfasern haben eine hohe Festigkeit, einen kühlen Griff und eine seidige Optik, was dieser Fasergeneration neue Anwendungsgebiete öffnet, die bisher den traditionellen zellulosischen Stapelfasern nicht zugängig waren.

Die Entwicklung der Synthesefasern beginnt um 1940 mit Polyamidfasern und 1950 mit Polyacryl- und Polyesterfasern, 10 Jahre später kommen Polypropylenfasern auf den Markt (Abb.4).

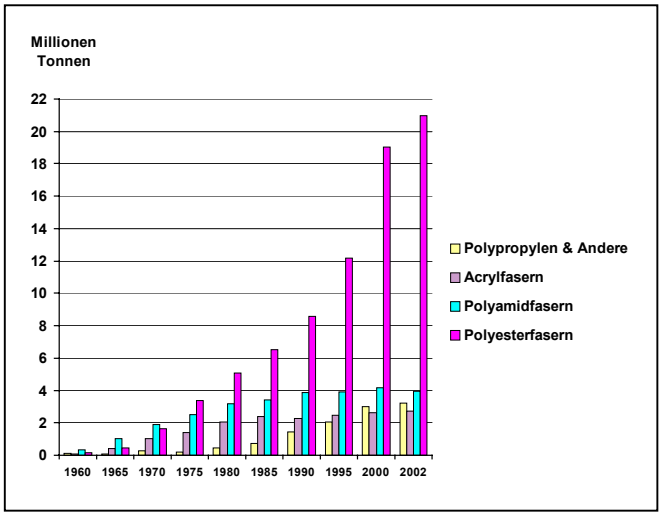

Abb. 4. Weltproduktion Synthesefasern

Hauptsächlich Polyesterfasern mit einer durchschnittlichen jährlichen Wachstumsrate von 13 % sind für den rasanten Anstieg der Chemiefasern verantwortlich. Im letzten Jahr wurden bereits an die 21 Millionen Tonnen Polyesterfasern produziert, davon 9 Millionen Stapelfasern und 12 Millionen Filamente. Der Großteil der weltweiten Polyesterfaserproduktion erfolgt heute in Fernost. China, Südkorea und Taiwan stellen zusammen mehr als die Hälfte der Weltproduktion. Vorallem in der VR China wurden die Polyesterfaserkapazitäten stark ausgeweitet. Der damit verbundene niedrigere Importbedarf der VR China hat das Problem der weltweiten Überkapazitäten verschärft. Davon betroffen sind in erster Linie die Hersteller in Südkorea und Taiwan, welche mit Produktionskürzungen, Unternehmenszusammenschlüssen oder z.T. mit Produktionsverlagerung in Länder mit noch billigeren Herstellkosten (z.B. Vietnam, China) reagieren. Trotz dieser Maßnahmen könnte das Problem der weltweiten Überkapazitäten noch auf Jahre hinaus weiter bestehen, da im Nahen und Mittleren Osten (Saudiarabien, Iran, Pakistan, Ägypten) neue Kapazitäten auf den Markt kommen werden.

Im Gegensatz zu Polyesterfasern zeichnet sich bei Polyacrylfasern mit 2,7 Millionen Tonnen weltweit gesehen eine gewisse Stagnation ab. Neue Kapazitäten sind in großen Verbrauchsländern wie China oder Pakistan in Betrieb genommen worden, wodurch dort der Importbedarf sinkt. Auch bei Polyacrylfasern wird daher der Konkurrenzdruck unter den Anbietern zunehmen.

Eine gewisse Stagnation verzeichnen auch Polyamidstapelfasern und Teppichgarne, wofür maßgeblich die starke Konkurrenz von Polypropylen am stagnierendem Teppichmarkt ausschlaggebend ist. Im Gegensatz dazu steigt die Produktion von Polyamid Hochfest Filamenten weiter an, wachsende Einsatzbereiche sind airbag und Reifencord.

Unter den Polypropylenfasern wachsen Filamente, welche hauptsächlich in Teppichgarnen und Non-wovens ihre Verwendung finden, am stärksten.

Waren Chemiefasern einst die alleinige Domäne der sog. „Klassischen Industrieländer“ wie Westeuropa, USA und Japan, so hat sich diese Bild - was das mengenmäßige Aufkommen betrifft - in den letzten 10 bis 20 Jahren grundsätzlich geändert. Heute werden bei Chemiefasern bereits mehr als 70 % in Asien bzw. der Übrigen Welt hergestellt (Abb. 5).

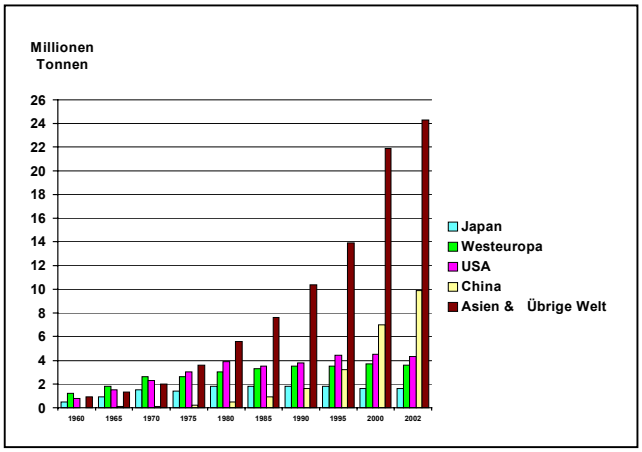

Abb. 5. Weltproduktion Chemiefasern nach Weltregionen

China ist mit einem jährlichen Ausstoß von 10 Millionen Tonnen zum weltweit größten Produzenten aufgestiegen, man erzeugt heute dort bereits mehr als in Taiwan, Korea und Indien zusammengenommen.

Trends am Weltfasermarkt

- der weltweite Faserverbrauch wächst überproportional zur Weltbevölkerung mit einer durchschnittlich jährlichen Wachstumsrate von 3,5 % in den letzten 50 Jahren.
- deutliche Verlagerung des Faserverbrauches und der Textil- bzw. Bekleidungsproduktion nach Asien. China hat sich zum weltweiten Textil- und Fasermarkt entwickelt zu Lasten anderer asiatischer exportorientierter Länder.
- der Pro-Kopf Verbrauch an Textilien und Bekleidung steigt mit wachsendem Einkommen.
- der Anteil der Chemiefasern am weltweiten Faseraufkommen liegt bereits bei über 60 %.
- hohe Überkapazitäten bei Chemiefasern vorallem in Fernost, Restrukturierungen werden sich fortsetzen.
- auch bei Baumwolle übersteigt das Angebot die Nachfrage, Baumwolle wird im Anbau und Verarbeitung stark subventioniert.
- starker Preisdruck durch Überangebot an Fasern.
- starke Konzentration auch bei den Zulieferern der Faser- und Textilindustrie (Anlagenbau, Textilmaschinen, Farbstoffe, Textilhilfsmittel).
- Konkurrenzdruck wird sich durch Wegfall der Quoten ab 1.1.2005 verstärken.
- zunehmende regionale Blockbildungen und Einsatz von handelspolitischen Maßnahmen (Antidumping, Strafzölle).
- Filamentgarne wachsen schneller als Stapelfasern.

Stapelfaser versus Filament

Teilt man das gesamte Faseraufkommen nach Stapelfasern und Filamente, so fällt vorallem auf, daß in den letzten 20 Jahren die Filamentproduktion auf ca. 18 Millionen Tonnen stark angestiegen ist. Filamente haben heute bereits einen Anteil von mehr als 30 % am weltweiten Faseraufkommen (Abb.6). Das starke Wachstum der Filamente ist umso erstaunlicher, als die Expertenmeinung bisher von einem stärkeren Anstieg der Stapelfasern ausgegangen ist.

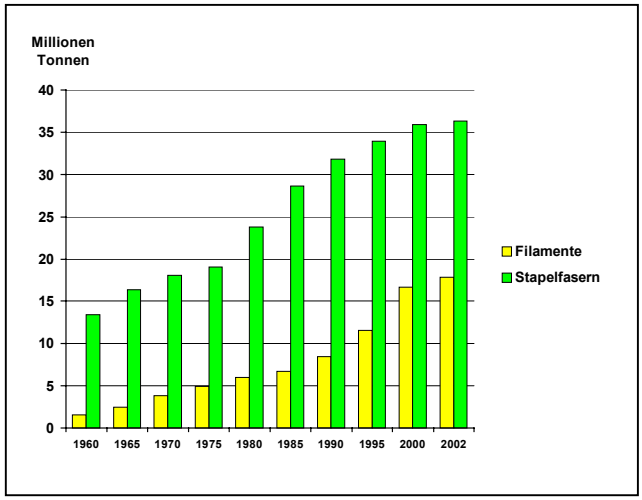

Abb. 6. Weltproduktion Stapelfaser versus Filament

Die weltweite Stapelfaserproduktion liegt bei ca. 36 Millionen Tonnen, wobei Baumwolle nach wie vor die wichtigste Faser darstellt (Abb.7).

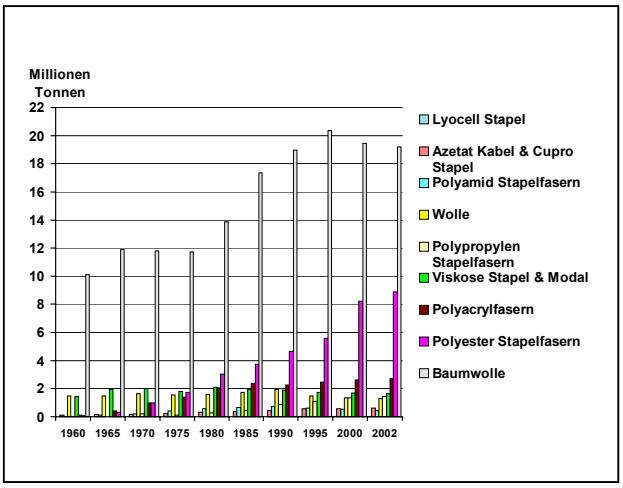

Abb. 7. Weltproduktion Stapelfasern

Während jedoch das Baumwollaufkommen in den letzten 10 Jahren stagniert, ist die Produktion von Polyester Stapelfasern um das Doppelte angestiegen und erreichte im letzten Jahr mit mehr als 9 Millionen Tonnen bereits an die 40 % des Baumwollaufkommens. Auch die Produktion von Polypropylen Stapelfasern und Azetat Kabel hat zugenommen, wenngleich nicht so rasant, wie dies bei Polyester der Fall ist. Die Produktion der anderen Stapelfasern wie Wolle, Viskose, Polyacryl und Polyamid stagniert bzw. ist mehr oder weniger rückläufig.

Stapelfasern werden zunehmend zu Non-wovens verarbeitet, mit 28 Millionen Tonnen findet jedoch der überwiegend größte Teil seine Verwendung in der Kurzstapelspinnerei (Abb. 8).

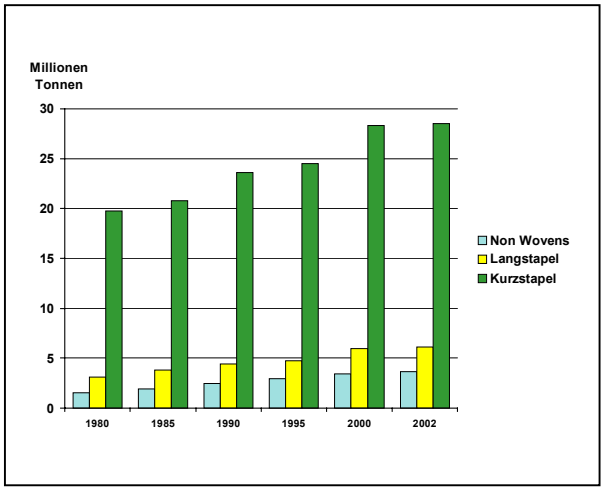

Abb. 8. Stapelfaserverbrauch nach Einsatzgebieten

Betrachtet man die Entwicklung in der Kurzstapelspinnerei etwas näher, so fällt die starke Zunahme der Synthese bzw. Polyesterfasern auf, während Baumwolle und Viskosefasern stagnieren. Regional gesehen ist die Produktion der Baumwollspinnerei in den sog. „Klassischen Industrieländern“ rückläufig, heute werden alleine in Asien an die 20 Millionen Tonnen Kurzstapelfasergarne produziert (Abb.9).

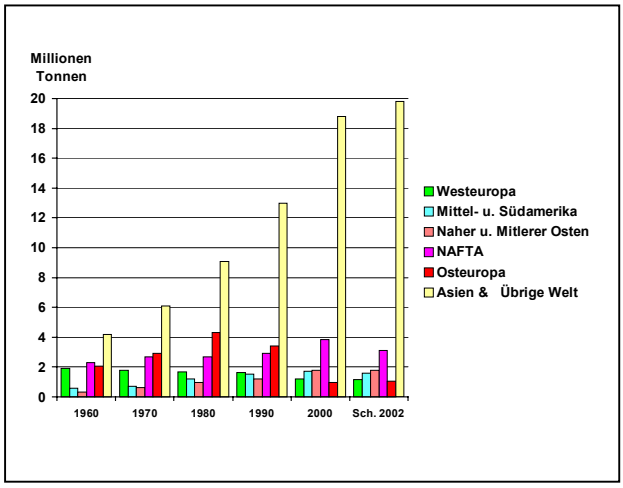

Abb. 9. Faserverbrauch Kurzstapelspinnerei nach Weltregionen

Die weltweite Filamentproduktion beträgt wie bereits erwähnt ca. 18 Millionen Tonnen, alleine 12 Millionen Tonnen davon sind Polyesterfilamente. In den letzten 10 Jahren hat vorallem die Produktion von textilen Polyesterfilamenten für Bekleidung und Heimtextilien stark zugenommen auf 11 Millionen Tonnen. Aber auch Polypropylenfilamente für Teppiche gewinnen zunehmend an Bedeutung zu Lasten von BCF Garnen (Abb.10).

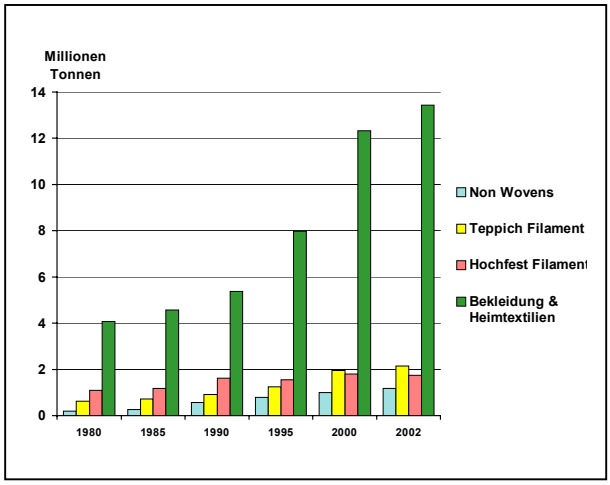

Abb. 10. Filamentverbrauch nach Einsatzgebieten

Stellt man die Produktion von Textil Filament jener der Baumwollspinnerei gegenüber, so fällt die Zunahme der Textil Filamentproduktion besonders stark ins Gewicht (Abb.11).

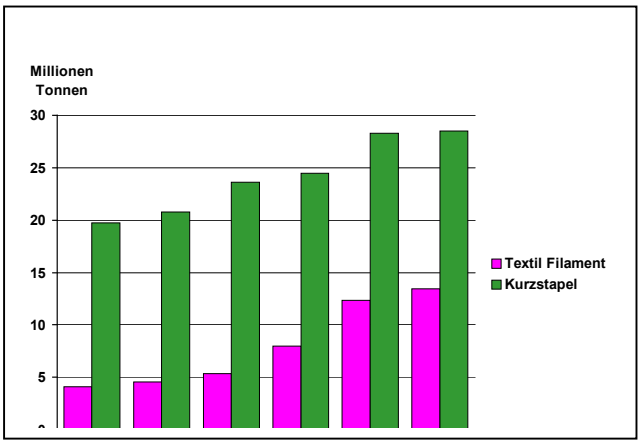

Abb. 11. Faserverbrauch Kurzstapel versus Textil Filament

Hand in Hand mit der Zunahme der textilen Filamentproduktion wurde in den letzten 10 Jahren verstärkt in Texturiermaschinen investiert. Man nimmt an, daß heute bereits an die 80 % der weltweiten Textil Filament-produktion texturiert wird, der Großteil davon ist bei den Filamentherstellern selbst angehängt. Diesen Garnen wird eine sehr hohe Flexibiliät nachgesagt, in der Weise, daß sie sehr leicht mit anderen Filamenten gemischt werden können. Weitere Vorteile sind der gute Griff, hohe Produktivität in Weberei und Wirkerei, sowie generell ein gutes Preis- Leistungsverhältnis. Vorallem in Sportbekleidung, Heim- und Autotextilien haben sich diese Fasern in letzter Zeit durchgesetzt.

Lenzinger Berichte, 82 (2003) 12-19

LENZING VISCOSE® RAINBOW EINE INNOVATION FÜR DIE FÄRBEREI

Dr. M. Crnoja Cosic[a], Dr. P. Sulek, Ing. G. Emlinger, Dr. J. Schlangen

[a]Lenzing AG, Faser Service, Österreich, A-4860 Lenzing, tel. ++43 7672 701 3676, fax. ++43 7672 918 3676, m.crnoja@lenzing.com

Einleitung

Die Lenzing Viscose® Rainbow ist eine Viskosefaser mit besonderen Färbeeigenschaften. Durch intensive Forschungs- und Entwicklungsarbeiten ist es gelungen eine kationische Viskosefasern zu kreieren, die ein äußergewöhnliches färberisches Verhalten zeigt. Die kationischen Ladungen befinden sich überwiegend im Inneren der Faser, so dass die Oberflächenkonzentration der kationischen Ladung auf der Faser relativ gering ist. Diese Eigenschaft ermöglicht eine gleichmäßige und reproduzierbare Färbung der Lenzing Viscose® Rainbow. Die Kationizität ist homogen in der Faser verteilt, lässt sich nicht auswaschen und ist resistent gegenüber allen Prozessen und Substanzen, die bei der Verarbeitung von Viskosefasern eingesetzt werden.

Färberischen Eigenschaften der Lenzing Viscose® Rainbow

Die Lenzing Viscose® Rainbow lässt sich mit Reaktivfarbstoffen auf herkömmliche Weise ohne Probleme färben. Es ist dabei zu beobachten das der Farbauszug und Fixiergrad signifikant steigt. Mit Direktfarbstoffen kann bei 80 bis 95°C mit sehr geringen Salzkonzentrationen (2 bis 3 g/L) bei Ausziehgraden zwischen 95 und 99% gefärbt werden. Die 60°C Waschechtheiten liegen dabei auch bei dunkleren Farbtönen auf dem Niveau einer Reaktivfärbung. Es ist keine kationische Nachbehandlung nötig.

Lenzing Viscose® Rainbow lässt sich zum Unterschied zu herkömmlichen Cellulosefasern auch mit Wollfarbstoffen färben. Dabei eignen sich Metallkomplex- und ausgesuchte Säurefarbstoffe sehr gut. Auch bei diesen Färbungen werden 60°C Waschechtheiten auf dem Niveau von Reaktivfärbungen gemessen.

Einsatzgebiete der Lenzing Viscose® Rainbow

Die Lenzing Viscose® Rainbow befindet sich zur Zeit noch nicht auf dem Markt. In Zusammenarbeit mit ca. 20 Entwicklungspartnern aus den unterschiedlichsten Bereichen der Textilindustrie wird eine intensive Produktentwicklung betrieben, bei der in den verschiedenen Anwendungsbereichen die entwickelten Verfahren getestet und optimiert werden. Die besonderen färberischen Eigenschaften der Lenzing Viscose® Rainbow entwickeln den größten Anwendernutzen in Mischungen mit anderen Fasern.

Lenzing Viscose® Rainbow kann in Intim- und System-Mischung mit Polyester in einem einstufigen und einbadigen Auszieh-Färbeprozeß in ca. 4 Stunden gefärbt werden. Je nach Artikel und Farbton kann diese Zeit noch verkürzt werden. Bei diesem Verfahren wird mit Dispersions- und Direkt- oder Metallkomplexfarbstoffen unter Polyesterfärbebedingungen (130 °C, pH 4,5 bis 6) gefärbt, heiß und kalt gespült und die Färbung ist fertig. Die Produktivität kann gegenüber dem bisher üblichen Verfahren, einer nacheinander durchgeführten Färbung mit Dispersions- und dann mit Reaktivfarbstoffen, verdoppelt oder sogar verdreifacht werden. Über diese Lenzing Viscose® Rainbow-Anwendungen wurde bereits auf den Chemiefasertagungen 2001 und 2002 von der Lenzing AG und der DyStar berichtet.

Durch die spezielle Eigenschaft, dass die Cellulosefaser Lenzing Viscose® Rainbow auch mit Wollfarbstoffen (Metallkomplex und

ausgesuchte Säurefarbstoffe) gefärbt werden kann, ergibt sich die zweite Anwendung mit einem hohen Kundennutzen. Die Mischungen von herkömmlichen Cellulosefasern (Viskose, Modal, Lyocell, Baumwolle, Leinen, ...) mit Lenzing Viscose® Rainbow wird als Webware oder Gestrick in System- oder Intimmischung hergestellt und als Rohware einem Färbeprozess unterzogen, bei dem auf Rainbow ein anderer Farbton gefärbt werden kann als auf der Standard-Cellulosekomponente. Es ist möglich sehr kurzfristig bestimmte, sich gut verkaufende Farbdesigns, nachzuproduzieren. Dieses System ist nicht neu und unter dem Namen Benetton-Prinzip bekannt. Neu ist, dass sich dieses Prinzip auf reine Celluloseartikel ausdehnen lässt. In Kombination mit Polyester, Cellulose und Rainbow sind sogar Tricolor-färbungen möglich. Diese neue Anwendung der Lenzing Viscose® Rainbow soll in den weiteren Ausführungen genauer dargestellt werden.

In der Zukunft könnten sich noch Vorteile bei der Färbung und im Druck von Polyamid- und Wollmischungen mit Lenzing Viscose® Rainbow ergeben, über die jedoch erst später berichtet werden soll.

Konkurrenzfärbungen von Mischungen aus Lenzing Viscose® Rainbow mit anderen Cellulosefasern

Das Färben mit Direktfarbstoffen

In folgenden Untersuchungen soll ermittelt werden, wie sich Direktfarbstoffe in Konkurrenzfärbungen von Lenzing Viscose® Rainbow und anderen Cellulosefasern (Viskose) jeweils auf diese Materialien verteilen. Dabei soll geklärt werden, welchen Einfluss dabei folgende Parameter besitzen:

1. Temperatur
2. pH-Wert
3. Färbezeit
4. Salzkonzentration
5. Farbkonzentration bei 2g/L Salz
6. Farbkonzentration bei 10g/l Salz

Für die Untersuchungen wurden folgende Standardparameter festgelegt:

Färbetemperatur	80°C (30min)
Salzkonzentration	2g/L
pH-Wert	7
Sirius Rubin K-2BL	2%
Flottenverhältnis	1:30
nichtionisches Netzmittel	

Bei diesen Färbeversuchen hat sich gezeigt, dass die Parameter pH-Wert, Färbezeit und Farbstoffkonzentration nahezu keinen Einfluss auf das Verhältnis der Farbtiefen (Helligkeiten ΔL) auf Lenzing Viscose® Rainbow - und Viskose-Gewebe gehabt hat. Die Salz-konzentration und die Färbetemperatur besitzen einen deutlichen Einfluss auf die Farbstoff-verteilung. In Abbildung 1 und 2 sind die Ab-hängigkeiten als Balkendiagramm dargestellt.

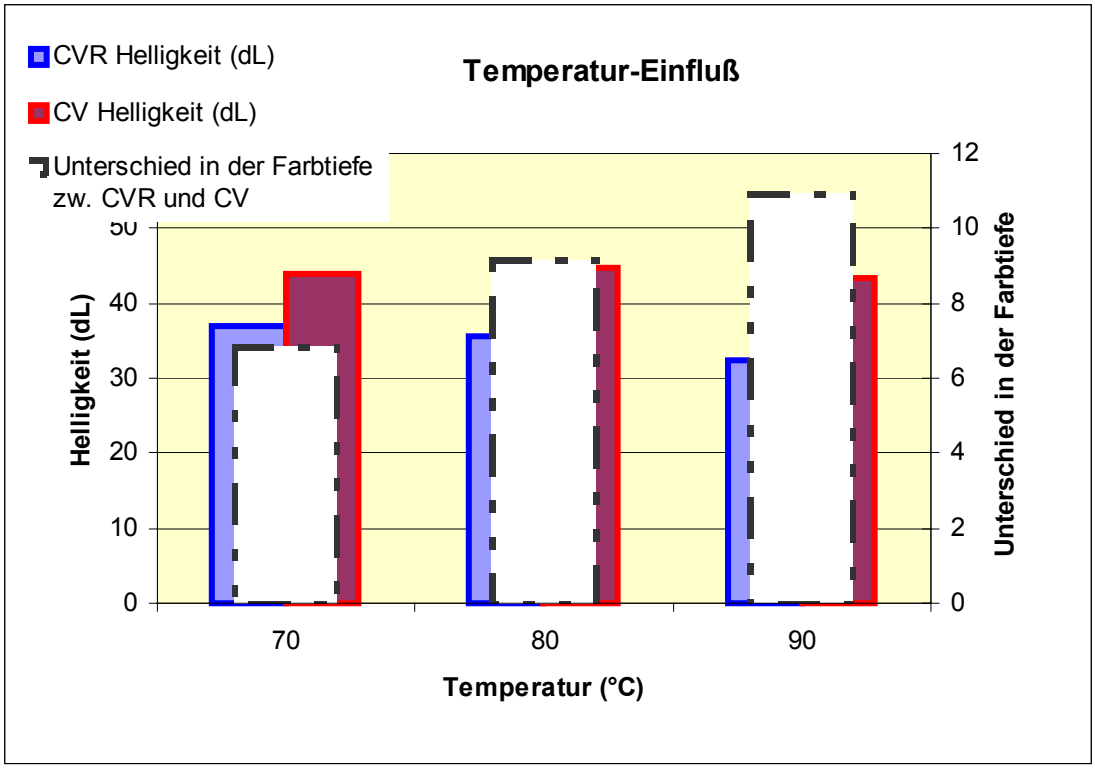

Abbildung 1. Einfluss der Temperatur auf die Farbstoffverteilung bei der Konkurrenzfärbung von Lenzing Viscose® Rainbow (CVR) und Standard-Viskose (CV)

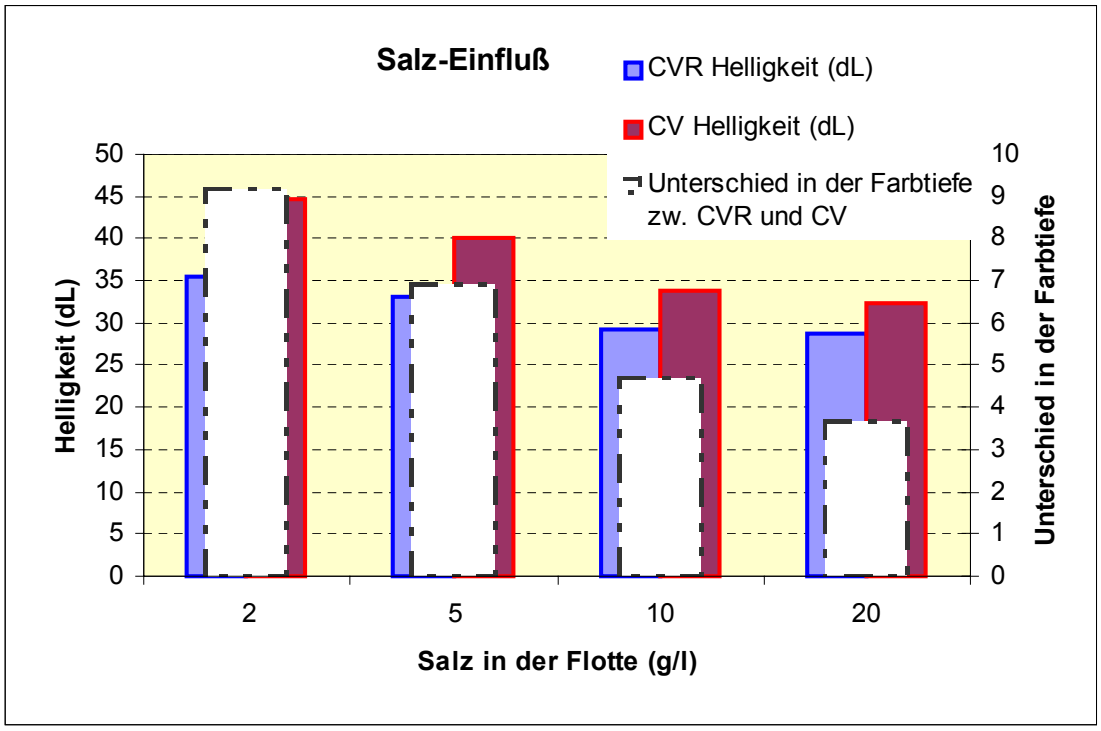

Abbildung 2. Einfluss der Salzkonzentration auf die Farbstoffverteilung bei der Konkurrenzfärbung von Lenzing Viscose® Rainbow (CVR) und Standard-Viskose (CV)

In Abbildung 1 ist deutlich zu erkennen, dass mit höherer Temperatur die Differenz in der Helligkeit der beiden gefärbten Komponenten zunimmt. Bei 70°C ist ein Unterschied von ca. 7 und bei 90 °C ein Unterschied von 11 Cielab-Einheiten zu beobachten. Weitere Untersuchungen haben gezeigt, dass sich dieser Trend bei höheren Temperaturen fortsetzt. Dieser Zusammenhang zwischen Färbetemperatur und Farbstoffverteilung ist auch stark von dem verwendeten Farbstoff abhängig.

Die Salzkonzentration hat einen sehr großen Einfluss auf die Verteilung des Direktfarbstoffes. Je höher die Salzkonzentration in der Flotte umso geringer ist der Helligkeitsunterschied auf den Geweben (bei 2 g/l Salz beträgt das ΔL 9 und bei 20 g/l nur 3,5 Cielab-Einheiten). Eine weitere Erhöhung der Salzkonzentration führt nicht mehr zu einem signifikanten Effekt. Aus dieser Eigenschaft ist abzuleiten, dass es für die Reproduzierbarkeit der Konkurrenzfärbung von Lenzing Viscose® Rainbow mit herkömmlichen Cellulosefasern günstig ist, bei hohen Salzkonzentrationen zu färben, da sich die Farbstoffverteilung nicht mehr ändert wenn die Salzkonzentration schwankt. Die Farbstoffverteilung in Abhängigkeit der Salzkonzentration ist ebenfalls stark vom verwendeten Farbstoff abhängig (siehe Abbildung 3).

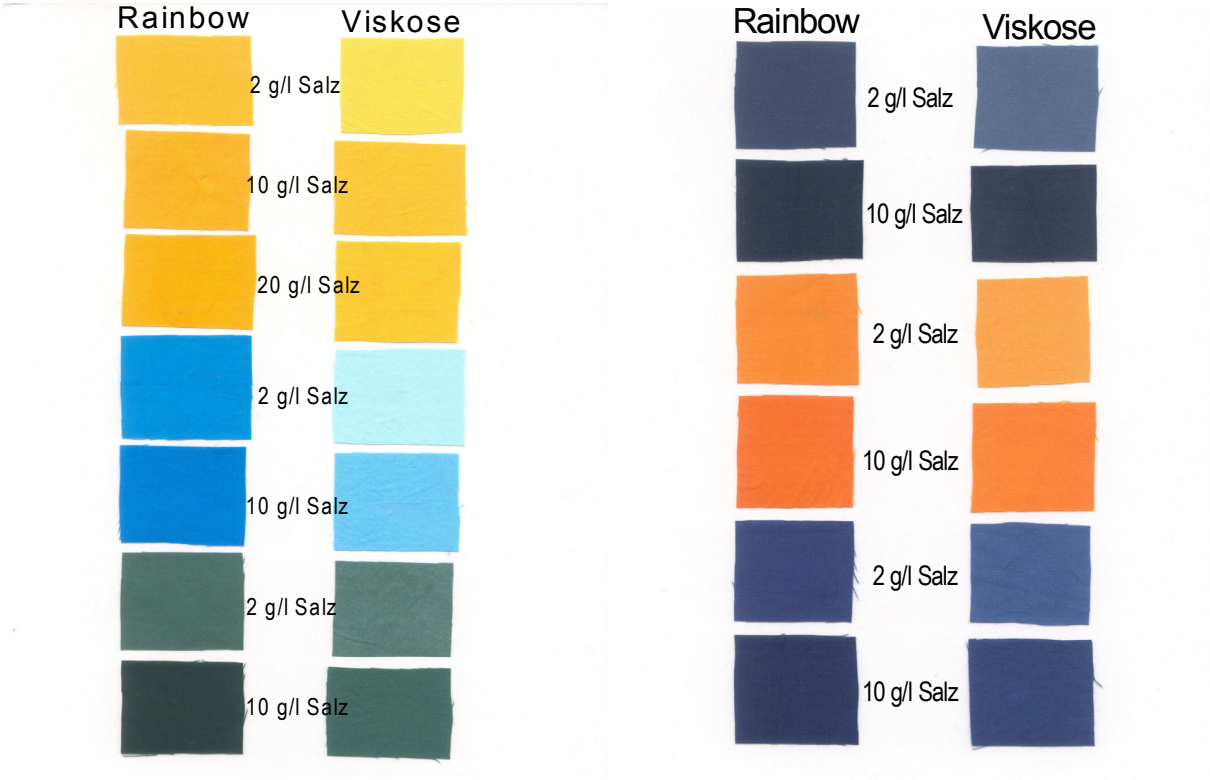

Abbildung 3. Abhängigkeit der Farbstoffverteilung von der Salzkonzentration in der Flotte und des eingesetzten Farbstoffes

Das Färben mit Reaktivfarbstoffen

Bei der Konkurrenzfärbung mit Reaktivfarbstoffen sind grundsätzlich die gleichen Abhängigkeiten im Vergleich mit Direktfarbstoffen zu erkennen. Diese Abhängigkeiten sind jedoch noch stärker ausgeprägt. So ist es bei den meisten Reaktivfarbstoffen möglich bei 130 °C selektiv nur die Lenzing Viscose® Rainbow zu färben und die andere Cellulosekomponente farblos zu belassen. Der Reaktivfarbstoff wird dabei thermisch fixiert. Nach der Färbung wird ein Seifprozess empfohlen um Hydrolysate von den Fasern zu entfernen.

Bei Färbetemperaturen von 60°C und Salzkonzentrationen zwischen 60 und 80 g/l

kann die Farbstoffverteilung stark verändert werden. Es ist unter diesen Bedingungen möglich, in Abhängigkeit des verwendeten Farbstoffs Lenzing Viscose® Rainbow und Standard-Viskose Ton in Ton zu färben. Die Art der eingesetzten Reaktivfarbstoffe besitzt jedoch einen großen Einfluss. Hier sind weitere Arbeiten notwendig um die Eigenschaften der verschiedenen Reaktivfarbstoffe zu charakterisieren..

Abbildung 4. Konkurrenzfärbungen mit Lenzing Viscose® Rainbow und Standard-Viskose mit Reaktivfarbstoffen bei verschiedenen Temperaturen.

In Abbildung 4 ist am Beispiel eines Lenzing Viscose® Rainbow/Viskose-Karogewebes dargestellt, wie bei verschiedenen Temperaturen und unterschiedlichen Reaktivfarbstoffen die Farbstoffverteilung aussieht. Die Ausschnitte des Karogewebes sind so gewählt, dass sich links oben 100% Lenzing Viscose® Rainbow, rechts unter 100% Viskose und in den beiden anderen Feldern Mischungen von Lenzing Viscose® Rainbow- und Viskose-Garn befinden.
Die eingesetzte Farbstoffmenge ist jedoch unterschiedlich (bei 130°C 0,3% und bei 60°C 2%).

Das Färben von Mischungen aus Lenzing Viscose® Rainbow und herkömmlichen Cellulosefasern mit Direkt- und Metallkomplexfarbstoffen:

Lenzing Viscose® Rainbow kann im Gegensatz zu herkömmlichen Cellulosefasern auch mit Wollfarbstoffen gefärbt werden. Metallkomplexfarbstoffe eignen sich neben einigen ausgewählten Säurefarbstoffen besonders gut. Diese Eigenschaft kann genutzt werden um System- oder Intimmischungen aus Lenzing Viscose® Rainbow und herkömmlichen Cellulosefasern bicolorgig zu färben. Dazu wurde Gewebe aus Lenzing Viscose® Rainbow, Lyocell, Viskose und Modal in einer Konkurrenzfärbung mit verschiedenen Kombinationen aus Direkt und Metallkomplexfarbstoffen gefärbt. Die Färbungen wurden unter folgenden Standardbedingungen durchgeführt:

Färbetemperatur
Salzkonzentration
Flottenverhältnis

peratur 45 min
7
ittel

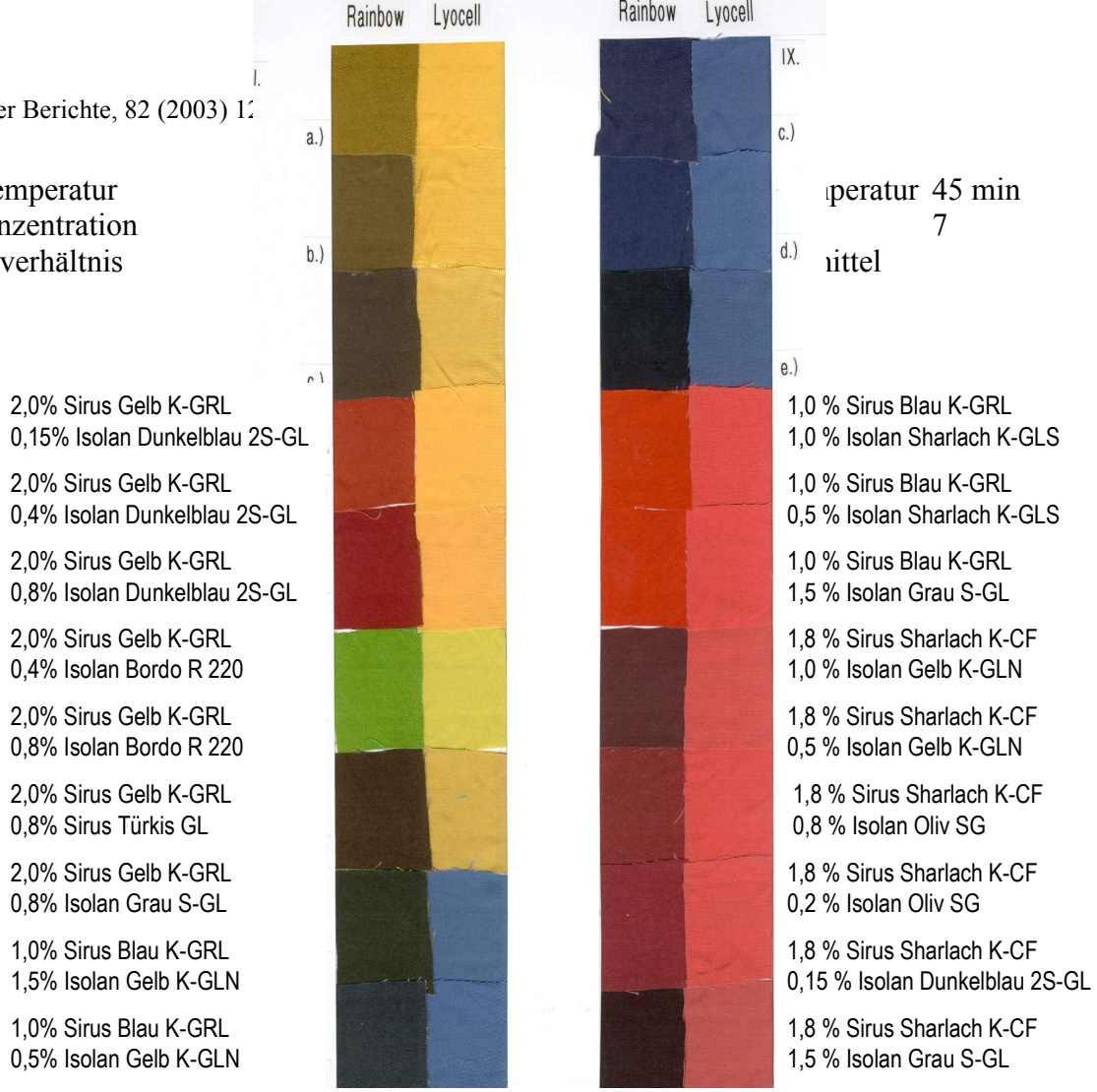

Abbildung 5. Bicolorfärbungen von Lenzing Viscose® Rainbow und Lyocell mit Direkt- und Metallkomplexfarbstoffen

Aus Abbildung 5 ist ersichtlich, dass nur der Direktfarbstoff das Lyocellgewebe und beide Farbstoff das Lenzing Viscose® Rainbow-Gewebe gefärbt haben. Lyocell eignet sich besonders gut für Bicolorfärbungen dieser Art, weil die Lyocell nahezu nicht von Metallkomplexfarbstoffen angeschmutzt wird. Entsprechende Versuche mit Viskose und Baumwolle zeigten leicht schlechtere Ergebnisse bezüglich der Anschmutzung.

Diese Bicolor-Färbe-Technologie ermöglicht eine sehr flexible und kostenschonende Produktion von Buntwebartikeln und –strickartikeln. Bei der bisherigen Produktion dieser Artikel muss man mit einer Vorbereitungszeit von mindesten 2 Monaten rechnen. Erst nachdem die Garne gefärbt wurden, kann die Web- oder Strickware produziert werden und damit muss man schon frühzeitig Farbdesign und Produktionsmenge festlegen und kann nicht mehr auf Markttrends reagieren.

Mit der hier erläuterten Lenzing Viscose® Rainbow Bicolor-Färbetechnologie kann die produzierte Web- oder Strickware sehr kurzfristig mit den unterschiedlichsten Farbdesigns im Stück gefärbt werden. Man ist nicht schon frühzeitig auf die Mengen für das jeweilige Design festgelegt und kann je nach Kundenwunsch sehr flexibel das jeweils benötigte Farbdesign auswählen. Mischungen aus Lenzing Viscose® Rainbow und herkömmlichen Cellulosefasen sind jedoch nicht völlig frei in der Farbeinstellung, weil der für die herkömmliche Cellulose verwendete Direkt- oder Reaktivfarbstoff immer auch die Lenzing Viscose® Rainbow mitfärbt. Es sind alle Farben in Kombination mit weiß (Lenzing Viscose® Rainbow farbig, herk. Cellulose

weiß) und schwarz (Lenzing Viscose® Rainbow schwarz, herk. Cellulose farbig) möglich und zahlreiche Bicolor-Kombinationen.

Die Reproduzierbarkeit der Bicolorfärbungen ist gut. Es wurden jeweils mehrere Färbungen an einem 10 kg Jet-Färbeapparat und einem Labor-Jigger durchgeführt. Dabei wurden an einer gemusterten Ware (Jet-Färbung, Abbildung 6) keine signifikanten Farbtiefen- oder Farbtonunterschiede festgestellt.

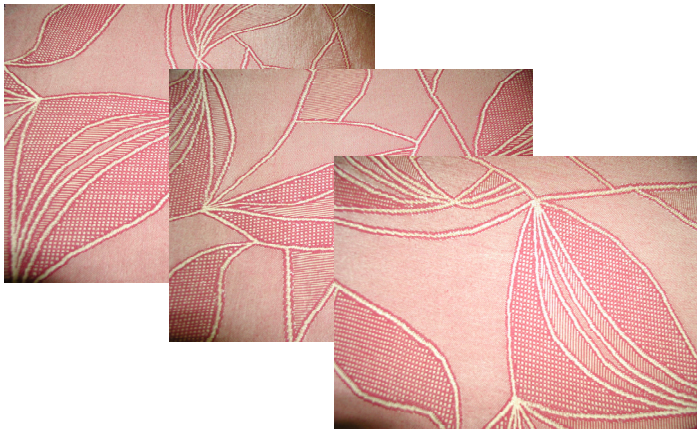

Abbildung 6. Vergleich mehrfach wiederholter Färbungen am Jet zur Überprüfung der Reproduzierbarkeit von Bicolor-Färbungen mit Lenzing Viscose® Rainbow

Tricolorfärbungen von Mischungen aus PES-, Lenzing Viscose® Rainbow- und anderen Cellulosefasern

Die zielstrebige Weiterentwicklung dieser hier vorgestellten Bicolor-Färbetechnologie führt zur Tricolorfärbung von Mischungen aus Lenzing Viscose® Rainbow ‚Polyester und herkömmlicher Cellulose. In diesem Verfahren ist es möglich in einem Stückfärbeprozess die drei Faserkomponenten mit unterschiedlichen Farben zu färben. Im Labor und Technikum wurde folgendes Verfahren (Temperatur/Zeit-Diagramm) ausgearbeitet:

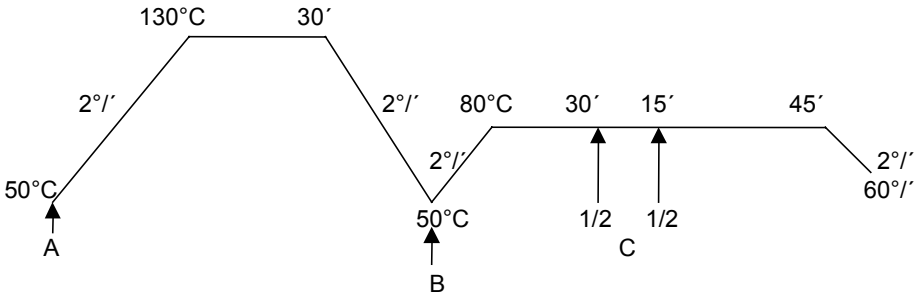

An Position A werden die notwendigen Prozesschemikalien, der Dispersionsfarbstoff und der Metallkomplexfarbstoff zudosiert. An Position B wird Salz (zwischen 20 und 80 g/l je nach Farbstoff) und ein Direkt- oder Reaktivfarbstoff zugegeben. Die dann zu erreichende Färbetemperatur richtet sich ebenfalls nach dem verwendeten Farbstoff an Position B (Direktfarbstoffe 80 bis 90°C, Reaktivfarbstoffe 60 bis 80°C). An Position C kann, die für eine Reaktivfärbung notwendige Menge Alkali hinzugegeben werden. In Abbildung 7 wird ein Gewebe gezeigt, dass in einer Stückfärbung nach dem hier erläuterten Verfahren gefärbt wurde.

Dieses Verfahren wurde jedoch noch nicht unter industriellen Bedingungen getestet.

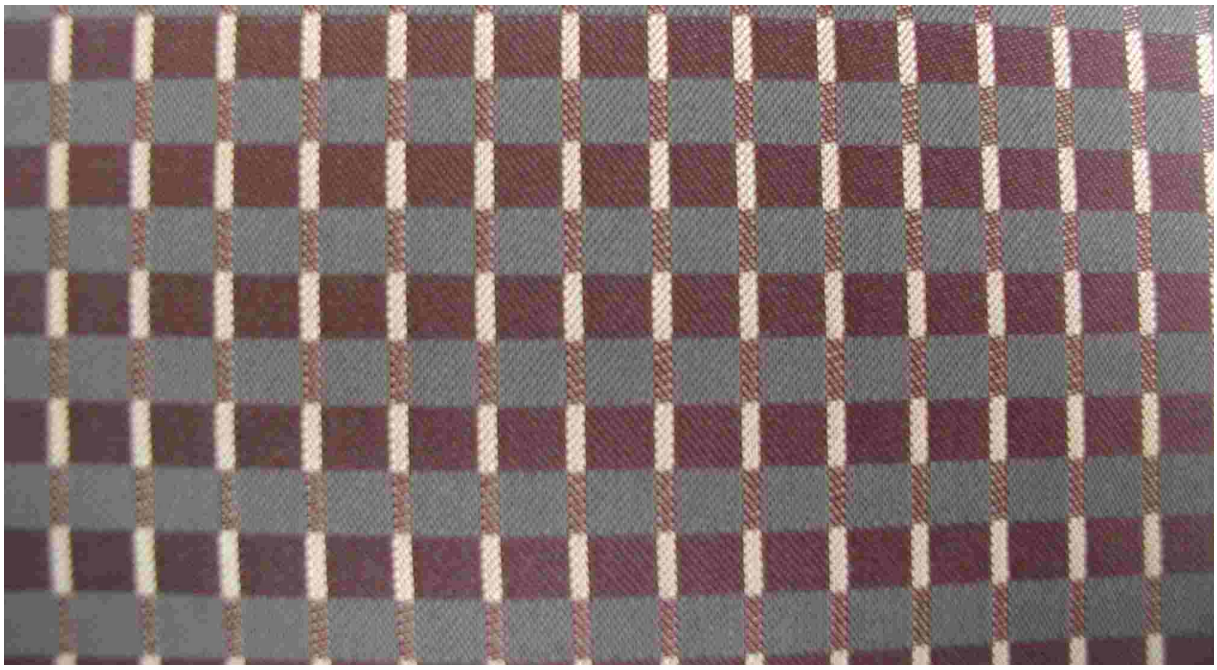

Abbildung 7. Tricolorfärbung von Lenzing Viscose® Rainbow (oliv), Polyester (braun) und Viskose (gelb)

Zusammenfassung und Ausblick

Die Entwicklungen von Lenzing Viscose® Rainbow-Anwendungen mit einem hohen Kundennutzen haben folgende Ergebnisse erbracht:

a) Polyester/ Lenzing Viscose® Rainbow-Mischungen können in 3 bis 4 Stunden Färbezeit in der Ausziehfärberei mit guten 60°C-Echtheiten gefärbt werden.

b) Bicolor-Stück-Färbungen von Mischungen aus Lenzing Viscose® Rainbow und herkömmlichen Cellulosefasern bieten ein hohes Maß an Flexibilität und Kostenreduktion bei der Herstellung von Buntweb- und Buntstrickartikeln.

c) Tricolor-Stückfärbungen von Mischungen aus Lenzing Viscose® Rainbow, Polyester und herkömmlichen Cellulosefasern.

Weitere Anwendungen mit Lenzing Viscose® Rainbow könnten in folgenden Bereichen einen Kundennutzen generieren:

a) Mischungen mit Lenzing Viscose® Rainbow und Polyamid im Bereich Druck und Stückfärbung

b) Mischungen mit Lenzing Viscose® Rainbow und Wolle

Lenzinger Berichte, 82 (2003) 20-30

IONTEX
Special Fibres for Filtration and Water Purification

Harald Schobesberger[a], Josef Schmidtbauer[a]
Patrick Gayrine[b], Richard Martinetti[b]

[a] Lenzing AG, R&D, 4860 Lenzing, Austria,
tel.: ++43/7672/701-0
h.schobesberger@lenzing.com; j.schmidtbauer@lenzing.com
[b] IFTH, Avenue Guy de Collongue, 69134 Ecully, France
tel.: ++33/472/861600
pgayrine@ifth.org; rmartinetti@ifth.org

Abstract

The selective removal of toxic ionic species from diluted waste streams requires effective filtration systems. The development of new filtration systems based on cellulosic textile materials with ion exchange capacities is the objective of the EU-funded research project IONTEX. In cooperation with other European partners Lenzing and IFTH are developing cellulosic fibres respectively nonwovens with ion exchange properties.
The advantages of such IONTEX textile filter materials compared to traditional technologies are a much bigger surface available for ion exchange reactions, which means at the same time faster process kinetics, and a lower pressure drop at higher flow rates.
In order to introduce ion exchange groups into cellulosic textile materials, two different approaches have been investigated: a reactive surface treatment of the cellulosic textile or nonwoven on the one hand and the introduction of homogeneously distributed functional groups into the cellulosic fibre on the other hand. In a process developed and patented by IFTH, functional monomers are grafted onto the surface of the textile material after activation by electron beam treatment. For the functionalisation of cellulosic fibres, Lenzing's well established incorporation technology is used by preparing micro-dispersions of ion exchange substances and introduction into the viscose spinning dope.
IONTEX filters are characterised by high efficiency and selectivity, they can be easily regenerated and provide sufficient mechanical and chemical stability in the respective media.

Keywords: *cellulosics, ion exchange, filtration, nonwovens*

Introduction:

Water is one of our most important but limited resources. Global fresh water consumption amounts to more than 4,000 km³/a and demand is growing twice as fast as population. We are moving towards a global water crisis: 50% of the people living in developing countries suffer from diseases associated with insufficient water supply and every 8 seconds a child dies due to the lack of clean and safe water [1].

Efficient and flexible technologies are therefore required to reduce aqueous pollution. The purification of waste streams will allow recycling of process water in industrial processes and also contribute to improve the quality of drinking water. In Europe, a major source for the emission of toxic ionic species into water are the surface treatment and plating industry with more than 15.000 SMEs and the nuclear power industry with more than 200 nuclear power plants [1].

EU-funded Project "IONTEX"

The selective removal of heavy metal ions from diluted waste water streams requires highly efficient filtration systems. The development of such new and innovative filtration systems

based on cellulosic textile materials with ion exchange capacities is the objective of the EU-funded research project IONTEX. The project started in the GROWTH program of FP5 in April 2001.
The Consortium of 6 European partners is coordinated by Institut Français Textile et Habillement (IFTH) and well distributed across the value chain from fibre manufacturer, nonwoven producer, filter manufacturer to the end-user. This complementary organisation guarantees, that tailor-made (intermediate) solutions are developed for the subsequent process step.

The objective is to realize an industrial filter capable of removing traces of ionic pollutants (heavy metal ions and nitrates) and to deal with very high flow rates at the same time. Traditional separation systems based on evaporation, ion exchange resin beads or membrane technologies are too costly or not sufficiently effective for such applications. A textile filter system combining both features is currently not on the market and is highly desired by the surface treatment industry.

In order to introduce ion exchange functional groups into cellulosic textiles and nonwovens, two different approaches were investigated:

- the reactive surface treatment of cellulosic textiles or nonwovens and
- the introduction of homogeneously distributed functional groups into the cellulosic fibre followed by subsequent processing of the fibre into textiles or nonwovens.

IFTH has developed a proprietary process to graft functional monomers onto the surface of textiles and nonwovens by electron beam activation. The other approach is based on Lenzing's well established incorporation technology for introducing micro-dispersions of ground ion exchange resins into the viscose spinning dope.

Grafting of ion exchange groups on textiles and nonwovens

IFTH developed a process for reactive surface treatment of nonwovens by electron beam grafting: selected monomers are bonded onto the surface of webs made of special cellulosic fibres with superior grafting behaviour. The chemical reaction takes place in the nonwoven fabric under activation by means of irradiation.

Grafting technology [2]:

Grafting is a chemical way to attach new properties on a polymeric framework by covalent bonds. The chemical grafting process is carried out in three steps:

a. First phase: *activation of the polymer matrix*
On the unreactive polymer framework reactive sites (free radicals) are created to initiate the grafting reaction.

Several ways are used to obtain activated sites onto a polymer:

- Ozonization
- Redox potential salts
- Peroxides
- Radiation (UV, γ rays, β rays, accelerated electrons)

b. Second phase: the *grafting reaction*
In presence of an unsaturated monomer, the free radical sites react with the double bond of the monomer to create a new polymeric chain.

c. Third phase: *propagation and termination*
The reaction stops when all monomers are consumed or when certain additives are added.

In the following example, the functionalised monomer is bearing ion exchange termination which gives a strong acidic cation exchanging functionality onto the cellulose polymer chain.

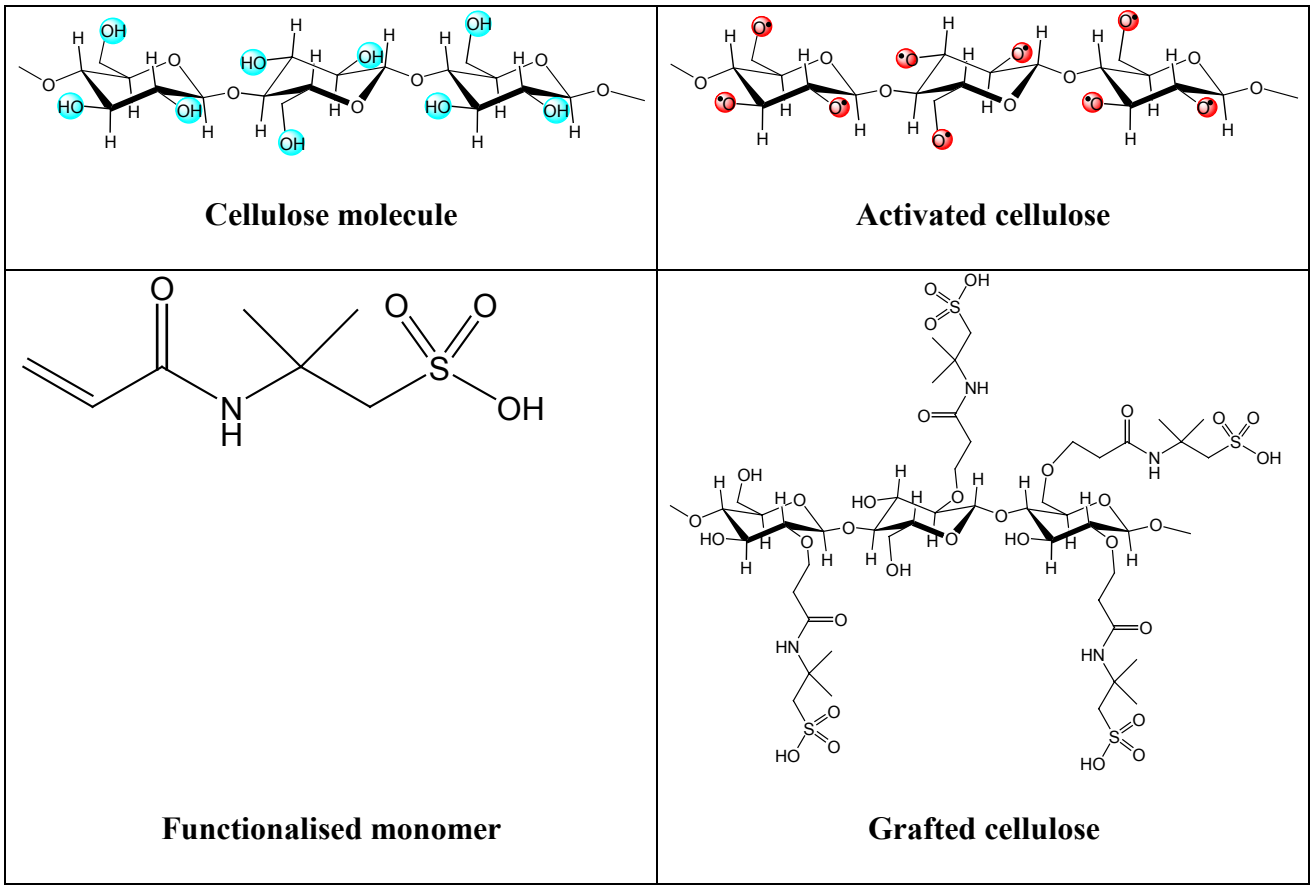

Figure 1: chemical structures during the grafting of cellulose

Electron beam technology

The e-beam process is carried out with needlepunched or hydroentangled nonwoven fabrics. The fabric is impregnated with a solution of monomer, which should be grafted onto the fibre surface. Wettability and adsorption behaviour of fibres are the important parameters for the impregnation step. After the wetted fabric is squeezed, activation in the irradiation unit takes place. The unsaturated monomers react with the generated radicals in the cellulose. Normally a grafting yield of 30-45% is reached. Therefore the unconverted monomers as well as by-products (homopolymers) must be eliminated in multistage washing steps.

The e-Beam treatment is quantified in the ISO system using a dose unit called “GRAY”.
The Gray unit (Gy) represents an amount of energy brought into material and is expressed in “Joules” per kilogram of product :

1 Gray = 1 J/kg

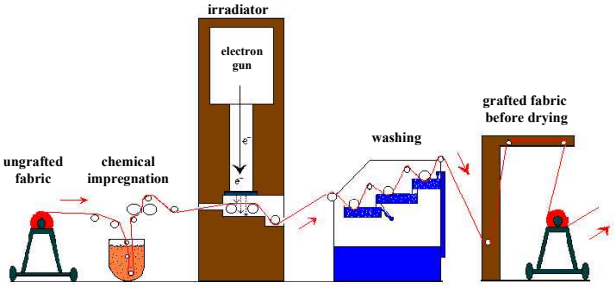

Figure 2: line for grafting of textiles and fabrics

In case of cellulosic materials grafting and crosslinking doses commonly range from 5 to 30 kiloGray, which means 5 to 30 kJ/kg of nonwoven fabric.

The e-beam treatment on cellulosic fibres effects a drop in the degree of polymerisation (DP). The higher the initial DP, which depends on the type of fibre, the more significant is the decrease of DP at higher irradiation doses (see Fig. 3).

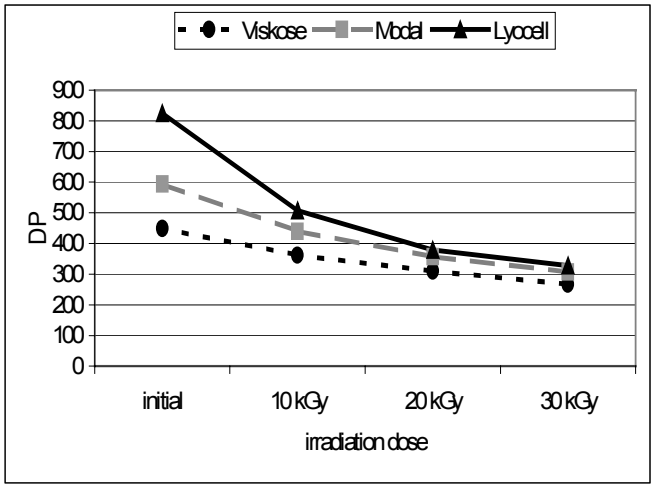

Figure 3: effect of e-beam treatment on cellulosic fibres: comparative loss in DP depending on dose

Compared to traditional chemical treatment processes the Electron Beam Processing cumulates both technologies: activating and grafting.

The advantages of using the e-beam technology are:

- Initiator free
- Material may have significant weight of max. 500 g/m² and thickness up to 4 mm.
- Insensibility to pigments and charges contained into the impregnation slurry.
- The greatest advantage is the possibility to create free radicals into polymeric fibrous supports that induce reactions of grafting.

After the evaluation of the influence of fibre properties on the electron beam grafting, selected monomers have been screened and new monomers with higher ion exchange capacity have been developed and synthesised (see Fig. 4).

Extended grafting trials followed, producing specific cation and anion exchangers with ion exchange capacities from 1,5 to 2,8 mequ/g fibres.

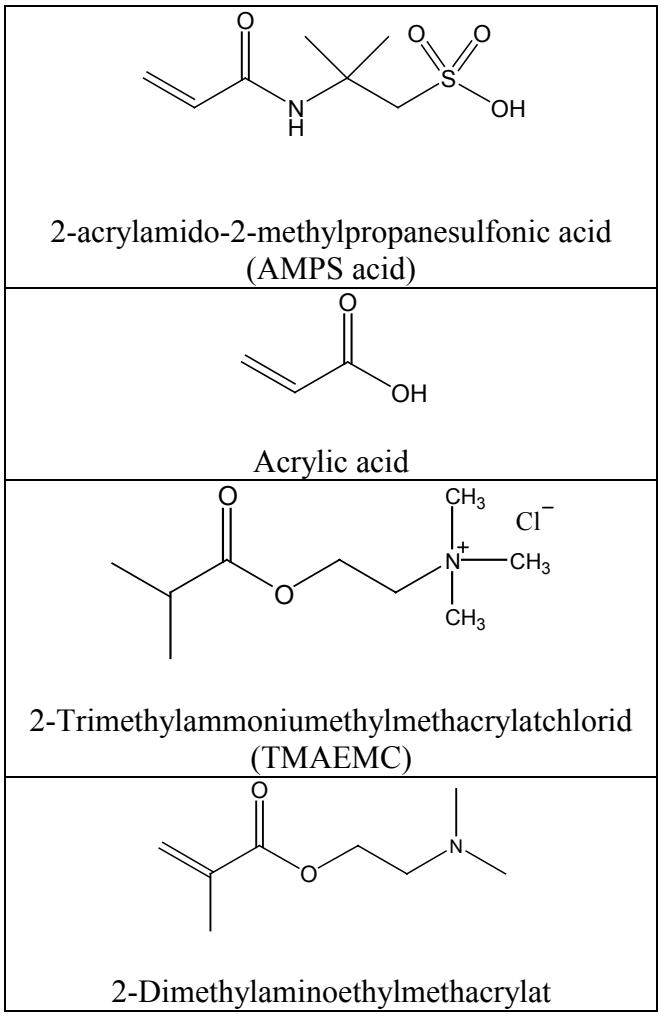

Figure 4: chemical structures of functional monomers used for grafting.

Besides the attainable ion exchange capacity the grafting yield is significant for the grafting process. Cellulosic fibres are porous, have hydrophilic properties and can swell when they are impregnated with monomer solution. Good adsorption capacity of cellulosic fibres corresponds with high grafting yields due to high monomer concentration in the swollen fibre. This is an advantage of cellulosics compared to synthetic fibres, which can also be grafted by e-beam treatment.

All these products were obtained by grafting functionalised monomers onto various cellulosic fibres from Lenzing.

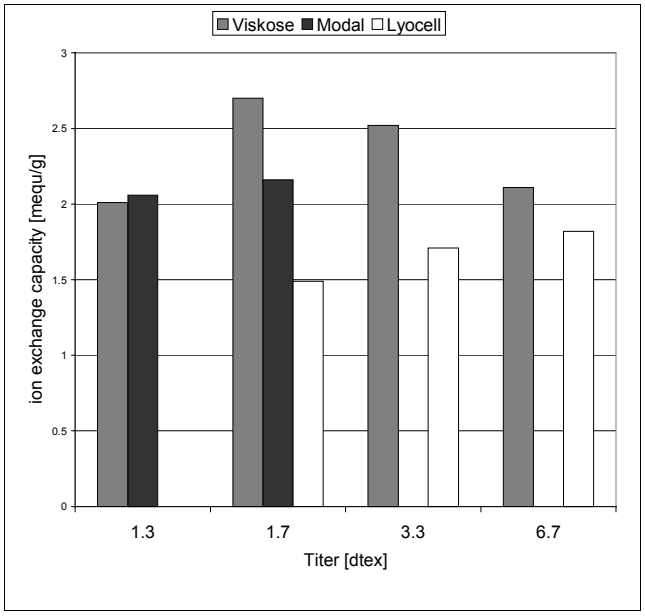

Figure 5: examples for ion exchange capacity of grafted Viscose, Modal and Lyocell fibres

Incorporation of ground ion exchange resins into cellulosic fibres

Parallel to the electron beam grafting of cellulosic fabrics as described above, the research work at Lenzing concentrated on the introduction of homogeneously distributed functional groups into the cellulosic fibre during the fibre manufacturing process. The immobilisation of the ion exchange functions in viscose fibres was achieved by incorporation of insoluble polymers bearing ion exchanging groups into the viscose spinning dope.

It was obvious to use commercially available ion exchange resins, to prepare stable microdispersions from these resins and to mix the dispersion into the viscose solution using the same technology as applied for spun-dyed or flame retardant fibres.

As the suppliers of the ion exchange resins could not provide products in the demanded fineness, it was our first task to grind the resin pearls to an applicable fineness.
The requirement for the preparation of resin dispersions was, that the particle size of the ground resins should not considerably exceed 7 µm. An example for a particle size distribution is shown in Fig. 6.

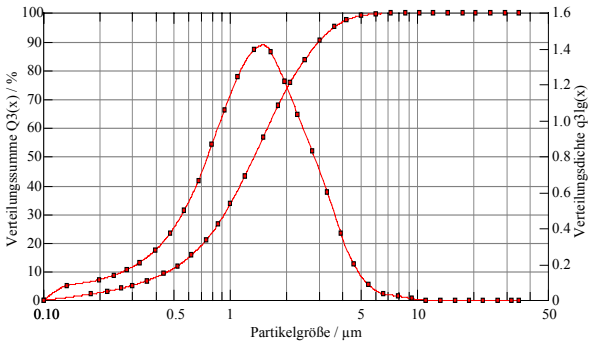

Figure 6: particle size distribution of ground dispersion (Lewatit MP S100)

Meanwhile we have acquired the knowledge how to grind the resins most effectively to the demanded fineness. The grinding has to be done in two steps, because the resin pearls cannot be cracked in the pearl-mill, which is most effective for the fine grinding operation. It must be mentioned, that the grinding process of the different resins most probably depends on the type of polymer, the degree of polymerisation and the cross-linking.

After we were able to grind ion exchange resins, which are available in a spherical shape with a diameter of 0,4-1,7 mm, the milling process had to be improved and in some cases the dispersion had to be stabilised against sedimentation by addition of dispersants. If the dispersion is not stabilised, nozzles get clogged and spinning behaviour is bad. We could find some combinations of chemicals which can be used for the stabilisation of the resin particles if necessary.

The resin dispersions were incorporated into Viscose and Modal fibres in our pilot plant, where we could assess the processability of the dispersions as well as the attainable ion exchange capacity. We found the expected correlation between increasing incorporation rate and ion exchange capacity. Depending on the dispersion fineness, we were able to realize incorporation rates up to 45% with fibre capacities between 1-2 meq/g.

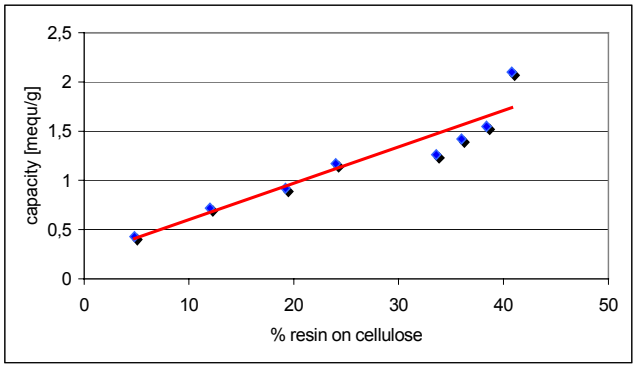

Figure 7: ion exchange capacity of Viscose fibres with increasing amount of incorporated resin

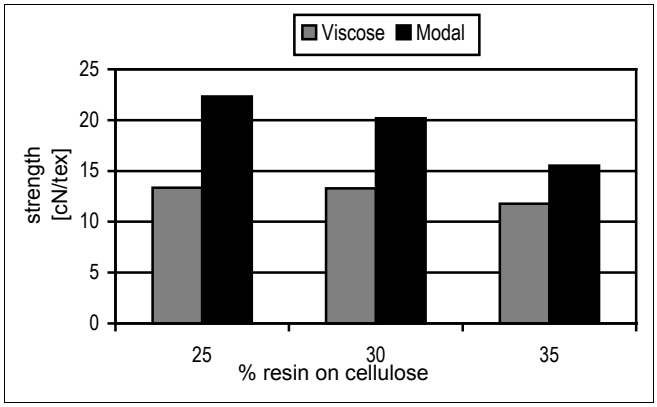

Figure 8: tenacity of Viscose and Modal fibres with increasing amount of resins incorporated

The ion exchange capacity was determined following DIN 54403 [3]. After rinsing the fibres with demineralised water they were treated with a standard solution of caustic soda. After a short time a certain volume of the caustic soda solution was titrated with hydrochloric acid.

Because the fibre tenacity decreases proportional to the incorporated quantity in case of Viscose fibres, we carried out the incorporation on the basis of Modal. The advantage of an ion exchange fibre made of Modal is, that despite high resin concentrations in the fibre, the achieved fibre tenacities are still high enough to guarantee processability for needlepunch or hydroentanglement (Fig. 8).

Comment	Viskose		Modal	
	mequ / g fibre	Strength cond. cN/tex	mequ / g fibre	Strength cond. cN/tex
25% Lewatit MPS112H	0,88	13,3	0,83	22,3
30% Lewatit MPS112H	0,93	13,3	0,91	20,2
35% Lewatit MPS112H	1,13	11,8	0,98	15,5

Table 2: fibre tenacity and ion exchange capacity of Viscose and Modal fibres with increasing amount of resins incorporated

We have already tested some resins with different characteristics focusing on cation exchangers and resins with chelating properties (Table 1). Naturally the list of tested resins can be extended at will according to the requirements and operational area.

name	matix	type	functionality
Lewatit MP S100	Styrene-divinylbenzene copolymer	Strongly acidic	Sulfonic acid
Lewatit MP SP112H	Styrene-divinylbenzene copolymer	Strongly acidic	Sulfonic acid
Lewatit TP208	Styrene-divinylbenzene copolymer	Weakly acidic	Iminodiacetic acid
Duolite C467	Styrene-divinylbenzene copolymer	Weakly acidic	Aminophosphonic acid
Amberlite GT73	Styrene-divinylbenzene copolymer	Weakly acidic	Thiol groups
Lewatit MP 500	Styrene-divinylbenzene copolymer	Strongly basic	Quarternary amine (I)

Table 1: list of applied resins

REM investigations at the Technical University of Graz have shown a homogenous distribution of resin particles over the total fibre cross section and a very porous fibre surface. It could also be seen, that due to the high porosity of the cellulosic fibres heavy metal ions can penetrate into the fibre, where the ion exchange reaction takes place (Fig. 9 and 10). Thus the fibre surface is by far not as influencing as the total fibre volume and the rate of incorporated resin.

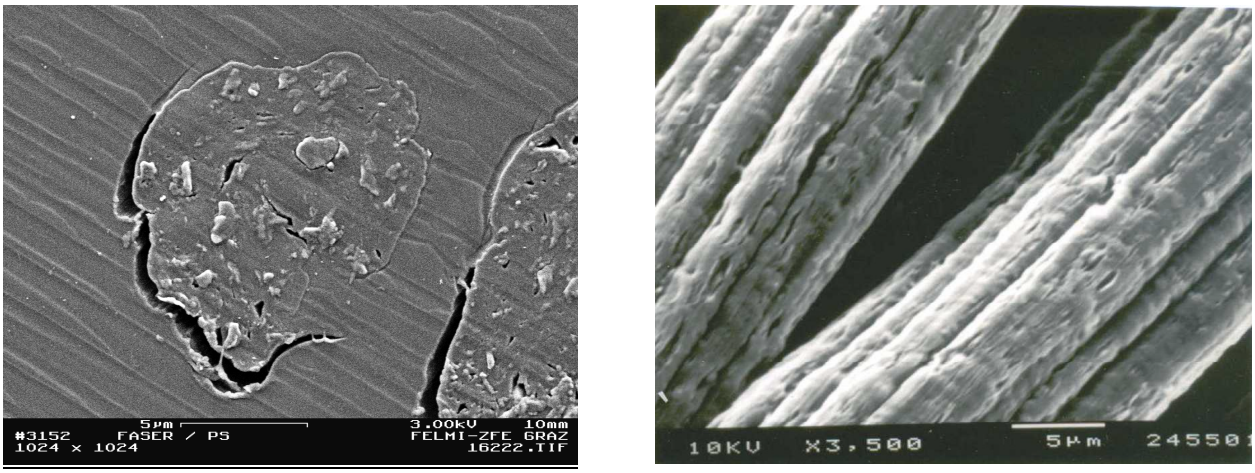

Figure 9: REM of Viscose fibres with resin particles embedded

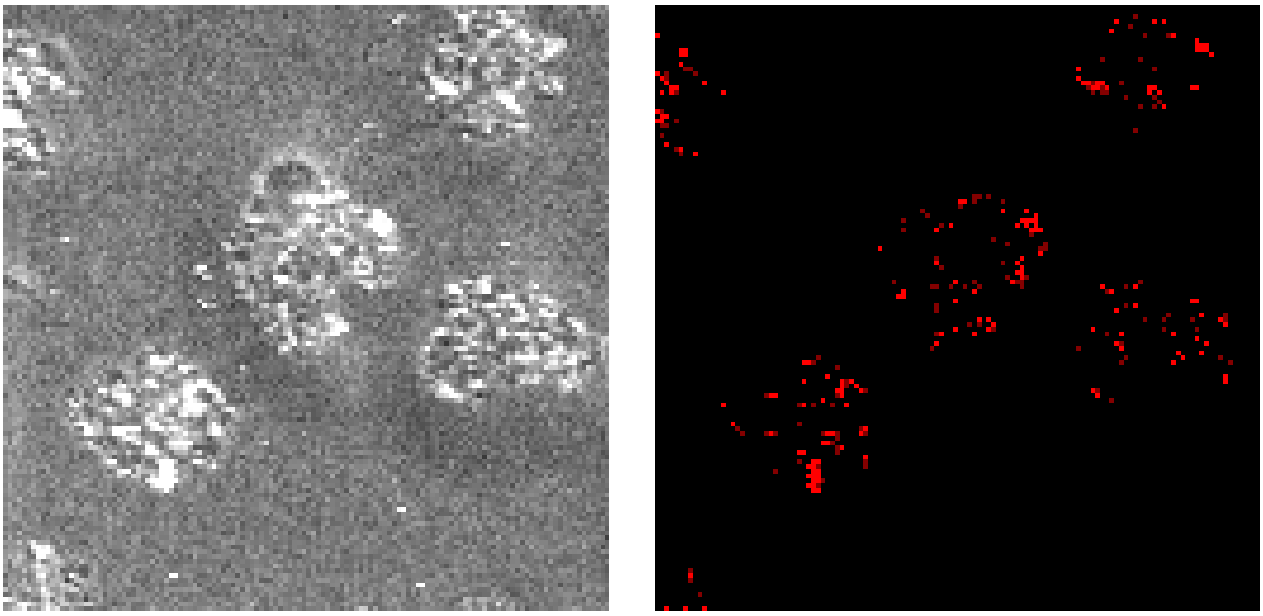

Figure 10: REM of Viscose fibres with embedded resin particles (left) and distribution of lead over the cross section of exhausted fibres (right)

Nevertheless, ion exchange fibres are completely regenerable. Series of operation and regeneration cycles have shown that the capacity of an ion exchange fibre remains unchanged for several cycles. Trials with a filter cartridge containing IONTEX fabrics, loaded with sodium and regenerated with hydrochloric acid illustrate the reliable recovery of the metal for many times.

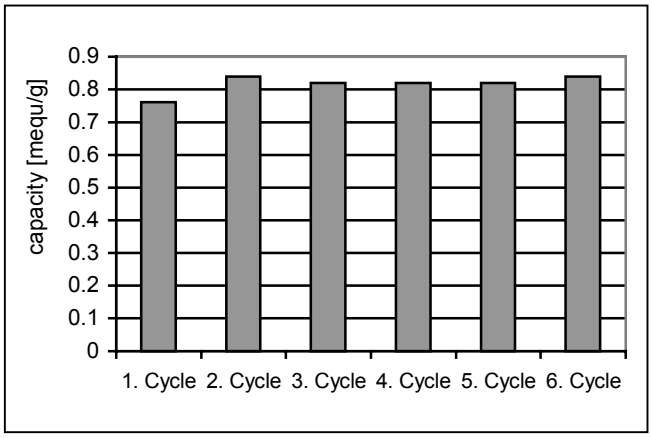

Figure 11: ion exchange capacities of fabric containing 35% resin on cellulose, after several operation cycles

Since ion exchange fibres are applied in liquid systems, degradation of the fibre plays an essential role. The fibre should not be degradable in media out of those toxic agents should be removed, neither by a chemical nor by a biological process.

As there do not exist any specific data in this field, we tested the stability of Viscose fibres in liquid systems. As a first solution the outflow of our waste water treatment was chosen as the medium containing a specific microorganism, which can favor the degradation of cellulose (Fig 13). Another solution did not contain any micro-organisms, but heavy metal ions (Pb, Ni, Sn, Cu), which are typical for effluents from the plating industry (Fig. 12). To estimate degree of degradation, we measured the TOC, DOC of the liquids, and the difference in weight of the treated fibre and the fibre strength. After a testing period of 50 weeks no significant degradation reactions could be determined.

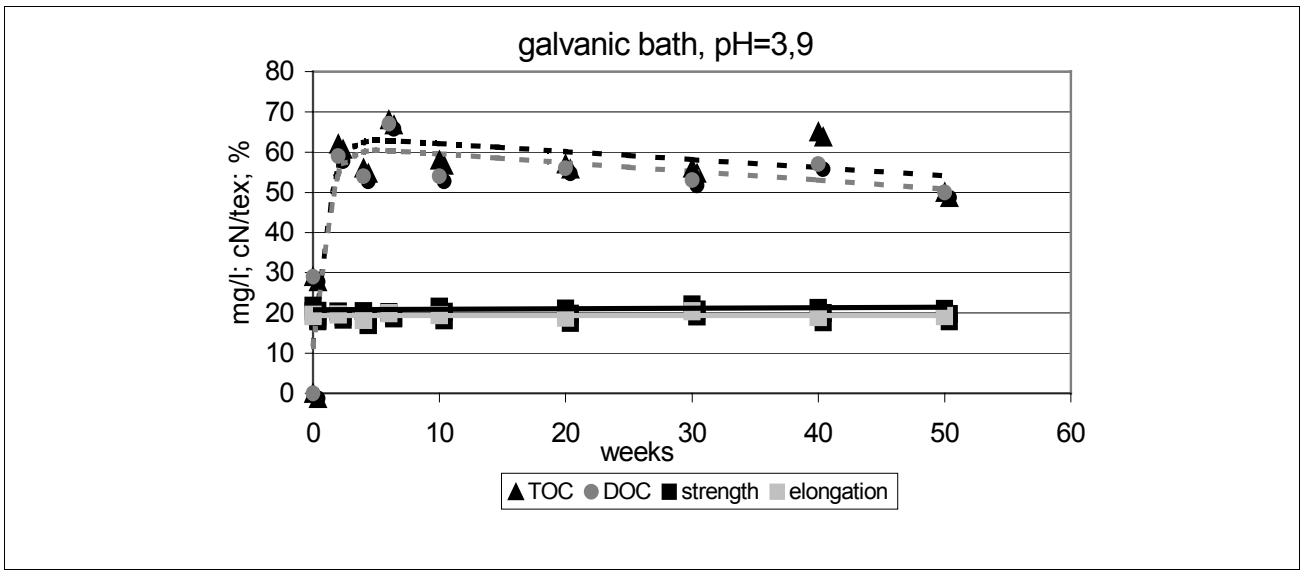

Figure 12: fibre properties and carbon content of the solutions for determination of the resistance of Viscose fibres in galvanic industry

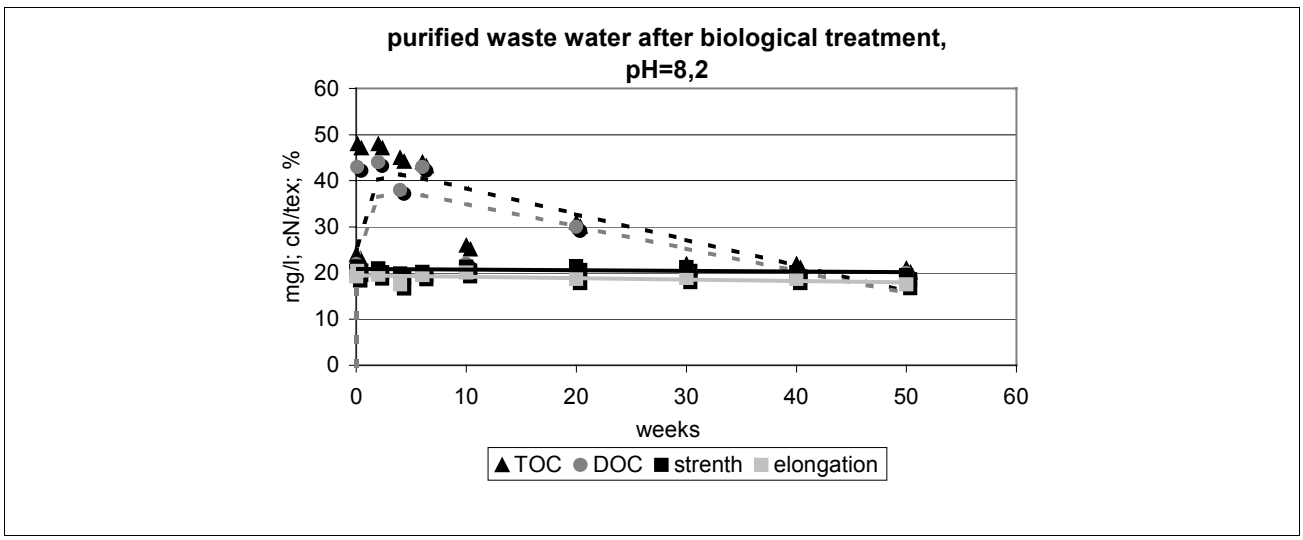

Figure 13: fibre properties and carbon content of the solutions for determination of the resistance of Viscose fibres in waste water containing microorganism.

Ions Exchange Fabrics

Non-grafted fabrics for irradiation are processed according to the usual techniques. Depending on the application needlepunched or spunlaced webs with required properties can be produced from Viscose and Lyocell fibres.

The processing of resins containing ion exchange fibres into nonwovens works as well. Although the fibre finish has not been optimized so far, the entanglement of Viscose fibres with resins incorporated was satisfying.

	Standard Viscose 1,7dtex/40mm	**IONTEX textile, made from resin containing Viscose fibres**
Weight	424 g/m²	401 g/m²
Thickness	4,1 mm	5,4 mm
Density	103 g/dm³	74,3 g/dm³
Strength dry (MD)	313 N	121 N
Strength dry (CD)	607 N	133 N
Elong. dry (MD)	72 %	59 %
Elong. dry (CD)	50 %	62 %

Table 3: mechanical properties of ion exchange fabrics compared with a standard

The ion exchange fabrics produced by e-beam grafting or by incorporation of resins are different from ion exchange resins.

- Difference in presentation:
  - ⇨ Nonwoven cellulosic felts instead of polystyrene beads
- Difference in properties
  - ⇨ Natural hydrophilic web
  - ⇨ Superior accessability for ions due to enlarged surface
  - ⇨ Different fluid flow, and low pressure drop

With all these properties the cellulosic framework and to the particular ion exchange function it follows that ion exchange fabrics are characterised by high process kinetic allowing very high flow rate in comparison with classic ion exchange resins.

Lab-scale trials illustrate these differences between IONTEX textile and resins. The removal of copper ions was studied with a column containing Lewatit MP S100H and another column stuffed with ion exchange fabrics. The fabric was made from fibres incorporated with 30 % Lewatit MP S100H. Both columns provide the same capacity, but the flow rate was chosen much higher in case of the fabric in order to adjust the same ratio of $vol_{filtrate}/vol_{bed}$ (see Table 4 and Fig. 14).

	IONTEX fabric	**resin Lewatit MP S100H**
total bed volume of column	902 ml	70,7 ml
mass of ion exchange material	108 g	32,6 g
total bed capacity	141 mequ	141 mequ
flow rate	3060 ml/h	240 ml/h
$vol_{filtrate}$ / vol_{bed} / h	3,4	3,4
feed concentration	5 g/l Cu^{2+}	5 g/l Cu^{2+}
time to breakthrough	22 min	160 min
capacity at breakthrough point	121 mequ	86 mequ
capacity utilisation*	86 %	61 %

Table 4: parameters for the determination of the breakthrough behaviour of ion exchange materials in lab scale
consumed capacity at the breakthrough point related to total capacity

Figure 14: column trial in lab-scale: ion exchange fabrics in the left column, resin in the right column

The experiment demonstrates that the fabric is able to exchange more heavy metal in shorter times by applying higher flow rates. Despite the sub-optimal fluid flow through the manually filled column, the IONTEX textile permits a better ion exchange efficiency explainable by higher process kinetics compared to resin beds.

Some main advantages of ion exchange fabrics are:

- Classic resins used in water processing allow flow rates in the range of 20 to 40 volumes of filtrate by volume of resins ($vol_{filtrate}/vol_{bed}$). Ion exchange fabrics allow flow rates up to 300 $vol_{filtrate}/vol_{bed}$.
- In regeneration state, the flow rate of classic ion exchange resins is 10 to 20 $vol_{filtrate}/vol_{bed}$ on an average. The regeneration of IONTEX textiles is carried out at the same flow rate as the purifying process. Lower consumption of regenerants and rinsing water can be predicted.
- Good accessability and high flow rates permit better process kinetics of IONTEX fabrics compared to resin beds. Although the total ion exchange capacity per volume is lower in case of ion exchange fabrics, the available capacity can be used more effectively.
- The IONTEX textile is resistant to poisoning caused by macro-ions such as metal complexes or proteins, oils and fats. All theses species can be removed from saturated IONTEX fabrics during the phase of regeneration.
- Filtration devices made from IONTEX fabrics cumulate both properties: physical separation from solids out of the liquid phase and ionic purifying of the liquid phase by ion exchange processing due to the ion exchange capacity of the fibres.

Summary

Two technologies to produce ion exchange fabrics were presented. The electron beam grafting of cellulosic fabrics as well as the modification of fibres by incorporation of ground resins with subsequent processing into nonwovens are both suitable to produce ion exchange fabrics with tailor-made properties for filtration and adsorption of undesired ionic species from liquids.
In a process developed by IFTH functional monomers are grafted onto the surface of the textile material after activation by electron beam treatment. Ion exchange fabrics providing capacities between 1,5 to 2,8 mequ/g and bearing selective ion exchange functions offer wide possibilities in terms of waste water purification.

The substantial development of a new product by Lenzing is based on the incorporation of ground resins into Viscose and Modal fibres.
Commercially available ion exchange resins can be dispersed and processed into IONTEX fibres yielding well defined ion exchange capacities up to 2,2 meq/g. Based on Modal technology, more than 40% of the fibre mass can be replaced by an ion exchange resin while the fibre still retains sufficient strength for industrial processing into yarns, textiles or nonwovens. Investigations by electron microscopy confirmed that even functional groups inside the fibre are accessible for ion exchange reactions.

The fibres can be processed into nonwoven filter materials by needlepunch or hydroentanglement. IONTEX filters are characterized by high efficiency and selectivity; they can be easily regenerated and provide sufficient mechanical and chemical stability in the respective media.

In comparison with ion exchange resins the superior exchange characteristics of ion exchange textiles permit a faster regeneration process as well as an eco-efficient filtration process requiring less rinsing water, time and energy. This filter medium is also convenient for treatment of radio-active effluents from the nuclear industry. The fast process kinetics allow the removal of traces of undesired ions from polluted water, moreover, made from combustible textiles the filter can easily be incinerated reducing the volume of contaminated waste.

Prospective investigations with ion exchange filters at the end users site should confirm these experimental findings.

References

[1] Der Fischer Weltalmanach; Fischer Taschenbuchverlag GmbH, Frankfurt, 1999; S 1215, S 1289

[2] E. Letournel; P. Gayrine: Industrial Applications of Electron-Beam Processing, Grafted Material for Technical Textiles; presentation at Techtextil 2001, Frankfurt

[3] DIN 54403: Prüfung von Ionenaustauschern - Bestimmung der Totalen Kapazität von Kationenaustauschern

Entwicklung von Ionentauscher-Fasernauf der Basis von modifizierten ALCERU®-Fasern

R. Büttner, F. Wendler
Thüringisches Institut für Textil- und Kunststoff-Forschung e. V. Rudolstadt

---

Die nach dem ALCERU®-Verfahren hergestellten Lyocellfasern waren ursprünglich für eine rein textile Anwendung konzipiert. Die Eigenschaften dieser Fasern sind aber im besonderen Maße für Modifizierungen geeignet mit dem Ziel, der Faser bestimmte funktionale Eigenschaften zu geben. Das Ziel unserer Arbeiten lag in der Entwicklung einer Faser mit Ionentauschereigenschaften. Die Ionentauscherkapazität sollte einstellbar und in ihrem Maximum mit der Kapazität kommerzieller Ionentauscher vergleichbar sein. Ein weiterer Anspruch war, diese Fasern mit den bekannten textilen Techniken der Garn- und Vliesherstellung verarbeiten zu können. Ein weiteres Ziel bestand darin, den Faserherstellungsprozess durch die Modifizierungstechnologie nicht wesentlich zu verkomplizieren und zu verteuern.

Zur Erreichung der letzt genannten Zielstellung wurde das Prinzip der physikalischen Inkorporation von gemahlenen Ionentauschern angewandt.
Anwendungen für diese Ionentauscherfasern sehen wir als Filter für die Aufbereitung von Trinkwasser oder anderen Wässern und wässrigen Lösungen. Eine weitere Anwendung für diese Fasern eröffnet sich in der Medizin als Träger von bakteriziden Metallionen und ionogenen Wirkstoffen.

Die zu entwickelnden Ionentauscherfasern sollten nach dem ALCERU®-Verfahren hergestellt werden. Das ALCERU®-Verfahren basiert auf der Lösung der Cellulose im Monohydrat desN-Methyl-Morpholin-N-Oxid (Bild 1).

Eine Lösung von Cellulose im Monohydrat des N-Methyl-Morpholin-N-Oxid wird extrudiert in einem Luftspalt verzogen und die Cellulose in einem wässrigen Spinnbad regeneriert.

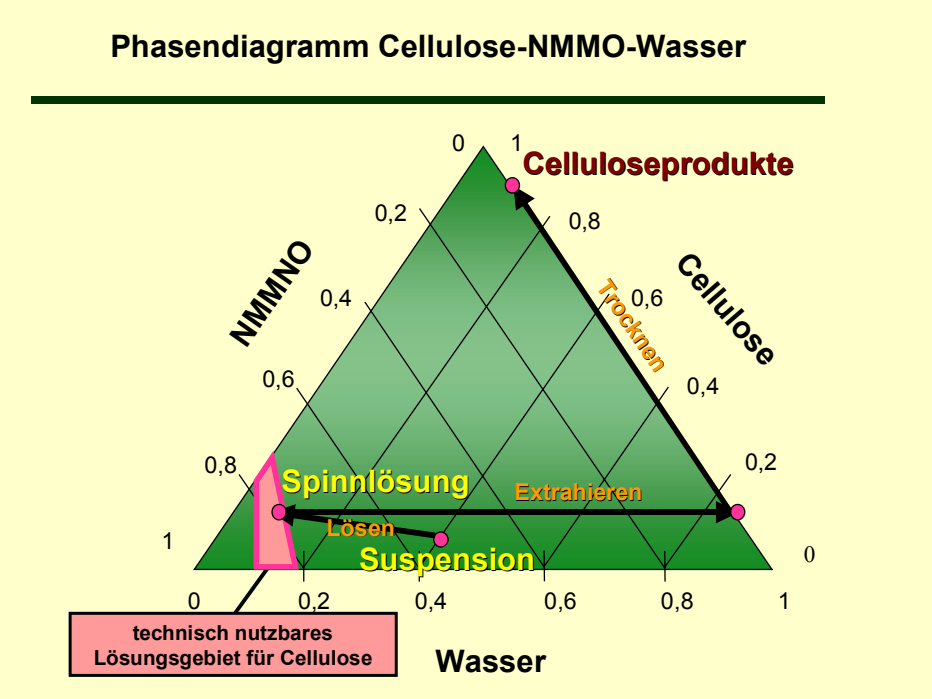

Bild 1. Grundlage des ALCERU®-Prozesses

In diesem Verfahren ist die Herstellung der Fasern auf einen rein physikalischen Prozess zurückgeführt im Gegensatz zu den bekannten Viskose- oder Kupferammoniakverfahren. Diese Änderung der Prozessführung führt nicht nur zur Vereinfachung des Verfahrens, sondern auch zu neuen textil-physikalischen Eigenschaften der Fasern (Tabelle 1).

Parameter	Dim.	Lyocellfasern	Normal-viskose	Cellulos. Chemie-fasern HWM
Reißkraft	**cN**	**6 – 8**	**3 – 4**	**5 – 6**
Dehnung kond.	**%**	**10 – 15**	**18 – 23**	**14 – 16**
Dehnung nass	**%**	**10 – 18**	**22 – 28**	**15 – 18**
Feinheitsbez. Reißkraft	**cN/tex**	**42 – 48**	**20 – 25**	**34 – 38**
Feinheitsbez. Nassreißkraft	**cN/tex**	**26 - 36**	**10 – 15**	**18 – 22**
Feinheitsbez. Schlingenreißkraft	**cN/tex**	**18 – 20**	**10 – 14**	**12 – 16**
Nassreißkraftverhältnis	**%**	**55 – 65**	**55 – 60**	**60 – 65**
Nassmodul	**cN/tex**	**200 – 350**	**50**	**120**
Cellulose	**DP**	**550 – 600**	**290 – 320**	**400 – 450**
Anfangsnassmodul	**[5 %]**	**250 – 270**	**40 – 50**	**180 – 250**
Wasseraufnahme-vermögen	**[%]**	**65 - 70**	**90 - 110**	**75 - 80**

Tabelle 1. Vergleich textilphysikalischer Werte von Cellulosefasern

Die Spezifik des Verfahrens und die hohe Naß- und Trockenfestigkeit der ersponnenen Fasern erlaubt es, hohe Anteile von unlöslichen Ionentauschern in die Spinnlösung einzubringen und in der Faser homogen zu verteilen [1].

Voraussetzung für das Einbringen der Ionentauscher in die Spinnlösung ist eine feine Aufmahlung dieser Tauscher in Fließbett-Gegenstrahlmühlen.

Das Oberkorn des Mahlgutes sollte ca. 10 – 15 µm nicht überschreiten. Der gemahlene Ionentauscher wird in der Spinnlösung homogen verteilt .
Über die inkorporierte Menge des Ionentauschers kann die Austauschkapazität gesteuert werden. Gleichzeitig wird damit die Reißkraft der Faser festgelegt. Bis zu ca. 33 Gew.% inkorporierter Ionentauscher ist eine Garnherstellung möglich. Höhere Füllgrade können mit der Nadelvliestechnik oder Nassvliestechnik verarbeitet werden. Mit steigendem Ionentauscheranteil steigt die Austauschkapazität und fällt die Faserfestigkeit (Bild 2).

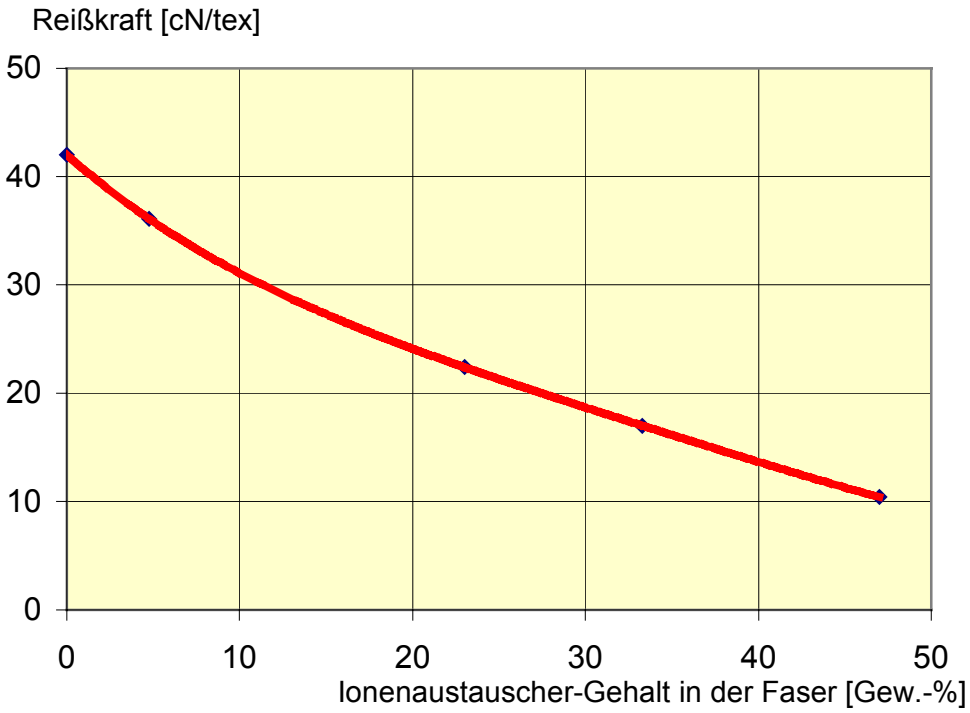

Bild 2. Faserfestigkeit - Füllgrad

Im Bild 3 wurde die Oberfläche eines Ionentauscherfilamentes dargestellt. Man erkennt eine raue Oberfläche, was auf die Inkorporation der Ionentauscherpartikel mit der genannten Korngröße zurückgeführt werden kann.

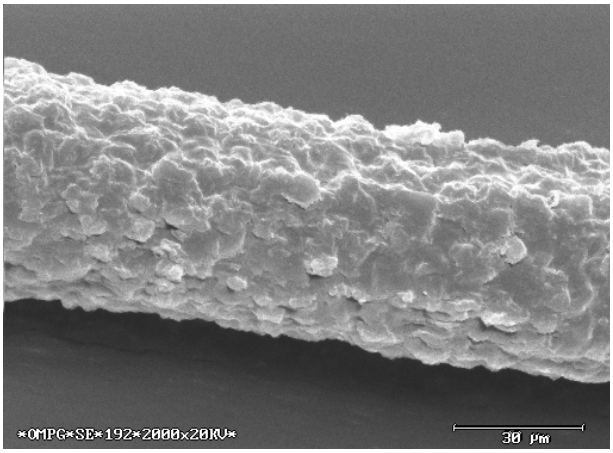

Bild 3. Rasterelektronenaufnahme

Nach dem aufgezeigten Verfahrensprinzip können unterschiedliche Ionentauscher in die Cellulosematrix eingearbeitet werden und den Lyocellfasern spezielle Ionentauschereigenschaften verleihen. Es ist auch möglich, unterschiedliche Ionentauscher in Kombination zu inkorporieren. Die Ionentauscherfasern zeichnen sich gegenüber dem bekannten Ionentauschergranulat durch eine sehr hohe Austauschgeschwindigkeit aus, wobei die Zugänglichkeit der Ionentauscherpartikel voll gegeben ist. Die möglichen Anwendungsformen reichen vom Filtervlies bis zu textilen Flächengebilden.

Im Bild 4 wird die Schwermetallbindung in einem mit Kupfer- und Blei-Ionen aufgestockten Trinkwasser demonstriert. Die Schwermetallbindung kann durch Inkorporation von schwachsauren Ionentauschern auf der Basis von vernetztem Polyacrylat mit Carboxylgruppen oder besser noch mit schwachsauren chelatbildenden Iminodiacetat-Gruppen erreicht werden.

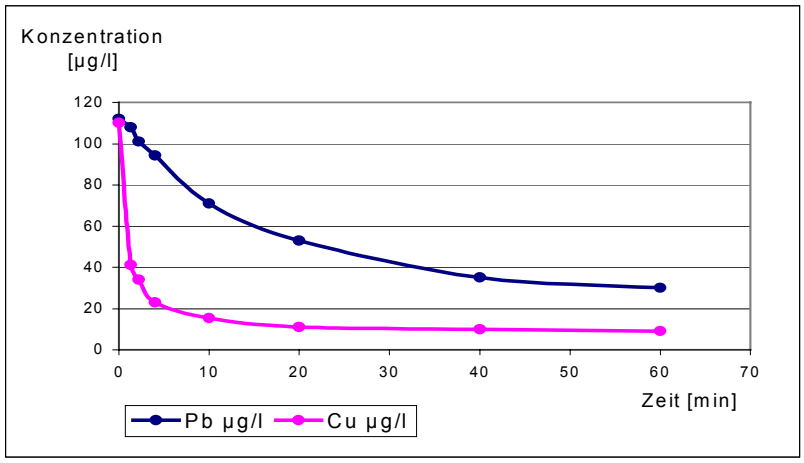

Bild 4. Schwermetallreduzierung im Trinkwasser

Die Nitratbelastung im Trinkwasser ist in einigen Gebieten ein Problem und kann durch Ionentausch reduziert werden. Die Nitratreduzierung mit selektiven Ionentauschern auf der Basis von vernetztem Polystyrol mit quaternären Ammonium-Gruppen ist im Bild 5 dargestellt.

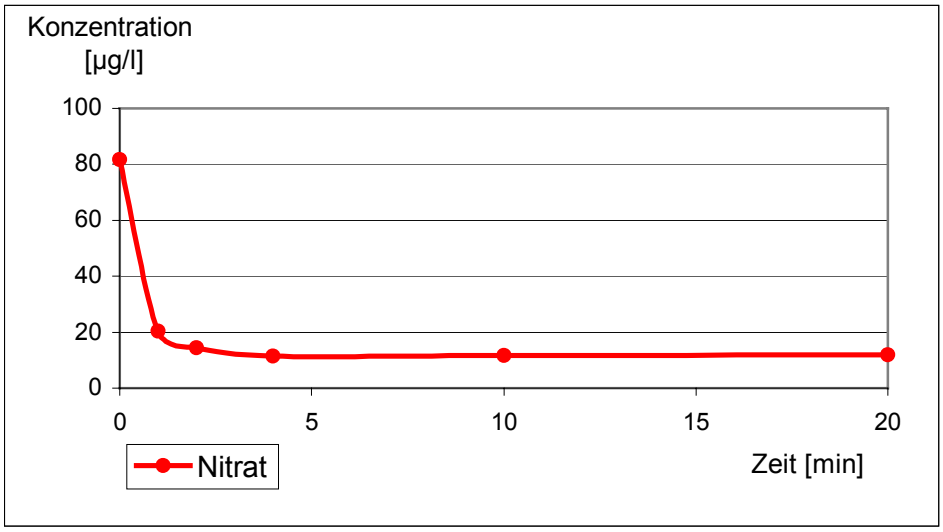

Bild 5. Nitratreduzierung im Trinkwasser

Eine weitere Anwendung kann die Reduzierung der temporären Wasserhärte in Trinkwasser sein. In der Literatur wird beschrieben, dass insbesondere Carbonate die Qualität der zubereiteten Getränke negativ beeinflussen, es ergeben sich bittere flach schmeckende Kaffees, abgestanden schmeckende Tees [2, 3].

Es wird weiter darauf hingewiesen, dass Wasser mit entsprechender Alkalität die Säuren des Kaffee neutralisiert und so den unangenehmen Geschmack bedingt [4].
Neben der Geschmacksbeeinflussung hat die temporäre Härte auf die Optik von Teegetränken Einfluss (Bild 6) [5].

Probe	Temporäre Härte in mval/l	Gesamthärte in °dH
259	2,81	71,07
260	3,20	12,24
261	1,41	35,50
262	1,60	6,12

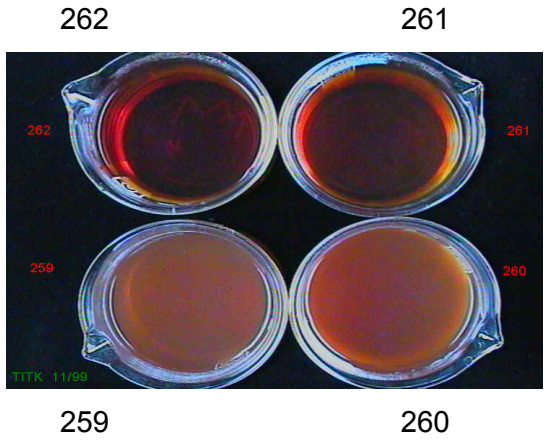

Bild 6. Einfluss der temporären Wasserhärte auf die Trübung

Im Bild ist der Einfluss der temporären Härte auf die Trübung eines Teegetränkes zu sehen. Nach unseren Untersuchungen ist die Trübung ausschließlich von der Höhe der temporären Härte abhängig. Für eine gute Optik des Tees sollte sie auf einen Gehalt von < 1,6 mval/l HCO3- abgesenkt werden.

Die Leistungsfähigkeit der Ionentauscherfaser auf der Basis eines schwachsauren vernetzten Polyacrylates wird im Bild 7 gezeigt. Die eingesetzte Faser hat eine Kapazität, die mit bekannten Ionentauschergranulaten vergleichbar ist. So genügen etwa 150 mg Faser zur ausreichenden Reduzierung der temporären Härte für 150 ml Wasser.

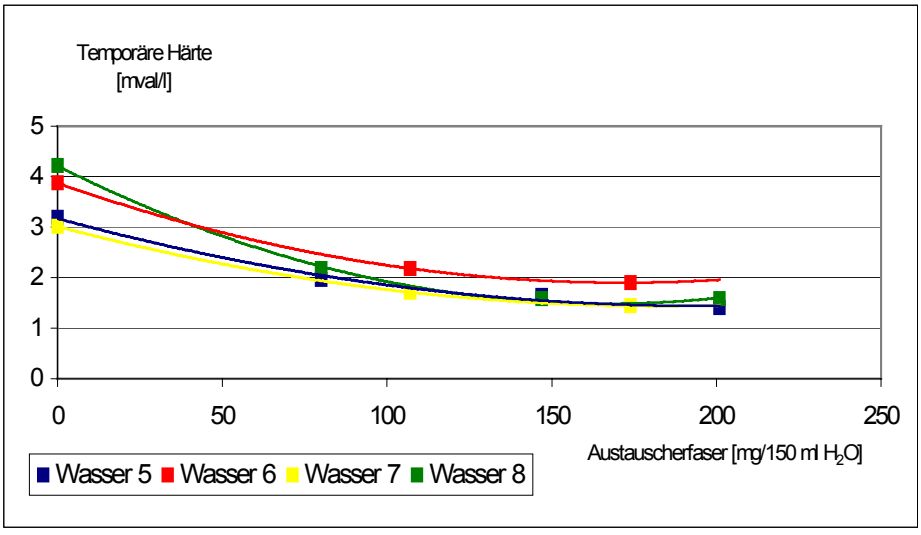

Bild 7. Einfluss des Austauschfasergehaltes auf die temporäre Härte

Neben der Möglichkeit, mit Ionentauscherfasern bestimmte Ionen aus wässrigen Lösungen zu entnehmen, ist auch der umgekehrte Weg möglich: das Einbringen von speziellen Ionen. Durch die Inkorporation ausgewählter Ionentauscher in die ALCERU®-Faser ist die Beladung mit Schwermetallionen wie z. B. Silber, Kupfer und Quecksilber möglich. Dies führt zu einer bakterizid funktionalisierten Cellulosefaser. [6 – 8] Die Beladung mit z. B. Silberionen führt zu folgenden Vorteilen gegenüber bisherigen Silberapplikationen:
Die Silberbeladung ist in weiten Grenzen einstellbar.
Durch die Auswahl der Ionentauscher und die Silberkonzentrationen in der Faser kann die Silberionenkonzentration in der wässrigen Lösung und somit die bakterizide Wirkung gesteuert werden.
Der textile Charakter und die Wasseraufnahme der Cellulosefaser bleiben erhalten.

Diese bakteriziden Cellulosefasern finden sicher eine breite Anwendung in der Medizin als Wundauflagen und als medizinische Papiere. Die bekannten Resistenzen von Bakterienstämmen gegen verschiedene Antibiotika unterstützen die Wiedereinführung eines der ältesten Bakterizide,
Silber, in neuen Applikationen.

Zusammenfassung:

Die Entwicklung von funktionalen Fasern auf der Basis von modifizierten ALCERU®-Fasern führte zur Entwicklung von Ionentauscherfasern. Durch Inkorporation von gemahlenen Ionentauschern können Fasern mit einstellbarer Austauschkapazität hergestellt werden. Die Zugänglichkeit der Ionentauscher ist voll gegeben. Die maximal erreichbare Austauschkapazität entspricht der kommerzieller Ionentauscher.

Eine Kombination unterschiedlicher Ionentauscher in der Faser ist möglich. Diese Fasern können nach der bekannten ALCERU®-Technologie hergestellt werden. Bis zu einem Füllgrad von ca. 33 Gew.% mit Ionentauschern ist eine Garnherstellung möglich. Höhere Füllgrade können mit der Nadelvliestechnik oder der Nassvliestechnik verarbeitet werden.
Ionentauscherfasern können zur Entfernung von Ionen aus wässrigen Lösungen eingesetzt werden. Aber auch ein Eintragen spezieller Ionen in Lösungen in geringen Konzentrationen ist möglich. Die Beladung der Ionentauscherfaser mit bakterizid wirkenden Ionen führt zu bakteriostatischen oder bakteriziden Fasern mit breiter Anwendung in der Medizin und bei der Sport- und Freizeitbekleidung.

Wir danken dem Bundesministerium für Wirtschaft und Technologie für die finanzielle Förderung des Forschungsvorhabens (BMWi-Projekt Nr. 37/99).

Literatur:

[1] Büttner, R.; Claußen, F.; Knobelsdorf; C.; Krieg, M.; Taeger, E.; Patent DE 19917614 C2
[2] Maier, H. G.; „Kaffee“, Berlin, Ham burg (1981) ISBN 3-489-61414-3
[3] Pangborn, R. M.; Trabue, I. M.; Lizzle, H. C.; Analysis of coffee, tea and artifi cally favoral drinks prepared from min eralized waters; J. Foods Sci., 36, 355 – 362 (1971)
[4] Sivetz, M.; „Coffee technology“, West port 1979
[5] Pangborn, R. M.; Influence of water composition, extraction procedures, holding time and temperature on quality of coffee beverage; Lebensm.-Wiss., U. Technologie 15, 161 – 168 (1982)
[6] Pies, I.; Immun mit kolloidalem Silber, VAK-Verlag 1998
[7] Ullmann´s Encyclopedia of Industrial Chemistry, 5. Auflage; VCH Verlagsge sellschaft, 1993, S. 160
[8] Thurman, R. B. ; Gerba, C. P., CRC Cvit; The molecular mechanism of copper and silverion disinfecting of bacteria and viruses; Rev. in Environ. Contr. 18 (4) 295 – 315 (1989)

Lenzinger Berichte, 82 (2003) 37-42

TENCEL®
A VERSATILE, HIGH PERFORMANCE FIBRE FOR NONWOVENS

Andrew Slater and Dr. Andrew Wilkes, TENCEL Ltd.

ABSTRACT

TENCEL® is a high performance, solvent spun, 100% cellulosic fibre, which is ideal for use in many nonwoven applications because of its high strength, durability, absorbency, purity and biodegradability. Over the past 2-3 years the use of TENCEL® fibre has expanded significantly in nonwoven end-uses worldwide. This is as a direct result of the fibre's unique attributes, which are particularly suited for wiping products, currently one of the fastest growing nonwoven market sectors. Also during this period a range of new TENCEL® grades has been developed with enhanced processing performances and fibre properties. This paper reviews the reasons for the recent growth in the use of TENCEL® in nonwovens, discussing aspects such as how the key TENCEL® fibre properties benefit nonwoven producers and consumers, how the processing performance of the fibre has been improved and how to achieve the optimum fabric characteristics from the fibre through spunlacing, needlepunching, latex bonding, wet-laying or air-laying. Particular reference is made to the benefits of TENCEL® in hydroentangled wet and dry wipes.

INTRODUCTION

In the early 1990's a new cellulosic fibre was launched commercially under the brand name of "TENCEL®". TENCEL® was classed as a new generic fibre type (lyocell), the first addition to the fibre classification system for some 20 or more years. TENCEL® is 100% natural in origin as it is made from regenerated cellulose derived from wood pulp. The resultant fibre is of high purity, fully biodegradable and produced from one of the most eco-friendly processes available. It is fair to say that the initial market focus for TENCEL® was into the traditional textile apparel sector. However, this has changed over the last few years. To counteract the cyclical nature of the fashion driven textiles business TENCEL® is now targeted equally into the industrial sector, with particular emphasis on the key nonwovens markets of wipes, filters and feminine hygiene products. The fibre's basic properties fit very well with this strategy.

TENCEL® MANUFACTURING PROCESS

The TENCEL® manufacturing process has been in commercial operation for 10 years now and has proved to be very successful technically, economically and environmentally.

TENCEL® manufacture is a simple process to describe (see Fig 1). The primary raw materials are purified, dissolving grade wood pulp and an amine oxide solvent. The pulp is a renewable resource obtained from FSC (Forestry Stewardship Council) approved and fully managed forests, growing on marginal land. It is dissolved directly in the amine oxide solvent to form a viscous dope. This dope is filtered and extruded through spinnerets to form continuous filaments. These are washed to recover the solvent, dried, mechanically crimped, cut if required, and baled. TENCEL® can also be sold uncrimped in continuous filament, or tow form. The process has been engineered from the outset to have minimal environmental impact and to guarantee excellent ecological credentials for the

fibre. The solvent recovery is by necessity, extremely efficient.

The resultant product is a pure, 100% cellulose fibre. The long chain molecules within the fibre are arranged in a highly orientated crystalline form, resulting in high strength, absorbency and excellent retention of mechanical properties, particularly in the wet state.
The baled TENCEL® fibre is supplied to roll goods manufacturers and converters who make a wide range of engineered nonwoven products from it. At the end of the product's useful life, it can be safely disposed of, as TENCEL® biodegrades completely during normal biological treatment, such as soil burial or anaerobic digestion, into carbon dioxide and water. These natural decomposition products are released back into the atmosphere, elegantly closing the loop of the product lifecycle.

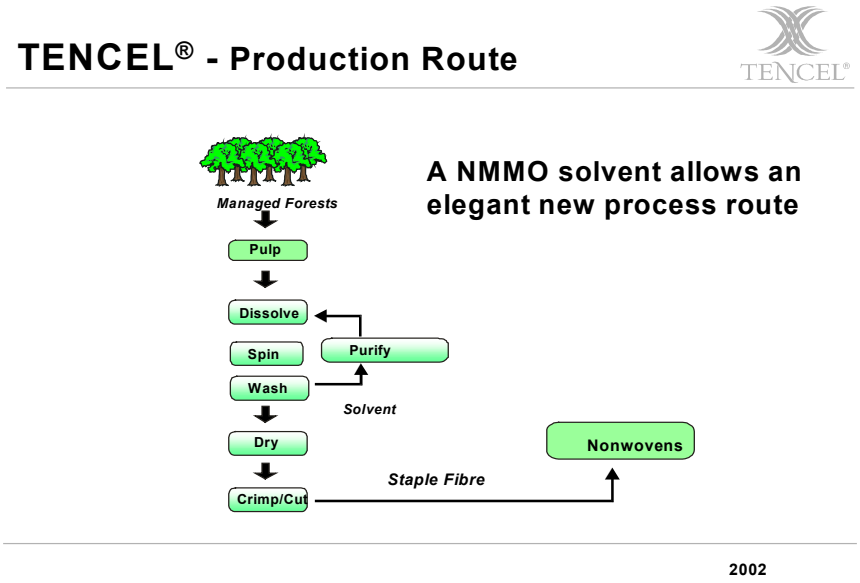

Figure 1. TENCEL® Production Process

TENCEL® PROCESSING PROPERTIES

Staple fibres usually provide the starting point for many nonwoven processes. Because the staple based technologies are so diverse in terms of machinery design, a range of fibre types must be developed to suit individual needs and to ensure optimum conversion efficiencies and fabric properties.

For carding based technologies, TENCEL® fibres have been designed to open consistently and easily prior to the carding step. This gives uniform and nep-free webs. To ensure adequate web cohesion and high running speeds, high crimp TENCEL® variants have been introduced; sometimes in conjunction with more cohesive surface finishes, to provide for efficient web transfer and to minimize fibre fly. Fully optimized TENCEL® variants such as the new TENCEL® HS260 grade have been shown to run at greater than 250m/min on commercial nonwoven carding lines. This is significantly faster than the speeds at which viscose can be run, and with greater web quality and control. This improvement has been achieved through recent advances in crimper design, filament presentation and static control, allowing high levels of fibre crimp to be achieved consistently and without structural damage to the fibre or compaction of the tow. Appropriate selection of surface treatments has also been necessary to compliment this approach and to ensure both consistency and stability in the crimping process.

Crimp levels anywhere in the range 20-55 crimps per 10 cm are now available ensuring that the fibre processes well on current commercial carding lines.

It is vitally important with TENCEL® to match the crimp level to the surface cohesion. This is done on a 'machine by machine' basis by employing a selection of surface lubricants and antistats, which complement the action of the crimp and ensure that opening, carding and web transport are all equally efficient.

The benefits in terms of maximum card speed achieved with TENCEL® HS260 on the newest Thibeau card are outlined below (Fig 2). The webs formed in the trials were set at 30 gsm weight.

FIBRE TYPE	MAXIMUM CARDING SPEED (Meters/min)
TENCEL® HS260	250+
POLYESTER	200-250
STANDARD LYOCELL	150-200
VISCOSE	~150

Figure 2. Comparative Carding Speeds

The higher crimp and surface modified TENCEL® HS260 grades are supplied in a form which is very similar to that of polyester staple, so blending with this fibre type is very efficient. However, TENCEL® can also be produced in a lower crimp form but with a highly cohesive surface finish, giving it somewhat similar processing characteristics to that of a standard viscose. This variant is selected when it is necessary to maximize fabric strengths and dimensional stabilities.

The TENCEL® HS260 variants offer higher bulk and softer handle in fabrics compared to normal TENCEL®.

FABRIC PROPERTIES

A large amount of work has been carried out over the last five years to understand and enhance the attributes of TENCEL® in nonwoven structures. These basic attributes are now being exploited to significant commercial advantage by an increasing range of nonwoven producers.

SPUNLACING

The basic properties of TENCEL® fibre are particularly well suited to the spunlacing (water-jet entanglement) method of bonding. The fibre strength is very high, particularly in the wet state, being at least twice as strong as that of viscose. TENCEL® also entangles efficiently, because of its smooth surface and because its fibrillar cellulose structure plasticizes when wet. This results in very strong and stable spunlaced nonwovens, compared to viscose (Fig 3), but it is still entirely possible to preserve the drape and softness of the final fabric through appropriate choice of bonding pressure profile, belt design and fabric basis weight.

Fabric wet strengths can sometimes be higher than the dry values because the TENCEL® filaments swell predominantly in the diameter. This causes the entangled fibres to lock together even more efficiently. Consequently very soft fabrics with adequate strength can be produced, by using relatively low water pressures. Also

significant basis weight reductions can be achieved, either to generate cost savings, or to reach new markets such as thin, highly permeable coverstocks with basis weights below 20gsm (10gsm for some latex bonded structures). When using apertured entangling belts, fabric hole clarity is the best of any fibre, leading to a superior wiping action and an improved appearance. The combination of a strong fibre and efficient entanglement also results in exceptionally low lint levels, a key requirement for many nonwoven wipers in critical task situations. High fibre modulus and relatively low fibre elongation gives superior fabric stability, which improves the efficiency of conversion from fabric to finished product and acts as an excellent base material for many coating processes. The flexibility in the possible basis weights and bonding levels possible with TENCEL® permits an expanded range of absorbent fabric properties to be achieved. The working range of water pressure for TENCEL® is about 40 to 100 bar (compared to viscose rayon at 55 to 70 bar). The range of consolidation is therefore greater, and capacity, wicking, bulk and softness can be engineered within a much larger envelope. The increased crimp available from TENCEL® HS260 can be used to advantage in the fabric giving higher bulk/thickness and hence improving the fabric aesthetics.

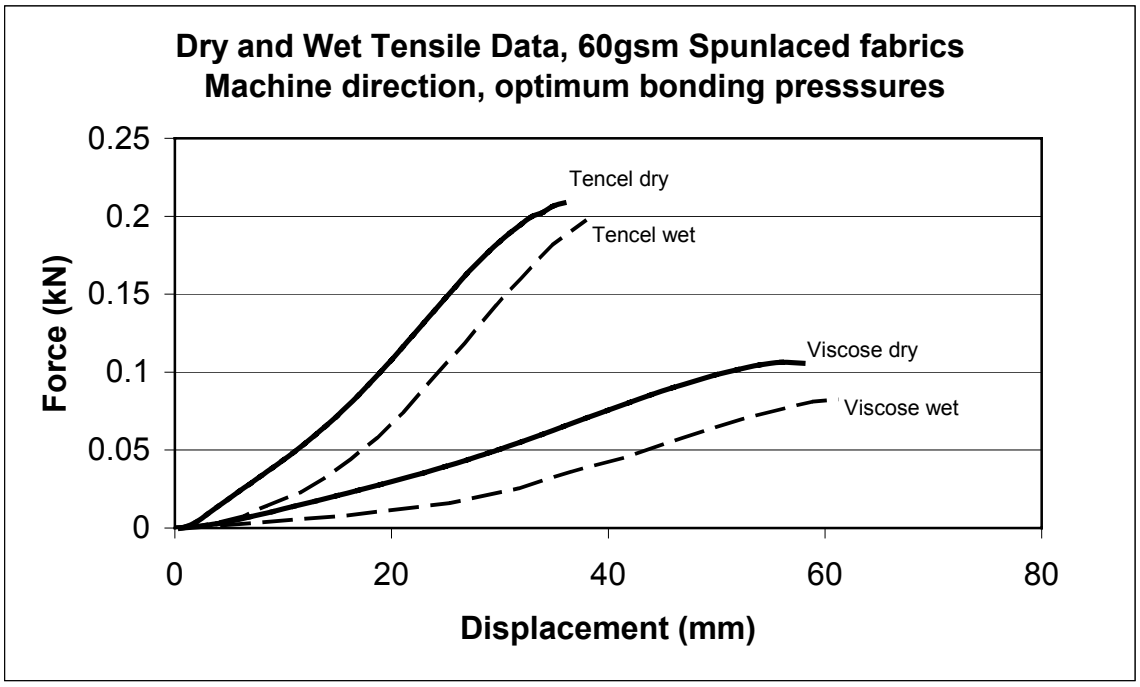

Figure 3. Dry & Wet Spunlaced Fabric Strengths for Viscose and TENCEL®

NEEDLEPUNCHING

In needlepunching applications where bonding is achieved through the use of mechanical needling of the fibre web, very efficient bonding is seen with TENCEL®, even with what for this market sector is traditionally perceived as a low decitex product. For example 1.7 decitex TENCEL® is now used routinely in needlepunched nonwovens, whereas the lowest practical decitex limit for viscose rayon is about 3.0 or above. This is achieved without significant fibre breakage and leads to softer, more absorbent structures, which have a unique ability to retain and release fluid. The high wet resiliency of the fibre allows the fabrics to retain bulk in the wet state, leading to superior handling aesthetics and wiping action.

LATEX BONDING

In latex bonding, fabrics are created by bonding the webs with latex emulsions, starch sizes, or other adhesives. This is usually followed by a curing step. For this technology, which is still used extensively to produce dry wipes, the high fabric strength produced from TENCEL® enables binder levels to be reduced by as much as 50%. This enhances both fabric absorbency and softness. Binder levels can be reduced to such an extent that the flushability and biodegradability of the final fabric can be significantly enhanced. These are useful features in today's environmentally aware market place. If binder levels are maintained, then very strong and stable fabrics can be obtained with good abrasion resistance and hence increased product lifetime.

AIR-LAYING

Air laying technology requires very different fibres to those used for the main staple processing routes described above. Here fibre webs are created using air dispersion, usually followed by deposition on a suction belt. For optimum air-laying, low cohesion and static free fibre surfaces are advisable, combined with a short fibre cut length. The inherently open nature of a tow washed and mechanically crimped fibre like TENCEL® makes it more suitable for web formation in an air stream than many other cellulosic fibres. High fibre crimp can also be employed to enhance this performance and improve filament dispersion within a matrix of other fibre types. Substituting for modest percentages of normal fluff pulp with TENCEL® can significantly increase the softness, strength, bulk and absorbency of air-laid fabrics. The longer TENCEL® fibres support the pulp matrix leading to higher tear and burst resistance, and better fluid transport because pores in the structure collapse less easily.

WET-LAYING

An alternative method of dispersing short fibres to form a fabric is to use water. This is the basis for wet-laid nonwoven manufacture or traditional papermaking. When wet-laying to form a fabric the high modulus of TENCEL® allows relatively long length fibres to be processed without dispersion problems. This results in low defect webs with excellent tear and burst strength and good dimensional stability. In addition, the unique fibrillar, crystalline structure of TENCEL® can be broken down through mechanical wet abrasion, for example at the beating stage of a traditional papermaking process. This can be very readily achieved because the fibre swells so much radially when wet. The wet abrasion generates submicron diameter fibrils, which are retained within the fibre matrix, creating a micro-porous network, which is ideal for fine filtration.

FINISHED PRODUCT BENEFITS

Much of the impressive growth in the use of TENCEL® in nonwovens has coincided with the substantial growth in, and segmentation of the consumer and industrial wipes sectors.

TENCEL® is the ideal fibre for many categories of wiping. It is free of sulphurous odors because the manufacturing process is effectively a simple dissolution and regeneration process. This permits the production of fragrance free wet wiping products, where the liberation of unpleasant sulphurous odors has been a perennial problem when using viscose rayon. Also for many wet-wiping applications, the use of TENCEL® means the absorbent properties of the wipe can be engineered to ensure that gravitational drainage in tubs and canisters can be reduced to a minimum and yet all the wiping layers are equally wetted out. Because less liquid is trapped within the fibre structure, compared again to viscose, the volume of expensive lotion required for an effective wiping performance can be significantly reduced.

As already mentioned, TENCEL® produces low lint fabrics because of its strength and durability as a fibre and the efficiency with which it can be bonded. This low linting feature is mandatory for many critical-task wiping applications. This includes clean-room use, surface preparation in

the automotive, aerospace and printing industries and many medical wipes, gauzes and swabs.

Chemical purity and a good regulatory history and compliance record commend the fibre's use in personal hygiene and hospital products. TENCEL® has excellent wet resilience. This gives improved aesthetics and efficient skin exfoliation in cosmetic wipes.

High fabric strength can extend the life of many wiping products. In particular, TENCEL® wipes stand up well to overnight bleaching, which is common in the food service industry. Also, as bonding levels can sometimes be reduced to take advantage of the filament strength, fabric flushability and biodegradability can be enhanced making disposal cheaper and easier.

TENCEL® is ideal for food contact use in hot oil and beverage filtration, as a result of very uniform fabrics and good regulatory clearance. Papers containing fibrillated TENCEL® are an economic alternative to other sources of nanofibres in high efficiency air and liquid filtration.

TENCEL® contributes strength, stability and uniformity to synthetic leather substrates.

CONCLUSION

The case for specifying TENCEL® fibre in nonwoven products is compelling. Priced cost effectively, with unique attributes and excellent environmental credentials, its future in absorbent nonwoven products is assured.

Lenzinger Berichte, 82 (2003) 43-48

FLUOROPOLYMER FIBRES MEET NONWOVEN TECHNOLOGY

Adalbert Wimmer, Jean-Luc Cialdini, D.I. Volker Stumpf

Lenzing Plastics GmbH & Co KG,
4860 Lenzing, Austria
phone: ++43 7672 701 2279, fax: ++43 7672 918 2279, email: v.stumpf@lenzing-plastics.com

Abstract

Lenzing Plastics GmbH & Co KG will introduce their very unique products made out of polytetrafluoroethylene and some of the features of the products made of them.
PTFE has certain chemical, as well as physical properties. These are temperature- and chemical resistance, high insulation and low friction. Based on these properties, such products will withstand harsh filtration conditions and do a very good job in a lot of other applications.
These features are the reason that PTFE-filtermedia are used mostly in hot-gas-filtration of waste-incinerators, power plants and other industrial incinerators.
Last but not least, the absolutely irregular cross-section of the staple-fibres furthermore contribute to an outstanding filtration efficiency.
It was also a question of interest to determine the removal efficiency for various particle sizes, hence this topic will become more evident in future emission regulations. Three standard needle-felts, two of them with an additional surface treatment (one coated, one spunlaced) were tested for their filtration parameters at the STFI in Chemnitz on their filter test rig. A report regarding the results of changing cycle times, differential pressure, dust emission and removal efficiency by particle size has been issued.

I. What is PTFE?

1. Chemical structure:

PTFE (polytetrafluoroethylene = $(C_2F_4)_n$) is a plastic material that was discovered by Dr. Roy Plunkett at the DuPont research laboratories on April 6, 1938. Dr. Plunkett was working with gases related to Freon refrigerants when upon checking a frozen, compressed sample of tetrafluoroethylene, he and his associates discovered that the sample had polymerized spontaneously into a white, waxy solid powder. PTFE was first marketed under the DuPont's Trademark Teflon® [1)] in 1945.

The molecular weight of PTFE can exceed 9,000,000 [2)] making it one of the largest molecules known. It is made up of linear chains of molecules (figure 1) which boast excellent chemical inertness and thermo-stability.

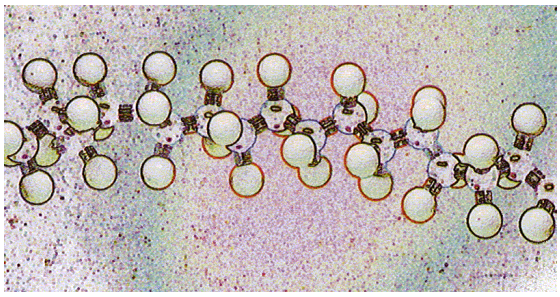

Figure 1: PTFE molecule

In view of the special properties of PTFE, it is impossible to use methods commonly employed in fibre manufacturing. There are only a few companies that are able to process PTFE into fibres and filaments worldwide.

2. Physical properties:

a Chemical resistance:
The strength of the carbon bond and the fact that this is almost entirely covered by fluorine atoms means that PTFE is

almost entirely chemically inert (figure 2). It does, however, swell when exposed to fluorinated hydrocarbons and will be destroyed by molten alkali metals [1].

It is resistant against acids, alkalines and solvents even at high temperatures. This excellent chemical resistance made PTFE to be used in applications such as hot gas filtration for incinerators where no other materials have been suitable for it.

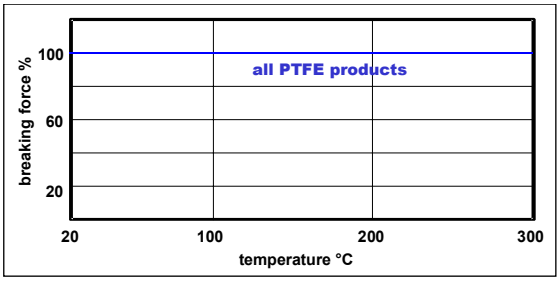

Figure 2: Chemical resistance of PTFE against acids, alkaline, humidity

b Temperature resistance:
This polymer has a crystallite melting point of 327 °C and can be exposed from –200 °C up to sustained high temperatures of 260 °C and for a short period of time up to 300 °C [2) 3)]. This properties make it the ideal filter-media for harsh and hot environments.

c Flammability:
Self-fire extension is crucial when dealing with chemical environment and high temperature. PTFE has once more proved its outstanding performance with its limiting oxygen index (LOI) of 95% (figure 3). This means, it requires 95% of oxygen to start igniting and support of flame.

d Atmospheric aging:
It is 100% UV stable and non aging. [1]

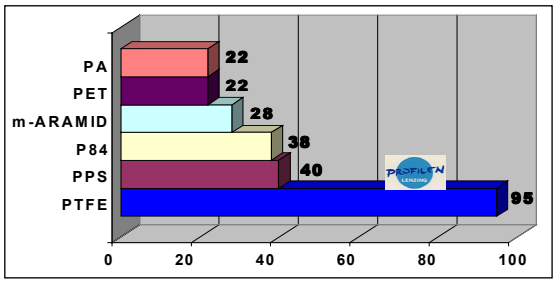

Figure 3: Limiting oxygen index of different fibres

e Low friction and excellent dust-cake-release:
PTFE with his lowest coefficient of friction [1] of all solid materials makes it ideal for the release of dust contamination on filters and in numerous of technical applications (e.g. slide bearings).

f Water repellency and washability:
PTFE does not absorb water and it is easily washed even at high temperatures and with strong detergents. Its surface rejects water, dirt and other contaminants, hence it is an outstanding stain proof material.

3. "Lenzing PROFILEN"® [4)] PTFE fibres cross-section and titre distribution:

"Lenzing PROFILEN"® fibres have an irregular cross-section (figure 4) and as a result not an uniform titre. They have a titre distribution as shown in figure 5. This irregularity gives, contrary to the fibres with a round cross section – made by the matrix spinning process - a more dens filter-media. The micro-denier fibres fill into the voids, resulting in a denser felt and a higher filtration efficiency. This high amount of small denier fibres increases the surface to volume ratio.

Commonly used weights of needle-felts are in between 700 and 900 g/m².

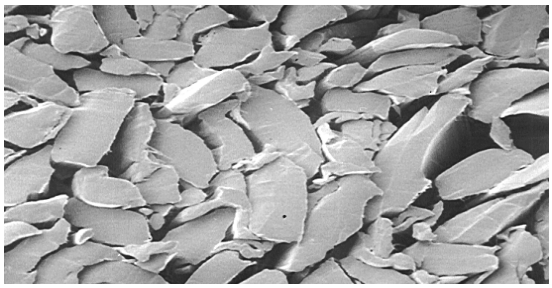

Figure 4: Cross section of "Lenzing PROFILEN"® fibres

PTFE-filter-media made from matrix-spun fibres in comparison to felts made of "Lenzing PROFILEN"® fibres are much lighter, but offer the same level of performance.

Lenzing-Plastics GmbH & CoKG started marketing and selling this unique type of staple-fibre in the late nineties (90's).

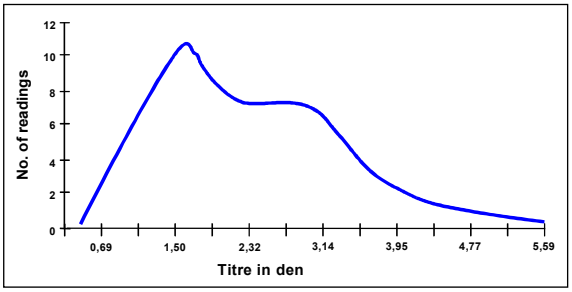

Figure 5: Typical titre distribution of "Lenzing PROFILEN"® fibres

The properties and features of our products, which guarantee an outstanding performance of the filter-media, contributed to a big growth of LPG, which finally become one of the major and leading PTFE-yarn and fibre manufacturer in the world.

II. Filtration Test

1. Objectives of the filtration tests:

Objectives of this study are to verify the benefits of processes to modify the surface of industrial standardized needle-felts.

Various surface structures will directly effect the filtration efficiency or in consideration of it, the needle-felt design (e.g. weight/m²) will get influenced subsequently.
Furthermore it might be worth to investigate, if these benefits of surface modification can be used for applications such as liners for safety and protective clothing.

2. Options available to achieve our objectives:

a Heavy weight needlefelts: Adding more fiber per square meter will improve the filtration efficiency of the filter media but will also cost more. We have decided not to include a heavier needle-felt in the test. We decided to do the test with a felt of about 750 g/m².

b Surface coating based on fluoropolymers: Existing products are on the market. The purpose is to improve filtration efficiency and the release of the dust cake. Such felts are established in filtration and therefore we included this felt in our test.

c Hydro-dynamic surface treatment: Spunlacing is not a new technology but using it for surface modification of needle felts might be a future break through of enhancing properties.

3. Test rig information:

The tests have been carried out by the STFI (Sächsisches Textilforschungsinstitiut e.V., Chemnitz, Germany) using the following filtration test equipment:

- Filter Test Rig Type „AFC 130", Topas GmbH, Germany
- Test in accordance of VDI 3926
- Type of test dust: Plural SB

4. Comparison of 3 constructions of needle-felts:

The following three samples have been used:

- **Standard needle felt:**
  Air permeability: 299 l/m2/s
  Weight approx. 750 g/m²
- **Same felt coated:**
  Air permeability: 200 l/m2/s
  Coating approx. 30 g/m²
- **Same standard felt spunlaced:**
  Air permeability: 126 l/m2/s
  The spunlacing was conducted by STFI using an "Aqua-Jet" pilot plant made by Fleissner/Germany [5].

III. Test results

1. Cycle time:

Figure 6 shows the time intervals between each cleaning cycle. When reaching the differential pressure due to dust cake build up, the filter medias get cleaned automatically by pulsing compressed air (jet pulse cleaning).

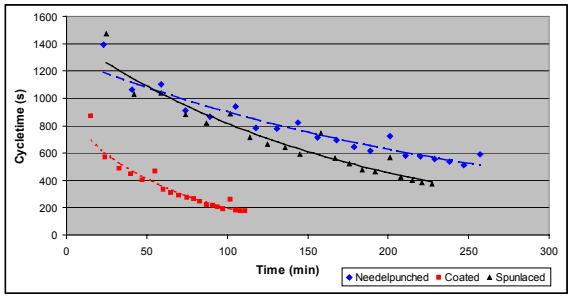

Figure 6: Comparison of cycle time

Standard felt and the hydro-dynamic treated felt performed better than the coated felt as far as time cycle between cycles. This is due to less differential pressure and to less blinding of the media. The dust that cannot get properly removed during the cleaning cycle blocks off small openings in the felt and creates blinding over a period of time.

2. Differential pressure:

The differential pressure is the static pressure increase in between the raw gas side and the clean gas side of the filter unit. This pressure change is caused by the gradual build up of the dust cake which restricts the air flow through the filter media.

In figure 7 we can see, that the differential pressure of the spunlaced felt is much better in comparison to the coated one. The difference to the standard needle felt is naturally, due to a more compact fibre structure of the spunlaced felt, hence the air-permeability is different.

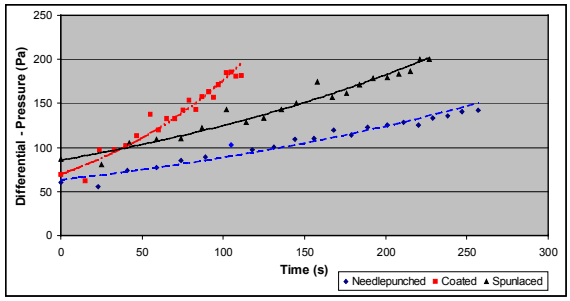

Figure 7: Comparison of differential pressure

3. Dust emission:

This is the total amount of dust which still could pass through the filter system. The value is determined gravimetrically and expressed in mg/m³. The results are showing reduced dust-emission levels in comparison to the standard needle-felt and the coated one.

Explanation for this improvement (see figure 8) is the smooth, more closed surface-structure of the spunlaced felt. A standard needle-felt, which normally works by the basic principles of depth filtration. Adding the spunlacing process creates a surface oriented filtration due to its smoother surface.

4. Removal efficiency by particle size:

This test provides data of the filtration efficiency in regard of the sizes of the particles. This figure is expressed in percentage of particle-sizes in micron which will get captured.

The smaller the particles in size, the more difficult to filter!

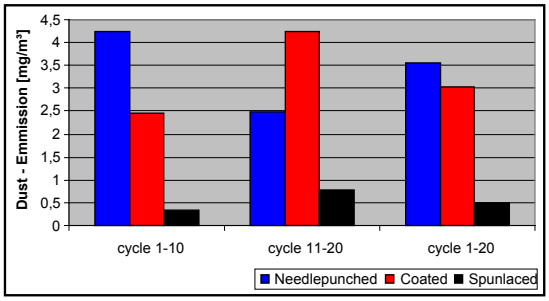

Figure 8: Comparison of dust emission

We see in figure 9, that the spunlaced felt is removing small particles (sub micron range) much better than the standard needle felt and has a better performance than the coated felt. Already at a particle size of around 2.5 micron and bigger all felts achieved removal efficiencies of 100%.

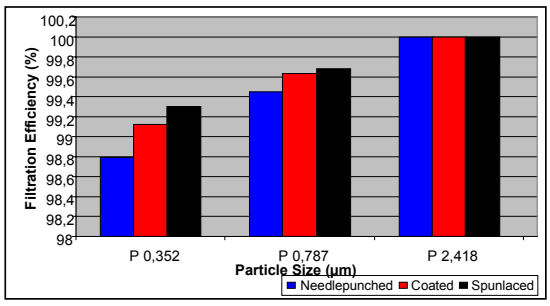

Figure 9: Comparison of removal efficiency by particle size

IV. Conclusion

Spunlaced materials are already dominating many markets for nonwovens, but not the filtration market. Based on the results of this study, the filtration market can also benefit from this technology.

Based on the very dense spunlaced products in combination with a very smooth surface, this technology provides a better performance than needle punched and even coated felts.

The dust emission levels are already very low (down 0.5 mg/m³) but more research might improve emission levels in the future.

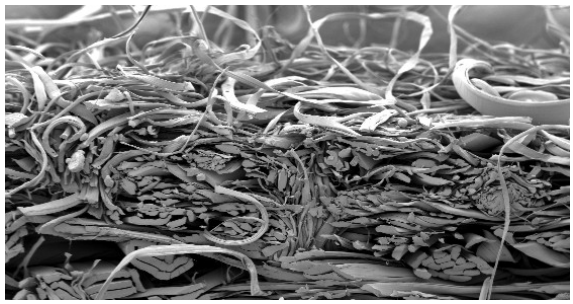

Figure 10: SEM photograph from a cross-section of the standard needle-felt, showing a hairy surface

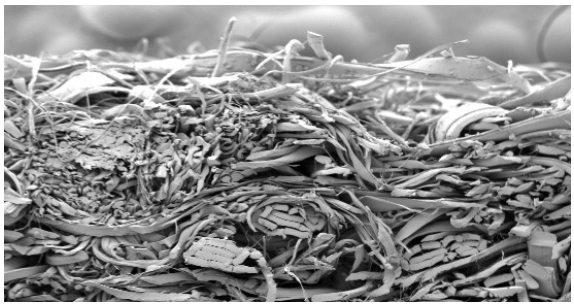

Figure 11: SEM photograph from a cross-section of the same standard needle-felt, but spunlaced, showing a closed, much smoother surface

Also the removal efficiency by particle size looks more than promising. Up to 99.8 % of submicron particles are already captured.

These results might lead to an optimisation of processing nonwovens and will contribute either a better filtration performace or to a reduction of the felt weight, hence reducing the costs.

Also other applications might be more feasible in the near future, e.g. breathable, water repellent and extreme light weight PTFE-liners for garments like safety and protective clothing to enhance functionality and comfort.

a Hydro-dynamic treatment shows a benefit in filtration efficiency of sub-micron particles without the negative effect of loss of pressure drop and air permeability.

b This surface treatment could also be used to lower the weight of the felt. This will create

a filter media as good, or slightly better than a standard felt but cheaper than standard felt.

c Based on these test results, it is unnecessary to coat a PTFE felt with a fluoropolymer coating. It was not beneficial for the pressure drop and did not really show an improvement as far as dust emission is concerned.

d Lastly, the smooth and closed surface of the hydro-dynamic treatment could be applied in the garment industry to make light weight, breathable and water repellent liners. Tests are already initiated and the results will follow soon.

[1] Teflon® registered trademark of DuPont
[2] Hans Dominghaus, Die Kunststoffe und ihre Eigenschaften, ISBN 3-18-400738-3
[3] Hoechst Plastics, Hostaflon Information, H KR 103 E-8124/022, Dec. 1984
[4] "Lenzing PROFILEN"® registered trademark of Lenzing AG
[5] http://www.fleissner.de/aj_e.htm

Lenzinger Berichte, 82 (2003) 49-57

Protection of Lyocell Fibres against Fibrillation: Mode of Action of the Cross-linking Agent 2,4-Dichloro-6-(β-Sulphatoethylsulphonyl) anilino-s-Triazine (Cibatex AE 4425).

A.H.M. Renfrew and D.A.S. Phillips

Christian Doppler Laboratory for Textile & Fibre Chemistry in Cellulosics, UMIST, P O Box 88, Manchester M60 1QD, UK.
Phone: +44 (0) 161 200 4162 / 4148 Fax: +44 (0) 161 200 4589
Email: a.renfrew-2@umist.ac.uk, duncan.phillips@umist.ac.uk

ABSTRACT

2,4-Dichloro–6-(β-sulphatoethylsulphonyl) aniline-s-triazine (Cibatex AE4425) was used as a cross-linking agent to improve the wet abrasion resistance of Lyocell fibres. The agent, which exhibits poor water solubility, was sold as an aqueous dispersion. During application to Lyocell in the presence of alkali, the agent entered the solution phase before reaction with the fibres. HPLC analysis and solution studies support the view that the two electrophilic species taking part in the cross-linking reaction are vinylsulphone plus one of the chlorine atoms of the dichlorotriazine (DCT) residue and that preliminary hydrolysis of one of the chlorine atoms is not the cause of the observed solubility changes.

Keywords: *Cibatex AE 4425, cross-linking, dichlorotriazine, vinylsulphone*

INTRODUCTION

Abrasion of cellulosic fibres, particularly in the wet state, gives rise to fibrillation, i.e. the formation of micro fibrils on the fibre surface. While this phenomenon is observed for both natural and synthetic cellulosic fibres, it affects Lyocell to a greater degree than cotton, flax and viscose. Although fibrillation can be used to create special fabric aesthetics for Lyocell, e.g. peach skin effects, for many outlets it has a negative impact on the appearance, surface properties and structure of a garment [1,2,3].

The source of this problem lies with Lyocell's high wet swelling characteristics [4] (approximately 65% increase in volume) and weak lateral links between the crystallites [5], which render it susceptible to mechanical abrasion.

It has been shown that Lyocell's wet abrasion resistance can be improved by the application of cross-linking agents either to the never-dried fibre [6] or to textile substrates [7]. A few cross-linking agents have been used commercially for application to the dried fibre, usually in fabric form prior to dyeing. One such agent is 2,4-dichloro–6-(β-sulphato-ethylsulphonyl)anilino-s-triazine (1) (Cibatex AE 4425 ex Ciba; now withdrawn). A synthesis of compound (1) has been described by Lewis [8].

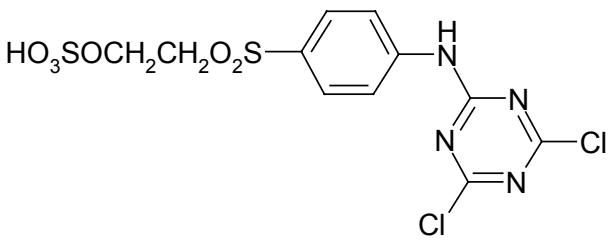

1

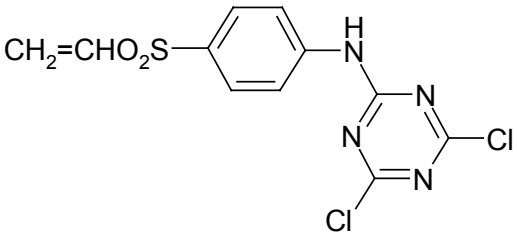

2

Compound (1) exhibits very poor water solubility and was sold and applied as an aqueous dispersion. During its application the suspension was added to an aqueous bath at 60°C, containing fabric and Glauber's salt followed by the addition of alkali to give an approximate pH of 11. These changes resulted in the dispersion of compound (1) forming a clear solution. However, it is well known [9] that the application of both heat and alkali to a compound containing a sulphatoethylsulphone group will result in β-elimination of the sulphato group. Such a process would result in the loss of the water solubilising group of compound (1) and convert the agent to the vinylsulphone form (2). A priori, this would be expected to be even less soluble than the parent compound.

Despite the loss of its only anionic group in alkaline medium, compound (1) dissolves completely during application. This work was undertaken to rationalise the technical success and mode of action of 2,4-dichloro–6-(β-sulphatoethylsulphonyl)anilino-s-triazine (1) as a cross-linking agent.

EXPERIMENTAL

HPLC Method A

HPLC was performed with a Hewlett Packard 1050 series fitted with a quaternary pump and diode array detector. The column was a Hypersil ODS, 250 x 4 mm, 5µm; solvent A, water with 2 g/l tetrabutylammonium chloride; solvent B, acetonitrile with 2 g/l tetrabutylammonium chloride; flow rate 1.2 mL/min; Temperature 40°C; injection volume 10 µl; wavelength 254nm. The following gradient programme was used:

	min.	% A	% B
	0	65	35
	1	65	35
	20	45	55
	25	20	80
	26	10	90
	30	65	35
Stop time	35		

HPLC Method B

HPLC was performed with a Hewlett Packard 1100 series fitted with a quaternary pump.
The column was a 10 cm Purospher RP-18 (5µm) packing and a LiChrocart 125-4 HPLC column cartridge; solvent A; acetonitrile; solvent B, water with 0.25% dicyclohexyl-ammonium phosphate; flow rate 2ml/min; temperature 40oC; injection volume 5µl; samples were analysed using a diode array detector at a wavelength of 450 nm (BW 400nm). The following gradient programme was used:

	min.	% A	% B
	0	30	70
	5	50	50
	6	40	60
	7	30	70
Stop time	7		

Retention times (t_R) are in minutes.

Mass spectra were recorded with a Micromass Instruments LCT orthogonal time-of-flight mass spectrometer fitted with a Z-Spray electrospray ion source operating in negative mode at 3Kv needle potential. Nitrogen was used as a drying and sheath gas. Data was stored in the continuum mode on a Micromass Instruments MassLynx data station utilizing Version 3.5 software pack. Infusion was at a rate of 20µl/minute with a Harvard Instruments syringe pump utilized for sample introduction. Mixed phosphate buffer comprised potassium dihydrogen phosphate (2 parts) and disodium hydrogen phosphate (1 part).

Reaction of 2,4-dichloro–6-(β-sulphatoethylsulphonyl)anilino-s-triazine (1) with sodium hydroxide solution

1. <u>At room temperature</u>

A dispersion of commercially available 2,4-dichloro–6-(β-sulphatoethyl-sulphonyl-anilino-s-triazine (1) (90 g/l) was stirred in a beaker. Starting at pH 4.6, sodium hydroxide solution (1M) was added dropwise. After initial precipitation of a white solid, the suspension changed to an opalescent solution at pH 12.6 and a clear stable solution at pH 12.8-12.9.

(b) **<u>At 60°C</u>**

A suspension of laboratory prepared 2,4-dichloro–6-(β-sulphatoethylsulphonyl)anilino-s-triazine [8] (1) (2.5 g) in water (200 mL) was stirred at pH 6.8 at room temperature then heated to 50°C . Sodium hydroxide solution (2M) was added dropwise, with heating to give initially a white precipitate, then an opalescent solution and finally a clear solution at pH 12.9 and 60°C. The solution was stirred for 2 minutes at 60°C before the addition of dilute hydrochloric acid solution (2M) to give a pH of 6.8, resulting in the formation of a white precipitate. Mixed phosphate buffer (1 g) and sodium chloride (20 g) were added and the white solid that formed was filtered off. To the wet solid was added mixed phosphate buffer (1 g) and resulting solid dried in an electric oven at 65°C.

HPLC (Method B) showed a complex mixture with no starting material (tR 2.6) and a major peak at tR 4.13.

The solid gave a strong and instantaneous yellow coloration on treatment with pyridine and sodium hydroxide, indicative of the presence of a dichlorotriazinyl group [10].

Reaction of 2,4-dichloro–6-(β-sulphatoethylsulphonyl)anilino-s-triazine (1) with sodium carbonate solution

A small sample of laboratory prepared [8] 2,4-dichloro–6-(β-sulphatoethylsulphonyl)anilino-s-triazine (1) was placed in a HPLC sample vial and dissolved in aqueous acetonitrile. Five drops of sodium carbonate solution (2M) were added and the sample analysed by HPLC (Method B; see Table 1)

Peak	Retention Time	% Area	Assignment
1	0.50	2.27	-
2	0.68	5.85	-
3	1.92	4.75	-
4	2.53	12.50	Cibatex AE 4425
5	4.03	74.80	Compound (2)

Table 1

Synthesis of 4,6-bis-(p-β-sulphatoethylsulphonyl)anilino-1,3,5-triazin-2(1H)-one (9)

Cyanuric chloride (10g; 98%; 0.053 mol), dissolved in acetone (100mL), was added to water (200 mL) to give a white suspension. The suspension was stirred at 20°C, pH 7-7.4 for 4 hours to give a clear solution which was screened and allowed to stand overnight. The solution was then cooled to 1°C, and a pH 7.1, before the portion wise addition of solid p-aminophenyl-β-sulphatoethylsulphone (PABSES; 15.6g, 95.5%; 0.053 mol.), keeping the temperature at 1-2°C and pH at 3.0-4.5. The reaction, which was followed by HPLC (Method B), initially indicated the presence of only one new peak, at tR 1.20 (dichlorohydroxytriazine, tR 0.90, and PABSES, tR 0.80). After 3 hours, and

consumption of all the PABSES, HPLC analysis showed the presence of two peaks at tR 0.90 and 1.20, approximately in equal amounts.

A further addition of solid PABSES (15.6 g) was made at 3°C, pH 4-4.5. The reaction mixture was allowed to stir over the weekend to give, by HPLC analysis, 93% product and 7% PABSES and a pH of 3.4. Potassium chloride (10% w/v) was added portion wise to give a grey solid which was isolated by filtration, washed with potassium chloride solution (15%) and dried in an electric oven at 65°C for one week to give the product (42.2 g). HPLC analysis (Method B) gave a peak at tR 1.12 (100%) and mass spectral analysis showed ions at m/z 654 (M - H)- (78%), 574 (M-H-SO3)- (5). There was also a doubly charged ion at 327 (M-2H)2- (100).

Attempted synthesis of 6-chloro-4-(p-β-sulphatoethylsulphonyl)anilino-1,3,5-triazin-2(1H)-one (8).

Cyanuric chloride (9.3 g; 99%; 0.05 mol) was dissolved in acetone (100 mL) and the solution poured into water (300 mL) containing mixed phosphate buffer (2 g). The suspension was stirred at 25°C and a pH of 6-7 maintained by the addition of 2M sodium hydroxide solution. After 1 hour a faintly turbid solution was given which was filtered through filter aid to give a clear solution. The solution was allowed to stand for a further 2 hours at pH 6-7, then mixed phosphate buffer (5 g) was added.

ρ-Aminophenyl-β- sulphatoethylsulphone (PABSES; 14.7; 95.5%; 0.05 mol) was suspended in water (200 mL) and mixed phosphate buffer (1 g) was added. The suspension was cooled to 10ºC and 2M sodium hydroxide added with stirring to give pH 3. Finally 2M sodium carbonate solution was added to give pH 5.6, and a brown solution, at a temperature of 13 ºC.

The PABSES solution was added to the solution of sodium dichlorohydroxytriazine (NHDT) and heating commenced until a temperature of 75-80ºC was reached while maintaining the pH at 6.4-6.5 with 2M sodium carbonate solution. The reaction was very slow, as evidenced by HPLC and a falling pH.

Heating was maintained at 79-80ºC for 3 hours. During this period the reaction solution became cloudy and HPLC showed a main peak (approx. 50%) at tR 1.03 (method B) but also the build up of impurities. The reaction was stopped and allowed to stand overnight. Filtration of the white solid (4.8 g) gave a gross mixture containing PABSES, NHDT, a new band at tR 1.03, bis-condensation and six minor bands at higher tR. A pure sample of the desired material was not obtained by selective salting of the filtrates.

Results and Discussion

A prerequisite for effective cross-linking of Lyocell with any agent is good substantivity for the fibre. In turn, substantivity can only be achieved through a solution state. Accordingly, the anticipated loss of solubility of compound (1), by elimination of the water solubilising sulphato group seemed to run counter to expectations for good solubility and good substantivity. One possible explanation for its mode of action is that, following the elimination reaction to the corresponding vinylsulphone (2), the more reactive dichlorotriazinyl group hydrolyses to the potentially more alkali soluble chlorohydroxytriazine, (3; Scheme 1). Chlorohydroxytriazines are tautomeric and depending on pH compound (3) can exist also as 4-chloro-6-(p-vinylsulphonyl)anilino-1, 3, 5-triazin-2(1H)-one.

This potentially more soluble derivative (3) might then be regarded as the effective cross-linking agent.

Chlorohydroxytriazines are weakly acidic and readily form sodium salts, e.g. compound (4) exists as the anion in neutral solution and 2-(N-methylpyrrol-2-yl)-4-chloro-6-hydroxytriazine (5) has a pKa of 5.2 [11].

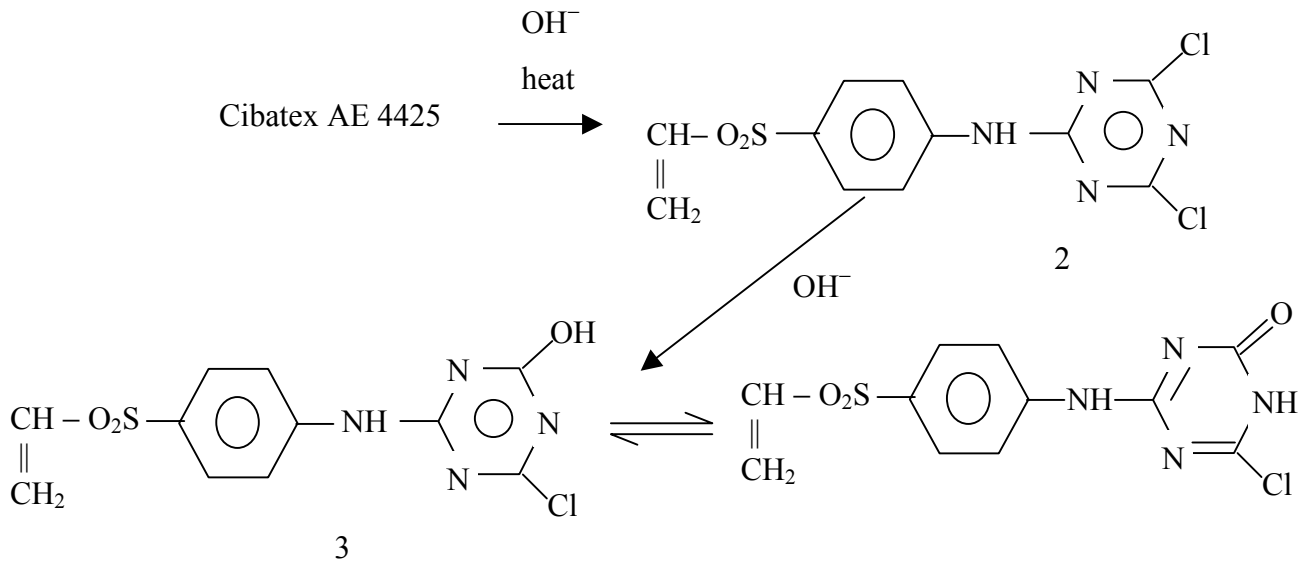

Scheme 1

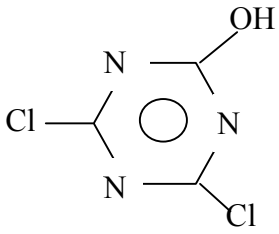

4

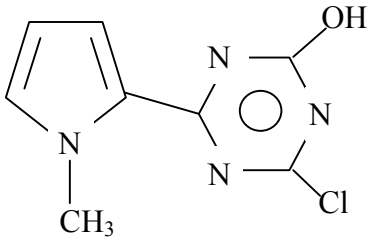

5

While the hydroxyl group on the triazine ring in structure (3) would be expected to improve prospects for alkali solubility, it would also have a deactivating effect on the remaining chlorine atom on the triazine ring. Indeed dyes of general structure (6; R = a chromophore residue) do not readily react with cotton in the presence of alkali. On the other hand dichlorohydroxytriazine (4) is an effective cross-linking agent for Lyocell in the presence of alkali [12]. However, in this case the mono reacted species (7), containing an alkoxy substituent attached to the triazine ring, is more susceptible to nucleophilic attack by cellulosate anions than compounds of type (7; R = a chromophore residue).

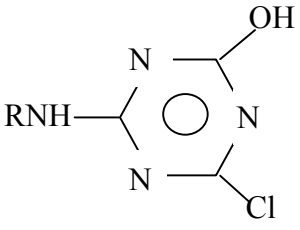

6

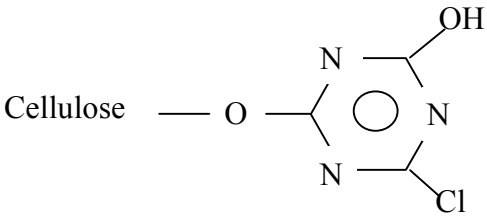

7

In an attempt to resolve the efficiency of compound (3) (or its masked sulphato precursor (8) as a cross-linking agent for Lyocell, its synthesis via dichlorohydroxytriazine was attempted (see Scheme 2).

Cyanuric chloride was initially converted to its monohydroxy derivative (4), which, in turn, was reacted with ρ-aminophenyl-β-sulphatoethylsulphone (PABSES). When this reaction was conducted at pH 3-4.5 and at 0-2ºC, it was not possible to isolate, nor indeed detect, a stepwise substitution of the two remaining chlorine atoms and the product was the bis-arylaminotriazine (9). This is in keeping with the previously observed [11] pH dependency of the relative rates of displacement of the first and second chlorine atoms of 2-substituted dichloro-s-triazines. In acidic media k2 > k1 (Scheme 3).

In an attempt to reduce the role played by protonation, this reaction was run at pH 6.4-6.5 (a greater pH was desirable but could not be used for fear of eliminating the sulphato group).

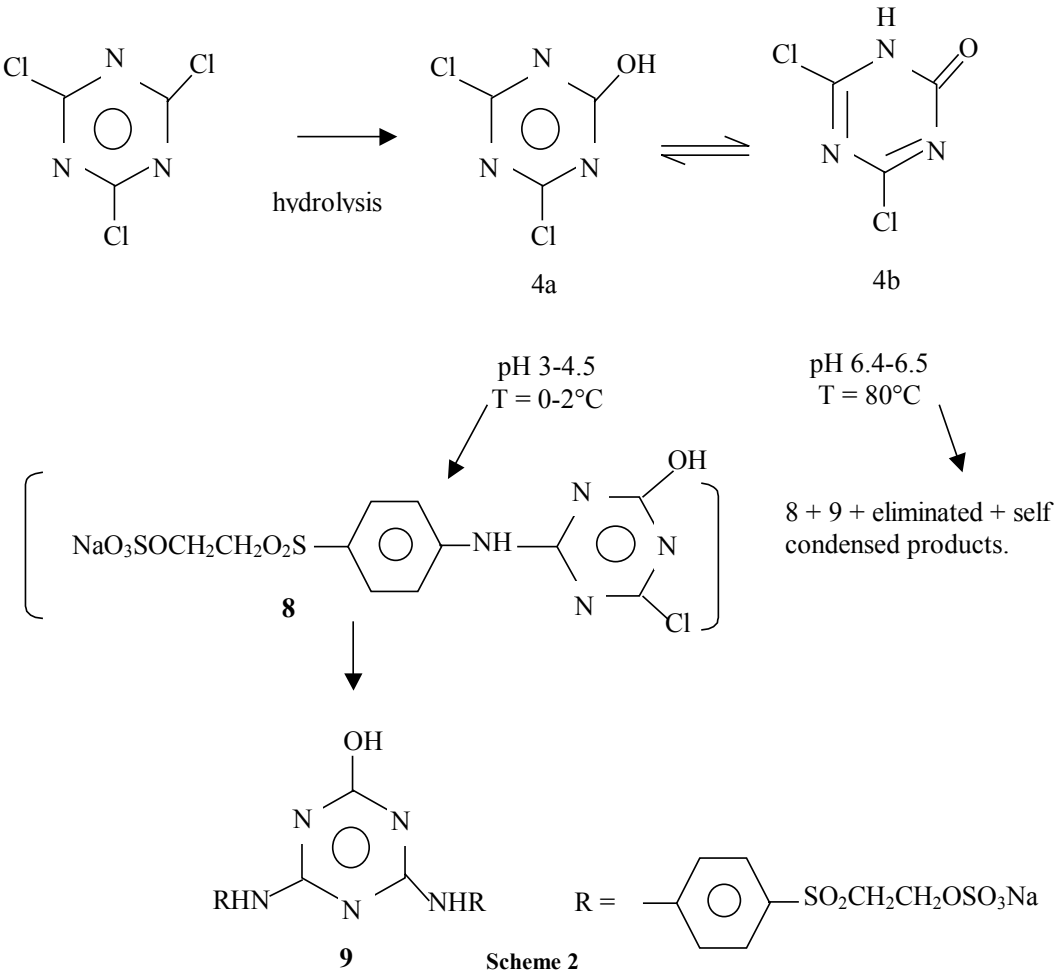

Scheme 2

However under these conditions relative high temperatures were necessary (80ºC) to induce the reaction to take place. In this case a stepwise substitution appeared to occur (see experimental) but a gross mixture resulted and the desired product could not be isolated cleanly.

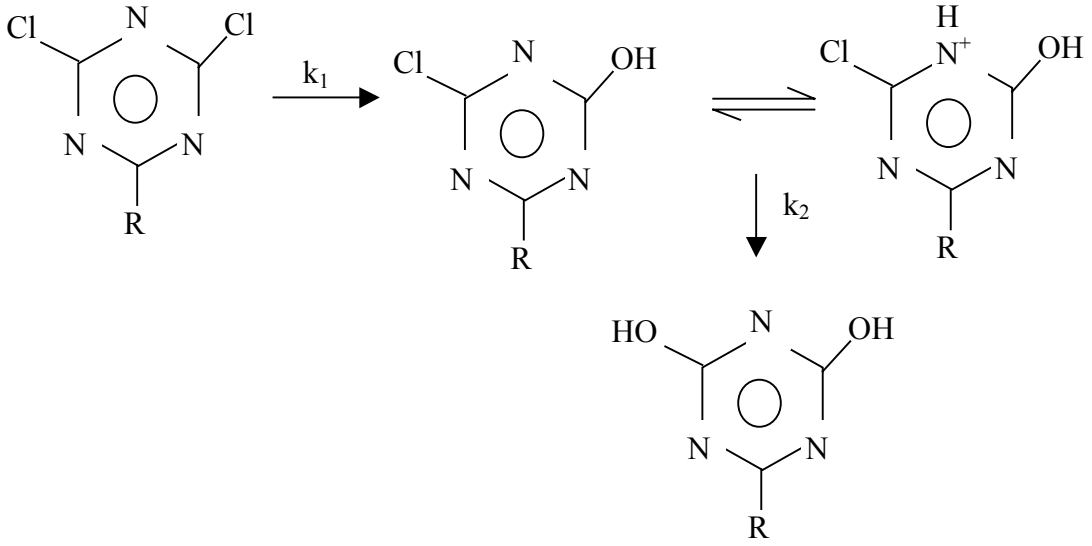

Scheme 3

HPLC studies of 2,4-dichloro–6-(β-sulphatoethylsulphonyl)anilino-s-triazine (1) in alkaline solution also suggested that selective alkaline hydrolysis to yield compound (3) would prove difficult and this approach was not examined. Addition of sodium hydroxide solution to a suspension of compound (1) at room temperature initially caused a precipitate to form and this is consistent with elimination of the sulphato group taking place to furnish compound (2). As the pH was increased the solid began to dissolve and a clear solution resulted at pH 12.8 – 12.9. Repeating this procedure at 50-60°C, similarly resulted in a precipitate firstly forming, with a clear solution being produced at pH 12.9. After 2 minutes at 60°C the pH was reduced from 12.9 to 6.8 with dilute hydrochloric acid to give a white solid. HPLC showed this solid to be a complex mixture, with the most abundant component (peak area 27%) exhibiting an tR of 4.13 (Method B). The solid gave a strong and instantaneous yellow coloration with pyridine and caustic soda indicative of the presence of a dichlorotriazinyl group [10].

The assignment of the major peak at tR 4.13 as compound (2) was supported by treatment of compound (1) with a milder alkali. The addition of dilute sodium carbonate solution to a solution of compound (1), at room temperature, in an HPLC sample vial resulted in the immediate formation of a peak at tR 4.03 (Table 1).

It is well documented [9] that β-sulphatoethylsulphones, in alkali media, undergo instantaneous β-elimination to give vinylsulphones. The increase in tR from 2.54 [sulphato compound (1)] to tR 4.03 [vinylsulphone compound (2)] is entirely consistent with the loss of the anionic group (reverse-phase chromatography).

Further HPLC studies (Method A; Table 2) showed that compound (1), at pH 6-7, exhibited one major band at tR 8.89 (sample No. 1) with minor bands at tR 9.39 and 5.65. However at pH 12, compound (1) formed a clear solution due to the presence of a component with an tR at 9.39 (samples No. 3 and 4). This species was also present in sample No. 1, as a minor band, which is consistent with some β-elimination having taken place during synthesis or storage of compound (1). However the compound responsible for this band at tR 9.39 was insoluble in water at pH 6-7, as it was completely removed by filtration through a 0.45 µm filter before analysis (sample No. 2). This also supports the view that the alkali soluble form of the cross-linking agent (1) is the anion derived from compound (2) and not compound (3), as the latter would exist predominantly as

the sodium salt at pH 6-7 and would be expected to show some water solubility.

Sample No.	pH	Temperature (°C)	Stirring Time(min)	Peak Retention Time
1	6 - 7	60	10	8.89, 9.39 (minor), 5.65 (minor)
2*	6 - 7	60	20	8.89, 5.54 (minor)
3	12	RT	< 1	9.39, 5.4 (minor), 3.35 (minor)
4	12	RT	2	9.39, 5.4 (minor), 3.35 (minor

* Sample was passed through a 0.45 μm filter before analysis

Table 2 - The concentration of 2,4-dichloro–6-(β-sulphatoethylsulphonyl)anilino-s-triazine (1) (commercial material) for HPLC studies (Method A) was 10 g/l.

Accordingly, the solubility of compound (1) under alkaline conditions is explained in terms of the abstraction of the weakly acidic hydrogen atom from the arylamino group attached to the dichlorotriazinyl group (Scheme 4), and not as a result of initial formation of a chlorohydroxytriazine derivative.

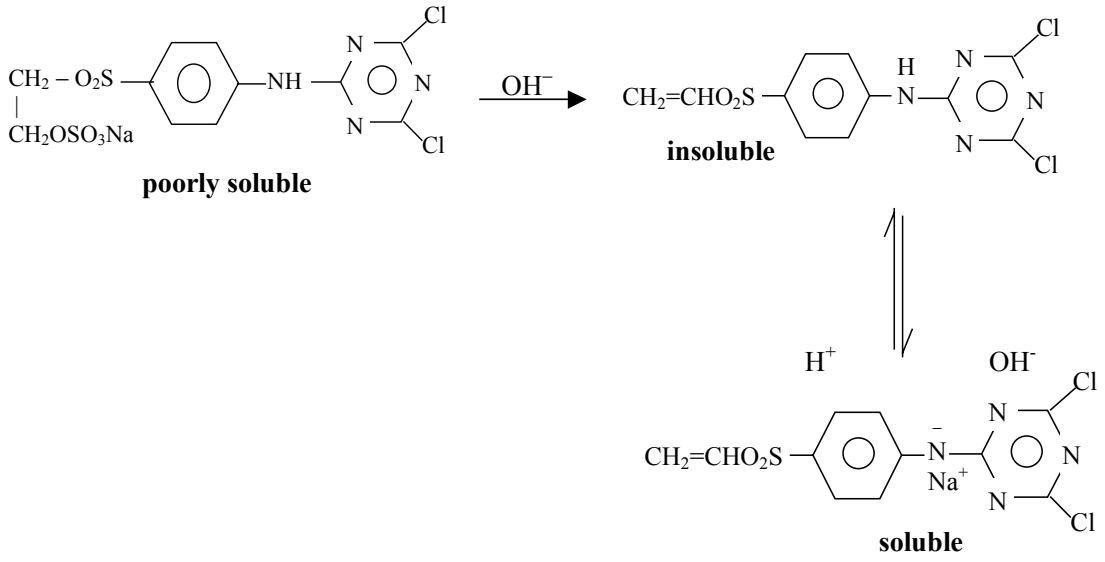

Scheme 4

This scheme is strongly supported by the work of Horrobin and others [13,14], who showed that arylaminodichlorotriazines, devoid of water solubilising groups are soluble in dilute sodium hydroxide solution. That this was due to acidity and not a chemical reaction was confirmed by measurement of the dissociation constants of water soluble derivatives, e.g. dichloro-p-sulphoanilino-s-triazine has a pKa = 10.5 at 25°C. Compound (2), which has a p-sulphonyl group, would be expected to be more acidic. Accordingly, both experimental and literature evidence support the view that the two reactive groups responsible for the cross-linking of Lyocell with Cibatex AE 4425 are vinylsulphone and dichlorotriazine.

CONCLUSION

In alkali medium 2,4-dichloro–6-(β-sulphatoethylsulphonyl)anilino-s-triazine (1) undergoes the expected elimination reaction to give a less water-soluble non-anionic vinylsulphone species (2). HPLC analyses and solution studies support the view that, as the pH is raised, the increased aqueous solubility of the cross-linking agent is the result of deprotonation of the weakly acidic arylaminodichlorotriazinyl group and not the formation of a chlorohydroxytriazine derivative. Accordingly, the effective cross-linking groups are vinylsulphone and dichlorotriazine.

REFERENCES

1. K.P. Mieck, M. Nicolai and A. Nechwatal, Melliand Textilberichte, 5, (1997), 336.
2. M. Nicholai, A. Nechwatal and K.P. Mieck, Melliand Textilberichte, 10, (1999), 848.
3. M. Nicholai, A. Nechwatal and K.P. Mieck, Melliand Textilveredlung, 31(9/10), (1996), 191.
4. 4.K. Brederek, M Gruber, A Ottertbach and Schulz, Textilveredlung, 31 (9/10), 1996, 194.
5. 5.M. Nicolai. A. Nechwatal and K.P. Mieck, Textile Res. J., 66 (9), 1996, 575.
6. 6.Courtaulds Patent, WO 95/28516, 26.10.95.
7. 7.A. Nechwatal, M. Nicholai, K.P. Mieck, B. Heublein, G. Kühne and D. Klemm, Die Angewandte Makromoleculare Chemie, 271, (1999), 84.
8. 8.D.M. Lewis and J. Yao, J.S.D.C., 116, (2000), 285.
9. 9.A. Hunter M Renfrew, Reactive Dyes for Textile Fibres, Society of Dyers and Colourists, (1999), p2.
10. 10.H.P. Burchfield and P.H. Schuldt, J. Agr. Food Chem., 6, 106, 1958.
11. 11.A.F. Cockerill, G.L.O. Davies and D.M. Rackham, J, Chem. Soc., Perkin Trans. 2, (1974), 723.
12. 12.Lenzing AG Patent, WO 99/19555, 22.4.99.
13. 13.S. Horrobin, J. Chem. Soc., 1963, 4130.
14. 14.A.M.H. Renfrew, J.A. Taylor, J.M. Whitmore and A. Williams, J. Chem., Soc., Perkin Trans., 2, 12, (1994).

Lenzinger Berichte, 82 (2003) 58-63

MODIFICATION OF FIBRILLATION BY TEXTILE CHEMICAL PROCESSING

Wangsun Zhang, Satoko Okubayashi and Thomas Bechtold

Christian-Doppler-Laboratory for Chemistry of Cellulosic Fibers and Textiles
Institute of Textile Chemistry and Textile Physics of Leopold-Franzens-University Innsbruck
Höchsterstrasse 73, A-6850 Dornbirn, Austria
Tel: +43(0)5572 28533, Fax: +43 (0) 5572 28629, e-mail: textilchemie@uibk.ac.at

Abstract

Lyocell fibres are known for their high wet strength, silky lustre and strong fibrillation tendency. The tendency of fibres to fibrillate, in particular, opens up a number of possibilities for researchers to modify the textile surface. In textile processing, alkali treatment is an important stage. This paper is a report on a study of the fibrillation tendency in different types of alkali-treated fibres. The effect of alkali type on fibrillation tendency was observed to follow the order: TMAH>LiOH>NaOH>KOH. In a separate set of experiments, fibre samples were first treated with alkali, neutralised and then treated with distilled water. It appears that treatment with NaOH and KOH decreased fibrillation tendency in fibres. Alkali retention values and water retention values of treated fibre samples were also determined. It was also found that softening agents, such as Siligen SIN can also decrease fibrillation tendency. Two different methods were used to determine fibrillation tendency. Furthermore, the effect of drying, at different temperatures, on fibrillation tendency of fibres treated with softening agent was studied. The result shows that drying samples at high temperatures could reduce fibrillation.

Keywords: fibrillation, alkali treatment, softening agent, abrasion test, Lyocell fibre

INTRODUCTION

Lyocell fibre is a new regenerated cellulose fibre produced by a novel route. Compared to viscose, Lyocell is eco-friendly, since it is manufactured by a non-polluting manufacturing process and the fibres are 100% biodegradable by both aerobic and anaerobic processes [9]. Lyocell fibres are widely used in making artificial leather, coating substrates, medical swabs and gauzes, filters bicomoposites, battery separators, durable and disposable clothing. They can also be used to produce high-strength fabrics. Due to its special physical properties, a wide variety of novel effects can be obtained on Lyocell fibres such as peach skin, silk touch and soft denim. Knit goods produced from Lyocell are characterised by a pleasing soft handle and excellent drape. Like cotton, Lyocell exhibits outstanding wear comfort. Fabrics produced from Lyocell fibre are breathable, moisture absorbent and have excellent dimensional stability i.e. virtually no shrinkage occurs in household laundering. Lyocell fibres, alone or in blends, are used widely in apparel and other fashion [1].

Lyocell fibres distinguish themselves from other fibres in the specific property of fibrillation in wet state under impact of external mechanical effects. Although the fibrillation characteristics of Lyocell fibres makes possible the creation of entirely new effects, an appropriate selection of textile chemical processing is necessary to avoid uneven fibrillation on the fibre surface.

During abrasion of wet Lyocell fabrics, only the surface fibres are fibrillated; a process is referred to as “pre-fibrillation” or “primary fibrillation”. Most reports on treatments of Lyocell to reduce pre-fibrillation describe treatments such as dyeing with reactive dyestuffs or treating fabrics with crosslinking

agents [8]. Textile chemical processing of Lyocell fabric and their blends is an important feature for optimising the use of such fabrics for apparels. It is, therefore, essential that conditions for such processes are optimised to minimise fibrillation. (It has been observed that most important stage in chemical processing of different cellulose fibres and blends is response of these fibres to treatments involving alkali at different concentrations [2, 11]. During scouring, mercerisation and dyeing with reactive dyes, sodium hydroxide or sodium carbonate is normally used. It is well known that the fibrillation tendency of Lyocell fibres is related to swelling state [4, 6, 7]. There is little information on the effect of alkali treatment or treatment with softening agents on fibrillation tendency. In view of this, it is necessary to examine the effect of different types of alkali at room temperature on Lyocell fibres. In present study effect of different types of alkali and softening agents on fibrillation tendency have been examined.

Experimental

(1) Materials

Lyocell yarns, Lyocell fibres supplied by Lenzing AG were used for experiments. Lithium hydroxide, sodium hydroxide, potassium hydroxide and tetramethyl-ammonium hydroxide (TMAH, 25% sol.) were AR grade and used without further purification. Siligen SIN and Siligen VN were supplied from BASF AG.

(2) Methods

Pre-t*reatment of fibres with alkalis and softening agen*ts

Lyocell fibre was soaked into alkali solutions of certain concentration for 30 minutes at room temperature. After neutralization with an acetate buffer solution (pH=5) and rinse with hot and cold water, it was dried at 60 °C. Solutions of Siligen SIN and Siligen VN were prepared at concentrations of 1, 2, 5, 10 and 20 g/l. A 0.5 g of fibre was immersed into the Siligen solution for 5 min at ambient temperature and squeezed. The pick-up rate of the solution was about 100 %. Then the sample was dried at 60, 120 and 150°C.

Fibrillation and abrasion test

Method 1: Untreated Lyocell yarn was cut into 24 mm of length and placed in a 250ml metal dye pot with an alkaline solution and 20 (0.5 cm of diameter) ball-bearings [10]. The pot was then capped and tumbled end-over-end at normal tumble at room temperature for 2 hours. After this the sample was neutralized with an acetate buffer solution (pH=5) and rinsed with hot and cold water. Then the sample was dried in an oven at 60°C for 1 hr. A Canon digital camera (Power shot S40) was attached to a microscope and used to take photographs of the fibrils on fibre surfaces. Number of fibrils in the range of 380 µm longitudinal length was counted using another microscope with a monitor.

Method 2: Fibrillation test for the fibre pre-treated with alkali or softener was conducted according to the method for untreated yarn (Method 1) with distilled water instead of alkaline solution.

The abrasion test of the fibre treated with softener was performed with a DELTA-100 (Lenzing AG). A sample fibre was hung on the abrasion bar and number of rotations of an abrasion bar attached to the equipment was counted till the fibre was torn.

Alkali and water retention values

0.5 g of sample material was put into alkali solutions or distilled water for 2 hrs, centrifuged at 4000 G for 10 min and weight of the sample was measured (W_w). The sample was neutralized with a buffer solution, rinsed with hot and cold water since alkaline solution was used for the experiment. The wet sample was dried at 105 °C for 2 hr (W_d). Alkali retention (ARV) and water retention values (WRV) were calculated with equation (1).

$$A(W)RV(\%) = \frac{W_w - W_d}{W_d} \times 100 \qquad (1)$$

Weight loss

Yarn was weighed in standard atmosphere of 20 °C, and 65 % relative humidity, then put into different types of alkaline solution for 2 hr. After neutralization with an acetate buffer (pH=5) and rinsing with hot and cold water, the sample was put in an oven for drying at 105°C for 1 hr, then kept for 24 hr under condition of 20°C, 65 % relative humidity. Then the sample was weighed again. The weight loss (WL) was calculated with the following formula,

$$WL(\%) = \frac{W_a - W_b}{W_a} \times 100 \qquad (2)$$

where W_a is the weight of untreated sample, W_b is the weight of the treated sample.

Results and Discussion

Effects of alkali treatment on fibrillation tendency

Relation between fibril number and concentration of alkalin solution for fibrillation test is shown in Figure 1. The fibril number increased with increase in concentration of alkali for all alkalis. TMAH shows greatest increase of fibril number as compared to other alkalis, which indicates that TMAH has the greatest effect to induce fibrillation on Lyocell fibres.

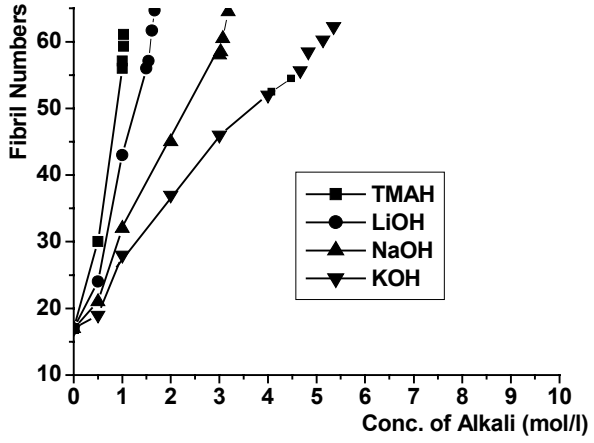

Figure 1. Plots of fibril number on untreated Lyocell fibre against alkali concentration of fibrillation test.

Figure 2 shows the plots of ARW against concentration of alkali for untreated Lyocell yarn. ARV for TMAH shows remarkable increase till a concentration of approximately 1 mol/l and then the increase is observed to be retarded. Sodium hydroxide shows constant and higher increase of ARV. The low fibrillation tendency of Lyocell treated with potassium hydroxide as shown in Figure 1 could be due to lower ARV of KOH. The lower ARV of KOH could be because of small ion diameter of hydrated K^+ as given in Table 1.

Cation	Li^+	Na^+	K^+
Diameter (Å)	5.7	4.3	2.9

Table 1. Size of hydrated cations [5]

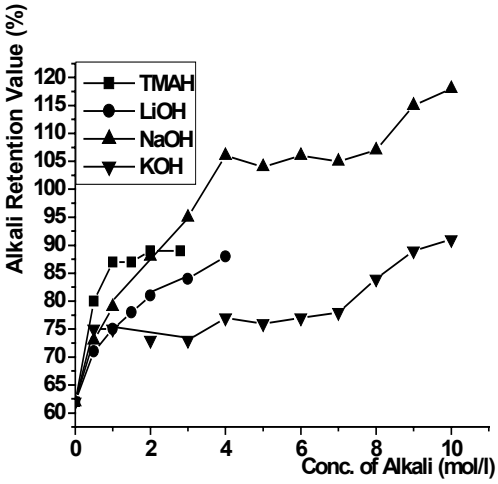

Figure 2. Plots of ARV of untreated Lyocell yarn against alkali concentration.

Effect of concentration of alkalis for untreated Lyocell yarn on weigh loss of fibre during alkaline treatments is shown in Figure 3. The WL is increases in the order of TMAH>LiOH>NaOH>KOH concurring with the order of fibril number at the same concentration of alkali as shown in Figure 1. This suggests that fibril tendency is strongly related to strength of alkalis. It was obvious that different alkali resulted in different fibrillation tendencies and swelling extents in Lyocell fibre.

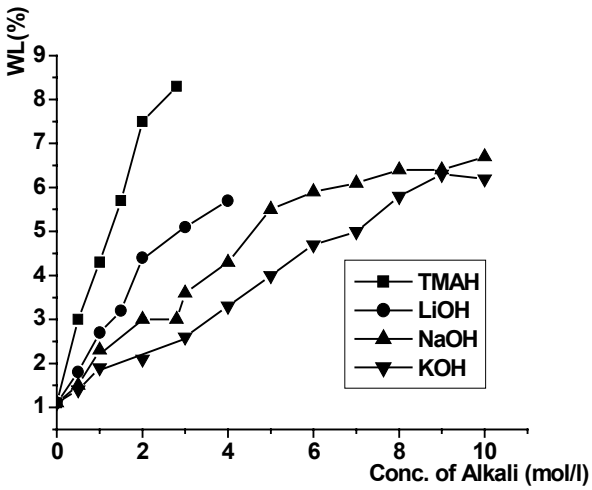

Figure 3. Plots of WL of untreated Lyocell yarn against alkali concentration**.**

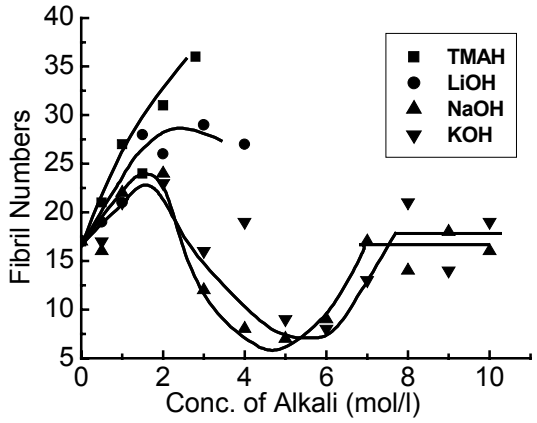

Figure 4. Plots of fibril number on alkali pre-treated Lyocell fibre against alkali concentration of pre-treatment.

Effects of alkali pre-treatment on fibrillation tendency

Figure 4 shows the relation between fibril numbers, after fibrillation test in water and the alkali concentration used for pre-treatment of Lyocell fibres. The fibril number increases with increase in alkali concentration up to 2 mol/l and then decreases down to 5 mol/l and then increases again up to 9 mol/l for NaOH and KOH. These results are quite different from the results for untreated Lyocell fibre which was abraded in alkaline solution as shown in Figure 1. Alkali pre-treatment retards fibrillation under certain conditions though alkali treatment with abrasion promotes fibrillation.

WRV of Lyocell fibre pre-treated with alkali was plotted against the alkali concentration of pre-treatment in Figure 5. WRV increases with increase in alkali concentration for all alkalis, which could indicate that pores in the fibre become larger after alkali treatment [3] and the increase in pore volume is affected by the strength of alkali. Considering the results of fibril number and alkali concentration in Figure 4, there is no direct relation between water retention value of Lyocell fibre and fibrillation property after alkali treatment.

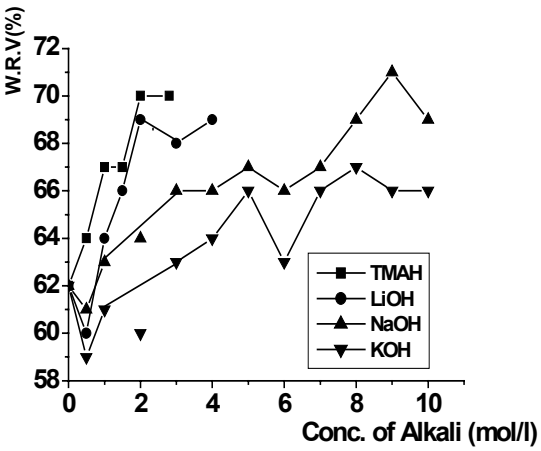

Figure 5. Plots of WRV of alkali pre-treated Lyocell fibre against alkali concentration of pre-treatment**.**

Effect of softener pre-treatment on fibrillation

Fibrillation test of fibre pre-treated with softener was done in distilled water with ball-bearings. The fibril number counted was plotted against concentration of softener in Figure 6. Fibril number dramatically decreases with increase in the amount of Siligen SIN added to Lyocell fibres while no decrease in fibril numbers is observed for Siligen VN. These results suggest that softener Siligen SIN improve fibrillation property of Lyocell but Sliligen VN does not. It could be due to a difference in chemical structures of softeners. Siligen SIN is a polysiloxane and Siligen VN is a polyethylene wax. Regarding the effect of

treatment temperature, fibrillation was retarded more greatly with increase in treatment temperature.

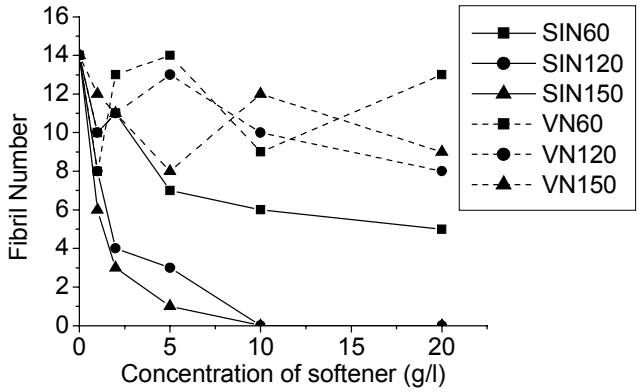

Figure 6. Plots of fibril number on softener pre-treated Lyocell fibre against concentration of softener. SIN and VN indicate softener and a number after SIN and VN indicate temperature used for pre-treatment of Lyocell fibre.

In Figure 7 the effect of concentration of softener on WRV is shown. The WRV decreases with increase of concentration in Siligen VN though there is no improvement in fibrillation for Siligen VN. However, WRV and fibril number of Lyocell fibre treated with SIN are lower than those with VN. These results could imply that water retention capacity is not directly indicative of fibrillation property but of other factors that indirectly relate to fibrillation. Further investigation is required to clarify the details.

An abrasion experiment of the fibre treated with softener was done using an abrasion tester. In Figure 8 count of rotation of abrasion bar till the fibre was torn was plotted against the concentration of softener. Large count of rotation means high resistance against abrasion. As can be expected, rotation number increases with increase in concentration of softener especially for fibres treated with SIN at 150 °C, showing lowest fibrillation. The fibre with high abrasion resistance has low fibrillation property.

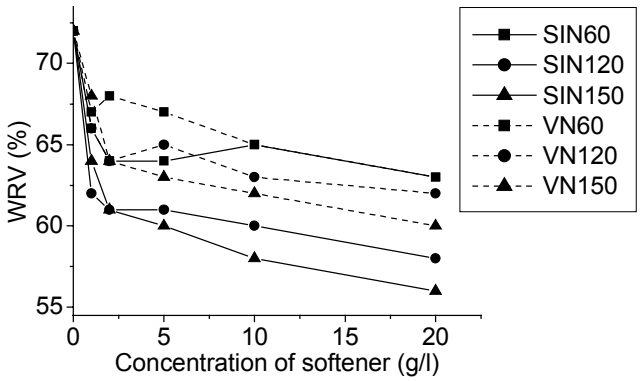

Figure 7. Plots of WRV of softener pre-treated Lyocell fibre against concentration of softener. SIN and VN indicate softener and a number after SIN and VN indicate temperature used for pre-treatment of Lyocel fibre.

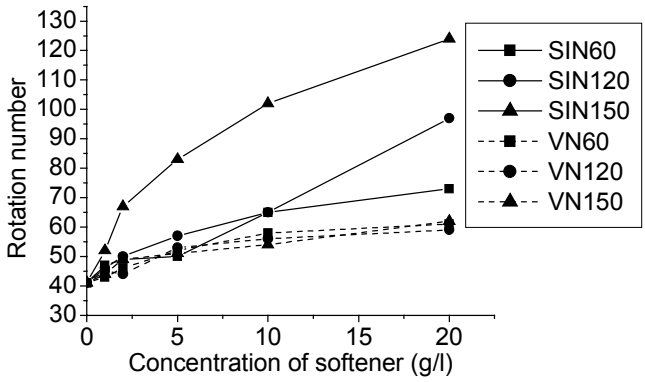

Figure 8. Plots of rotation number against concentration of softener. SIN and VN indicate softener and a number after SIN and VN indicate temperature used for pre-treatment of Lyocel fibre.

CONCLUSIONS

The effects of treatments with alkali and softener on fibrillation tendency of Lyocell fibre were investigated. Much more fibrillation was observed on untreated Lyocell fibres tested in alkaline solutions compared to those shaked in water. Grade of fibrillation and weight loss in Lyocell fibre decreased in the order of TMAH>LiOH>NaOH>KOH. The fibre pre-treated with NaOH or KOH at a concentration of 5-6 mol/l, however, had less fibrillation after fibrillation test with water. Pre-treatment of Lyocell fibre with softeners also induced decrease in WRV, increase in abrasion

resistance and improvement of fibrillation property. The fibre pre-treated with 10 g/l of Siligen SIN at 150 °C showed excellent anti-fibrillation property.

ACKNOWLEDGMENTS

The authors gratefully acknowledge the financial support received from the Christian-Doppler Research Society and Lenzing AG, Austria. The authors also thank Fluka Production GmbH, Buchs, CH, for providing TMAH solution, and BASF AG for Siligen SIN and VN.

REFERENCES

[1] Brauneis, F. and Eibl, M. *Melliand International*, 1998, **79**(3), E-38, 155.

[2] Bredereck, K. *et al., Melliand Textilberichte*, 2003, 58-64.

[3] Bredereck, K., Gruber, M., Otterbach, A. and Schulz, F., *Textilveredlung*, 1996, **31**(9/10),94-200.

[4] Ibbett, R. N. *et al., Textile Research Journal*, 2001, **71**(2), 164-173.

[5] Kielland, J., J. Am. Chem. Soc., 1937, **59**, 1675.

[6] Mortimer, S. A. *et al., Journal of Applied Polymer Science,* 1996, **60** (10), 1747-1756.

[7] Nemec, H., *Lenzinger Berichte*, 1994, **9/94**, 69-72.

[8] Schafer, K, *Melliand International*, 1998, **79**(4), E-64, 247.

[9] Sheth, G. N. et al., 2-3 March, 2002, 43rd Joint Technological Conference, NITRA.

[10] Taylor, J. M., *European Patent Application,* 1992, 0538977 A1.

[11] Toth, T., Tanczos, I. *et al., Textile Research Journal*, 2003, **73**(3), 273-278.

Lenzinger Berichte, 82 (2003) 64-69

NEW LENZING TECHNIK WET OPENER SYSTEM BLOW-DRY: OPERATIONAL EXPERIENCES

Herbert Hummer

Lenzing Technik, A-4860 Lenzing, Austria
e-mail: h.hummer@lenzing.com
Fax: +43-7672/96857

Abstract

The new wet opener system blow-dry for staple fibre has been introduced by Lenzing Technik. On basis of actual operation data the performance of the system is verified and discussed. The system reduces moisture of inlet fibre up to 30% and thus increases capacity of existing lines or reduces requirement of conventional dryercapacity in new lines. A main technological effect is the homogenisation of moisture across the working width. A computer-simulation model for the design of the system is introduced.
Keywords: fibre drying; capacity increase;homogenous moisture distribution; computer simulation

Introduction

This article makes reference to the report by Mr. H. Weber in *Lenzinger Berichte 2002* (1) and shall fulfill the purpose of adding operational data and experiences from a recently finished project and in that way compare the design expectations with reality. This means it can be considered also as an update of the status of this technology after a number of installations in different plants and configurations.

A brief explanation of the system shall be given as a repeat at this point with reference to figure 1. The system is implemented in the viscose staple fibre process between aftertreatment and dryer. It takes up the fibre after the mat opener in aftertreatment machine via a suction hood to the mixing box (C), where it gets in intensive contact with preheated air from the fresh-air-fan (A) and heat-exchanger (B). The fibre is conveyed by the hot air through the transportation fan and piping (D) to the air-separator (E) while the turbulent flow creates proper heat transfer and evaporation of water that is carried along with the fibre. After separation from transport air the fibre falls into a feeding chamber and is passed through the opening device and transmitted to the main dryer as a uniform fleece.
The main features can be summarised as follows:

- Technological step of predrying before opening
  Benefits:
  - Better specific opening effect
  - Less damage to fibre
- Mixing of fibres across working width
  Benefits:
  - Homogenous distribution of moisture
- Elimination of inclined spike apron
  Benefits:
  - Reduced repair and maintenance
  - Elimination of possible contamination of fibre
- Flexibility in layout arrangement
  Benefits:
  - Implementation in existing plants
  - Interconnection of production lines
- Modular concept of system with modules
  - Transportation and opening
  - Heating and drying
  - Heat recovery

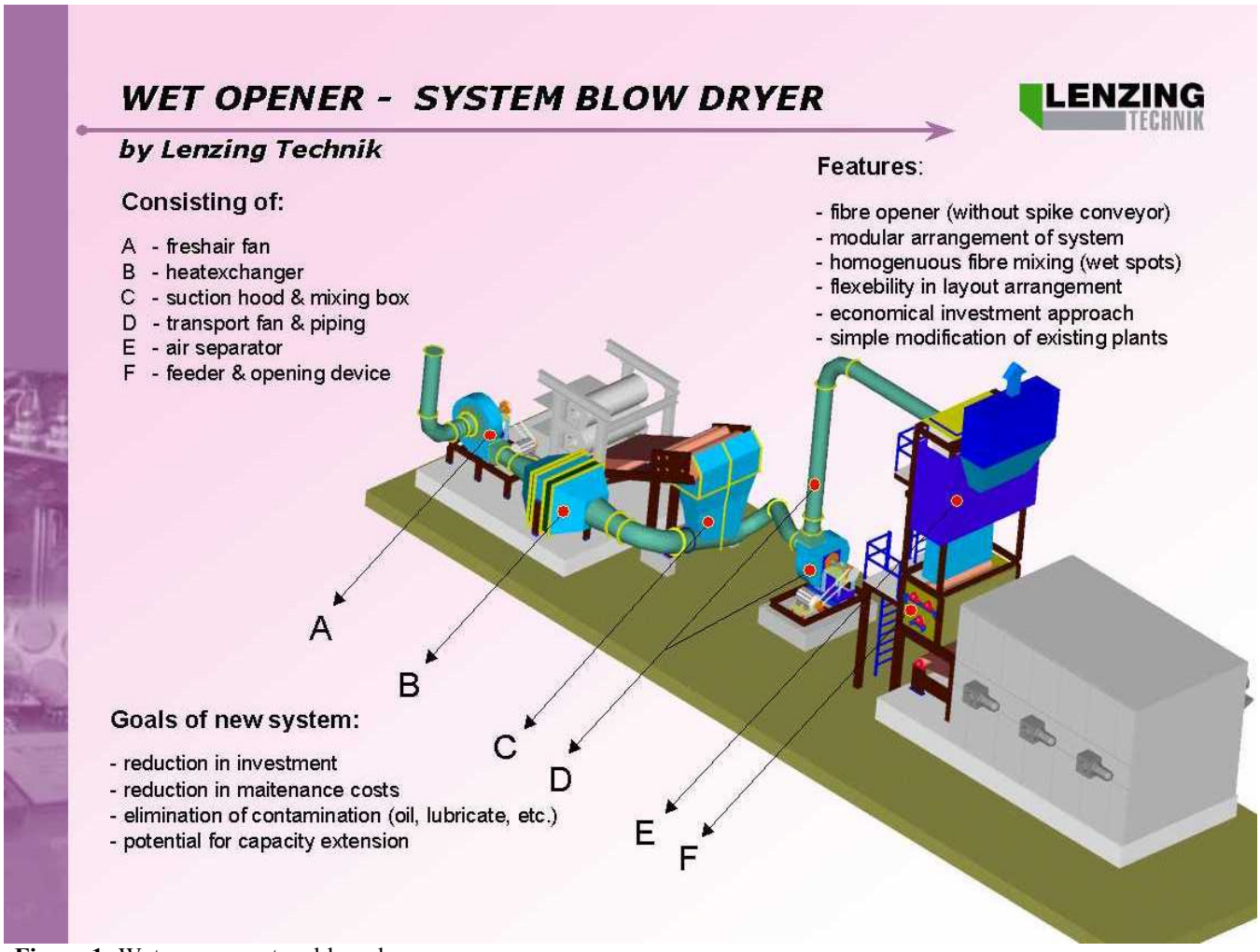

Figure 1: Wet opener system blow-dry

Description of an actual project

The actual project is characterised by the main goal to increase production of an existing line, which is operated with a two-stage belt-dryer.
The alternatives to the solution with our system blow-dryer had been extension of belt-dryer or addition of a new belt-dryer. They were excluded after evaluation of cost for equipment and requirement of space (new building).

The key-data have been:

- Reduction of moisture by min. 20 %
- Increase of capacity by 20 tons/day
  The scope of project included the modules fibre transport and opening and heating/drying. No heat recovery was requested.

Methods and instruments

The task was analysed as a complex system covering existing belt-dryer and new blow-dryer. It was decided to use the computer simulation model SIMEX (2) for the complete dryer system. At this point only the section of blow-dryer shall be discussed.

The structure of the computermodel for the section blow-dryer is explained in figure 2.
It is based on a closed material and energy-balance and operates with the following parameters:

- Fibre:
  - actual production [t/h]
  - water content [t/h]
  - temperature [°C]
- Airflows:
  - temperature [°C]
  - water content [kg/h]

- actual flow [m³/h]
- Steam and condensate:
  - flowrate [t/h]
  - pressure [bar]
  - temperature [°C]

Each single figure for material data can be selected and adjusted. The theoretical basis for the model is that through the turbulent flow of hotair and fibre a certain heat transfer rate will occur and from that the necessary duration of exposure of the fibre can be calculated. This means that for a certain flowrate the length of heat exchanger (i.e. transportation pipe) can be determined. The theoretical heat transfer rate must be calibrated with experimental data

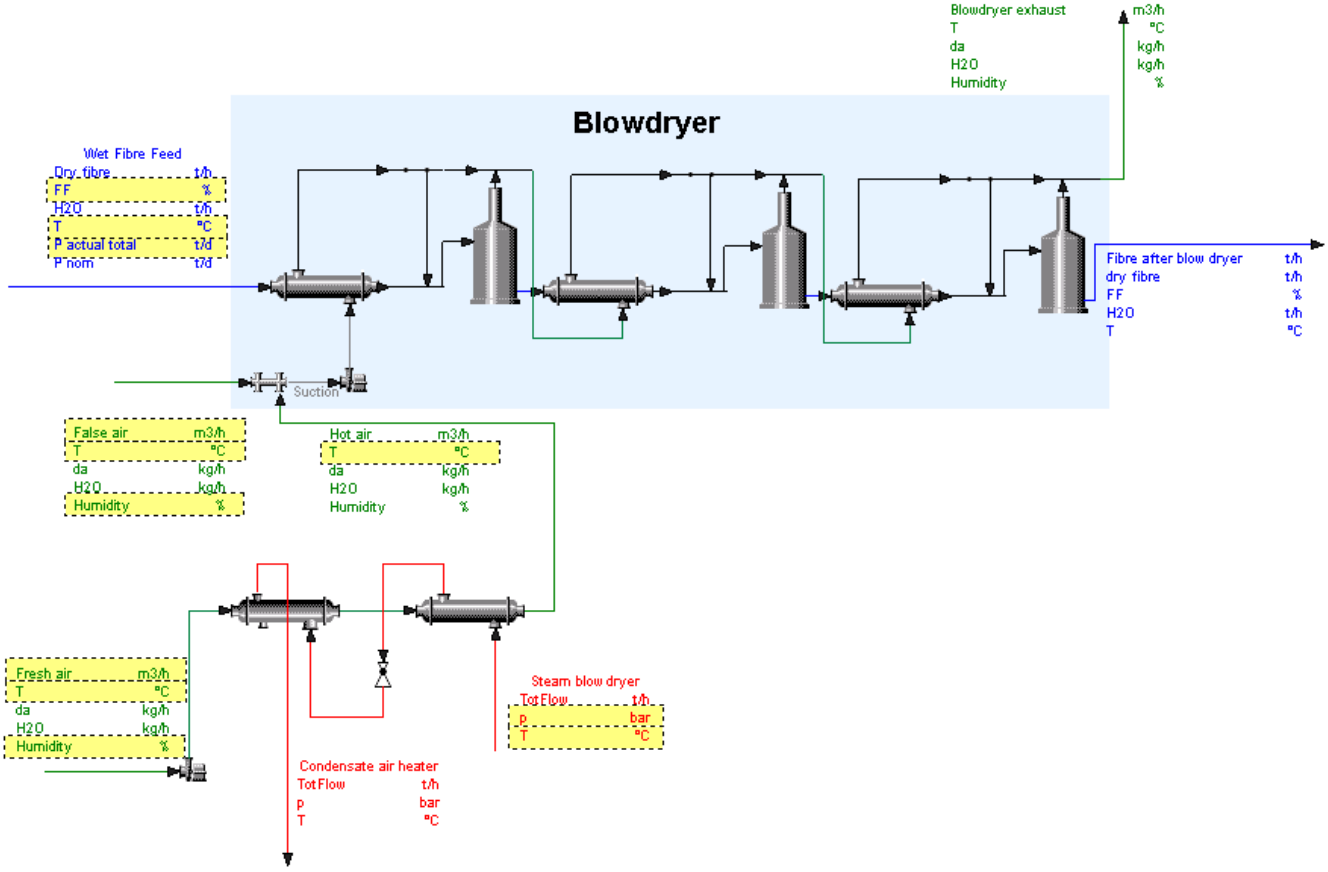

Figure 2: Computer-simulation model for section blow-dryer

For the total airflow fresh air and false air through inlet of fibre are calculated.
The input data are parameters for fibre, fresh air and false air, which are marked in yellow in figure 2.

The others are calculated data, i.e. the main results of interest e.g.:

- outlet moisture of fibre [t/h]
- moisture of exhaust air [kg/h]
- temperature of exhaust air [°C]
- steam consumption [t/h]
- condensate flow [t/h]

A series of iterative calculations has been carried out with the model before freezing the design.

Results and discussion

The system is in operation since 8 months and has passed the performance test successfully.
For the purpose of that test numerous operational data have been collected which are taken for discussion as follows.

	Fiber Moisture - inlet (%)							Fiber Moisture - outlet (%)						
Sample	Sampling point							Sampling point						
	1	2	3	4	5	STD	Avg	1	2	3	4	5	STD	Avg
A	175,5	92,7	117,9	103,6	216,3	52,7	**141,2**	95,6	97,5	103,2	96,1	97,7	3,0	**98,0**
B	163,6	226,7	156,1	93,3	271,0	68,5	**182,1**	93,8	87,8	105,7	92,3	93,6	6,6	**94,6**
C	132,1	85,6	139,0	79,7	137,4	29,5	**114,8**	94,4	92,8	95,6	94,0	92,1	1,4	**93,8**
D	131,9	105,3	120,0	118,0	147,3	15,9	**124,5**	94,5	87,8	96,1	87,6	87,4	4,3	**90,7**
E	172,6	90,9	149,1	100,8	145,9	34,6	**131,9**	91,8	88,0	104,9	104,2	108,5	9,0	**99,5**
F	121,5	98,6	148,6	76,6	108,8	26,8	**110,8**	80,4	87,5	98,0	99,5	99,2	8,6	**92,9**
G	146,5	96,4	124,8	135,2	179,2	30,3	**136,4**	98,5	78,7	111,0	96,9	90,6	11,8	**95,1**
Average	149,1	113,7	136,5	101,0	172,3		**134,5**	92,7	88,6	102,1	95,8	95,6		**95,0**
Minimum	121,5	85,6	117,9	76,6	108,8	20,0	**102,1**	80,4	78,7	95,6	87,6	87,4	6,7	**85,9**
Maximum	175,5	226,7	156,1	135,2	271,0	55,3	**192,9**	98,5	97,5	111,0	104,2	108,5	6,0	**103,9**
St.-deviation	21,7	50,2	15,5	20,7	55,2	**42,9**		5,8	5,7	5,7	5,3	7,0	**7,1**	
CV(%)	14,5	44,1	11,4	20,5	32,1	31,9		6,3	6,5	5,6	5,5	7,3	7,5	

Table 1: Fibre data inlet and outlet

1. Fibre inlet (ref. Table 1)

Five sampling points have been selected at the end of after treatment (after final pressing) over the working width, the sampling interval was 4 hours.

The samples have been dried in a laboratory oven, the difference in weight between dry and wet condition was calculated as moisture content.

Following aspects are to be remarked:

- Moisture of taken samples is not homogenous; standard deviation of five samples of one set is up to 68,5; even the average of the single sets is ranging from 110,8 % to 182,1%, the standard deviation for the whole dataset is 42,9.

- The inhomogeneous distribution of moisture is found in many applications and represents a major problem with conventional drying as it means that the fibre has to be overdried and remoisturized .

- The samples 1 and 5, which represent the outer edges of the fleece, are showing the highest moisture figures which is also in accordance with operational data from many applications where the technology of fleece forming and squeezing does not specifically eliminate this effect.

- The deviation of the maximal figures out of the sets is 2,5 times the standard deviation of the minimum figures.

2. Fibre outlet (ref. Table 1)

The samples of outlet fibre have been taken directly from the belt before entrance to the beltdryer. The moisture determination has been done with the standard laboratory method as described above.

The figures in table1 provide the following positive results:

- The average reduction of moisture is 39,5%, which is high above the requested capacity. Due to big deviation of single samples at inlet it is permitted for example to devaluate the figures of sample 1 and 5 by 50% which results in a theoretical average inlet moisture of 125,8%. Even under that assumption the moisture reduction still is 30,95%.

- The moisture distribution across working width is considerably homogenous compared to the fibre inlet. The maximum standard deviation within one set is 11,8 (compared to 68,5 before) and the deviation of all figures is reduced to 7,1 from 42,9 before. This means that a much more homogenous fibre fleece is entering the

main dryer and reducing energy consumption in that step of the process. The impact on moisture distribution is shown obviously in figure 3 by comparison of the fibre moisture and deviation at inlet and outlet of blow-dryer system for the average of the samples in table 1.

- The outer samples 1 and 5, which appeared as wet edges at inlet, are no more deviating from the other samples in the center of the working width. This means that the turbulences in the transportation pipe create the necessary mixing effect to ensure uniform drying.

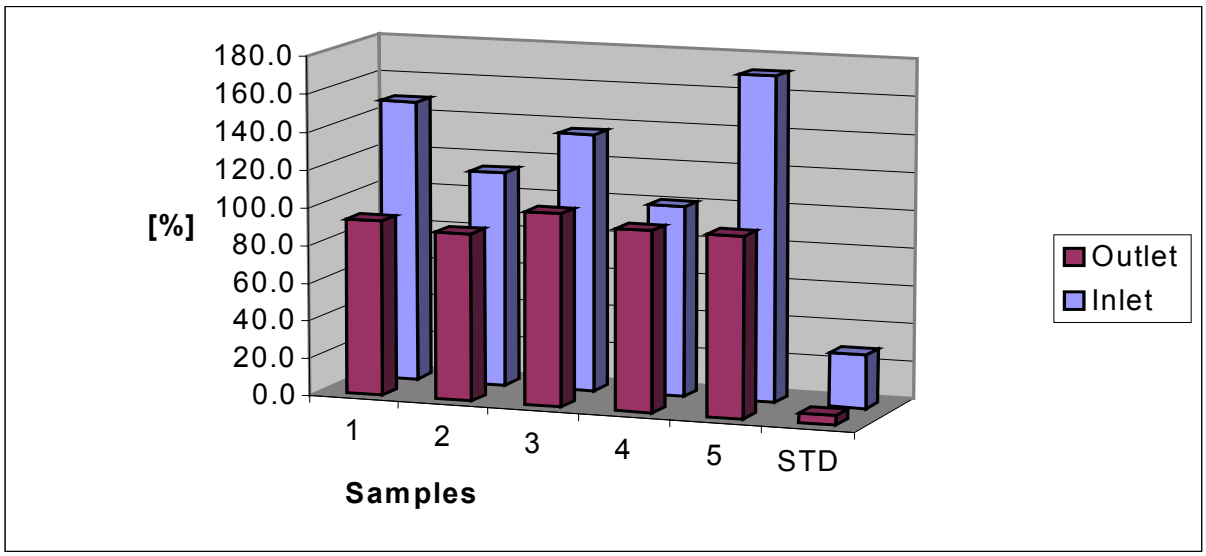

Figure 3: Fibre moisture inlet and outlet including standard deviation

Conclusions

The conclusions out of the operational experiences and data as described above can be summarised as follows.

- The system is capable of considerably reducing moisture of wet fibre. The range of 30% as above is at the higher end according to data available now.
- The system reduces deviation of moisture across working width to a level that is up to 6 times lower than before the system.
- The system eliminates wet edges on both sides of the working width of a fibre fleece.
- The above features lead to a reduction of specific energy consumption in main dryer and more homogenous final moisture after dryer.
- The design of tailor-made systems is supported by a computer simulation model that is well calibrated by experimental data and can predict the influence of variation of single parameters with high precision.
- The wet opener system blow-dryer is suitable for implementation in existing plants to achieve increased capacity as well as for new plants.
- The remaining features as described in the introduction have not been discussed in this paper however can be summarised in a general statement that the expectations have been fulfilled and proved in the actual project.

Acknowledgement

My sincere thanks goes to all the colleagues in Lenzing Research & Development and in Lenzing Technik who have contributed to the development and successful implementation of this system.

References

(1) Weber, H. in *Lenzinger Berichte Nr. 81* 2002; 76-79

(2) SIMEX: Computer-simulation-software by Lenzing Technik

Lenzinger Berichte, 82 (2003) 70-75

AUTOMATED BOBBIN INSPECTION SYSTEM

Josef Baumgartinger [a] , Roman König [b]

[a] Lenzing Technik GmbH&CoKG, Div. Lenzing Technik,
Werkstrasse 2, Lenzing, Austria
[b]Glanzstoff Bohemia s.r.o., Lovosice, Czech Republic

Abstract

Automated bobbing inspection systems will take over the present monotonous visual inspection which is difficult and tiring for human operators and which causes so many wrong or faulty decisions in today's manual inspection. Latest technology and the fast progress in the field of laser optics, data and image analysis do offer further progress and time saving possibilities, which will continue to increase the profitability of such automated systems like Lenzing Instruments LIS.

Keywords: bobbin detection; optical inspection; artificial vision inspection

Introduction

In a filament production process (POY, HOY, FDY) and also during texturing usually a certain number of bobbins do not comply to higher quality levels because of either obvious structural faults like deformations, oil or dirt stains, etc., or because of faults in the fine structure – like overthrown ends or broken filaments which usually are very difficult to detect.

Certainly a desired ideal case would be a 'zero-error-production', and more and more companies are undertaking big efforts in this direction.

However, to identify problematic components within a production plant, it is necessary to check and inspect every single bobbin thoroughly and to evaluate the detected faults statistically. The resulting statistics may allow one to fully sort out some problems and to at least minimize others.

With an online data connection to the SQL database the quality level of the production is always present. The traceability within the production flow improves significantly. To achieve as well as to maintain zero-error-production it is and always will be crucial to inspect the product before it leaves the plant site.

Nowadays usually a significant number of human inspectors are responsible for this sophisticated task. However, for human reasons (tiring and monotonous work, varying ability of concentration) as well as for technical reasons (shiny or glossy bobbin surfaces, light conditions etc.) human inspection is never as constant and reliable as an automated inspection could be. See figure 1.

Hence reliability and the cost of manpower have been the reasons for quite a few institutions and companies to think about how to automate the process of bobbin inspection in recent years.

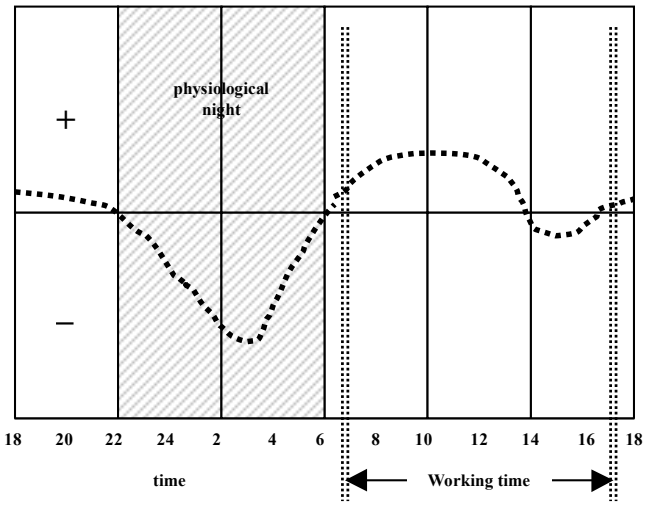

Figure 1. Physiological variation of human performance / ability of concentration [1]

1 Classification of Nonconformity

The classification of bobbin defects has always been an individual matter for each company, depending on requirements and quality levels. An automatic inspection system should easily comply with individual classifications and of course also threshold values for different defects have to be selectable individually.

Different kinds of quality parameters, depending on the application of the filaments, have to be classified:

- **Geometry:**
  Diameter
  Winding length and position
  Density / weight
  Taper angle
- **Macro structural defects:**
  Bulges and ridges
  Saddle
  Tube- / bobbin damages
- **Micro structural defects:**
  Overthrown ends
  Dirt spots or colour defects
  Whiteness differences
  Transfer tail and waste bunch
  Broken filaments, loops, fluff
  Tight spots

The design of the LIS in hardware and software is very flexible and allows of course an individual combination of quality parameters, which have to be detected.

Anyway, to make a system like the LIS 200 feasible, all required inspections have to be taken over by the system.

2 Automated Inspection

It seems to be obvious that a human optical (visual) inspection can only be replaced by an automatic system, which works on an optical basis. However, a series of comparative experiments has proven that a plain camera system is not suitable to identify the above-mentioned errors at a satisfactory level as compared to the human eye. The quality and repeatability of the results have been poor, particularly in the range of micro structural defects.

Therefore the *Lenzing Instruments* automated bobbin inspection system LIS 200 is based on latest laser technology, illumination and digital camera systems, which shows a tremendously better detection quality, resolution and repeatability compared to common camera based systems.

2.1 How does the LIS 200 work?

The LIS measurement is based on different technologies.

While the bobbin is being rotated around its axis in the testing position by a handling robot, the surface of the bobbin is inspected with digital cameras and / or lasers including special illumination.

The basic method of the LIS 200 as described before, and the sophisticated evaluation software allow one to detect defects of a bobbin in the geometry, macro structure and micro structure at a result rate comparable to the human inspection – except for the reliable detection of broken filaments.

Detection of Broken Filaments:

Single filaments are usually too fine to be identified at the resolution used for scanning the topography of the bobbin's surface. A laser beam (wave length of the laser is 685 nm) is emitted on to a bobbin's face side under a flat angle and a CCD matrix camera, which is mounted under a flat angle as well, records the reflection of the surface.

While the surface of the bobbin itself appears as a solid line for the CCD camera, single filaments sticking out from the surface appear like flash lights, when they are hit by the laser beam.

Counting the number of such flashes during one full rotation of the bobbin allows one to detect broken filaments, loops or fluff at a very high accuracy and reliability. Due to the fact that the counting takes place on two different levels the

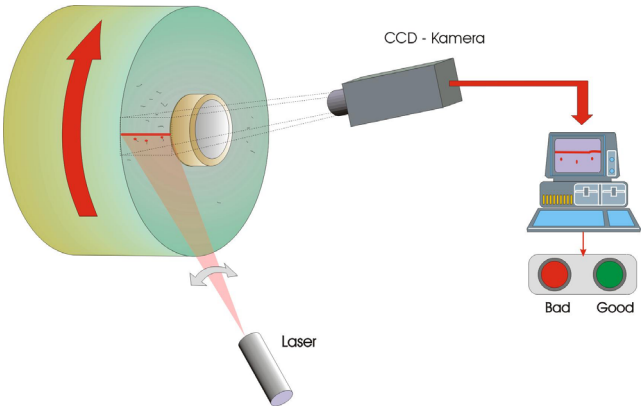

Figure 2. detection of broken filaments

quantity is separated into long and short broken filaments.

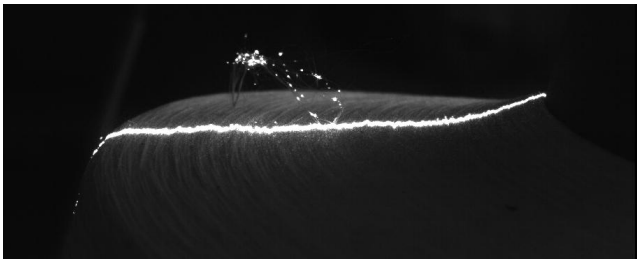

Figure 3. Flash lights when the laser hits the broken filaments

With the same detection system some other quality parameters (winding length, bulges and ridges, saddle) can be detected.

Detection of Overthrown Ends

Extremely difficult is the recording of overthrown ends because they hardly show a difference from the bobbins face structure. The intelligent human vision system is able to automatically ignore unimportant structures therefore it can concentrate on certain patterns and identify them quite easily.

An automatic system has to obey to the fact that besides the unique pattern of one or more overthrown ends every picture contains usually a lot of noise and insignificant disturbances.

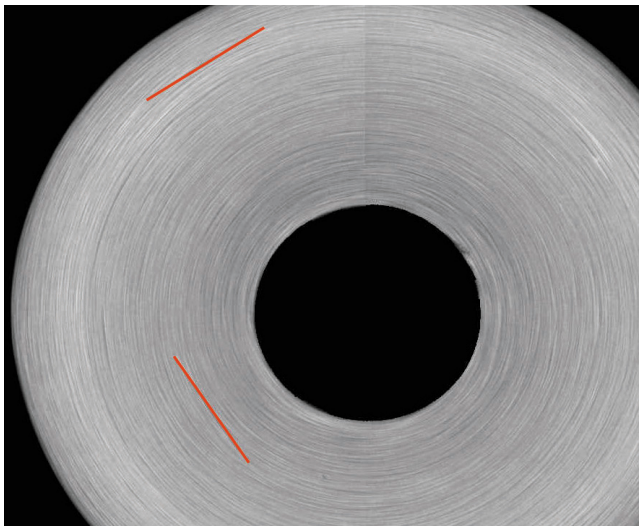

Figure 4. Overthrown ends detected by LIS 200.

The detection of overthrown ends by the LIS 200 has been realized by introducing a learning mode, which enables the system by comparison to distinguish between bobbins with overthrown ends exceeding a certain length and others without.

Detection of Dirt

The detection of dirt is done under special illumination by 3 line sensor color digital cameras with more than 2000 pixels.. The cameras scan 100 % of the surface and system determine the RGB-value [2]. A color difference (dirt) leads to a different RGB-value, which is used for the classification.

Detection of Diameter

This is done with a triangulation laser distance sensor. The resolution is in the range of 0.5 mm.

2.2 Evaluation System

Digital image processing requires significant computing resources; on the other hand bobbin inspection is a highly time critical task - therefore every sensor of the LIS 200 is connected to its own evaluation PC.

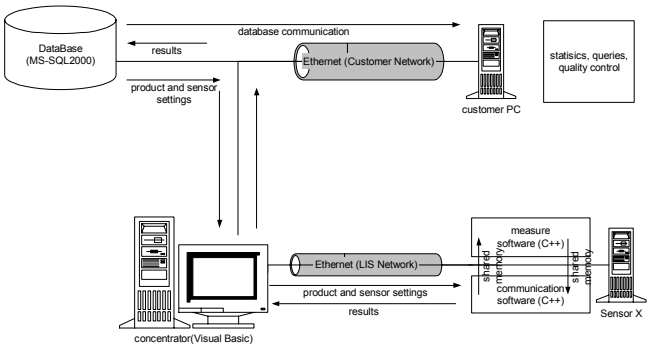

Figure 5. Data communication between measurement PC, database and customer PC.

The evaluation system is built by a complex hierarchy of personal computers (see Figure 5 and Figure 6), featuring rapid parallel calculation of the inspection results with a highly sophisticated digital image processing software and a flexible and simple user interface.

The front end allows interfacing to many common computer systems, enabling an easy integration of the LIS 200 into existing Process Control Systems as can be seen on Figure 6, which represents the installation at Glanzstoff-Bohemia / CZ.

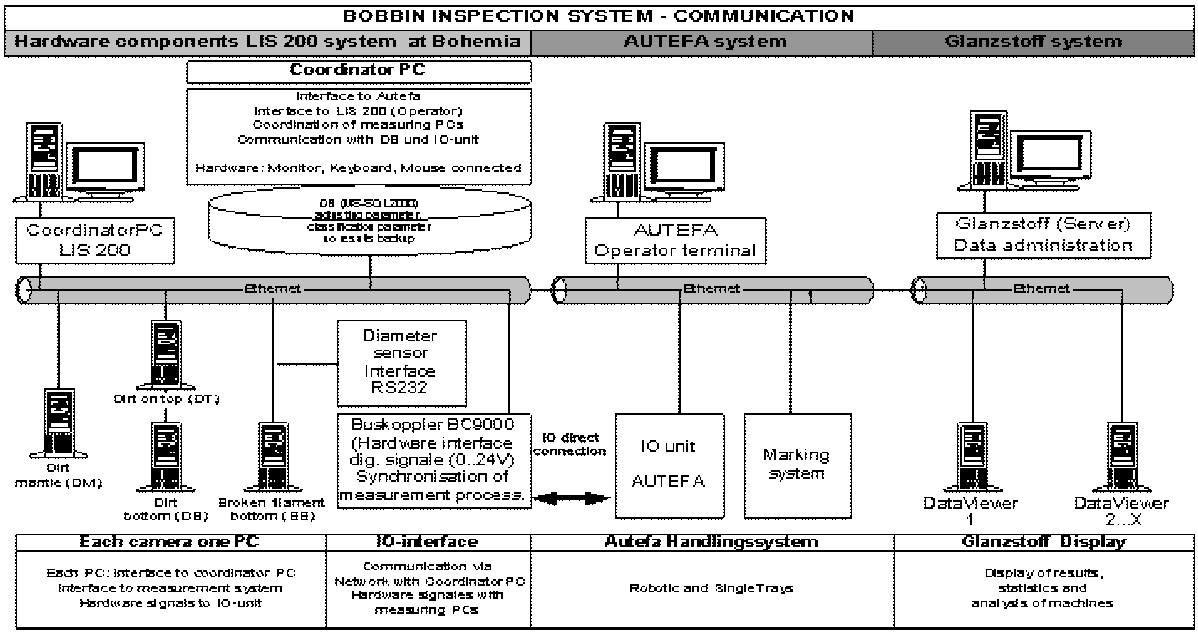

Figure 6. Data communication between LIS200, automation unit and customer database. As realised at Glanzstoff – Bohemia / CZ.

Evaluation and tolerance limits

The results are transferred to a data concentrator, which collects all results of the sensors installed, and compares them to the tolerance limits defined by the operator. The system allows one to issue a simple 'Good – Bad' decision, or to differ between 3 or more different quality grades or to issue a complete result sheet with single inspection results for each bobbin.
The LIS allows one to determine tolerance values for each detectable defect. However, human inspectors hardly go for fixed tolerances – by experience they develop a feeling for whether a bobbin complies to the required quality level by only looking very shortly at it. Often a quality decision is not unanimous but will depend on the individual inspector. In such an ambiguous environment the introduction of an automatic inspection system will create a lot of discussion; the definition of significant tolerances will require a certain time for every individual customer. Here the learning software of the LIS is a tremendous advancement to optimize the correspondence of quality decisions by the human and by the machine.

Once an acceptable inspection level has been thought out and achieved by the LIS 200, additional units will work at exactly the same quality level continuously, which is a significant advantage compared to the ambiguous human inspection.
Apart from issuing quality decisions and inspection results for single bobbins the LIS 200 stores all results into a database system. With a flexible query interface it is easy to set up statistics, which show certain trends and regularities of repeated defects (e.g. machine regularities, shift wise differences, etc.) and hence to eliminate them.

2.3 Handling Unit

The physical interface between the LIS 200 inspection and the process flow is realized by the handling unit. Depending on the type of transport system (e.g. conveyor, buggy or shuttle) a range of transport means are possible:

- robots from 2 axes up to 6 axes
- conveyor with single trays and portal robots
- or manual supply

can be used to take one after the other bobbin for presenting them to the inspection system and putting them back into the process flow.

3 Economic Benefit

The return of investment on an automatic bobbin inspection with the LIS 200 will be determined by many different factors, e.g. the technical and automation level of a production unit, the cost of manpower and certainly the quality level and cost of customer claims.
In general an automatic system like the LIS 200 yields the following major economical effects and benefits:

- **Cost reduction**
  Cost effects include the reduction of manpower, reduction of inspection costs as well as of B-grade products and waste.
  Immediate reaction on detected malfunctions and hence a reduction in internal quality costs and customer claims.

- **Increasing product quality**
  The unanimous and repeatable inspection level of the automatic system leads to an exact reliable product quality at the end of the process.

The statistical evaluation of defect occurrences and trends allows one to immediately identify and react on problems in the production process. The actual status of the quality is monitored online.

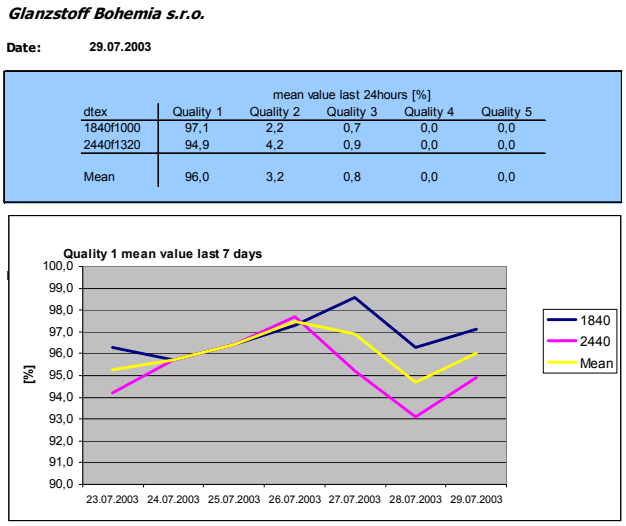

Figure 7. Statistical evaluation of the quality level based on data from LIS 200.

For each product, which is running there is an overview or a comparison between different days as shown in Figure 7 for 7 days. If there is a need for some more detailed information the traceability to the single spinning machine and position is possible. Due to continuous evaluation faults are systematically detected.
On the other hand the investment for installing an automatic bobbin inspection depends on three main parameters:

- **Throughput**
  How many bobbins have to be inspected per hour, shift or day?
  As an upper time limit for inspection the LIS 200 requires approximately 5 seconds per bobbin from scanning to the final result. The handling time to get the bobbin from the transport system into the testing position and back again depends on the transport system and the logistic concept. In ideal cases handling time may even overlap the inspection time. A realistic handling time shall be in the range of 0 to 4 seconds per bobbin.
  The production or testing volume has to be

divided by the performance of a system including inspection and handling time – the result is the number of complete LIS 200 units required. The standard measuring including handling of 7 to 10 seconds per bobbin enables a fully automated inspection of approx. 8.600 bobbins per day and line.

- **Inspection level**
  Answering the question which defects are to be inspected for in an individual case leads to the configuration of a LIS 200, and the number of sensors required does certainly determine the price of a LIS 200 unit.

Handling unit

Finally the optimal integration of the LIS 200 into the product flow requires a certain robotic system laid out to be strong enough for handling the bobbins, and to flexibly interface with the transport system.

Proper system integration and an adequate logistics concept are important to optimise the handling time and hence to increase the throughput as discussed above.

The large number of variables determining the feasibility of an automatic bobbin inspection makes it very difficult to issue general statements about the cost-benefit ratio. But realistic payback times of installing an automatic inspection with the LIS 200 shall range from 12 to 30 months.

References

[1] Uni Freiburg; Leistungsfähigkeit und Leistungsbereitschaft, www.forst.uni-freiburg.de/.../awi/awi_lehre/pruefungsmaterial/loeffler/2Leistungsfaehigkeit+Bereitschaft.pdf

[2] A color value expressed in the RGB color space is composed of red, green, and blue component values.

Lenzinger Berichte, 82 (2003) 76-78

CIRCULAR KNITS OF MODAL/ELASTANE LYOCELL/ELASTANE

Egon Duenser [a]

[a] Lenzing AG, Lenzing, e.duenser@lenzing.com

Abstract

Core yarn containing an elasthane core covered by cellulosics (Modal, Lyocell) offer new aspects in production of elastic knitted fabric. As an alternative way to classical plating techniques the introduction of elastic core yarns permits a broad range of new variations in the production of elastic knitwear [1].

Keywords:
Modal, Lyocell, core yarn, elasthan, knitting

Classical plating techniques and new possibilities using elastic cellulosics core elastane yarns

The classical plating technique has established itself in the market as a standard procedure. In fact each stitch comprises two single yarns. The core yarn Spun Modal from Feldkirch spinning / *Lenzing AG*, Austria) is made with a bare elastane yarn inside. This conveys permanent elasticity on the fabric.

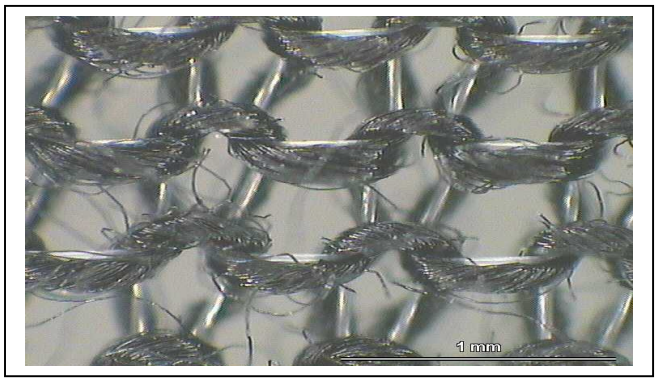

Figure 1. Left side of a plated fabric

In this classical structure the Modal/Lyocell yarn is located on the outer side /showing side of the knitted fabric. The elastane is on the skin side as a result of plating.
Yarn components and the desired knit fabric elasticity can be selected and determined in agreement with the product from the designer or knitter. Three-dimensional elasticity can be obtained. The yarn components and the elastane pretension do, however, have to be defined with the manufacturer of the core yarn. Yarns cannot be exchanged by the knitter as he sees fit.

Since core yarns are available to - an increasing extent sheathed elastane core - an elastic jersey can for example be produced as an alternative to the fabrics classically plated (Figure 2, 3). When using core yarns only spun fibres are located on the surface of the yarn. The elastane share is hidden on the inside. This means that these fabrics have the natural hand of Modal and Lyocell fibres even on the skin / inner side, and the appearance of the outer side is left intact.

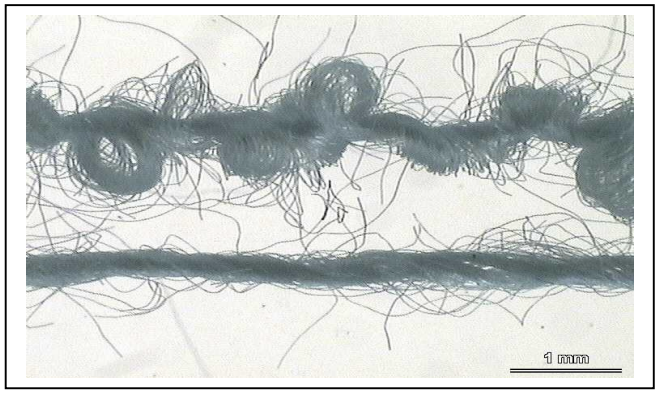

Figure 2. Core yarn of modal, relaxed and with pretension for knitting

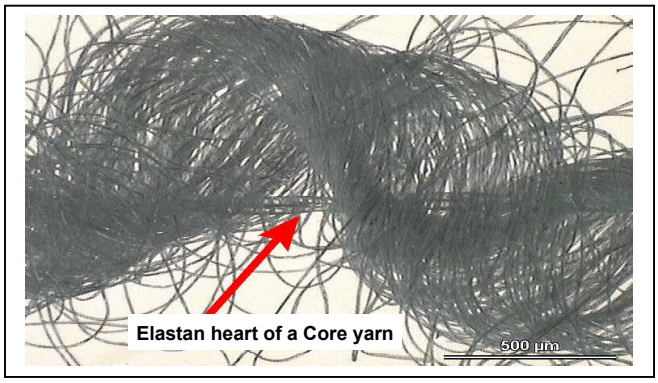

Figure 3. Core tread considerably enlarged

Yarn counts and technical yarn data

Most of the processed core yarns comprise a core of Dorlastan with a count or fineness of 44 dtex and these are covered by spinning with Micromodal, Lyocell or /cotton of Nm 85 or 100. This results in a twisted thread fineness of around Nm 68 or 50.

The fineness of the twisted thread depends enormously on the stretching of the Dorlastan yarn used as the core. This can and should in fact be agreed between the knitter and spinner, respectively with the yarn manufacturer. This stretching determines the elastic power of the finished knitted fabric and its mass per unit area.

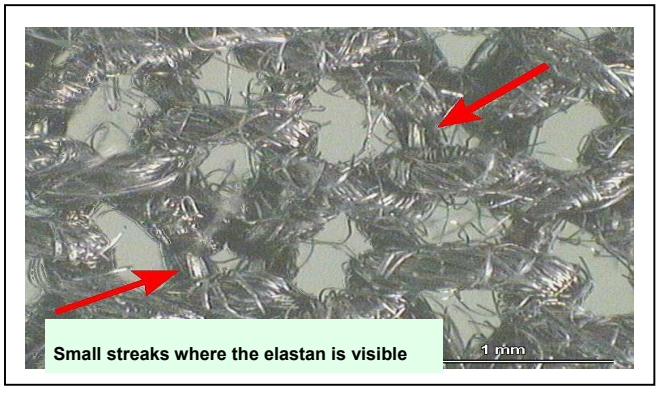

Figure 4. Elastic pique made with core yarn

What yarns suit which knitted fabrics

When a fabric is to be made of or with core yarns, the main task is to make the elastane disappear, in addition to three-dimensional elasticity. The selection of the yarns (fineness of twisted thread and stretching) will be influenced by the knit you wish to have, the machine set-up, the density of the knitted fabric and the mass per unit area. There is a significant advantage in that with this core yarn you have nature next to the skin 100 % (Lyocell, Modal fibre fabric), the fish-skin hand of the elastane side of the plating goods of former years no longer applies. It might be possible to do without dyeing the Dorlastan, when the core yarn manufacturer has spun a super yarn with no elastane peeking out of it (Figure 4).

Fabrics can obtain a super-elastic effect with core yarns even those which have a highly irregular yarn /thread consumption /row whereas to date rows always had to be constructed with a very regular yarn consumption in-between to make the fabric elastic to some extent with an even plating effect.

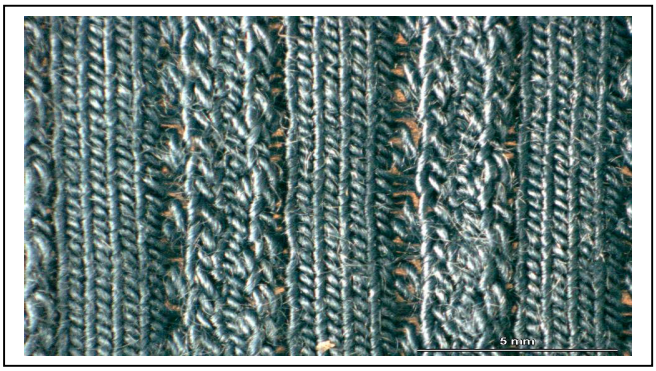

Picture 5 Elastic fabrics with different thread consumption

Core yarns do not require an investment in new machinery

These can be processed with tape feeders and / or single feeder. This ensures that the machinery can be used in a flexible manner.
Knitted fabric effects can be achieved with core yarns which would barely be possible with classical plating techniques.

The list includes structures, jacquards, jacquard and embossed effects (light and heavy). In the same way all drop stitch and rib effects can now be knitted with a different pattern repeat and thread consumption (Picture 5 - 7). New

kinds of embossed patterns, elastic and light, can be knitted with these sheathed yarns in a 3D and much more economic manner.
With Modal and Lyocell core yarns knitted fabrics become clearer, softer and they have a smooth and silkier surface. The serviceability, with structured patterns in particular, improves enormously since there are no longer any bare elastane threads on the reverse side of the fabric as an underlap. These bare elastane yarns are extremely prone to damage and snagging which means that knitters frequently had to do without generous elastane effects such as these.

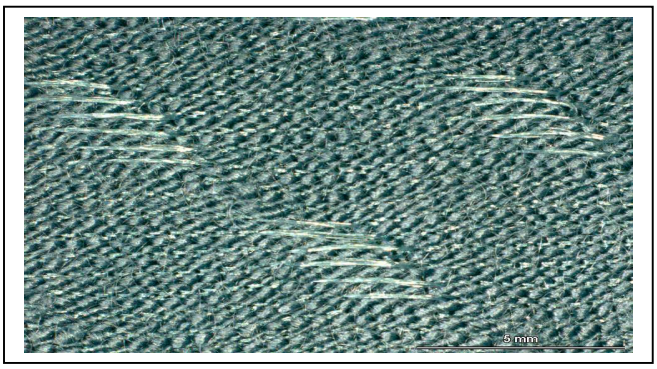

Picture 6 jacquard single with reverse stitch effect

Processing and finishing

The tension of the core yarns should be set so that one obtains approximately the mass per unit area one was aiming for. The adjustment should in any case be looser than for classical plating products. The knitted fabric becomes solid enough after finishing.

It makes sense to use the same finish as is used with conventional plated products. The knitted fabric = elastane share should be prefixed prior to dyeing.

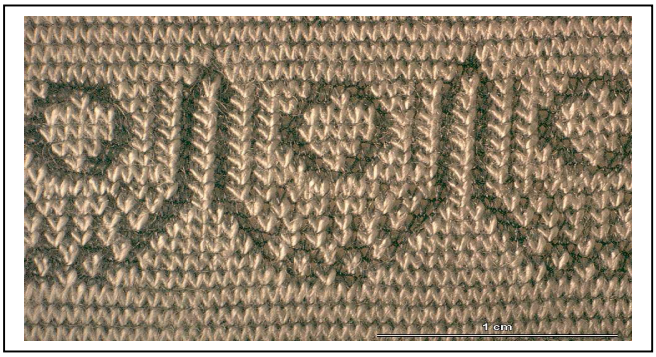

Picture 7 single jersey with jacquard sculptured design effect

References

1. Dünser E, Melliand Textilberichte **84** (2003) 176-177.

Lenzinger Berichte, 82 (2003) 79-82

WATER RELATED PROPERTIES OF CELLULOSE – SCIENTIFIC INVESTIGATIONS AND PRACTICAL IMPORTANCE

Satoko Okubayashi[a], Andrea Schmidt[b], Ulrich Griesser[b], and Thomas Bechtold[a]

[a]CD-Laboratory of Textile and Fibre Chemistry in Cellulosics,
Institute of Textile Chemistry and Textile Physics, Leopold-Franzens University Innsbruck,
Hoechsterstrasse 73, A-6850 Dornbirn, Austria,
Tel: +43 (0)5572 28533, Fax: +43 (0)5572 28629, e-mail: textilchemie@uibk.ac.at
[b]Institute of Pharmacy, Leopold-Franzens University Innsbruck, Innrain 52, A-6020 Innsbruck, Austria

Abstract

Effects of wash and dry treatments on pilling property of cellulosic knitted fabrics (Lyocell 1, Lyocell 2, Modal, Viscose and cotton) were studied. Degree of fuzz, fibril and pill formed on the fabrics were observed with a microscope and evaluated according to a description of assessment. Fuzz formation was observed on fabrics that were treated in a tumble drier while pills were observed on the fabric that was washed and dried. The results suggested a mechanism of pill formation in which mechanical abrasion causes fuzz in dry condition and the fuzz is developed to pill in wet condition accompanied by fibrillation of the fibre. Relations between liquid water retention, water vapour regain, BET constant, which indicates water accessibility in fibres, fibre-fibre friction in dry and wet states, contraction force and the pilling rating were also investigated and the results were found to support the model.

Keywords: *Lyocell fabric, wash-dry treatment, moisture sorption, water retention, fibre-fibre friction, contraction force, pilling, fuzz formation*

Introduction

Pill formation is a common problem in knit fabrics made not only from synthetic fibres but also from natural fibres, man-made cellulosics and their blends. There is little research into mechanism of pill formation for the cellulose fibres such as cotton, viscose and lyocell, while the mechanism in synthetic fibres has been investigated more intensively [4, 10]. Work on fibrillation in cellulosics have also been performed and reported [5, 6], however, relations between fibrillation, fuzz and pilling have not been focused on. On the other hand, it is well-known that cellulosic fibres are swollen in various polar solvents and show completely different chemical and physical behaviours [3]. As shown by the fact that fibrillation is promoted by swelling of fibres [11], water accessibility of the fibres is an important indicator of fibrillation and pilling properties. Fibre-fibre friction is also an important mechanical factor which is expected to support a mechanism of pill formation [1, 2].

In this study, accessibility of liquid water and water vapour on man-made cellulose fibres, Lyocell, Modal, viscose and cotton were investigated. Fibre-fibre friction in wet and contraction force of yarns in water were measured and a model of mechanism for pill formation was proposed considering the effects of water accessibility on grade of pilling and mechanical properties in wet.

Experimental

Materials

Two different lyocell knit fabrics (lyocell 1 and lyocell 2), Modal, Viscose and cotton knitted fabrics and their yarns were used in experiments. All samples have similar textile structures.

Methods

Wash-dry and pilling assessment: Sample fabrics were washed in a domestic washing machine using pH neutral detergent with liquor ration of 1:20 at 40 °C for 30 min. After one wash the fabrics were dried with a tumble drier at 60 °C for 30 min. The wash-dry cycles were repeated for 5, 10, 15 and 25 times and then pilling rating was evaluated according to the rating described in Table 1.

Pilling rating	Description
10	few or no fuzz
9	generation of short fuzz
8	increase of short fuzz
7	generation of long fuzz (growth of fuzz)
6	small amount of long fuzz
5	large amount of long fuzz
4	tangle of long fuzz
3	formation of pills
2	small amount of pill
1	large amount of pill

Table 1. Rating of pilling extent**.**

Images of fabric surface: Photo-images of the fabrics were taken with a digital camera (NIKON COOLPIX990) attached to an optical microscope (KRÜSS) at magnifications of 20 and 100.

Fibre/fibre friction: A defined length of 50 mm of yarn was fixed between two clamps of an apparatus to determine the number of counts (Zweigle D315) at a pretension 2 cN. The number of reverse turns T_r required to open the yarn twist to the point of slippage is obtained as experimental result. The experiments were performed at 50 cN of applied force F_R at 20 ºC and 65 % relative humidity (T_{rd}). T_r in wet (T_{rw}) was obtained according to the same method as described above after a yarn was mounted between the clamps and wetted with a few drops of water.

Water retention: A 0.5 g sample of fabric was soaked in distilled water for 24 hr at ambient temperature. After the wet fabric was centrifuged at 4000 G for 10 min the weight was measured (W_w). The sample was then dried at 105 °C for 4 hr and the sample was reweighed (W_d). The water retention (WR_l) was calculated from equation (1).

$$WR\ (g/g) = (W_w - W_d)/W_d \qquad (1)$$

Water regain and BET surface: Moisture regain (WR_m) on the fibre during sorption experiment was gravimetrically measured using an automatic analyzer SPS11 (MESSTECHNIK). The sample mass was approximately 1.0 g and relative humidity (R.H.) was varied from 0 to 90 % R.H. in sorption experiments and decreased from 90 to 0 % R.H. in desorption experiments at intervals of 10 % R.H. at 20 °C. The measurement was continued until the mass change was less than 0.02% at any given R.H.. BET surface (V_m) was calculated according to BET equation [7].

Contraction force: A yarn bundle with a length of 16 cm and 300 strings was mounted on an equipment at a pretension of 294 cN. After 10 min, the pretension was reduced to 49 cN, the bundle was dipped into distilled water for 15 min. The change in the contraction force was detected by a balance and recorded on a computer.

Results and Discussion

In order to clarify effects of domestic wash and dry cycles on the pill formation, fuzz formation and fibrillation, cellulosic knit fabrics were washed and dried 25 times and their surfaces were observed with a microscope. The photographs of the images are shown in Figure 1. Fuzz formed on the fabrics that were dried. Pills formed on the fabrics that were washed and dried. The results indicate that individual processes of washing and drying causes no pill formation. Only when the fabric is treated with both washing and drying, do pills appear. Similar results were obtained for all sample fabrics that were used in the experiments.

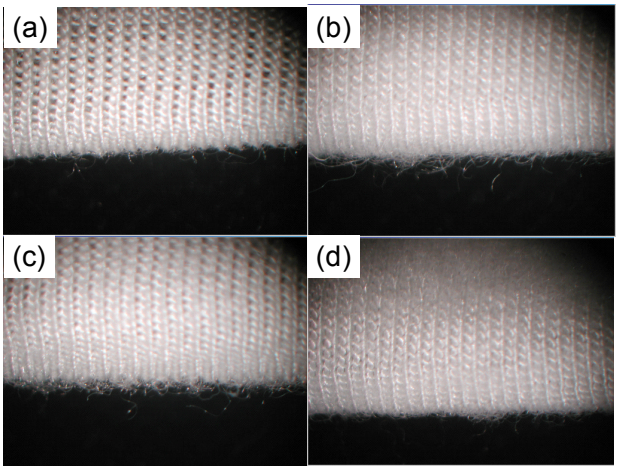

Figure 1. Images of Lyocell 2 knit fabric; (a) untreated, (b) after 25 washes, (c) after 25 dries and (d) after 25 wash-dry cycles**.**

Fibre-fibre friction is an important fibre property because it is expected to relate to pilling property of textiles. In this work, number of turns required to open yarn twist at 50 cN was measured and used to indicate fibre-fibre friction [8]. Higher values of T_r indicate increased fibre/fibre friction. Water retention is also an interesting parameter to indicate water accessibility of fibres [9]. It can help to prepare recipes for dyeing and finishing processes. Water retention was measured by the centrifugal method. Relation between T_{rd}, WR and number of times for wash-dry cycle for Lyocell 1 fabric is displayed in Figure 2.

T_{rd} increases with increase in wash-dry cycles while WR decreases, which suggests that inter-

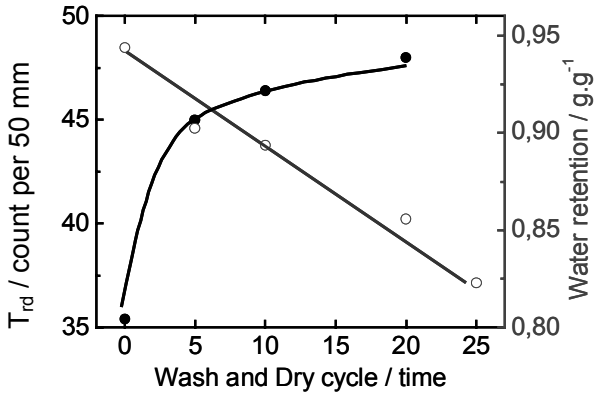

Figure 2. Plots of T_{rd} and water retention against number of times for wash-dry.

fibre and/or intra-fibre structures are changed and get tighter during wash-dry processes. Similar results for the relation between T_{rdry}, WR and the number of wash/dry cycle were obtained for other sample fabrics.

As shown in Figures 1 and 2, pilling property of knitted fabrics could be strongly related to the fibre properties in wet state which are definitely different from dry fibre. Fibre-fibre friction in wet state is a specific parameter to indicate change in fibre properties by water uptake. Water was dropped on the yarn mounted on a device and T_{rw} was counted by a similar method to the measurement of T_{rd}. Change in contraction force which occurs during swelling of fibre with some solvents could also indicate the characteristic fibre properties in wet condition [8]. Moisture regain and BET surface volume at 60 % R.H., and 20 °C were measured. The results are summarized in Table 2.

Material	WR_l	WR_m	V_m	T_{rw}/T_{rd}	Contraction force / g.dtex^{-1}	Pilling rating[1)]
	/ g.g^{-1}					
Lyocell 1	0.943	0.107	0.056	>>	0.45	2
Lyocell 2	0.799	0.097	0.052	1.11	0.59	4
Modal	0.642	0.096	0.054	1.26	0.46	1
Viscose	0.891	0.100	0.056	1.23	0.28	2
Cotton	0.555	0.055	0.029	1.28	0.13	2

Table 2. Relation between water accessibility and pill formation for cellulose fibres**.**

T_{rw}/T_{rd} is a ratio of T_{rw} to T_{rd}. Lyocell 1 fabric having higher WR and V_m shows large T_{rw}/T_{rd} compared to Lyocell 2. This suggests that fibres are swollen due to high capacity of water retention and the adjacent fibres get tight resulting in higher fibre-fibre friction in wet state. Pilling rating for Lyocel 1 fabric after 25 wash-dry is lower (greater pill formation) than that for Lyocell 2. Considering Lyocell 1 has larger value of T_{rw}/T_{rd}, higher swelling could induce much pill formation. Contrary to this assumption, much pill formed on Modal showing lower water accessibility. It could be due to the lower contraction force, which indicates that Modal fibre is softer in swollen state than Lyocell 2 fabric. It is presumed that the pilling property of the fabric is affected not only by water accessibility of the fibre but also

by other mechanical properties such as tenacity, tensile strength and flexural rigidity in wet.

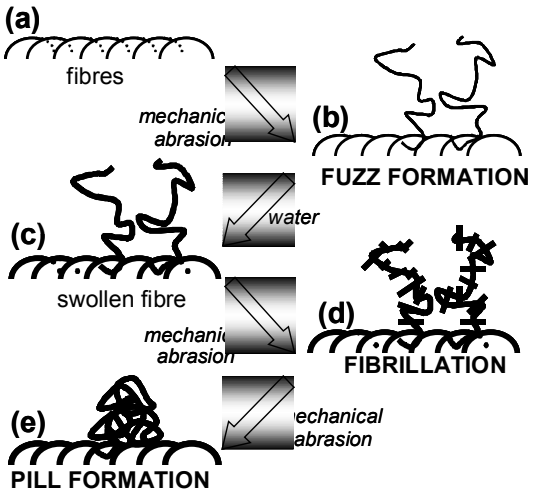

Figure 3. A schematic for a model of pill formation

Considering the relation between fuzz length, extent of fibrillation, fibre-fibre friction in dry and wet, water retention, contraction force, water regain, BET surface volume and pilling assessment, a mechanism of pill formation was suggested. The schematic presentation is given in Figure 3 [9]. Initially a mechanical abrasion is given to fabrics and a fibre end comes out from the inside the yarn, which corresponds to the process between (a) and (b). In this step a fibre having high fibre-fibre friction in dry would suppress fuzz formation. During wash the fibre is swollen, gets softer and fibre-fibre friction gets higher resulting large abrasion force between (b) and (c). A fibre having larger contraction force would show less fibrillation between the steps (c) and (d) because the softened fibre where softness is indicated by contraction force, is easily fibrillated. The fibrillated fibres are easily tangled with each other by mechanical abrasion and grow up to pills as shown by (d) and (e). Consequently, a cellulosic fibre showing large fibre-fibre friction in dry, small fibre-fibre friction in wet, small retention properties of liquid water and water vapour, and large contraction force would have excellent pill formation property.

Conclusion

A model for mechanism of pill formation was proposed for knit fabrics made from regenerated fibres from the results of degree of fuzz, fibril, pill formations after wash and dry, water retention of the fibres, contraction force and water vapour regain in the fabrics. The model suggests that fibre ends come out from inside yarn during dry process with mechanical abrasion and fuzz forms. The fuzz is swollen and gets soft during wash process and easily fibrillated because of the increase in the fibre-fibre friction. The fibrillated fibre is tangled and grows up to pills.

Acknowledgement

We are grateful to the CD-Research Society/Vienna and Lenzing AG for financial support

References

[1] Barella A., Manich A., *Textile Res. J.*, **5**, 314-317, 1984.
[2] Campos, R., Bechtold, T., *Textile Res. J.*, **73**(8), 721-726, 2003.
[3] Ibbett, R. N. and Hsieh, Y. L., *Textile Res. J.* **71**(2), 164-173, 2001.
[4] Latifi M., Kim, H. S. and Pourdeyhimi B., *Textile Res. J.,* **71**(7), 640-644, 2001.
[5] Lenz J., Schurz J. and Wrentschur E., *J. Appl. Polym. Sci.* **35**, 1987-2000, 1988.
[6] Mortimer S. A. and Peguy A. A., *J. Appl. Polym. Sci.,* **60**, 305-306, 1996.
[7] Morton, W. E., Hearle, J. W. S., 1997, "Physical Properties of Textile Fibres", The Textile Institute, UK.
[8] Okubayashi, S., Campos, R., Rohrer, C., Bechtold, T., International Textile Design and Engineering Conference INTEDEC 2003, 2003, Edinburgh.
[9] Okubayashi, S., Bechtold, T., Schuster, C., 3rd Central European Conference 2003, 2003, Portorose.
[10] Paek, S. L., *Textile Res. J.,* **59**, 577-583, 1989.
[11] Zhang, W.-S., Okubayashi, S., Bechtold, T., 13th International Symposium on Cellulose Chemistry and Technology, 2003, Iasi.

Lenzinger Berichte, 82 (2003) 83-95

CORRELATION OF REGENERATED CELLULOSE FIBRES MORPHOLOGY AND SURFACE FREE ENERGY COMPONENTS

Karin Stana-Kleinschek,[a] Volker Ribitsch,[b] Tatjana Kreže,[a]
Majda Sfiligoj-Smole,[a] Zdenka Peršin [a]
[a] University of Maribor, Laboratory for Characterisation and Processing of Polymers, Smetanova 17, 2000 Maribor, Slovenia
[b]Karl Franzens University, Institute of Chemistry, Reology & Colloid Science, Heinrichstraße 28, 8010 Graz, Austria

Abstract

Structural parameters of raw and pre-treated viscose, modal and lyocell fibres were determined using X-ray diffraction, and compared with data obtained from iodine adsorption and tenacity measurements. A good correlation was found between iodine adsorption and structural changes. These structural parameters are correlated with surface thermodynamic parameters obtained by surface tension experiments. Using several liquids of different polarities, the polar and disperse components of the polymers surface free energy were separated. The results obtained indicate that bleaching and mercerisation increases crystallinity and decreases tenacity. Both treatments increase the sorption abilities of all fibres due to a change of the fibre morphology. This is clearly expressed by an increase in polar surface free energies and a reduction -in the disperse components**.**

Key words: regenerated cellulose fibres, x-ray analysis, treatment, structure, tensiometry, surface free energy

Introduction

Regenerated cellulose fibres play an important role in the man - made fibre industry. Essential parameters in cellulose fibres are their chemical primary structure and the resulting fine structure - the amount of crystalline and amorphous regions, the microfibrilar structure and the morphology. They determine the fibres ability to adsorb low molecular weight compounds.

During fibre processing and finishing in aqueous systems, surface parameters such as interaction energies, surface tension and electro-kinetic properties determine the interaction with process components such as dyes, surfactants, ions and finishing chemicals. The fibres very often do not possess the surface properties needed for processing and other applications [3] and therefore various treatments (chemical processes) are applied to change hydrophilicity or hydrophobicity, to increase the number of special functional groups at the surface, for specific interactions with other functional groups (chemical treatments).

Alkaline washing, bleaching and mercerisation (alkaline treatment) are applied to remove hydrophobic impurities and to achieve a high and uniform adsorptivity of textile fibres for water, dyestuffs and finishing agents and a high and uniform degree of whiteness. Changes in fibre structure are observed due to alkaline treatment [32,28,21]. The size of the crystallites is affected and the crystalline orientation is changed when using mercerisation. Orientation is decreased in the case of slack mercerisation and increased when the process is carried out under tension [21]. Regenerated cellulose fibres, especially viscose are rather sensitive to chemical damage. Alkaline peroxide bleaching in the presence of sodium silicate drastically reduces the average molecular weight; sodium hypochlorite bleaching increases the crystallinity and in general the water retention capacity [22].

The differences in cellulose fibre structures (crystalline / amorphous), based on different manufacturing processes and structural modifications caused by processing steps (bleaching, mercerisation) are presented. These structural parameters are correlated with fibres

surface tension, sorption velocity, contact angle and finally the polar and disperse part of surface free energy.

Structure of man made cellulose fibres

Man-made cellulose fibres are produced from regenerated cellulose II which is obtained in two ways, either treating native cellulose with strongly alkaline solutions or precipitation from solutions. These fibres are generally described by a fibrillar structure model [15]. Depending on the spinning conditions, differences in the structural arrangement between different types of man-made cellulose fibres [9,20,9,28] are found, for example different density, crystallite size, crystallite orientation and pore structure. Fibres spun according to the viscose process (CV) have a skin-core structure and a transverse non-uniformity.

More uniform structured and spherical cross-sectioned modal fibres are obtained [9] if a modified viscose process retarding the cellulose regeneration is applied. This process causes increased molecular orientation especially in the crystalline regions and higher stretching ratios compared to the conventional viscose process, leading to high tenacity fibres.

NMMO or lyocell fibres (CLY), produced by the amine oxide process [9] are solvent spun and show characteristic round cross-sections and a smooth surface. Their high degree of crystallinity, molecular orientation and higher molecular weight causes special properties such as high wet fibre strength and comparatively low elongation, leading to the remarkable dimensional stability of fabrics produced from them [32,9,18,23].

No significant differences in the crystallite dimensions are reported, nevertheless the degree of crystallinity differs [9]. Lyocell fibre's degree of crystallinity is 16 % higher than that of modal fibres and much higher (43%) compared to viscose fibres. The fibrils in lyocell fibres are thinner than in CMD and CV fibres and molecular orientation is nearly the same (orientation function of lyocell fibres is 3% higher) as in modal fibres but much higher compared to viscose standard fibres (18%). Lenz and Schurz [15] determined the size of crystalline regions of regenerated cellulose fibres: length 12 - 14 nm, width 8 - 10 nm, and thickness 3 - 4 nm. The broad plane of the platelet-shaped crystallites is situated parallel to the $10\bar{1}$- lattice plane. The crystallites form strands with a length of 150 nm - 550 nm. They are partly bundled up in clusters with diameters of 30 - 60 nm, partly separated by less dense spacing regions.

Surface Tension

The above discussed crystallites size, orientation and distribution as well as the presence and size of amorphous regions and voids (void volume, inner surface) [19] are the parameters that determine the fibres adsorption and interaction abilities.

Polar and non-polar groups cause fibre's hydrophobic and hydrophilic nature obtained by various treatments. A lack of hydrophilicity is either due to the absence of polar groups or due to their non-accessible locations. The degree of hydrophilicity or wetting of a non-porous solid by a liquid is observed in two ways, either measuring the contact angle θ directly using goniometry or calculating it from data obtained by tensiometry.

From the known contact angle or the help of indirect methods [3,39] the surface energy of solid can be determined [3,25,27,36,40] and separated into a polar and a disperse part, according to the following considerations: If a liquid and a solid surface come in contact, an interaction between the polar parts as well as the disperse parts of both phases will take place at the interphase, but not between the polar and the disperse parts [14]. The interfacial tension of the two phases in contact is always lower than the total surface tension of separate phases due to interactions at the interphase. If one of the two phases in contact is non-polar, only dispersion interactions are possible. While dispersion forces exist in all molecules, the polar forces only exist in special molecules. They arise from the difference in electro negativity between different atoms in the same

molecule [14]. Therefore one can determine the polar and disperse part of the surface free energy measuring the contact angle between a solid and several liquids of different polarity [14,27].

Material and methods

Fibres and fibres treatment processes

One solvent spun cellulose fibre (Lenzing Lyocell - CLY) and two conventional cellulose fibres made by the viscose process (Lenzing Viscose CV and Lenzing Modal CMD) were investigated and are summarized in Table 1.
The fibres were treated using a Turbomat Ahiba laboratory dyeing apparatus according to the processes conventionally used in textile praxis (Table 2). The alkaline treatment was performed without any tension on the fibres (usually called slack mercerisation); we will refer to it as "mercerisation".

Fibre type	**Viscose**	**Modal**	**Lyocell**
Symbol	CV	CMD	CLY
Linear density T_t [dtex]	1.88 ±0.15	1.78 ±0.23	1.82 ±0.3
Fibre length l [mm]	39.9 ±0.51	40.1 ±0.33	39.4 ±0.44
Fibre diameter d [µm]	14.3 ±1.39	14.2 ±1.10	12.8 ±1.00
Density ρ [g/cm^3]	1.5045	1.5141	1.5205
Degree of polymerisation DP_η	235 ±5.13	507 ±3.61	642 ±4.58
Molecular mass M_η	38.000 ±880	82.100 ±540	104.000 ±730

Table 1. The specifications of investigated regenerated cellulose fibres

X-Ray analysis

The influence of different treatment processes, e.g. bleaching and slack mercerising (alkaline treatment), on the structural changes in different types of regenerated cellulose fibres was investigated by means of x-ray analysis, the procedure is described in detail in several references [24,1,6,2,29,34,35]. Ni filtered copper radiation from a conventional x-ray tube (50 kV / 45 mA) was used in all scattering experiments.

Bleaching	**Alkaline treatment**
6 ml/l H_2O_2	40 g/l NaOH
2 ml/l Tanatex Geo (mineral stabilizer for H_2O_2 stabilization)	7 ml/l Tanawet BC (wetting agent, anionic)
pH = 10.7	pH = 12.8
t = 30 min	t = 1 min
T = 98° C	T = 10°C

Table 2. Conditions of the treatment processes - bleaching and slack mercerisation (alkaline treatment without tension)

Determination of the long spacing by small angle x-ray scattering (SAXS). SAXS intensity curves were measured using a Kratky camera with a slit collimation using a PSD position sensitive detector counting scattered intensity in the meridional direction, i.e. parallel to the fibre axis. The experimental data was corrected for absorption and background scattering and long spacing was determined applying Bragg's law:

$$L = \frac{n.\lambda}{2.sin\theta} \qquad (1)$$

where L is the long spacing, n order of reflection, λ wavelength of x-rays and θ Bragg's scattering angle.

Determination of the crystallinity index and crystalline orientation by wide-angle x-ray scattering (WAXS). A two-circle goniometer equipped with a linear position sensitive detector (PSD was used to measure the two-dimensional WAXS scattering diagrams (azimuthal angular range from 0° to 180° in steps of 5°). The full pattern after the subtraction of the background scattering and the absorption and some steps of the evaluating procedure for one of the analysed fibres are presented in Figure 1.

A weighted integration of the two dimensional diagram (Eq.2) was performed to obtain a „randomized" scattering I(2θ) curve, which was corrected for Compton scattering.

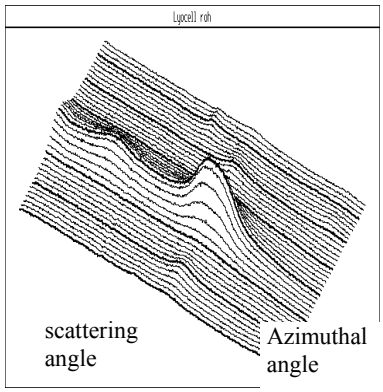

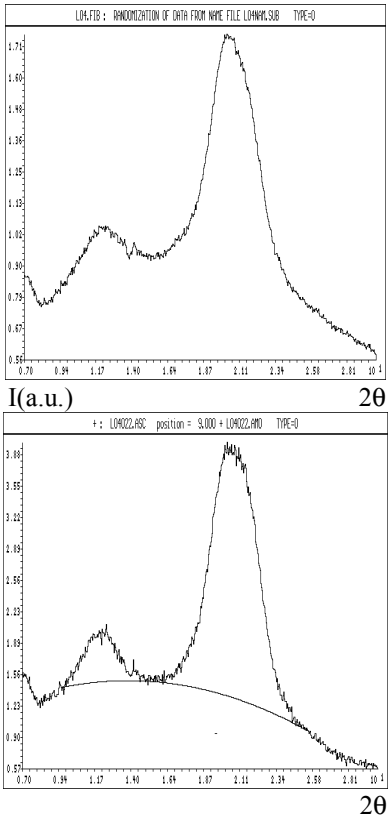

Figure 1. The full pattern for an analysed fibre, randomised curve and the separation of the crystalline and amorphous scattering

$$\bar{I}(2\theta) = \frac{\int I(2\theta(\varphi)\sin(\varphi)d\varphi}{\int \sin(\varphi)d\varphi} \qquad (2)$$

The amorphous contribution was approximated by a polynomial approximation and the curves were than analysed for crystallinity. The degree of crystallinity x_{cr} was estimated by the ratio of the crystalline scattering versus total scattering (Eq.3) [1,6]:

$$x_{cr} = \frac{\int_{2\theta_1}^{2\theta_2} I_c(\theta).\, d\theta}{\int_{2\theta_1}^{2\theta_2} I(\theta)\, .d\theta} \qquad (3)$$

where I is the entire coherently scattered intensity, I_c is the coherent intensity in the crystalline peaks and 2θ = diffraction angle.

The orientation parameter f_c was determined through the integral azimuthal distribution-width of the 101 reflections and Hermans' orientation function f_c was calculated according to:

$$f_c = \frac{3.\overline{\cos^2\varphi} - 1}{2} \qquad (4)$$

where φ is the angle between the c crystallographic axis and the fibre axis.

A strong interference of (101) and (021) crystalline reflection existed, therefore, an approximation using Gauss and Lorentz distribution was carried out to separate the two maxima as shown in Figure 2, and determination of the azimuthal intensity distribution of (101) reflections followed.

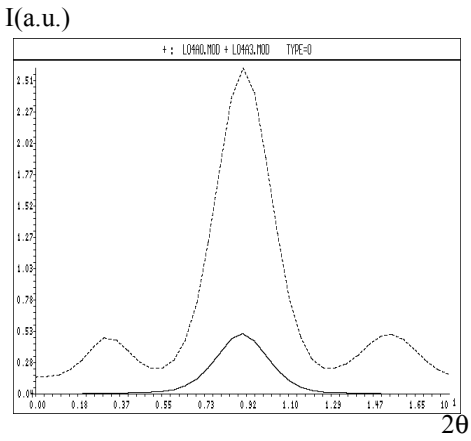

Figure 2. Approximation of the (101) and (021) crystalline reflections by Gauss and Lorentz distribution after the subtraction of amorphous background

Iodine sorption

The Schwertassek method was used for determining iodine-sorption [31,28]. The fibres were first treated with KJ_3 solution and afterwards the concentration of non-absorbed iodine was determined by titration. Iodine sorption value ISV is the amount of iodine adsorbed by one gram of cellulose substrate. It is calculate in the following way:

$$ISV = \frac{(a - b \cdot 1{,}33) \cdot F \cdot 2{,}538}{m_a} \quad (5)$$

where a is volume [ml] of $Na_2S_2O_3$ solution (c = 0.01 mol/l) for aliquot of blank KI solution, b is volume [ml] of $Na_2S_2O_3$ solution (c = 0.01 mol/l) for aliquot of sample solution, c is constant (for cellulose: 1.33), F is aliquot factor of $Na_2S_2O_3$ solution, determined by $KMnO_4$ (0.02 mol/l) and m_a is weight of absolutely dry fibre sample [g].

Mechanical properties

Stress-strain curves were measured using a Vibrodyn 400 dynamometer (Lenzing Technik Instruments) with a length between the clamps of 20 mm according to ISO 2062, linear density was determined using a Vibroskop 400 (Lenzing Technik Instruments). Testing conditions were T = 20ºC, Rh = 65%, the presented data are averages from 10 experiments.

Sorption measurements

Sorption measurements were carried out with fibres (raw and treated) placed in a cylindrical cell coming in contact with fluids of different polarity. The mass increase as a function of time (capillary velocity in a fibre plug) was monitored as described in earlier publications [4]. The results presented are statistically processed average values of 10 parallel measurements. The liquids (water, ethylene glycol, formamide, ethanol, and n-heptane) used in the sorption experiments (tensiometry) were chosen because of their specific polarities [12] which are appropriate to calculate contact angles and solid's surface energies from measured capillary velocities. A Krüss Tensiometer K12 GmbH Hamburg was used for these gravimetric measurements.

Calculation of contact angle and surface free energy. The modified Washburn Equation 1 [26,28,38] allows to calculate the contact angle θ from measured sorption velocities:

$$\cos\theta = \frac{mass^2}{t} \cdot \frac{\eta}{\rho^2 \cdot \gamma \cdot c} \quad . \quad (6)$$

$$c = \frac{1}{2} \cdot \pi^2 \cdot r^2 \cdot n_k{}^2 \, . \quad (7)$$

where $mass^2/t$ represents the sorption velocity (g^2/s), η is liquid's viscosity (mPa.s), ρ is liquid's density (g/cm^3), γ is the liquid's surface tension (mN/m), θ is contact angle between solid and liquid phase (°), c is material constant or c factor, r is the capillary radius (m), and n_k is number of capillaries.

The fibre's surface energy (γ_s) was determined indirectly - from the contact angle data. According to Young's Equation (3), the surface energy of a solid is given as [13]:

$$\gamma_s - \gamma_{SL} = \gamma_L \cdot \cos\theta \quad (8)$$

where γ represents surface tension of the solid (s) (mNm^{-1}), SL the solid-liquid interface, L the liquid and θ (°) is the contact angle between the solid and liquid phase.
Fowkes [7] proposed that the surface energy of a liquid or a solid could be separated into a disperse and a polar component:

$$\gamma_s = \gamma_s^d + \gamma_s^p \quad \gamma_l = \gamma_l^d + \gamma_l^p \quad (9, 10)$$

where γ represents the surface energies (mJm^{-2}) of the solid (s), and liquid (l) with the disperse part (d) and the polar part (p). The interfacial energy of liquids and solids with both disperse and polar components are described as [13]:

$$\gamma_{SL} = \gamma_S + \gamma_L - 2\sqrt{\gamma_s^d \gamma_L^d} - 2\sqrt{\gamma_s^p \gamma_L^p} \quad (11)$$

Introduction of the work of adhesion [36] and conversion leads to an equation of the type: $y = mx + b$

$$\frac{1 + \cos\theta}{2} \frac{\gamma_L}{\sqrt{\gamma_L^d}} = \sqrt{\gamma_s^p} * \sqrt{\frac{\gamma_L^p}{\gamma_L^d}} + \sqrt{\gamma_s^d} \quad (12)$$

The values γ_l, γ_l^d and γ_l^p are known material constants and the values of x and y can be determined. From the linear fit of the plot y versus x one gets the polar (Equation 13) and disperse (Equation 14) component of surface free energy [14,30]:

$$\gamma_s^p = m^2 \qquad (13)$$

$$\gamma_s^d = b^2 \qquad (14)$$

Results and discussion

X-Ray analysis

Small angle X-ray scattering SAXS. All types of regenerated cellulose fibres exhibit a well-defined maximum on the meridional SAXS diagram (Figure 3) indicating periodical structures due to alternation of crystalline and amorphous regions along the fibre axis. The long period values were calculated (Table 3) from the peak position and are almost similar for all untreated fibres (approx. 13.5 nm). This This This finding is in good agreement with the values reported [8,17]. Fibre's treatment in alkaline solution or a bleaching medium causes distinct changes. In the case of viscose fibres an increase of the long spacing for about 15% occurs regardless of the treatment conditions applied. Modal fibres show a significant change of long spacing (by about 15%) only in case of alkaline treatment. The opposite effect was observed with lyocell fibres showing a decrease of long spacing of about 10% (bleaching) and 5% (mercerisation).

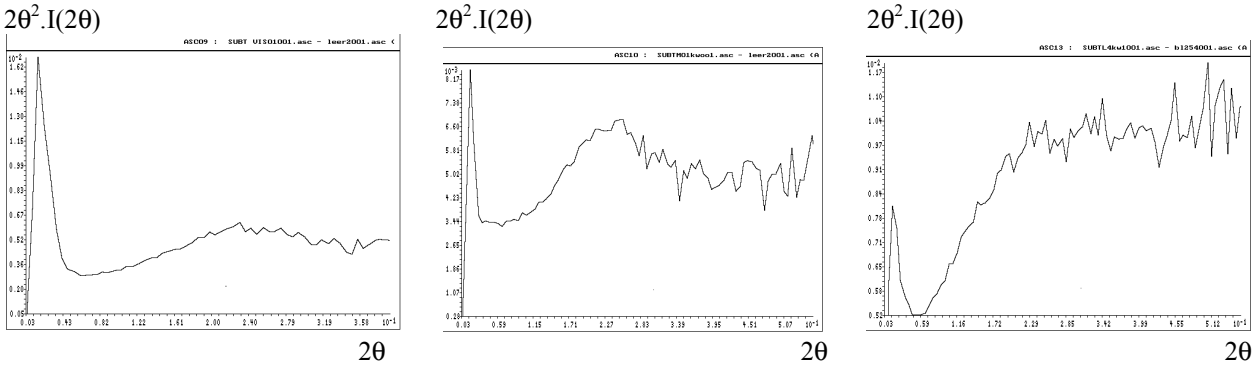

Figure 3. Plot of $2\theta^2$. I(2θ) vs. 2θ of meridional SAXS curve for the untreated viscose, modal and lyocell fibres, respectively.

Viscose fibres are of low crystallinity but highly accessible to different media due to their mainly amorphous molecular arrangement and an extensive inner surface. This morphology enables a better sorption of water and low molecular species, compared to the two other fibres [11,28] causing major structural reorganization shown by the changes in long spacing.

Cellulose molecules in CMD fibres are well oriented, have a higher degree of polymerisation and are densely packed. A non-extensive void system is formed because of the spinning process at high drawing ratios [9]. This structural parameter is the reason for the lower hydrophilic capacity of modal fibres in comparison to viscose or lyocell fibres. Mercerisation is the only treatment process that causes significantly increased long spacing and promotes the swelling process.

Lyocell fibres have a more complicated structure. They show high hydrophilicity caused by the fibres larger void system (comparable with viscose) and not by the fibre's superstructure. It was shown that water swollen solvent spun fibres contain more separated elementary fibrils and less non-swelling clusters than fibres spun from cellulose derivates [17]. The interstices that separate single elementary fibrils, the interfibrillar and intrafibrillar voids are accessible to water, sodium hydroxide and other treating media. The dense fibre inner structure prevents major structural reorganization if the lyocell fibres are bleached or mercerised without tension. Swelling does not create new voids nor do existing voids disappear; only the voids diameter is increased [16]. In the case of viscose and modal fibres the increase of long spacing is accompanied by a more pronounced crystallinity increase that could additionally influence changes in the periodical structure.

Fibre	Treatment	Long period nm	Crystalli-nity index x_{fc}	Orientation function f_c	*Voids volume cm^3/g	*Voids diameter nm	*Inner surface m^2/g	Tenacity cN/tex
Viscose	untreated	13.5	0.25	0.580	0.68	3.1	439	22.0
	bleaching	15.5	0.25	0.494				20.0
	mercerisation	15.6	0.38	0.722				19.5
Modal	untreated	13,5	0.37	0.706	0.49	2.4	409	34.0
	bleaching	13.7	0.44	0.583				32.0
	mercerisation	15.5	0.57	0.561				30.5
Lyocell	untreated	13.8	0.44	0.664	0.62	3.0	432	33.0
	bleaching	12.3	0.46	0.677				34.5
	mercerisation	13.0	0.50	0.768				27.0

Table 3. Long periods, crystallinity index, Herman's orientation function, *voids volume, diameter and inner surface of voids (determined using Size Exclusion Chromatography) and tenacity of untreated and treated fibres

Wide angle X-ray scattering WAXS. All analysed fibres show intensive scattering with negligible differences between the solvent spun and the two other fibre types. Fibre treatment always causes separation of the scattering function's peaks. The obtained results are presented in Table 3, one example of the randomised scattering curves of viscose is shown in Figure 5.

Crystallinity index. The crystallinity index (Figure 6) of viscose and modal fibres differ as expected, viscose has a lower crystallinity (0.25) than modal (0.37), lyocell fibres have the highest crystallinity index of 0.44. Any kind of treatment significantly increases the crystallinity index, which agrees very well with those results given in the literature [15].

Lyocell fibres are more stable than viscose or modal fibres in alkaline medium and therefore crystallinity increase is more pronounced for derivate spun cellulose fibres in comparison to solvent spun fibres. Viscose fibres crystallinity index is strongly dependent on the treatment conditions with an almost negligible increase caused by bleaching and a large increase caused by mercerisation (52%).

The bleaching of viscose fibres may cause some oxidative damage and therefore a limited increase of crystallinity, nevertheless, it causes a significant increase of long spacing.

A more pronounced crystallinity increase is observed after the bleaching of CMD (19%) and a strong one (53%) after alkaline treatment. Longer cellulose molecules in CMD fibres are less sensitive and more resistant to oxidative damages and therefore the influence of the alkaline environment predominates and an increase of crystallinity is observed.

The large degree of polymerisation of about 640 and the more complex structure are the reasons why lyocell fibres are more stable under any of the treatment conditions. A comparable small increase of crystallinity index occurs, however, and a correlation between the pH value of the treating medium and the crystallinity increase can be assumed. The pH value at bleaching is 10.7 and at mercerisation 12.8, the increases of crystallinity 5% and 14%, respectively.

Iodine sorption data confirms the X-ray results of crystallinity changes (Figure 7) especially when chemical changes caused by the oxidative bleaching process are taken into account. The lower the ISV the higher is the degree of crystallinity. This data also show that there are only very small differences in lyocells crystallinity caused by both treatments. However, the degree of cellulose products oxidation influences the iodine sorption.

Crystalline orientation. Fibres reactivity and accessibility as well as tensile properties are mainly influenced by crystalline orientation. This parameter shows such different trends for each fibre type, that no unique model for its explanation could be established. Warwicker

[37] has reported that the extent of crystallites disorientation in cotton depends on the extent of swelling and this may also be true for regenerated cellulose fibres

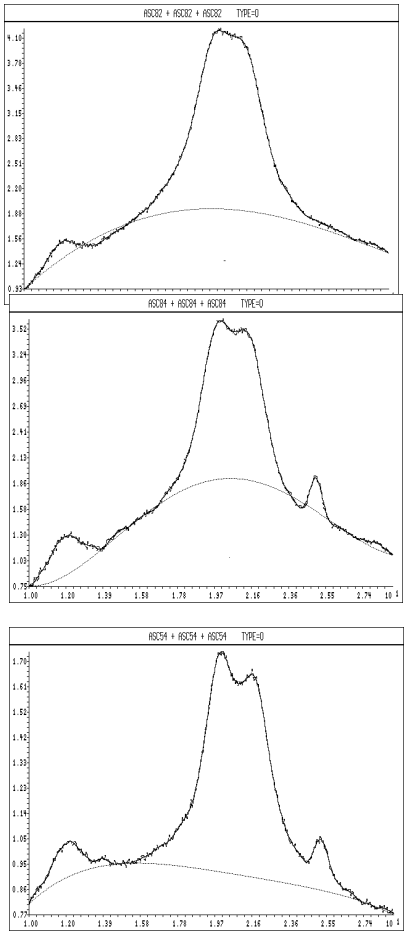

Figure 5. Randomised scattering curves with amorphous scattering for untreated, bleached and mercerised viscose fibres

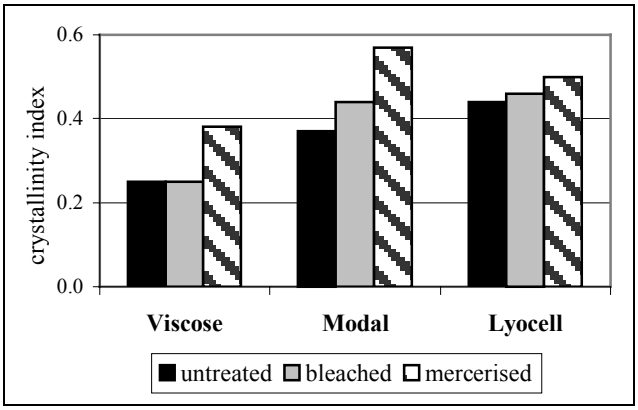

Figure 6. Crystallinity index of untreated and pre-treated regenerated cellulose fibres

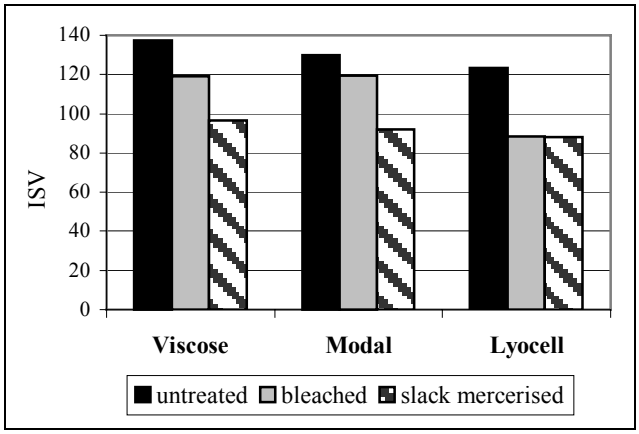

Figure 7. Iodine sorption value of untreated and pre-treated regenerated cellulose fibres

. The results of crystalline orientation for treated regenerated cellulose fibres are presented in Figure 8.

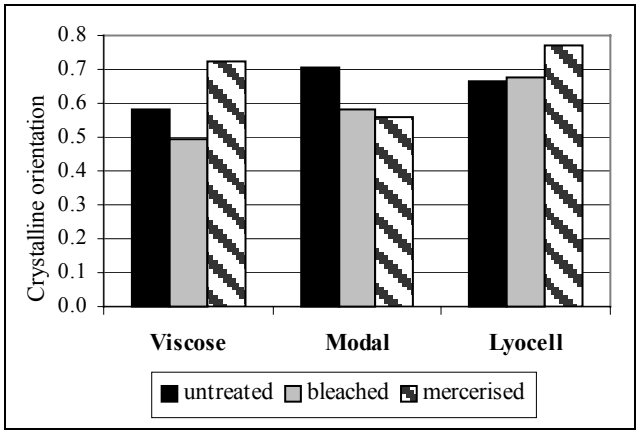

Figure 8. Crystalline orientation of untreated and pre-treated regenerated cellulose fibres

Different degrees of crystallites orientations of untreated fibres were expected and finally observed because it is conditioned by the differences in production processes. The orientation increases from CV to CLY and CMD. This does not correlate with earlier results, where CLY showed the highest degree of orientation [33], but it correlates well with the tensile strength reported here and explains the high tensile strengths of CMD and CLY fibres (Figure 9). Disorientation due to molecular relaxation is observed with viscose and especially modal fibres in the case of the bleaching process and happens also by the mercerisation of CMD. The increase of viscose fibres orientation due to mercerisation may be

promoted by high internal swelling under strong alkaline conditions in the treatment. It is connected with the penetration of the medium into the crystalline structures and, thereby, the crystalline reflections are extended. The same phenomenon is observed with lyocell fibres due to their high hydrophilicity, but to a lower extent because of lyocell fibre's more stable structure.

The changes in fibres tensile strength also correlate with crystallinity index and crystallites orientation. It is presumed that changes in the crystalline structure are also accompanied by changes in the amorphous domains. One explanation of our findings may be that the increasing crystallinity reduces the number of polymers strands in the amorphous area and this may be the reason of the decreased strength. The chemical influence (depolymerisation) under the treatment conditions will be an additional reason for the changed mechanical properties (Figure 11).

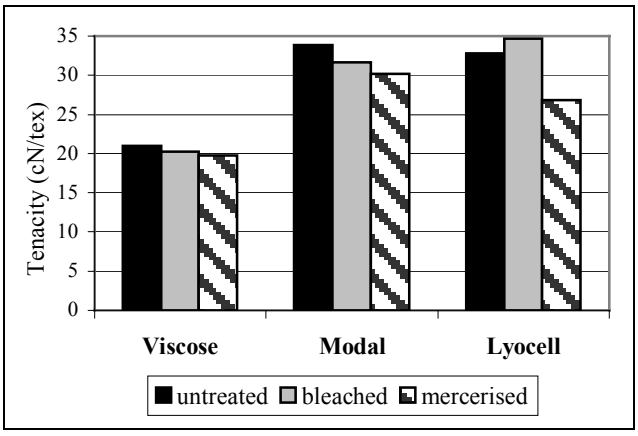

Figure 9. Mechanical properties of untreated and pre-treated regenerated cellulose fibres

Sorption measurements

Sorption velocity was measured using the fibre plug method and contact angles were calculated from these results. Figure 10 and Table 4 present the water sorption velocities of raw and mercerised viscose, modal, and lyocell fibres.

The observed sorption velocities show distinct differences between raw and mercerised fibres. Among raw fibres, viscose fibres have the fastest sorption velocity, even if the sorption velocity of modal fibres is the highest at the very beginning.

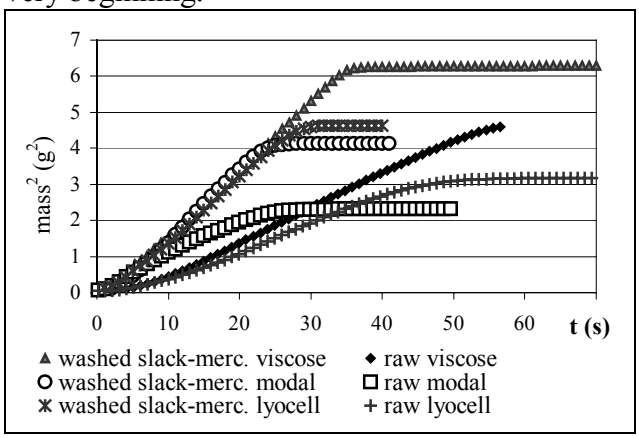

Figure 10. Water sorption velocities of raw and mercerised viscose, modal, and lyocell fibres.

CV adsorbs the greatest amount of water (133% of the fibres mass) due to the large amorphous regions and predominantly void systems. Raw modal fibres have the smallest sorption ability and a sorption velocity differing from the usual quadratic increase. It is very fast and non-linear at the beginning and approaches a linear increase before saturation. Calculated from that linear range it is found to be 2.2 times slower as compared to raw viscose fibres. Raw modal fibres adsorb the smallest amount (64%) of water because of their higher crystallinity index, better-orientated macromolecules and the smallest void system [11]. The diameter, volume and inner surface of the lyocell fibre's voids are similar to those of viscose [9], and so are the sorption characteristics. Raw lyocell fibres adsorb water 1.5 times slower, compared to viscose and 1.1 times faster compared to modal fibres. After water uptake their weight increases by 88 %.

The sorption abilities of all fibres are increased after mercerisation. The sorption velocity becomes almost identical although the amount of adsorbed water differs clearly. The mercerised viscose fibres are able to adsorb the greatest amount of water (177 %) at a 2.6 times higher speed then raw fibres. The adsorption speed of mercerised modal fibres is also increased; nevertheless they adsorb the smallest amount and show the smallest increase after treatment. Again, the reason for these differences is based on their structural and

morphological characteristics, the increased degree of crystallinity, high degree of polymerisation and molecular orientation and the smallest void system.

Fibre	Sorption velocity* (g^2/s)	Contact angle (°)	γ_s^p (mJ/m^2)	γ_s^d (mJ/m^2)
Raw viscose	0.089	80.66	25.54	8.24
STDEV	1.6E-03	1.16	0.28	0.25
Mer. viscose	0.175	69.26	39.95	5.46
STDEV	5.0E-04	0.89	3.16	3.13
Raw modal	0.052	82.38	25.01	7.99
STDEV	1.0E-04	2.36	3.40	3.13
Merc. modal	0.150	72.92	35.43	5.26
STDEV	1E-04	1.69	3.11	2.93
Raw lyocell	0.063	81.06	25.36	8.03
STDEV	9.5E-05	2.87	3.34	3.11
Merc. lyocell	0.157	71.52	36.69	5.41
STDEV	1.0E-04	1.29	3.16	2.96

Table 4. Sorption velocities, contact angles, polar and disperse components of the SFE of the raw and washed slack-mercerised viscose, modal and lyocell fibres.
* -calculated in the linear part of the slope

Due to the inner surface, diameter, and volume of the mercerised lyocell fibre's voids, they are able to adsorb more water then CMD fibres, beside the fact that they have the most crystalline structure [11]. In comparison to raw fibres, the mercerised lyocell fibres have a 5 times higher sorption velocity and after water absorption their weight increases by 133 %.
Comparing all three types of fibres, mercerisation caused an increase of absorption speed and amount and reduced the time needed to complete fibre wetting. The adsorption speed is almost identical; this correlates with the fact, that mercerisation reduces the differences in crystallinity index and crystalline orientation. The amount of adsorbed water correlates with the voids systems volume.

Contact angles

Contact angles were determined from the measured sorption velocities and using the modified Washburn Equation 1 [4]. The values of the contact angles define the wetting behaviour of the measured fibres (Figure 11, Table 4). Results are presented as average value of 10 parallel measurements.

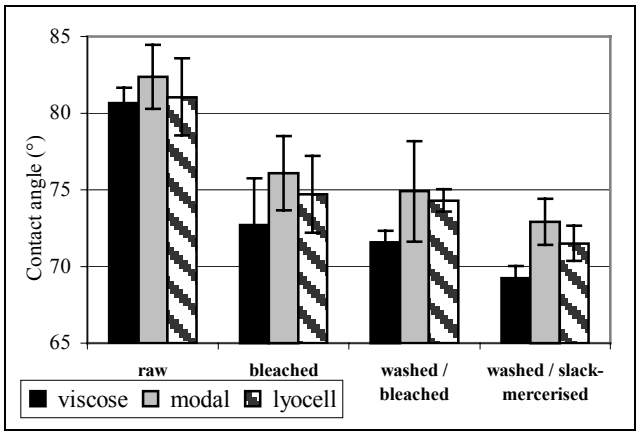

Figure 11. Water contact angles of raw and treated viscose, modal, and lyocell fibres as affected by the applied treatment.

Viscose fibres have the lowest degree of polymerisation, the lowest degree of crystallinity [9], and a large amount of amorphous regions [11,9], therefore showing the best wetting and sorption properties. Modal fibres have the smallest sorption ability because of a higher degree of crystallinity and crystallite orientation and a smaller ratio between crystalline and amorphous phases in comparison to viscose [9]. Lyocell fibres have, in comparison to viscose fibres, a higher degree of crystallinity, better orientation, and higher proportion between the crystalline and the amorphous phases (9:1) [9,9]. The lyocell fibres are, with regard to wetting and sorption ability, almost similar to viscose fibres despite the higher amount of crystalline phase.
Bleaching and mercerising decreased the contact angles (Figure 11), while the sorption velocities increased (Figure 10), resulting in a better sorption behaviour of the fibres. The result of bleaching is a 9% decrease, the use of mercerisation results in a 14% decrease of the contact angles. The reason of the contact angle's decrease is due to changes in the fibres structure. Mercerisation probably enlarges the area accessible for the aquatic medium, the bleaching process generates new groups (aldehyde, ketones, carboxyl), which are able to provide increased polar interactions with polar liquids.

Surface free energy – polar and disperse component

The calculated values of the contact angles between the fibres and liquids with known polar and disperse parts of surface tension were used to determine fibres surface free energy (SFE). According to equation 7 a linear correlation is obtained, whose slope is proportional to the polar and whose intercept to disperse part of SFE. There are no significant differences among the raw fibres, although the viscose fibres had the highest polar part of the SFE (25.54 ± 0.6 mJ/m^2), followed by lyocell (25.36 ± 6.29 mJ/m^2) and finally the modal (25.01 ± 7.07 mJ/m^2). The applied treatments increased the polar components of the fibres SFE. Bleaching has influence on the viscose fibres; it increased the polar component by 18.7%, while it had a smaller effect on modal fibres; the increase is only 5.4%.

Among all treatments, mercerisation has the biggest influence on all fibres. The mercerised viscose fibres have the biggest polar component (39.95 ± 6.55 mJ/m^2); it is 56.4% increased compared to raw samples. The mercerised lyocell fibres follow (36.69 ± 6.54 mJ/m^2) with 44.7% increase, and finally the mercerised modal fibres (35.43 ± 6.42 mJ/m^2) with 41.76% increase to raw samples.

Just the opposite trend but a less pronounced one is observed for the disperse components of the SFE (Figure 12, Table 4). Raw viscose fibres have the largest disperse component (8.2 ± 0.87 mJ/m^2), followed by lyocell fibres (8.0 ± 0.65 mJ/m^2), and modal fibres (8.0 ± 0.65 mJ/m^2).

The treatments have an almost similar reducing effect on the disperse components of all fibres. Bleaching decreased the disperse components, most of all for viscose (26.1%), followed by modal (24.7%), and lyocell fibres (19.7%).

Mercerisation caused the biggest decrease in viscose (33.7%) and modal fibres (34.2%); lyocell fibres are less influenced (32.6%).

The reason for the less influenced polar component is the structure of the modal fibres. They have higher density but lower void volume and inner surfaces [9] in comparison to viscose and lyocell fibres, so that treatments cause only a slight modification in the structure.

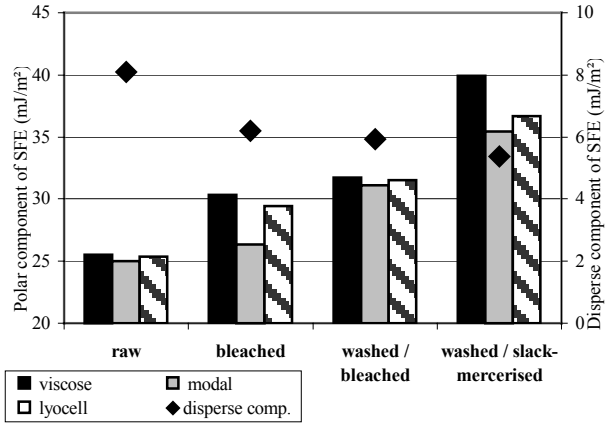

Figure 12. Polar and disperse components of the surface free energy of raw and treated viscose, modal, and lyocell fibres. The disperse components are the averaged values of all three fibres, because they do not differ significantly

The reason for the decrease of SFE´s disperse component are the increased number of polar groups created by the oxidation process and the increased accessibility for aqueous medium created by mercerisation. Viscose and lyocell show similar trends, caused by the similarity in diameter, volume and inner void surfaces.

Conclusions

We have studied the morphology, tensile strengths, sorption ability, polar and disperse surface free energy components of raw and treated man made cellulose fibres.

The fibres morphology depends on the fibre-forming process. The solvent spinning technique (NMMO fibre Lyocell) produces a highly crystalline (crystallinity index app. 0.44) and oriented fibre (f_c = 0.66). Crystallinity indices of high tenacity modal (0.37) and conventional viscose fibre (0.25) are closer, but there exist a significant difference in orientation function between these two types of fibres (CV 0.58, CLY 0.66). High levels of orientation are associated with the high tensile strengths of CMD and CLY fibres.

Sorption properties show a behaviour, which can be correlated with the differences in morphology. CV is able to adsorb the greatest amount of solvent and low molecular weight species (iodine). This is caused by a large amount of amorphous phase (crystallinity index = 0.25), and a large volume, diameter, and inner surface of voids. The polar component of SFE indicates a similar great number of accessible polar groups as in the case of CLY, which are able to interact with polar liquids.

CMD adsorbs the smallest amount of solvent and low molecular weight species; has the largest contact angle, and the smallest polar component of SFE. This is caused by the rather dense structure; the smaller void volume and inner surface area even if the degree of crystallinity is smaller than that of CLY.

CLY fibres sorption velocity is higher than CMD; they have contact angles and polar components of SFE similar to CV. The high hydrophilicity is caused by the fibres void system and not by the fibres superstructure, nevertheless the void system is less accessible for iodine adsorption.

The applied conventional treatment processes influence the fibres fine structure, increasing the crystallinity index and decreasing the tenacity. The changes in fine structure are especially pronounced in CV and CMD due to the chemical changes caused by alkali treatment. Crystallinity index increases as much as 51%. Lyocell fibres have a more complicated structure and are less affected with respect to the crystallinity index. The dense fibre inner structure prevents major structural reorganization. These findings are also reflected by the iodine adsorption. The influence on the crystalline orientation differs, it increases in the case of the less oriented CV and CLY, but decreases in case of the most oriented CMD fibres.

Mercerisation has the biggest influence on the sorption properties of all three types of fibres. The tensionless alkali treatment most likely causes an increase of the inner surface and the number of polar groups accessible for polar liquids. Hence an increase of the sorption velocities (≈115%) and the total SFE of the fibres follows, mainly due to the increase of the fibre's SFE polar component (≈48%). Bleaching causes less changes in fibres supra-molecular structure but it increases the SFE´s polar component by 20%. This is the consequence of the increased number of polar groups created by the oxidation process [5].

A good correlation between iodine adsorption and structural changes was observed. The increase in crystallinity decreases the accessibility of fibres and, thereby, the sorption of iodine becomes lower. The observed structural changes are not pronounced enough to significantly influence fibre's mechanical properties, with the exception of alkali treated CMD and CLY fibres where a significant decrease of tenacity was observed.

Viscose fibres (raw and treated) have the fastest sorption velocities, the lowest contact angle and the highest polar part of the SFE, and are therefore the most hydrophilic among regenerated cellulose fibres due to their structure (the greatest volume, diameter, and inner surface of voids) and above all due to the highest contribution of the accessible groups which are able to interact with polar liquids.

References

1. Alexander, L.E.: *X-Ray Diffraction Methods in Polymer Science,* Wiley Interscience New York, 1969.
2. Bodor, G.: *Structural Investigation of Polymers*, Ellis Horwood, New York, 1991.
3. Chan, C.M.: *Contact Angle Measurement, in Polymer Surface Modification and Characterization*, Hanser/Gardner Publications, Inc., Cincinnati, 1994, pp 35-45.
4. Filipič, Z., Stana-Kleinschek, K., Kreže, T.: *Tekstilec,* **2000**, 43 **(**7/8), 245-250.
5. Fras, L., Stana-Kleinschek, K., et.al.:*Tekstil*, **2000**, 52, 6, 263-276.
6. Glatter, O., Kratky, O.: *Small Angle X-ray Scattering*, Academic Press, London, 1982.
7. Gould R.F.: *Dispersion Force Contribution to Surface and Interfacial Tensions, Contact Angles, and Heats of Immersion*, in

"Contact Angle, Wettability and Adhesion," No. 43, American Chemical Society: Washington, DC, 1964, p 99.
8. Kiessig, H.: *Das Papier*, **1958**, 12, 117
9. Krässig, H.A.: *The Fiber Structure, in "Cellulose, Structure, Accessibility and Reactivity*," Gordon and Breach Science Publishers, Switzerland, 1992, pp 7-42.Kreže, T., Malej S.: *Text Res. J.,* **2003**, 73, (8), 675-684.
10. Kreže, T., Strnad, S., Stana-Kleinschek, K., Ribitsch, V.: *Mater.Res.Innov*., **2001**, 4**,** **(**2/3), 104-114.
11. Kreže, T., Stana-Kleinschek, K., Ribitsch, V.: *Lenzinger Berichte,* **2001**, 80, 28-33 .
12. Krüss: Test liquid main database.
13. Le, C.V., Ly, N.G., Stevens, M.G.: *Text Res. J.,* **1996,** 66, 389-397.
14. Lechner, H.: Die Kontaktwinkelmessung-Ein Verfahren zur Bestimmung der freien Grenzflächenenergie von Festkőrpern, Proceedings at the Universität für Bodenkultur, Wien, 1994, 12-17.
15. Lenz, J., Schurz, J.: *Cellulose Chem. Technol.,* **1990**, 24, 3.
16. Lenz, J., Schurz, J.: *Cellulose Chem. Technol.,* **1990**, 24, 679.
17. Lenz, J., Schurz, J., Wrentschur, E., Geymayer, W.: *Die Angewandte Makromolekulare Chemie,* **1986**, 138, 1.
18. Lenz, J., Schurz, J., Wrentschur, E.: *Colloid PolymSci*, **1993**, 271, 460.
19. Lewin, M., Sello, S.B.: *Interaction of Aqueous system with Fibers and Fabrics, in "Fundamentals and Preparation*"; Vol. 1, Part A, Marcel Dekker, Inc., New York and Basel, 1983, pp 57-58.
20. Lewin, M., Pearce, E.M.: *Handbook of Fiber Chemistry*; Marcel Decker, New York, 1998.
21. Lewin, M., Sello, B.S.: *Handbook of Fibre Science and technology,* Volume I, Marcel Dekker, New York Basel, 1983.
22. Lewin, M., Sello, B.S.: *Handbook of Fibre Science and technology*, Volume II, Marcel Dekker, New York Basel, 1984.
23. Marini, I., Brauneis, F.: *Textilveredlung,* **1996**, 31, 182.
24. Mark, H., Meyer, K.H.: *Z.physikal.Chem*., **1929**, B2, 115.
25. Neumann, A.W., Good, R.J., Hope, C.J., Sejpal, M.: *J. Colloid. Interf. Sci.,* **1974**, 49**,** (2), 291-304.
26. Neumann, A.W., Spelt, J.K.: *Thermodynamic status of Contact Angles*, in "Applied Surface Thermodynamics;" Vol.63, Marcel Dekker, Inc.: New York, Basel, Hong Kong, 1996, p 109.
27. Owens, D.K., Wendt, R.C.: *J. Appl. Polym. Sci.***, 1969**, 13, 1741-1747.
28. Peršin, Z.: *Master degree*; University of Maribor, 2001, 45.
29. Porod, G.: IV Internationaler Kongress für Biochemie, Wien, 1958.
30. Saito, M., Yabe, A.: *Text. Res. J*., **1983**, 53, 54-59.
31. Scholz, C., Flath, H.J.: *Textilveredlung,* **1991**, 26.
32. Schurz, J.: *Lenzinger Berichte,* **1980**, 48, 15Schurz, J.: *Lenzinger Berichte,* **1994**, 74, 37-40.Sfiligoj, Smole, M., Zipper, P.: *Prog. Colloid & Polym. Sci,* **1997**, 105, 85.
35. Sfiligoj, Smole, M., Zipper, P.: Colloid Polym Sci, **1998**, 276, 144.
36. Van Oss, C.J.: *Colloid Surface A*, **1993,** 78, 1-49.
37. Warwicker, J.O.: *Journal of Polymer Science*: Part A2, **1966**, 4, 571
38. Washburn, E.W.: *Phys.Rev.,* **1921**, 17**,** 3, 273-283.
39. Wu, S.: *Modifications of Polymer Surfaces: Mechanisms of Wettability and Bomndability Improvements*, in "Polymer Interface and Adhesion," Marcel Dekker, Inc., New York, 1982, p 257.
40. Wu, S.: *J. Polymer.Sci.,* Part C, **1971**, 34, 19-30.

Lenzinger Berichte, 82 (2003) 96-101

INVERSE SIZE EXCLUSION CHROMATOGRAPHY- A TECHNIQUE OF PORE CHARACTERISATION OF TEXTILE MATERIALS

Arunee Kongdee[a], Thomas Bechtold[a], Eduard Burtscher[b], Markus Scheinecker[c]

[a]Christain-Doppler Laboratory of Textile and Fibre Chemistry in Cellulosics, Institute of Textile Chemistry and Textile Physics, Leopold-Franzens University Innsbruck, A-6850 Dornbirn, Austria
[b]Institute of Textile Chemistry and Textile Physics, Leopold-Franzens University Innsbruck, A-6850 Dornbirn, Austria
[c]Lenzing AG, A-4860 Lenzing, Austria

Abstract

Inverse size exclusion chromatography is used to determine pore parameters such as volume, surface area and mean size, and to follow structural changes in regenerated cellulosic yarns; non-crosslinked type lyocell, CLY1; crosslinked type lyocell, CLY2 and CLY3; micromodal; CMD and viscose; CV. From the investigation in untreated yarns, CV provided the highest values of pore volume and surface area, but the lowest mean size, whereas the inverse was found in CLY1. As structures of the yarns change upon treatments, tension treatment in wet state was applied to yarns. With such treatments, the rearrangements in structures occurred and led to changes in pore parameters of materials. Pore volumes, surface areas and mean pore sizes of treated yarns tended to decrease. However, there was no significant change in pore parameters of treated yarns with and without tension.

Keywords: inverse size exclusion chromatography, tension treatment, pore volume, pore surface area, mean pore size, structural change

Introduction

Structural characteristics of textile materials play an important role in determining the accessibility, uniformity and sorption rate of reactions involved in production and treatment. Although, there are many methods available for pore characterisation such as gas adsorption [1], X-ray scattering [2] and electron microscopy [3], Inverse Size Exclusion Chromatography (ISEC) offers a great advantage over the other techniques as porous materials are analysed in the wet state. Materials with unknown pore characteristics were packed in the column while probe molecules with known molecular sizes were allowed to pass through the column. Residence times of molecules in the column are dependent on sizes of probe as illustrated in Figure 1 (a).

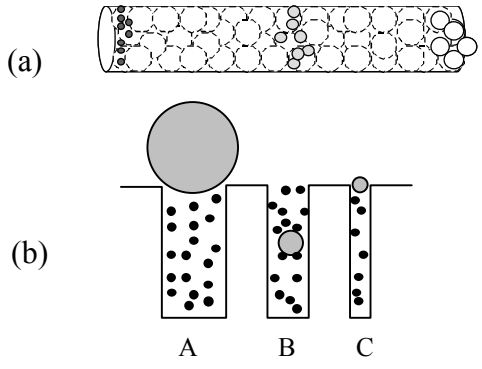

Figure 1. (a) Mechanism of size separation in column. (b) Illustration of accessible pore volume, grey circles = probe molecules, black circles = water molecules.

From Figure 1 (b), small probe molecules explore pores A, B and C, water in those pores will access them whereas water molecule in any pore accesses cannot access probes which

is too large to enter the pore. Volume of accessed water will provide accessible pore volume, but this technique is limited by the range of probe sizes available. As accessible pore volumes are determined by using probes to explore inside pores, probes must not be adsorbed on materials to be analysed and must present spherical shapes in water. Poly(ethylene glycol); PEG and dextran are suitable probes for cellulose analyses.

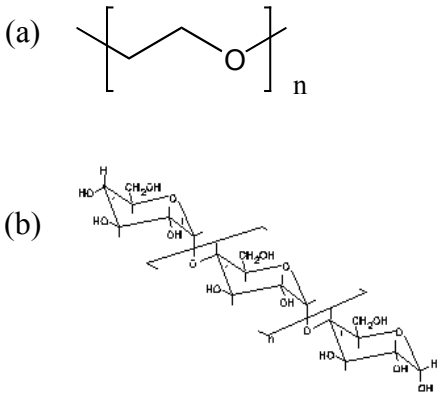

Fig. 2. Molecular structures of standards used. (a) PEG (b) Dextran.

Figure 2 shows molecular structure of PEG and dextran that were used as probes. Size of PEG and dextran increases with molecular weight with the relationships in equations 1 and 2 [4, 5].

For dextran

$$d = 0.53\ (M)^{0.5} \qquad (1)$$

For PEG,

$$d = 1.74\ (M)^{0.4} \qquad (2)$$

Tension treatment in wet state is a common treatment for textile materials and may cause structural changes in the substrate, in addition to changes caused by chemical or other physical treatments [6, 7, 8]. Therefore, it was of interest to us to apply tension treatments to yarns of regenerated cellulose and study the change of their structures by determining pore parameters using ISEC.

Experimental

Materials

Cellulose yarns of normal lyocell, CLY1 of 1.3/40 dtex, crosslinked lyocell CLY2 of 1.3/40 dtex and CLY3 of 1.4/38 dtex, micromodal (CMD) of 1.3/40 dtex and viscose (CV) of 1.3/39 dtex were used. Dextran and PEG with a series of different molecular weights were used as standards and Leophen MC (BASF, Germany) was used as de-aerating agent.

Methods

Tension treatment

CLY1, CLY2, CLY3, CMD and CV were treated by tension force in wet state as shown in Figure 3. 1000 m of each yarn were wound in hanks. A 1 kg weight was suspended on a 30 cm length of the hanks. These hanks were immediately immersed in water at room temperature for 2 hr, after which the hanks, with the weight attached, were dried in an oven at 105°C for 2 hr. A set of regenerated cellulose yarns without tension was prepared. The hanks, without tension, were wetted in water at room temperature, and then dried in an oven at 105°C for 3 hr.

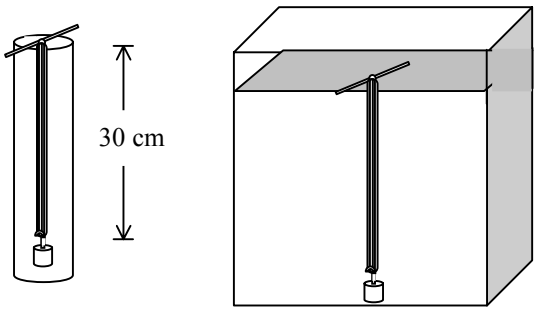

Figure 3. Tension treatment applied to cellulose yarns.

Inverse size exclusion chromatography

Treated yarns of CLY1, CLY2, CLY3, CMD and CV were cut into 2 cm. They were packed into stainless steel columns of 0.4x25 cm in dry state. Densities of columns were maintained in the range of 0.32 – 0.38 g/cm^3. 2 g/l of Leophen MC solution was flushed through columns at a flow rate of 1.0 ml/min for 12 hr. Distilled water was replaced at the same flow rate for further 12 hr. The operations were performed at room temperature at a flow rate of 0.1 ml/min.

A series of polymer standards of 0.1% dextran and PEG with various molecular weights were injected using AS-1555 auto-sampler, PU-1580 HPLC pump, detected by a differential refractometer model RI-1531 detector (Jasco) and analysed with a software. A schematic illustration of the process is shown in Figure 4.

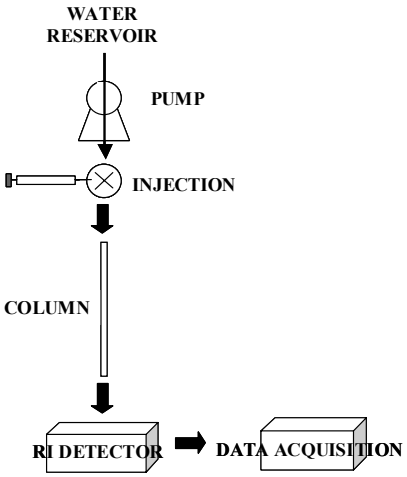

Figure 4. Instrument of ISEC.

Results and discussion

Elution profiles of separated molecules, were obtained by ISEC. Depending on the variation in their sizes, PEG 400, PEG 282, PEG 194, triethyleneglycol (TEG) 152, diethyleneglycol (DEG) 108 and ethyleneglycol (EG) 62 will be presented as shown in Figure 5. The relationship between log molecular weight of probes and retention time is illustrated in Figure 6. No distinct differences in retention times of probes were observed for probes with molecular weight from 1470 to 4500000 daltons (log MW from 3.17 to 6.65) indicating no separation of these probe molecules by cellulosic materials.

On the other hand, distinct differences in retention times were obtained for probes in the range of molecular weights from 62 to 940 dalton (log MW from 1.79 to 2.97), with the range of retention times obtained in untreated yarns being 3.97 min while that obtained for treated yarns being 3.47 min.

From the retention times of each probe, accessible pore volumes (V_i, ml/g) were determined using equation (3) [9, 10, 11].

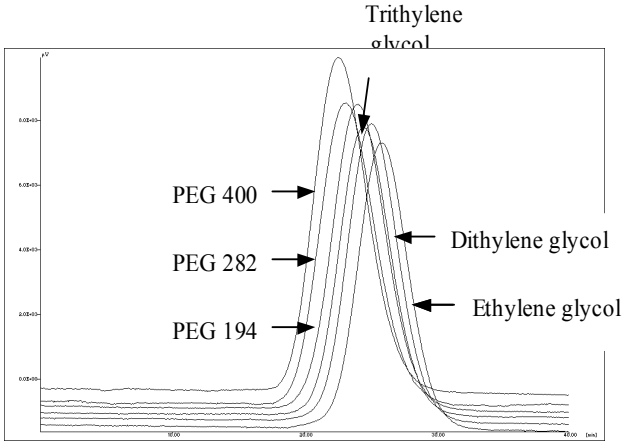

Figure 5. Typical chromatograms of PEG 400, PEG 282, PEG 194, TEG 152, DEG 108 and EG 62 on packing material; regenerated cellulose.

$$V_i = \frac{(T_e - T_o) \times F}{W} \qquad (3)$$

Where T_e is elution time of each probe (min), T_o is elution time of the biggest probe (min); PEG 4500000, F is the flow rate of mobile phase = 0.1 ml/min and W is the weight of yarn (g).

The resulting accessible pore volumes were plotted against diameter of probes as shown in Figure 7.

From Figure 7, it can be seen that accessible pore volume (V_i) is a linear function of diameter (d_i) for probes with size smaller than 26.9 Å. At diameter = 0 Å, total accessible pore volumes of yarns was obtained by extrapolation [8, 10]. Pore parameters of volume, mean size

and surface area were obtained using equations available in literature [12, 13]. Distribution coefficient of probe concentration (K), in external voids and internal pores is the ratio of probe radius (d) and pore radius (D_P) as given in equation (4):

$$K \approx 1 - n\frac{d}{D_P} \text{ when } d \ll D_P \qquad (4)$$

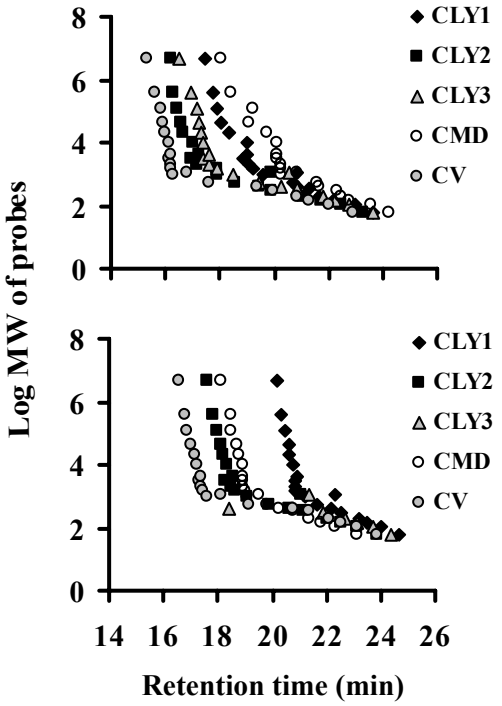

Figure 6 Retention time of probes on cellulosic yarns; (a) before tension treatment, (b) after tension treatment.

Where n is a constant, which is a function of pore configuration. If d is the diameter of probe, O_P is the surface area (m^2/g) and V_P is pore volume of material (ml/g), distribution coefficient is related to Σ; surface area (m^2/ml) as defined in equation (5):

$$K \approx 1 - \frac{d}{2}\frac{O_P}{V_P} \quad \text{where} \quad \Sigma = \frac{O_P}{V_P} \qquad (5)$$

By multiplying equation (5) by V_P, equation (6) is obtained.

$$KV_P = V_P - \frac{d}{2} O_P \qquad (6)$$

As accessible pore volume of material (V_i) is a function of pore diameter (d_i), the continuous plot between V_i and d_i give pore volume of material (V_P) as shown in equation (7).

$$KV_P = V_i \approx V_P - \frac{d}{2} O_P \qquad (7)$$

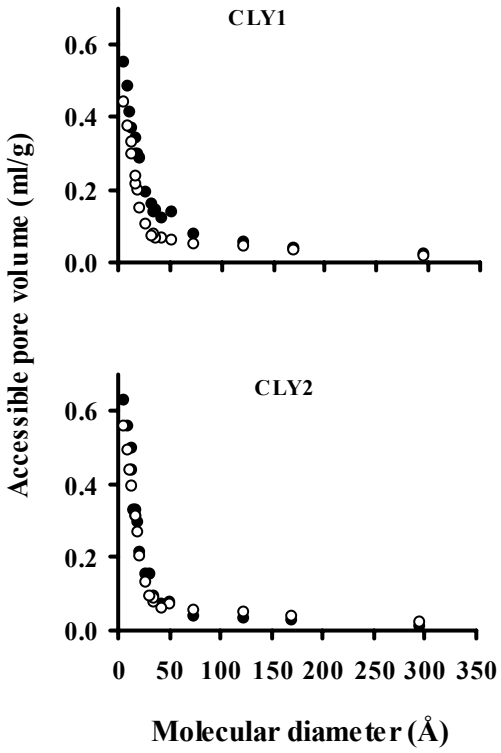

Figure 7 Relationship between accessible pore volume and diameter of probe of cellulosic yarns; ● before tension treatment, ○ after tension treatment

By replacing equation (5) in equation (4), the following equation is obtained.

$$1 - \frac{d}{2}\frac{O_p}{V_P} = 1 - n\frac{d}{D_P} \qquad (8)$$

Where n = 1 for slit pore model [6,13], mean pore size is obtained as the following equations. As V_p and slope ($\frac{O_P}{2}$) of a linear relationship between V_i and D_i are obtained from equation (7), $\overline{D}_P$ is obtained subsequently from equation (10). The calculated values of pore parameter: volume, mean size and surface area of original regenerated yarns and treated- regenerated yarns with and without tension are tabulated in Table 1.

$$\frac{d}{2}\frac{O_p}{V_P} = \frac{d}{D_P} \qquad (9)$$

Yarn	Pore volume (ml/g)			Surface area (m^2/g)			Mean pore size (Å)		
	Un-treated	Treated		Un-treated	Treated		Un-treated	Treated	
		Without tension	With tension		Without tension	With tension		Without tension	With tension
CLY1	0.63	0.51	0.56	334	312	372	38	33	30
CLY2	0.78	0.68	0.56	492	424	372	32	32	30
CLY3	0.78	0.72	0.68	454	426	410	34	34	33
CMD	0.72	0.51	0.57	360	336	384	37	40	30
CV	0.82	0.84	0.86	576	532	542	30	31	32

Table 1 Pore volume, surface area and mean pore size in regenerated cellulose yarns with and without tension treatment

$$\overline{D}_P = \frac{2V_P}{O_P} \qquad (10)$$

From the results, untreated yarns exhibited differences in pore parameters depending on type of material. The values obtained for pore parameters lied in the range of 0.63 - 0.82 ml/g for pore volume, 334 – 576 m^2/g for pore surface area and 30 – 38 Å for pore size. CLY1 exhibited the lowest pore volume and surface area, but highest mean pore size while the inverse was observed in CV. The pore parameters were also found to differ in yarns with tension treatments. Reduced values were found in all tension treated yarns, except in CV. Percentage of reduction in pore volumes, surface areas and mean pore sizes of materials were observed as 19, 13, 8, 29 and 4% for treated yarns without tension, and 11, 28, 13, 21 and 2% for the set of yarns treated with tension. By such treatment, it is believed that material structures reorganise, leading to structural changes. However, in a comparison of yarns treated with tension and without tension, pore parameters were rather similar. This indicates that both treatments cause the similar structural re-organisation in the material.

Conclusion

ISEC is a technique for determining pore parameters; volume, surface area and mean size in regenerated cellulosic materials in wet state. By using poly(ethylene glycol) and dextran with various sizes, accessible pore volumes in material are accessed. The initial relationship between accessible pore volume and molecular diameter of probe provides pore volume and surface area of material; mean pore size is subsequently obtained by the relationship of pore volume and surface area. From the investigation, pore parameters of regenerated cellulosic yarns were varied depending on type of materials and also tension treatment. Such changes can result from the different production routes and the applied textile chemical treatment.

Acknowledgement

Great thank is extended to the ÖAD (Österreichischer Austauschdienst), Christian-Doppler research society and Lenzing AG for financial support.

References

[1] Porter, B. R., Rollins, M. L., *J. Appl. Polym. Sci*. **1972**, 16, 217-236.
[2] Crawshaw, J., Cameron, R.E., *Polymer*, **2000**, 41, 4691-4698.
[3] Dolmetsch, H., Dolmetsch, H., *Das Papier*, **1969**, 22, 1-11.
[4] Haller, W., *Macromolecule,* **1977**, 10, 83-86.
[5] Squire, P. G., *J. Chromatogr*., **1981**, 210, 433-442.

[6] Rowland, S. P., Wade, C. P, Bertoniere, N. R., *J. of Appl. Polym. Sci.*, **1984**, 29, 3349-3357.
[7] Li, C., Ladisch C. M., Ladisch, M. R.. *Textile Res. J*. **2001**, 75(5), 407-414.
[8] Bredereck, K., Blueher, A. *Melliand Textilberichte*, **1992**, 73, 652-662.
[9] Gruber, M. *Ph. D. Dissertation*, Universität Stuttgart, **1998**.
[10] Casassa, E. F., Tagami, Y., *Macromolecules*, **1969**, 2(1), 14-26.
[11] Gorbunov, A. A., Solov'eva, L. Ya., Pesechnik, V. A., *J. of Chromatogr.*, **1988**, 448, 307-332.
[12] Stone, J. E., Scallan, A. M., *Cellulose Chem. Technology*, **1968**, 2, 343-358.
[13] Nelson, R., Oliver, D. W., *J. Polym. Sci.*: *Part C*, **1971**, 36, 305-320.

Lenzinger Berichte, 82 (2003) 102-106

Untersuchungen zur Bestimmung der Substituentenverteilung bei Viskosen

Thomas Lange [a], Elena Berger-Nicoletti [b], Paul Kosma [a], Antje Potthast [a] Herbert Sixta [c]

[a] Universität für Bodenkultur, Christian-Doppler-Labor für Zellstoffreaktivität, Muthgasse 18, 1190 Wien, Tel.: +431 36006-6051, Fax: +431 36006-6059, E-mail: tlange@edv2.boku.ac.at
[b] vormals Universität für Bodenkultur, Wien; gegenwärtige Adresse: Johannes-Gutenberg-Universität Mainz, Duesbergweg 10-14, Inst. f. Org. Chemie, 55099 Mainz
[c] Lenzing AG, R & D, A-4860 Lenzing, E-mail: h.sixta@lenzing.com

Übersicht

Es wurde eine Methode zur Bestimmung der Verteilung von Xanthogenat-Substituenten von Viskose untersucht. Hierzu wird die Viskose stabilisiert und durch Folgereaktionen in ein teilweise methyliertes Cellulosederivat überführt, was letztendlich eine Methylierungsanalyse ermöglicht. Als erstes werden die Xanthogenatgruppen derivatisiert, die freien Hydroxylgruppen substituiert, die Xanthogenatgruppen in einem zweistufigen Prozess entfernt und die freigesetzten OH-Gruppen methyliert. Die so erhaltene Methylcellulose kann mit bereits bekannten Methoden der Kohlenhydratchemie hinsichtlich ihrer Substituentenverteilung charakterisiert werden.

Stichworte: Viskose, Xanthogenat, Substituentenverteilung, Methylierungsanalyse

Einleitung

Der Viskoseprozess ist ein wirtschaftlich bedeutendes Verfahren: die Weltproduktion an Viskosefasern beträgt ca. 1950 kt pro Jahr. Obwohl das Verfahren schon lange bekannt ist, ist das Wissen um die molekularen Details sehr begrenzt. Dies liegt vor allem an der geringen Stabilität der Xanthogenat-Gruppen, die sich dadurch einer analytischen Untersuchung entziehen. Deshalb begnügt man sich bisher mit einer Bestimmung der Anzahl der Xanthogenate, dem sogenannten γ-Wert [1]. Dies ist ein Summenparameter, der über die Verteilung der Substituenten jedoch nichts aussagt. Da deren Verteilung, sowohl innerhalb der Anhydro-glucoseeinheiten (AGU) als auch entlang der Polymerkette die Eigenschaften der Viskose-lösung beeinflussen, ist ihre Ermittlung von großem Interesse.
Erste vielversprechende Versuche zur Ermittlung der Substituentenverteilung wurden bereits in den 1960er Jahren von Willard et al. [2] durchgeführt, wobei die Xanthogenatpositionen durch Methoxygruppen ersetzt wurden

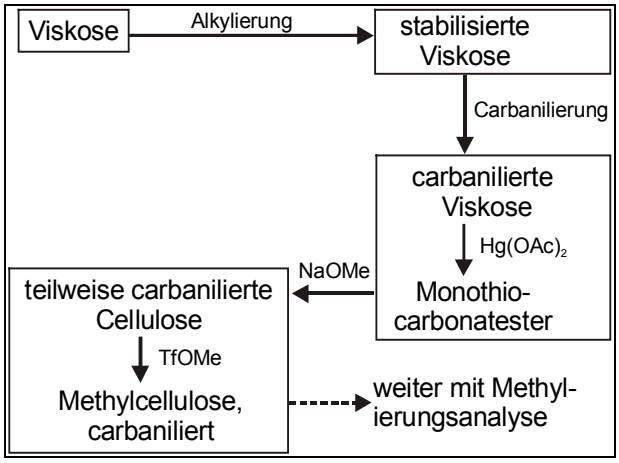

Abbildung 1. Schematische Darstellung zur Durchführung der Analyse. In Rechtecken zusammengefaßte Einzelschritte erfolgen ohne zwischenzeitliche Aufarbeitung.

Dies gelang jedoch nur bei einigen ausgewählten Viskoseproben, eine allgemeine

Anwendbarkeit war nicht gegeben. Eine Stabilisierung von Viskose erreichten Purves et al.[3] durch Alkylierung, wobei ein völlig unlösliches Produkt erhalten wurde, das - abgesehen von der Ermittlung der elementaren Zusammensetzung - nicht näher charakterisiert werden konnte. Einen anderen Weg beschritten König et al. [4] mit der Xanthogenierung von Alkalicellulose durch ^{13}C-angereichertes CS_2.

Für industriell verwendete Viskosen ist diese Methode jedoch unpraktikabel. Ziel der vorliegenden Arbeit war es eine Methode zu entwickeln die es erlaubt, die Verteilung der Xanthogenatgruppen an Viskosen zu bestimmen (Abbildung 1).

Ergebnisse und Diskussion

Es wurden zunächst verschiedene Modell-xanthogenate synthetisiert, um geeignete, selektive Reagenzien aufzufinden und die Reaktionsbedingungen zu optimieren.

Derivatisierungsreagenzien

Zur Stabilisierung der Viskosen wurden verschiedene Substanzen getestet (Abbildung 2), von denen einige kommerziell erhältlich sind. Die anderen konnten durch einfache Synthesen im Grammmaßstab hergestellt werden. [5]

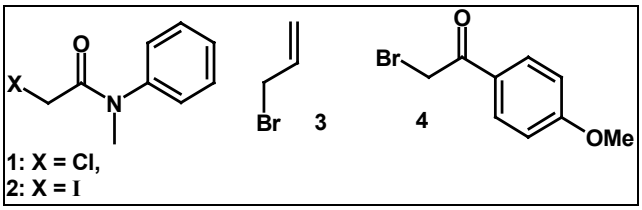

Abbildung 2. Geeignete Derivatisierungsreagenzien zur Stabilisierung von Viskosen.

Auf Grund der Instabilität der Viskose ist eine Stabilisierung der Xanthogenatgruppen als Grundvoraussetzung für die hier skizzierten Untersuchungen anzusehen. Dabei muss der ursprüngliche γ-Wert der Viskose so weit wie möglich erhalten bleiben. In Tabelle 1 sind die γ-Werte der stabilisierten und nichtstabilisierten Viskosen miteinander verglichen. Man kann der Aufstellung entnehmen, dass für die Stabilisierung der Modalviskose drei Reagenzien zur Verfügung stehen, die in Abbildung 2 gezeigt sind (2, 3, 4), während für die Normalviskose

Nr.	Bezeichnung	γ-Wert	γ-Wert stabilisiert
1	M-74	61.4	53.9
2	M-138	61.4	47.2
3	M-142	61.4	53.2
4	M-202	61.4	52.2
5	N-15	42.3	41.5
6	N-143	35.7	36.0
7	N-118	38.3	36.5
8	N-50	35.5	34.7

Tabelle 1. Vergleich der γ-Werte stabilisierter und nicht-stabilisierter Viskose.

mehrere Substanzen geeignet sind. Die γ-Werte für die stabilisierten Modal-Derivate sind deutlich geringer als jene der Ausgangsviskose. Das trifft unabhängig davon zu, ob die Reaktionsführung heterogen (Derivat fällt während der Reaktion aus) oder homogen (Derivat bleibt in Lösung) durchgeführt wird. Vermutlich handelt es sich hier um ein Problem der Zugänglichkeit: da beide Werte bei der N-Viskose nahe beieinander liegen, kann man einen systematischen Fehler wohl ausschließen. Aus praktischen Gründen wurde der Einsatz der Reagenzien auf die Verbindungen **2** und **3** beschränkt.

GPC-Untersuchungen

Die vorgeschlagene Analysenmethode erlaubt auch die Untersuchung der stabilisierten Viskose mittels Gelpermeationschromato-graphie (GPC), da die Derivate in DMAc/LiCl ausreichend löslich sind (Abbildung 3). Die UV-Detektion erfolgt im Aromatenbereich bei 290 nm. Bei Fehlen aromatischer Gruppen am Stabilisierungsreagenz - bzw. als Alternative hierzu - kann die Messung auch im Bereich der Xanthogenat-Absorption bei 313 nm erfolgen.

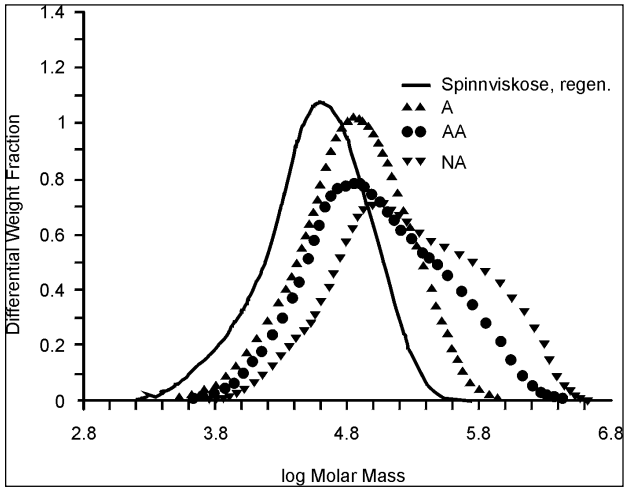

Abbildung 3. Chromatogramme vom Acetanilid- (A), p-Nitroacetanilid- (NA) und Acetamid-Derivat (AA) sowie von regenerierter Viskose.

Das Chromatogramm des Anilid-Derivates zeigt den gleichen prinzipiellen Verlauf wie das der regenerierten Viskose, was auf eine gleichmäßige Xanthogenierung über den gesamten Molmassenbereich hindeutet. Es erscheint lediglich etwas zu höheren Molmassen verschoben, da diese durch das Anbringen der Substituenten samt Xantho-genatgruppe zunimmt. Beim Acetamid-Derivat als auch beim *para*-NO_2-substituierten Anilid- Derivat zeigt sich Aggregationsbildung (Schulter), wodurch die Analysenwerte verfälscht werden. Generell bemerkt man bei sämtlichen Derivaten nach längerer Zeit in Lösung Aggregatbildung, wodurch die Filtrierbarkeit stark beeinträchtigt wenn nicht gar unmöglich wird. Eine Verbesserung des Lösungszustandes läst sich durch Carbanilieren erreichen.

Modellxanthogenate

Es wurden, von Cyclohexandiol bzw. ß-Methylglucosid ausgehend, die in Abbildung gezeigten Modellxanthogenate synthetisiert. Mit diesen wurden Stabilitätstests durchgeführt sowie die Orthogonalität der Schutzgruppen verifiziert.

Substituenten-Verteilung

Trotz der Alkylierung der Xanthogenate sind diese jedoch nicht stabil genug für die direkte Ermittlung der Substituentenverteilung [6]. Deshalb erschien es ratsam, das Problem mit Hilfe einer Methylierungsanalyse zu lösen.

Dazu müssen entweder die freien Hydroxylgruppen der stabilisierten Viskosen methyliert oder, quasi als Negativ davon, die Xanthogenat-Gruppen gegen Methoxylgruppen ausgetauscht werden.

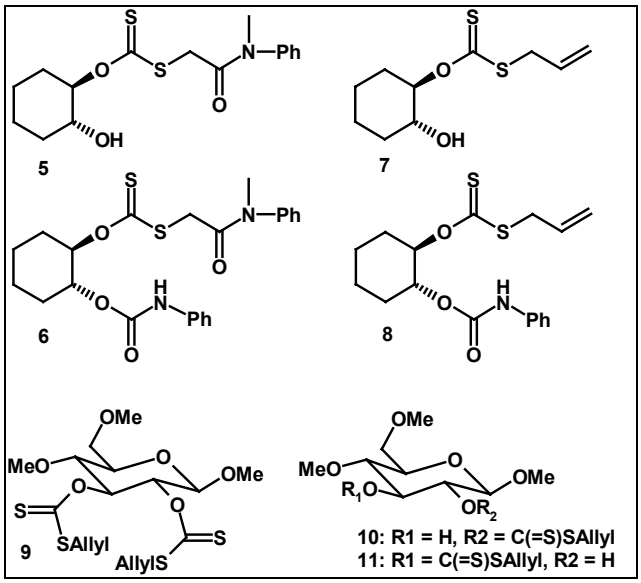

Abbildung 4. Modellxanthogenate zur Untersuchung der Stabilisierungsreaktion sowie der folgenden Reaktionsschritte.

Auf Grund der hohen Nukleophilie des Schwefels war es nicht möglich, die Verbindungen direkt zu methylieren; somit verbleibt nur die zweite Variante (Abbildung 5). Für die vollständige Substitution der Hydroxylgruppen erwiesen sich lediglich die Acetylierung und die Carbanilierung als günstig. Da Carbanilate stabiler sind als Acetate und auch eine geringere Tendenz zur Migration zeigen, wurde die Carbanilierung ausgewählt.

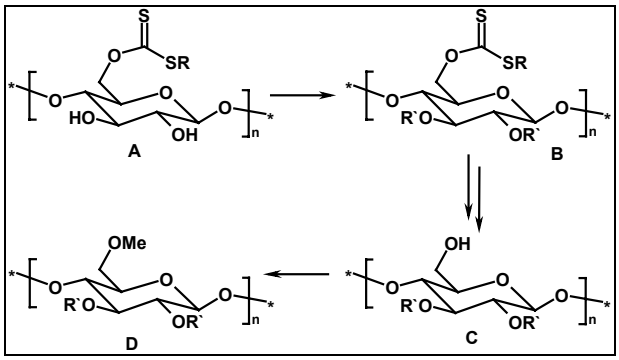

Abbildung 5. Generelle Analysestrategie zur Ermittlung der Substituentenverteilung. Nach Schritt „D" schließt sich eine klassische Methylierungsanalyse an.

Das selektive Entfernen der Xanthogenatester bereitete anfänglich Probleme, da diese sich als erstaunlich stabil erwiesen. Erst deren Umwandlung in die weniger stabilen Monothiokohlensäureester ermöglichte das Entfernen, ohne die Carbanilatgruppen mit abzuspalten. Für diese Reaktion sind in der Literatur verschiedene Reagenzien vorgeschlagen worden, wie das Nitrosylkation [7], Benzenselensäureanhydrid [8], Kaliumpermanganat [9] oder Quecksilber-(II)-acetat [2], wobei von der letzteren Methode die höchsten Ausbeuten angegeben werden.

Die Reaktion mit Quecksilberacetat zeichnet sich durch milde Reaktionsbedingungen (Rühren in feuchtem THF, Dioxan oder DMF bei Raumtemperatur) sowie vollständigen Umsatz nach wenigen Minuten aus. Bei den Reaktionen mit den Modellxanthogenate konnten keinerlei Nebenprodukte beobachtet werden (DC). Leider gelang es im Fall der stabilisierten Viskose nicht, die sehr toxische Quecksilberverbindung[i] durch ein anderes Schwermetallsalz zu ersetzen.

Die Abspaltung des so erzeugten Monothiocarbonatesters mit H_2O_2 oder mit Natriumchlorit nach Willard [2] erwies sich als nicht kompatibel mit den Carbanilat-Schutzgruppen, die teilweise abgespalten wurden. Ein Entfernen der Monothiocarbonate konnte schließlich mit Natriummethanolat in Trimethylphosphat/THF mit sehr hoher Selektivität erreicht werden. Versuche mit den Modellxanthogenaten zeigten, dass die Reaktion nach ca. 3 Stunden beendet ist. Selbst bei Verlängerung der Reaktionszeit auf 3 Tage tritt keine Abspaltung der Carbanilat-Schutzgruppen auf. Die Methylierung der freigesetzten Hydroxylgruppen erfolgt nach Prehm [10] mit Methyltriflat ohne vorherige Aufarbeitung der Reaktionsmischung. Auch hier konnte durch Versuche mit entsprechenden Modellverbindungen die Verträglichkeit der Methylierungsbedingungen mit den Carbanilat-Schutzgruppen nachgewiesen werden (Abbildung 6).

Es gelang somit die stabilisierte Viskose in ein partiell methyliertes Cellulosecarbanilat zu überführen, wobei die Methylgruppen die ursprünglichen Xanthogenatpositionen repräsentieren. Dieses Derivat kann anschließend einer konventionellen Methylierungsanalyse unterworfen werden. [11,12]

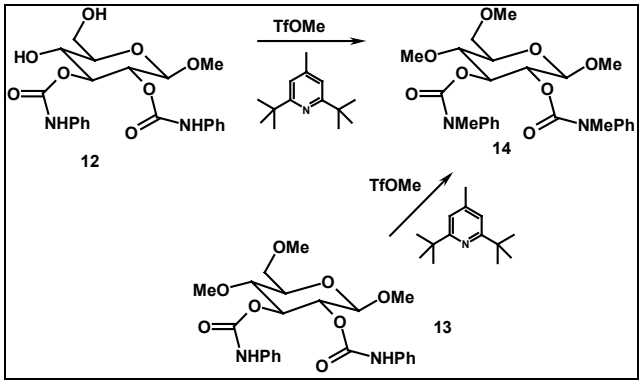

Abbildung 6. Untersuchung der Methylierungsbedingungen; beide Edukte (12, 13) sollten dasselbe Produkt ergeben, was sich bestätigte.

Zusammenfassung und Ausblick

Es gelang, Viskose unter weitgehendem Erhalt des ursprünglichen γ-Wertes zu stabilisieren. Die erhaltenen Derivate konnten unter schonenden Bedingungen carbaniliert werden. Eine Untersuchung der carbanilierten Derivate mittels GPC ist auf Grund der guten Löslichkeit und Stabilität des Lösungszustandes möglich.

In einem zweistufigen Prozess gelang weiterhin die Abspaltung der Xanthogenatgruppen: durch Reaktion mit Quecksilberacetat wurden diese in Monothiocarbonatester umgewandelt, die anschließend selektiv entfernt werden konnten. Die freigesetzten Hydroxylgruppen wurden methyliert; diese Methoxyfunktionen spiegeln die Positionen der ursprünglichen Xanthogenate wider. Alle Reaktionsschritte wurden an Modellsubstanzen hinsichtlich Umsatz, Ausbeute und - wo erforderlich - auf Orthogonalität mit den eingesetzten Carbanilat-Schutzgruppen untersucht.

Das methylierte Cellulosecarbanilat kann nun einer Methylierungsanalyse unterworfen werden, bestehend aus: Hydrolyse, Reduktion, Acetylierung und Analyse mittels GC-MS. Man erhält somit die Verteilung der Xanthogenate auf die Hydroxylgruppen 2, 3 und 6 der Anhydroglucoseeinheiten der Viskose.

Als langfristiges Ziel stellt sich die Aufgabe, auch die Verteilung entlang der Polymerkette zu ermitteln. Hierzu führt man nach dem Methylierungsschritt eine Teilhydrolyse durch:

[i] Ein spezieller Satz an Glasgeräten wird nur für diese Reaktion verwendet. Alle Lösungsmittelabfälle werden separat gesammelt und das Quecksilber als HgS gefällt.

man erhält oligomere Bruchstücke die deuteromethyliert werden. Anschließend können diese mittels Massenspektrometrie untersucht werden. Aus dem Vergleich der experimentell ermittelten Daten mit berechneten Werten erhält man die Information über die statistische Verteilung der Substituenten innerhalb der Polymerkette. [5] Die Abbildung zeigt die möglichen Verteilungsmuster in einem linearen Polymer.

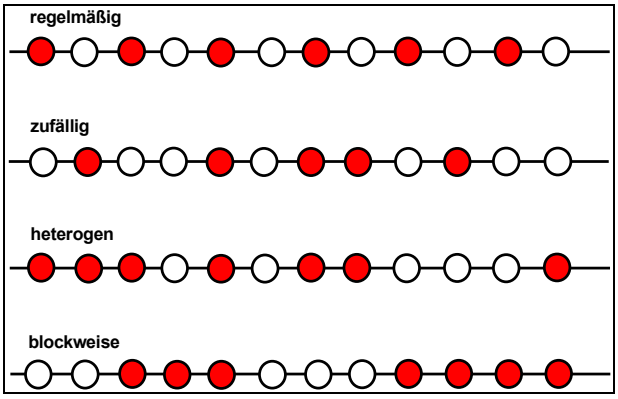

Abbildung 7. Mögliche Substitutionsmuster entlang der Polymerkette.

Danksagung

Ich möchte an dieser Stelle der Christian-Doppler-Gesellschaft sowie der Lenzing AG meinen Dank für die finanzielle Unterstützung aussprechen. Des Weiteren bedanke ich mich bei Prof. Kosma, Prof. Sixta, Prof. Potthast und Prof. Rosenau für die fachlichen Anregungen und Hinweise.

Literatur

[1] Götze, K.: "Chemiefasern nach dem Viskoseverfahren"; Springer-Verlag Berlin Heidelberg **1967**, 1173-77.

[2] Willard, J.J.; Pacsu, E.: JACS, *82*, **1960**, 4347-4350. ibid. 4350-4352.

[3] Purves, C.B.; Muller, T.E.: Methods of Carbohydr. Chem., 3, 1963, 239-251.

[4] König, L.; Dörig, R.; Postel, S.: Das Papier, *11*, **1993**, 641-644.

[5] Lange, T.; Berger-Nicoletti, E.; Kosma, P.: in preparation.

[6] Purves, C.B.; Vincent, D.L.; Falconer, E.L.; Sanyal, A.K.: Can. J. Chem., *35*, **1957**, 1164-1173.

[7] Jorgensen, K.A.; Ghattas, B-A.A.G.; Lawesson, S-O.: Tetrahedron, *38*, 9, **1982**, 1163-1168.

[8] Barton, D.H.R.; Cussans, N.J.; Ley, S.V.: J. Chem. Soc., Perkin 1, **1980**, 1650-1653.

[9] Hurd, R.N.; De LaMater, G.: Chem. Rev., *61*, **1961**, 45.

[10] Prehm, P.: Carbohydr. Res., *78*, **1980**, 2, 372-374.

[11] Lindberg, B.; Bouveng, H.O.: Methods of Carbohydrate Chemistry, vol. 5, 296-298.

[12] Biermann, C.J.: „Analysis of Carbohydrates by GLC and MS"; CRC Press 1989.

[13] a) Mischnick, P.; Gohdes, M.: Carbohydr. Res., *309*, **1998**, 109-115. b) Mischnick et al., Macromol. Chem. Phys., *201*, **2000**, 1985-1995. c) Mischnick P., Kühn, G.: Carbohydr. Res. *290*, **1996**, 199-207

Lenzinger Berichte, 82 (2003) 107-117

CHARACTERISING THE EMERGING LYOCELL FIBRES STRUCTURES BY ULTRA SMALL ANGLE NEUTRON SCATTERING (USANS)

K. Christian Schuster [(1)], Peter Aldred[(5)], Mario Villa[(2)], Matthias Baron[(2,3)], Rudolf Loidl [(2,3)], Olga Biganska[(4)], Stanislav Patlazhan[(4)], Patrick Navard [(4)], Hartmut Rüf [(1)] and Erwin Jericha[(2)]

1) Lenzing AG, Research and Development Lyocell, A-4840 Lenzing, Austria
2) Atominstitut der Österreichischen Universitäten, A-1020 Wien, Austria
3) Institut Laue-Langevin, F-38042 Grenoble, France
4) Centre de Mise en Forme des Matériaux, Ecole des Mines de Paris, F-06904 Sofia Antipolis, France
5) Christian Doppler Laboratory for Chemistry of Cellulosic Fibres and Textiles, A-6850, Dornbirn, Austria

Abstract

Ultra small angle neutron scattering (USANS) is a new technique that measures the elastic scattering from scattering length density fluctuations in the order of microns in real space, i.e. in the momentum transfer range of 2×10^{-5} - 2×10^{-3} $Å^{-1}$. This makes the technique ideal for studying Lyocell fibres in terms of their structure internally and their overall fibre diameter. In the present work, the USANS technique has been used to study the evolution of structure in a Lyocell fibre over a spinning line and also in ready made Lyocell fibres, which have undergone multiple wet/dry treatments.

Keywords: USANS, NMMO, Scattering curves, Q-range, Bonse-Hart split channel analyser.

Introduction

Lyocell fibre structure - a pending reaserch issue

In textile fibres the macromolecules generally are found to be oriented in the direction of the fibre. Due to attractive forces between the polymers highly oriented crystalline areas are formed, so called crystallites. These crystallites are bound to others via the lower oriented amorphous parts of the fibre. Depending on the strength of the molecular forces between the crystallites and within the amorphous zones a certain sensitivity for partial fibre splitting and formation of fibrils is resulting.
The phenomenon of fibrillation also is known with native fibres, e.g. cotton or flax where the crystalline structure of the cellulose is present in the so called “Cellulose I” form.

After swelling in concentrated caustic soda “Cellulose II” is formed which also is present in the crystallites of regenerated cellulose fibres[1].

Fibrillation as an undesired property first was detected with polynosic fibres because cotton, flax and viscose textiles show a lower impact of the fibre fibrillation on a change of their look, surface properties and textile structure[2].Various properties have been discussed and studied with regard to their importance for the fibrillation tendency:

Fibre properties of importance are: the degree of orientation, the crystallinity and dimensions of crystallites, the shape and homogeneity over the cross section, the pore volume, size and dimensions of the pores, the inner surface, the molecular flexibility within the fibre at different conditions[3-5].

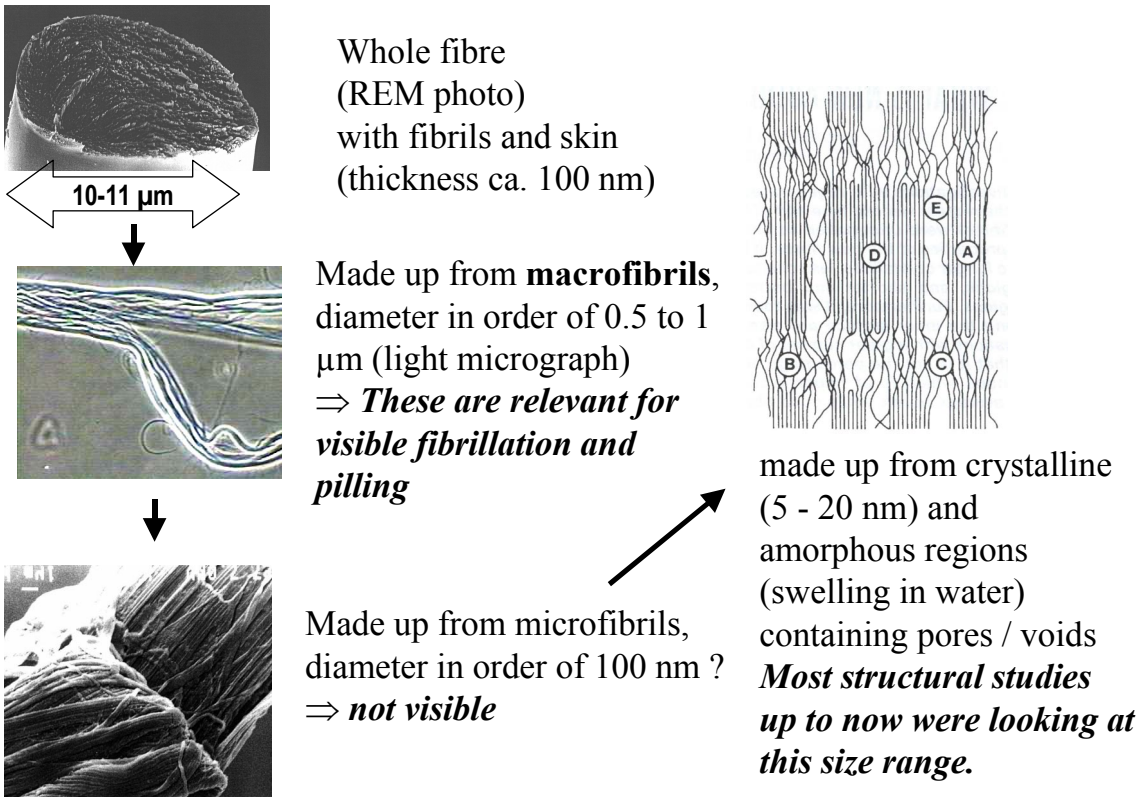

Figure 1. Proposed structures at different dimensional levels of Lyocell fibres.

Numerous studies to investigate main parameters that could influence fibrillation have been given in the literature. Considerable research has been performed to investigate the process of fibre formation e.g. geometry of the spinning line (distance between spinneret and coagulation bath) with regard to fibrillation tendency[6,7]. Others investigated the application of crosslinking substances or chemical treatment of the fibre in the never-dried state with regard to changes of the fibre properties.

The influences during yarn and textile production are these: Textile production includes the mechanical treatment of fibres during spinning and the textile formation by weaving or knitting. When the tendency of a textile to form fibrils is discussed this mechanical "history" has to be considered.

The effects during textile dyeing and finishing are these: Changes in the fibrillation tendency also result from treatments during dyeing and finishing processes[8,9]. While the mechanical abrasion during dyeing operations can result in an increased tendency to develop fibrils in the subsequent stage, crosslinking by bifunctional reactive dyes[10,11] or chemicals during finishing operations will lower the fibrillation tendency considerably[9,12]. Particularly for crosslinking of cellulose in textile finishing operations a distinct lowering in fibrillation is observed accompanied by an increase of crease angle, lowered swelling and wash shrinkage[13,14].

For the basic understanding of the fibrillation of a cellulosic fibre a suited model covering the whole textile pipeline, starting from the fibre manufacturing process has to be established and tested for its validity.

The first step however is to study the state of the formation of a fibrous substrate, and the changes in the primary state, including the fibre never – dried state, and the formation of the final fibre properties. The question to ask is: Which fibre properties and experimental conditions determine the tendency of a fibre to fibrillate?

Structure characterisation in cellulosic fibres, and specific properties of Lyocell

Structure characterisation of cellulosic and other polymer fibres has been concentrated for several decades mostly on scattering methods, especially X-ray scattering. Wide-angle X-ray scattering has revealed the different crystal modifications, especially cellulose I in natural fibres, and cellulose II in regenerated fibres. Small angle X-ray scattering (SAXS) resolves somewhat larger structures in the range of some ten nanometers, e.g. microfibrils in fibres[15]. Sizes and orientation of crystallites have been determined by small-angle X-ray scattering, as well as the sizes of voids between the crystallites[16,17]. These results have formed a structure model on the Ångström to nanometer scale. Special features of Lyocell fibres as compared to other cellulose regenerated fibres on this level are[15]:

(A) High crystallinity , high longitudinal orientation of crystallites
(B) High amorphous orientation
(C) Low lateral cohesion between fibrills
(D) Low extent of clustering
(E) Relatively large void (pore) volume

From these properties, it was tried to understand the fibre properties: swelling, wet rigidity, and especially fibrillation. Two important facts, however, make a direct connection between structures on the nanometer scale and fibrillation complicated and less relevant:

1. After the primary coagulation, the structure is formed in the spinning line[20]. Then the fibres undergo a process of structure reformation by drying, and further by repeated wetting and drying through the textile chain, which eventually leads to the final properties. The time scale of the first changes appears to be very short, therefore it was attempted early to use in-situ measurements to follow the emerging structures. Mortimer & Peguy[21] followed the filament diameter and birefringence as a measure for orientation in the air gap. Coulsey & Smith[20] reported temperature measurements of the spinning filament. NMMO concentrations over the spinning line were analysed in fast off-line measurements near real-time by Liu et al.[22].

Weigel et al.[23] followed crystallisation and nanoscale structure development during spinning by small and wide angle X-ray scattering using synchrotron radiation. The measurements were done in the air gap and after the spinning bath.

2. If fibrillation occurred only on the nanometer scale, it would not be a severe problem in textiles, as fragments of this diameter do not scatter light and thus are not visible. However, in practice the fibrils that split off from fibers are in the visible size range, several 100 nm to micrometers in diameter (Fig. 1). Substructures in fibres in this size range can be made visible by swelling in special reagents (Marshall's solution; Fig. 1) or by severe squeezing[20]. By scanning electron microscopy, Jianchin et al[25] showed the skin and macrofibrils. (See also Fig. 1). So, there are supposedly some substructures present which are held together only by relatively weak bonds, and which cannot be detected by the conventional scattering methods, but are most relevant for the phenomenon of fibrillation. A structure model taking in account these various orders of magnitude in structure size for the Lyocell fibre is proposed (Fig. 2)

Therefore, it is necessary to study structure formation in Lyocell fibres by methods which provide in-situ measurements at a size scale relevant for fibrillation. Some information can be gained by the recent space-resolved SAXS micro-method, e.g. on the orientation of microfibrils over the fibre diameter[26], and on structural differences between shell and core of regenerated fibres[27,28]. Spatial resolution here is in the range around 2 micrometers. A suitable technique to resolve the relevant size range was found in the lately developed USANS[29,30].

.

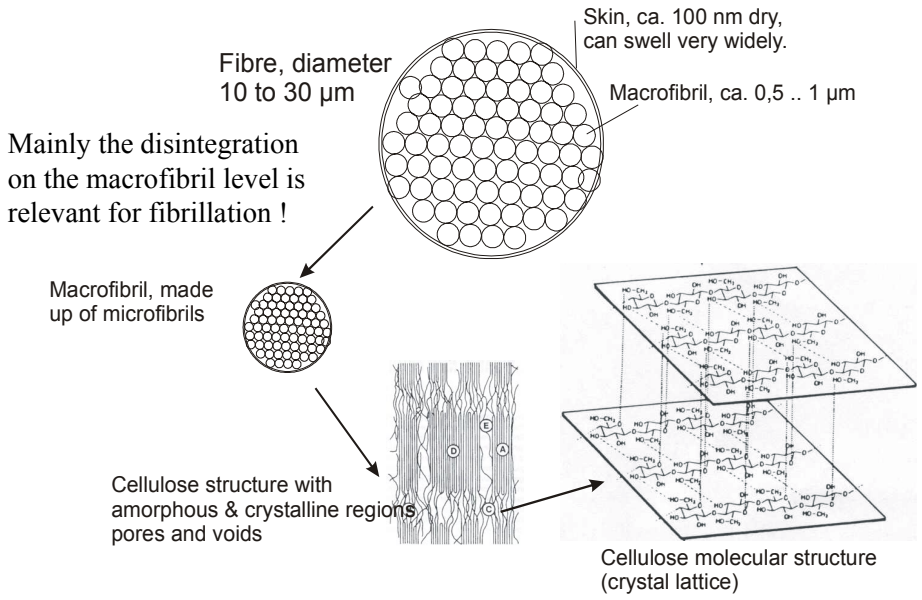

Figure 2. Proposed structure at different dimensional levels of Lyocell fibres.

Basic features of USANS

Neutrons are scattered by the atoms of any material, not just by the heavier elements. The specific scattering intensity does not follow a regular order in the periodic table. This feature enables contrast between otherwise very similar materials, as for example light and heavy water, or various organic polymers. Any regular structures in materials lead to neutron scattering.

Ultra Small Angle Neutron Scattering (*USANS*) measures the elastic scattering from scattering length density fluctuations in the order of microns in real space, i.e. in the momentum transfer range of 2×10^{-5} - 2×10^{-3} $Å^{-1}$.

The techniques of choice for studying the structure of micron sized particles are electron microscopy, light scattering and atomic force microscopy. There are however a number of cases where none of these techniques are applicable. Examples are in materials of low contrast, opaque materials (for light scattering) or in magnetic structures. In such cases, neutrons are a unique probe when contrast enhancement is necessary. Applications can be found in colloid science (mixtures of particles, strongly correlated colloid crystals, particles of micron size, silicon macropore arrays), materials science (filled polymers, cements, microporous media) and polymer science (constrained systems, emulsion polymerisation).

The angles measured are up to 1 mrad=0,05°. This corresponds to structures in a size between 0.1 µm and 30 µm. Therefore, the method *appears suitable to study structures in the size range relevant for fibrillation.*

USANS is a non-invasive method, so, *on-line in-situ measurements are possible without influencing the sample.* Heavy water (D2O) is fairly transparent to neutrons, giving a chance for in-situ measurements in the spinning bath. The different scattering intensity of light and heavy water can be used for studies of hydrated samples in contrast variation[18].

An interesting background detail is the theory of interaction on neutrons at small intensities: Neutrons only interact with nuclei of atoms. So, the probability of a collision of a neutron with a nucleus is very small, neutrons penetrate fairly deep into most materials. For measuring well-resolved scattering spectra at small angles, a narrow energy distribution of thermal neutrons is required, leaving only few neutrons from the source available for scattering experiments. At such low radiation intensity, no signal would be expected by particle collisions.

However, there are scattered neutrons detectable. It must be concluded that neutrons do not behave as *particles* here- USANS Scattering is a *wave* phenomenon (Fig. 3)

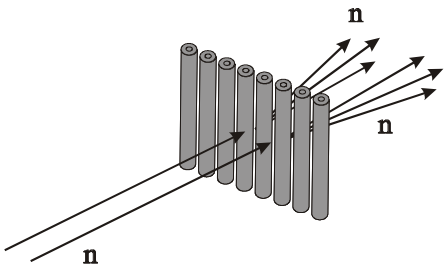

Figure 3. Scattering of neutrons incident on a row of cylidrical scatterers (lyocell fibres).

Experimental

Fig. 4 shows the USANS setup with the Bonse-Hart-Camera[31] and the neutron detectors. The laboratory spinneret was placed at the sample position, so that in-situ measurements of the spinning filaments could be performed. The number of filaments in one spinning line was 1 to 37.

The spinning bath was constructed as shown schematically in Fig.5. For off line measurements, up to 100 fibres were presented on glass carriers placed in the sample holder. The beam intensity was up to 10,000 neutrons per second and cm^2.

- Neutron source : research reactor at Institut Laue-Langevin, Grenoble
- USANS setup: „S-18“ of Atomic Institute Vienna
  - intensity: ca. 10,000 neutrons per sec.
  - very narrow energy / wavelength distribution
  - beam size: 1 x 1 cm

Fibre Spinning: laboratory spinning device built by Lenzing R&D.
- single fibres or up to 37 filaments
- spinning bath : heavy water (D2O)

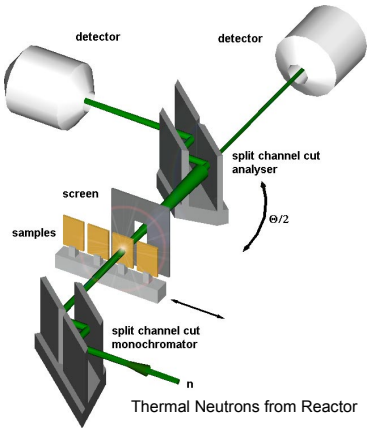

Bonse-Hart-Camera with sample position

Figure 4. Instrumental setup for Ultra-small angle neutron scattering (USANS).

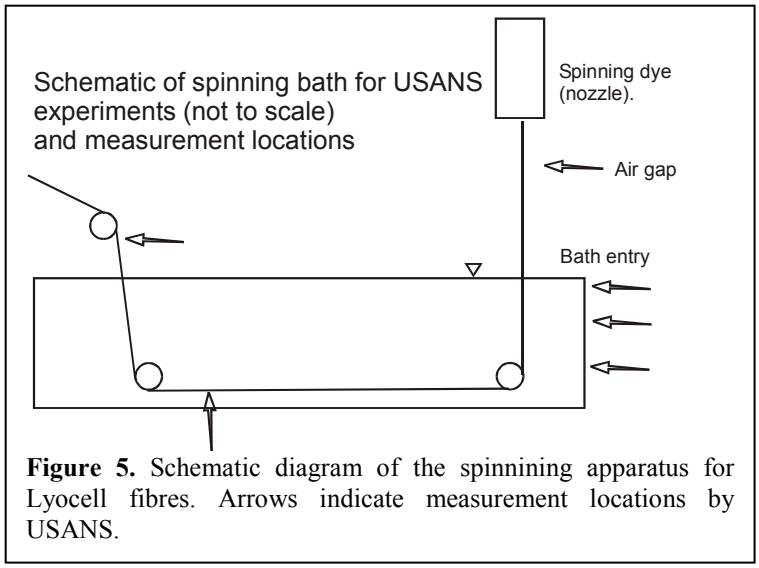

Figure 5. Schematic diagram of the spinnining apparatus for Lyocell fibres. Arrows indicate measurement locations by USANS.

Results and Discussion

Scattering curves: dependence on spinning conditions

By compairing the scattering patterns for the 0.9, 1.3 and 6.7 dtex fibres (Fig. 6), it can be seen that they are qualitatively different. By modelling it cannot be decided at present, if the differences between the scattering patterns are due to the thicknesses of the fibre, or due to their internal structure.

Scattering curves: structure development over the spinning line

When scattering curves were taken along the spinning line, signals could be detected in the air gap as well as in through spinning bath, which consisted of heavy water (Fig.7). Only in the position where the filament was running horizontally (Fig. 7: bath bottom), no signal was detected. It can be concluded that no regular structures in the measurement range were present along the filament axis.
The primary gel swelling is shown in the low Q range: The filament diameter increases in the spinning bath, goes through a maximum and then decreases. By analogy to the viscose process, it has been speculated that this swelling leads to instability in the formed fibre structure. Probably, low-fibrillating fibres have gone through a less severe primary gel swelling, suggesting an approach for improving the fibrillation problem.

Some structure formation over the spinning line can be seen in the higher Q range. The exact nature of these changes through the spinning line is yet to be interpreted. It has to be emphasized that better quality data, particularly a higher signal to noise ratio and resolution in the range $Q > 1.5 \times 10^{-4}$ Å^{-1} needs to be obtained if the nature of the internal structure (if any) and its evolution over the spinning line can be classified.

Scattering curves: structure development – effect of drying

It can be seen from the scattering curves in Figure 8, that the peaks become more pronounced from never-dried, to dried once, through to the fibres being wet/dried five times. Also, after the multiple wet/drying treatment, peaks appear in the higher Q range. This indicates that the never-dried fibres, or even the fibres after 1 drying treatment are not in their final state of development.

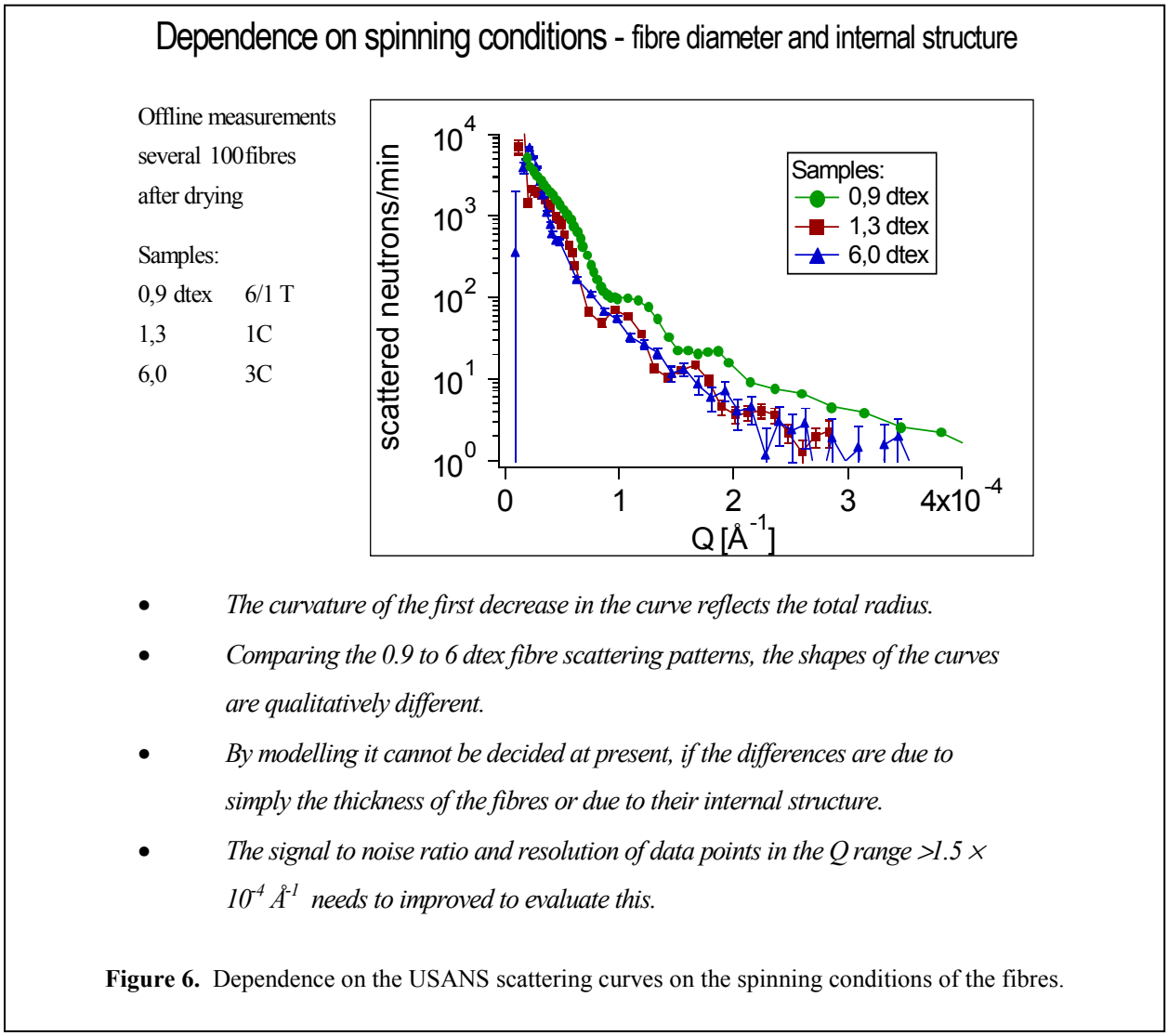

Figure 6. Dependence on the USANS scattering curves on the spinning conditions of the fibres.

Modelling of structures

In the present work, it was found that the simplest model, a solid cylinder, fits the scattering data in terms of peak positions (Fig. 9), for a 1.3 dtex (never-dried) fibre. However, a better fit was achieved when a gaussian radius distribution was applied to the solid cylinders. This has the effect of smearing the troughs between the peaks.

In future works, it is envisioned to employ more complex models resulting in simulated scattering curves fitting each data set more closely. For example, for fibre samples which have undergone multiple wet/dry treatments, or in following the development of fibre filaments over a spinning line, it is hoped this approach will facilitate characterisation of emerging internal structures in such samples, at each stage of the processes.

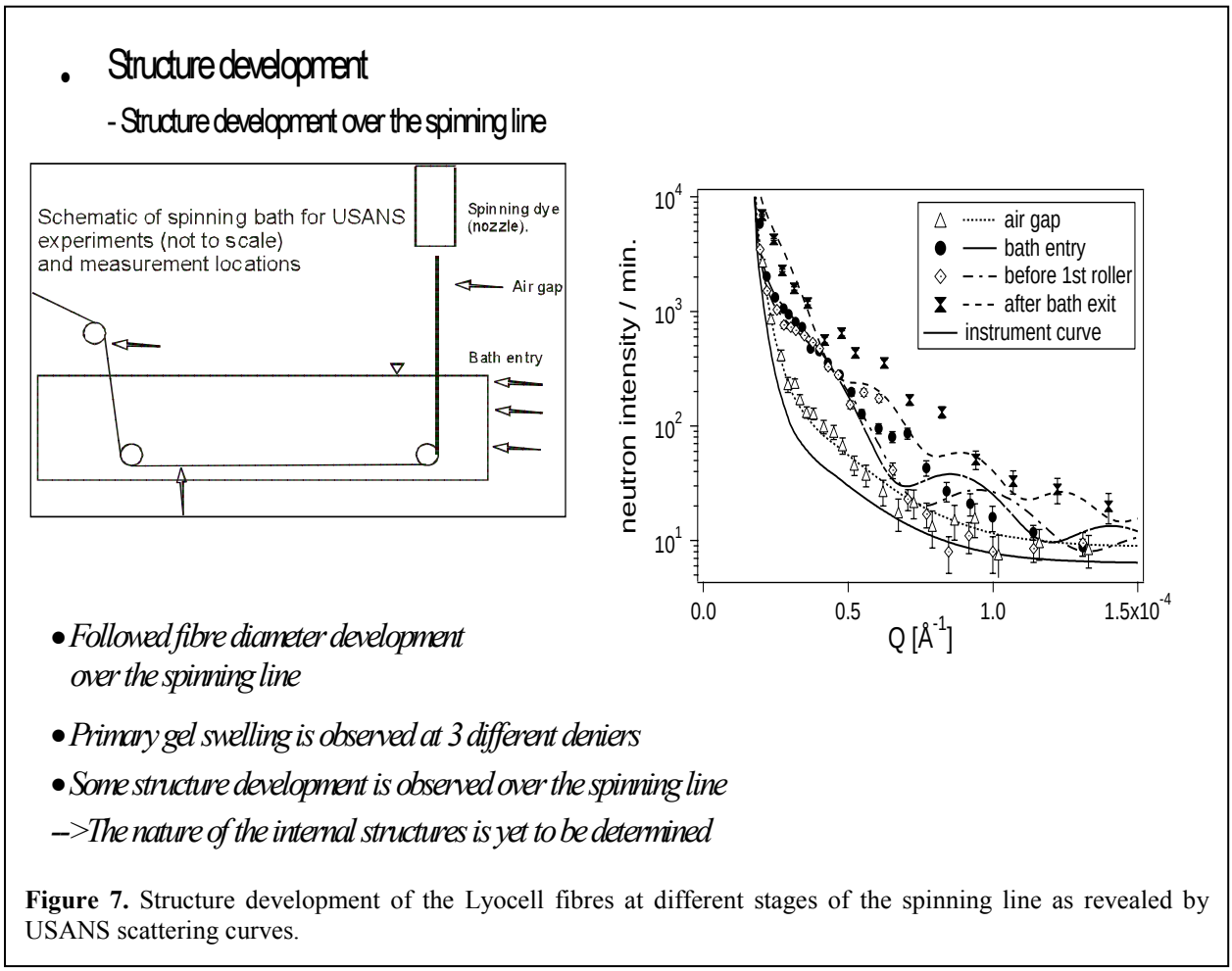

Figure 7. Structure development of the Lyocell fibres at different stages of the spinning line as revealed by USANS scattering curves.

Conclusion

From the results of the work described here, some preliminary conclusions can be drawn: Ultra Small Angle Neutron Scattering

- (USANS) yields novel structure information on Lyocell fibers
- Information can be obtained in the size range relevant for fibrillation, which is the micrometer to 100 nanometer range
- Some structure development over the spinning line, from the air gap through the spinning bath and after the spinning bath, could be observed in situ.

Perspectives

(1) For further interpretation, the following activities are suggested:

- Further modelling, in order to further explain the physical meaning of the scattering curves
- Interpretation connected with results from independent methods
  - ESEM and other imaging methods
  - chemical treatment for fibrillation (swelling)
  - light scattering
- Connect structural information from other size ranges
  - continue scattering curves into SANS range

Structure development - effect of drying: from never-dried to dried and over several drying cycles

Dry climate, 1.3 dtex
offline measurements
several 100 fibres

Samples:(5/5)

Treatment	
never dried D2O	*D*
dried once	*T*
dried 5 times	*T5*

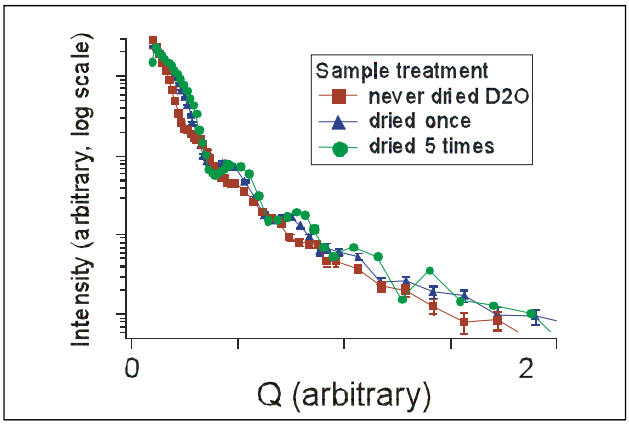

- *Scattering curves from dried samples show more pronounced oscillations*
- *also, more scattering in high q regions --> smaller structures*
- *Trend continues after 5 drying/re-wetting cycle*
- *Fibres are not in final state after 1st drying ?*

Figure 8. Structure development of the Lyocell fibres after multiple drying steps as revealed by the USANS scattering curves

"Solid Cylinder" model with radius distribution - fits the data best so far for fresh (never-dried) fibres

Scattering: Form factor

$$\frac{d\sigma}{d\Omega} = N.P(q).S(q) \cong N.P(q)$$

Differential cross section

Structure factor

$$P(q) = |F(q)|^2$$

Isolated solid rod of radius R: $F = \frac{2J_1(qR)}{qR}$

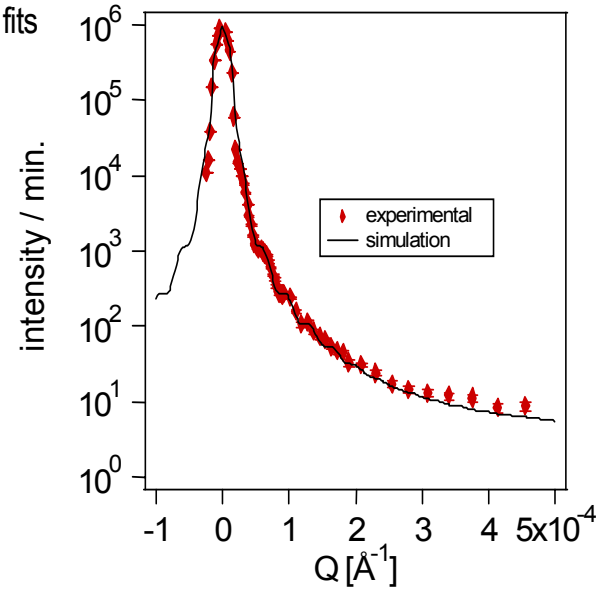

Figure 9. Description of a "solid cylinder" model function with radius distribution for the "Form factor", used in simulations of USANS scattering curves. The agreement between simulation (black line) and an experimental USANS curve (red dots: 1.3 dtex Lyocell (never-dried)) is quite good.

The findings from these first USANS experiments should be applied by performing spinning experiments leading to different fibrillation behaviour, and analysing these.

(2) For a more complete picture from USANS measurements, it is advisable to do more USANS measurements for assessing the reproducibility of the preliminary results. Data with higher signal to noise ratio and resolution in range $> 1.5 \times 10^{-4}$ Å^{-1} is needed to resolve internal structure within the fibre.

Acknowledgements

Thanks to Franz Dürnberger for highly skilled work with the spinning device, and to Ing. Helmut Fuchs who reconstructed the laboratory spinneret to fit into the USANS setup. Also, thanks to Cécile Danilo for her help with the modelling of the USANS curves. The support of the Austrian Academy of Sciences is gratefully acknowledged.

References

(1) Kadla, J. F. and Gilbert, R. D., Cellulose Structure: A Review, Cellulose Chem. Technol., 34, (2000), p. 197-216 Mieck, K. P., Nicolai, M. and Nechwatal, A., Zum Veredlungsverhalten von Lyocell-Geweben, Melliand Textilberichte, 5, (1997), p. 336-338.

(2) Nicolai, M., Nechwatal, A. and Mieck, K. P., Lyocell- Fasern - Alternativen zum Reduzieren der Fibrillierung, Melliand Textilberichte, 10, (1999), p. 848-851.

(3) Lenz, J., Schurz, J. and Wrentschur, Properties and Structure of solvent-spun and viscose-type fibres in the swollen state, Colloid and Polymer Science, 271 (5), (1993), p. 460.

(4) Mortimer, S. A., and Péguy, A. A., The Formation of Structure in the Spinning and Coagulation of Lyocell Fibres, Cellulose Chem. Technol., 30, (1996), p. 117-132.

(5) Lenz, J., Schurz, J. and Eichinger, D., Properties and structure of solvent-spun and viscose-type fibres in the swollen state, Lenziger Berichte, 9, (1994), p. 19-25.

(6) Nemec, H., Fibrillation of Cellulosic Materials- Can Previous Literature Offer a Solution ?, Lenzinger Berichte, 9, (1994), p. 69-72.

(7) Mieck, K. P., Langner, H. and Nechwatal, A., Untersuchung zur Fibrillierneigung Cellulosischer Chemiespinnfasern unterschiedlicher Faserbildungsmechanismen, Lenziger Berichte, 9, (1994), p. 61-68.

(8) Knobelsdorf, C., Mieck, K. P. and Nechwatal, A., Verfahren zur Reduzierung der Fibrillierbarkeit von lösungsgesponnenen Cellulosefasern, DOS 4,312,219, 14.4.1993.

(9) Nicolai, M., Nechwatal, A. and Mieck, K. P., Einfluβ von Veredlungsprozessen auf das Fibrillierverhalten von NMMO- Fasern, Textilveredlung 31 (5/6), (1996), p. 96-100.

(10) Achwal, W. B., Fibrillation tendency of Lyocell and its modification by reactive dyeing, Colourage, March (1999), p. 30-32.

(11) Bredereck, K., Schulz, F. and Otterbach, A., Die Fibrillationsneigung von Lyocell und deren Beeinflussung durch Reaktivfärbungen, Melliand Textilberichte, 10, (1997), p. 703-711.

(12) Nechwatal, A., Nicolai, M., Mieck, K. P., Heublein, B., Kuhne, G. and Klemm, D., Studies on the wet fibrillation of lyocell fibres, angew. Makromol. Chem. 271 (1999), p. 84-92.

(13) Pearson, L. and Taylor, J. M., Fabric treatment, WO 95/00697.

(14) Nechwatal, A., Nicolai, M. and Mieck, K. P., Crosslinking reactions of spun-wet NMMO fibers and their influence on fibrillability, Textile Chemist and Colorist, 28 (5), (1996), p. 24-27.

(15) O. Glatter, O. Kratky, Eds.: Small-angle X-ray scattering. Academic Press: New York (1982).

(16) J. Lenz, J. Schurz, E. Wrentschur: *„The length of the crystalline domains in fibres of regenerated Cellulose. Determination of the crystallite length of Cellulose II by means of Wide-Angle X-Ray Diffraction and Transmission Electron Microscopy“,* Holzforschung 42 (1988) Nr.2, p.117.

(17) J. Crawshaw, R.E. Cameron, *“A small angle X-ray scattering study of the pore structure in TENCEL cellulose fibres and effects on physical treatments”* Polymer 41, (2000), p. 4691.

(18) J. Crawshaw, M.E. Vickers, N.P. Briggs, R.K. Heenan, R.E. Cameron: The hydration of TENCEL© cellulose fibres studied using contrast variation in small angle neutron scattering. Polymer 41 (2000) 1873–1881.

(19) J. Schurz: *„What is new about new fibres of the Lyocell type“,* Lenzinger Berichte 9/94 (1994), p.37.

(20) H.A. Coulsey, S.B. Smith*: The formation and structure of a new cellulosic fibre,* Lenzinger Berichte 75, 51-61 (1996).

(21) S.A. Mortimer, A. Peguy: *„A device for on-line measurement of fibre birefringence“,* Textile Research Journal 64(9), (1994), p. 544.

(22) R. Liu , H. Shao et al., Studies on the coagulation process of lyocell fibers. Chemical Fibres International 51, (2001), p.432.

(23) P. Weigel, H.P. Fink, E. Walenta, J. Ganster, H. Remde: Structure fromation of cellulose man-made fibres from amine oxide solution. Cellulose Chem. Technol. 31 (1997), 321-333.

(24) S.A. Mortimer, A. Peguy: *„Methods for reducing the tendency of Lyocell fibres to fibrillate“,* Journal of Applied Polymer Science 60, (1996), Nr.3, p.305.

(25) Zhang Jianchin; Shi Meiwu; Zhu Hua; Kai Kan: *Study of the skin-core structure of Lyocell staple fibres,* Chemical Fibres International 49, (1999), p. 494.

(26) M. Müller, C. Czihak, G. Vogl, P. Fratzl, H. Schober, C. Riekel : *Direct observation of microfibril arrangement in a single native cellulose fiber by microbeam small-angle X-ray scattering* Macromolecules 31, 3953-3957 (1998).

(27) M. Müller, C. Riekel, R. Vuong, H. Chanzy : *Skin/core micro-structure in viscose rayon fibers analysed by X-ray microbeam and electron diffraction mapping.* Polymer 41, 2627-2632 (2000).

(28) C. E. Moss, M. F. Butler, M. Müller, R. E. Cameron: *Microfocus small-angle X-ray scattering investigation of the skin-core microstructure of lyocell cellulose fibers.* J. Appl. Polym. Sci. 83, 2799-2816 (2002).

(29) M. Hainbuchner, M. Villa, G. Kroupa, G. Bruckner, M. Baron, H. Amenitsch, E. Seidl and H. Rauch: The new high resolution ultra small-angle neutron scattering instrument at the High Flux Reactor in Grenoble. *J. Appl. Cryst.* (2000). 33, 851-854.

(30) M. Hainbuchner, PhD dissertation. Vienna University of Technology, 2000

(31) Bonse, M. Hart, Small-angle X-ray scattering by spherical particles of polystyrene and polyvinyltoluene. Appl. Phys. Lett. 7 (1965), 238

Lenzinger Berichte, 82 (2003) 118-127

Charakterisierung der Lösungsstrukturen in technisch relevanten Celluloselösungen

Thomas Röder[a], Roland Möslinger[a], Ursula Mais[b], Bernd Morgenstern[c] und Otto Glatter[d]

[a]R&D Lenzing , Werksstrasse 1, A-4860 Lenzing, Austria, phone: +43-7672-701-3082, fax: +43-7672-918-3082, email: t.roeder@lenzing.com
[b]Competence Centre WOOD - R&D Lenzing , Werksstrasse 1, A-4860 Lenzing, Austria
[c]FILK GmbH, Meißner Ring 1-5, D-09599 Freiberg, Germany
[d]Institut für Chemie, Karl-Franzens-Universität Graz, Heinrichstr.28, A-8010 Graz, Austria

Abstract

Zur Verformung von Cellulose und der Herstellung von Fasern muß die Cellulose in einem Lösungsmittel aufgelöst und nach der Verformung ausgefällt werden. Dazu werden hauptsächlich zwei Verfahren angewandt- das bewährte Viskoseverfahren und das neuere Lyocell-Verfahren.
Lyocell- und Viskoselösungen weisen unterschiedliche Lösungsstrukturen auf. Die Unterschiede sind mittels SAXS (Röntgenkleinwinkelstreuung), SLS (statische Lichtstreuung), DLS (dynamische Lichtstreuung) und DDLS (depolarisierte dynamische Lichtstreuung) deutlich aufzeigbar. Ein Vergleich der verschiedenen Ergebnisse soll die Möglichkeiten aber auch Grenzen der genannten Methoden aufzeigen. Außerdem wird das System LiCl-DMAc-Cellulose diskutiert, das für die Charakterisierung von Zellstoffen und anderen cellulosischen Substraten mit GPC (Größenausschlußchromatographie) von großer Bedeutung ist.
Celluloseaggregate in Lösungen sind ein altbekanntes Phänomen. In Abhängigkeit von Lösungsmittel und Cellulosekonzentration bilden die Celluloseketten in der Lösung ein Verhakungsnetzwerk mit Gelpartikeln (Viskose) oder ein Verhakungsnetzwerk aus hochgequollenen Aggregaten (Lyocell) oder sie liegen als Einzelmoleküle in der Lösung vor (0,9% LiCl-DMAc).

Characterization of the Solution Structure of Cellulose in Technically Relevant Solutions

Abstract

For the deformation of cellulose and the manufacture of cellulose fibres cellulose has to be dissolved in an appropriate solvent and precipitated after deformation. Therefore two techniques are used - the old viscose process and the new Lyocell process. Lyocell and viscose solutions vary in their solution structures. These differences can be observed with SAXS (small angle x-ray scattering), SLS (static light scattering), DLS (dynamic light scattering) and DDLS (depolarized dynamic light scattering). The comparison of the methods showed their possibilities and limits. Furthermore the system LiCl-DMAc-Cellulose will be discussed. This system has great importance for the characterization of pulps and cellulosic substrates by SEC (size exclusion chromatography).
The formation of cellulose aggregates in solution is a well-known phenomenon. In dependence of the solvent and the cellulose concentration the cellulose chains build up a loose network with gel particles (viscose), an entanglement network with high swollen aggregates (Lyocell), or a molecular disperse solution (0.9% LiCl/DMAc).

Keywords: cellulose solutions, NMMO, LiCl-DMAc, viscose

Einleitung

Für die Verformung der Cellulose ist ihre vorherige Auflösung erforderlich. Die technischen Verfahren basieren entweder auf der Direktauflösung, der Auflösung in einem komplexierenden Lösungsmittel oder der Derivatisierung mit anschließender Regeneration. Die zwei gegenwärtig wichtigsten industriell angewandten Verfahren sind das Lyocellverfahren (Direktauflösung) und das Viskoseverfahren (Derivatisierung).

Das Viskoseverfahren ist über 100 Jahre alt, gegen Ende des 19. Jahrhunderts wurden die ersten industriellen Anlagen gebaut [1]. Schurz [2] fand bereits 1960, daß der Lösungszustand von Viskose gut mit einem Verteilungsspektrum beschrieben werden kann. Er ging von einem geringen Anteil von maximal 5% der Cellulose aus, die als sogenannte Mikrogele in Form beständiger übermolekularer Strukturen vorliegen und nahm als Modell dieser Lösungsstrukturen ein ideales, unendliches Netzwerk an. Seger [3] beschrieb 1996 die Viskoselösung als hochgequollenes Verhakungsnetzwerk mit Inhomogenitäten, die durch eingebaute Aggregatstrukturen bedingt sind. Doch auch nach anderen intensiven Untersuchungen an Viskoselösungen sind noch viele Fragen unbeantwortet.

Die Geschichte des Lyocellverfahrens reicht bis zum Jahr 1939 zurück als das erste Patent für ein Verfahren zur Auflösung von Cellulose in verschiedenen tertiären Aminoxiden an Gränacher und Sallmann [4] erteilt wurde. Doch erst 1969 wurden diese Arbeiten von Johnson et al. [5] weitergeführt. Ab Mitte der 70er Jahre des vorigen Jahrhunderts wurde die Forschung an einem Verfahren zur Auflösung von Cellulose in Aminoxiden von Forschergruppen intensiviert, u.a. in den Vereinigten Staaten, in der damaligen Sowjetunion und in Frankreich. Die besten Ergebnisse wurden mit *N*-Methylmorpholin-*N*-oxid (NMMO) erzielt. NMMO wird in Form seines Monohydrates (NMMO-MH) verwendet. Anfang der 90er Jahre wurden die ersten Pilotanlagen errichtet, denen wenig später Großanlagen folgten.

Mischungen aus *N,N*-Dimethylacetamid (DMAc) und Lithiumchlorid sind als gutes Lösungsmittel für Cellulose bekannt [6]. Das System LiCl-DMAc ist für die großtechnische Celluloseverformung ungeeignet, es hat aber einen festen Platz bei der Analytik von Cellulose [7]. 1986 wurde von J. L. Ekmanis [8] die Gelpermeationschromatographie (GPC) von Cellulose in diesem Lösungsmittel beschrieben. Die Auflösung der Cellulose basiert auf einer Komplexierung. Die Art und Struktur des Komplexes wird in der Literatur kontrovers diskutiert [9].

Streumethoden eignen sich zu einer umfassenden Charakterisierung von Polymerlösungen. In verdünnten Lösungen werden mit der statischen Lichtstreuung (SLS) Molmasse, Trägheitsradius und zweiter Virialkoeffizient, mit der dynamischen Lichtstreuung (DLS) hydrodynamischer Radius sowie Translationsdiffusionskoeffizient und mit der depolarisierten dynamischen Lichtstreuung (DDLS) Rotationsdiffusionskoeffizienten bestimmt. Auch im Bereich konzentrierter Lösungen liefern Lichtstreuung und Röntgenkleinwinkelstreuung (SAXS) wertvolle Erkenntnisse zur Lösungsstruktur. Ein Vergleich der verschiedenen Ergebnisse soll die Möglichkeiten aber auch Grenzen der genannten Methoden aufzeigen.

Die Charakterisierung von verdünnten Celluloselösungen wird bereits von einem möglichen Vorhandensein von Aggregaten beeinträchtigt [10]. Technisch relevante Celluloselösungen weisen zusätzlich folgende Eigenschaften auf:

hohe Cellulosekonzentration und damit einhergehend eine hohe Viskosität sowie eine schlechte Filtrierbarkeit, Verfärbungen (Absorption) und Fluoreszenz, hohe Temperaturen (Lyocell), technisch bedingte Verunreinigungen und das Vorliegen von Mehrkomponentensystemen.

Experimentelles

Die statischen Lichtstreumessungen erfolgten an einem SLS-2 Goniometer der Fa. SLS Systemtechnik (Hausen, Germany) mit einem 5 mW He-Ne-Laser (632,8nm) bei Temperaturen von 20°C (Viskose, LiCl-DMAc) bzw. 85°C (Lyocell).

Die dynamischen Lichtstreumessungen wurden an einem Lichtstreugoniometer (Eigenbau Uni Graz) mit einem 5 W Argonionenlaser (514,5 nm, Spectra Physics, USA) und einem 10 mW

He-Ne-Laser (632,8 nm) bei einem Streuwinkel von 90° und einer Laserleistung von 200 mW durchgeführt. Im Fall der depolarisierten Messungen wurde die Laserleistung auf 1 W erhöht. Der Primärstrahl sowie das gestreute Licht wurden durch zwei Glan-Thomson-Polarisatoren (Glan Thomson, Halle, Berlin, Germany) mit einem Extinktionskoeffizienten kleiner als 10^{-6} geleitet. Die Detektion erfolgte über eine polarisationserhaltende Faser (OZ von GMP, Zürich, Schweiz), die über eine „grin" Linse mit einem Thorn-Emi-Photomultiplier (B2FBK/RFI) gekoppelt war. Das Signal wurde mit einem ALV-5000 Digital Multi-τ-Korrelator (ALV, Langen, Germany) mit 256 Kanälen analysiert.
Die Röntgenkleinwinkelexperimente wurden an einer Kratky-Kompaktkamera mit Göbelspiegel und Image-Plate-Detektion durchgeführt, als Strahlenquelle diente ein Generator Bruker-AXS (rotierende Cu-Anode, 18 kW, M18XHF22-V).

Ergebnisse und Diskussion

Verdünnte Lösungen - Cellulose in NMMO
Für die NMMO-Lösungen wurde die Cellulose in einen Glaskolben gegeben und die entsprechende Menge NMMO-MH zugegeben. Die Auflösung erfolgte unter Rühren bei 85-90°C [11]. Eine Aktivierung des Zellstoffes ist nicht notwendig. Um den Einfluß auf die Aggregatgröße zu untersuchen, wurden dennoch verschiedene Methoden der Aktivierung getestet. Die Ergebnisse von SLS-Messungen an V60-Zellstoff (DP 535) sind in Tabelle 1 zusammengefaßt. Je stärker der aktivierende Eingriff in die Struktur des Zellstoffes, um so kleiner und weniger kompakt sind die existierenden Aggregate. Durch den Einsatz eines Laborkneters konnten die Lösezeiten drastisch verringert werden, eine „Verbesserung" des Lösungszustandes wurde nicht beobachtet. Beim Lösen im Laborkneter wurde (abweichend) 78%iges NMMO eingesetzt und der Wasserüberschuß im Vakuum unter Scherung abgeführt. Die dann erhaltenen Ergebnisse (M_W, R_G) lassen darauf schließen, daß relativ kompakte Cellulose-teilchen vorliegen.

Aktivierung	t_{solv} [h]	M_w [10^6 g/mol]	R_G [nm]	A_2 [10^{-6} molml/g^2]	n_w	Lösungsherstellung
NH_3	5-10	10,7	167	4,0	123	Glaskolben
H_2O	10-15	17,5	171	1,9	202	Glaskolben
Keine	15-20	55,2	204	2,1	636	Glaskolben
NH_3	1	55	156	0,2	634	Laborkneter

Tabelle 1. Ergebnisse der statischen Lichtstreuung an unterschiedlich aktiviertem V60-Zellstoff

In Abb. 1 sind die experimentellen Formfaktorfunktionen [12] der Celluloseproben im Vergleich zu theoretischen Modellen angeführt (harte Kugel, weiche Kugel, homogen verzweigte Partikel, monodisperse Knäuel und polydisperse Knäuel). Der Kurvenverlauf für die Celluloseproben ist ähnlich und liegt zwischen dem einer weichen Kugel und dem einer homogen verzweigten Struktur. Beide Modelle sind denkbar, wenn man davon ausgeht, daß die Aggregate aufgequollene, ehemals kristalline Bereiche der Cellulose sind. Weil die Aggregate so groß sind, bewegt sich die Auswertung im Grenzbereich der Theorie. Das teilweise Ansteigen der Kurven bei großen Winkeln deutet darauf hin, daß Teile der Aggregate als separates Partikel detektiert werden.

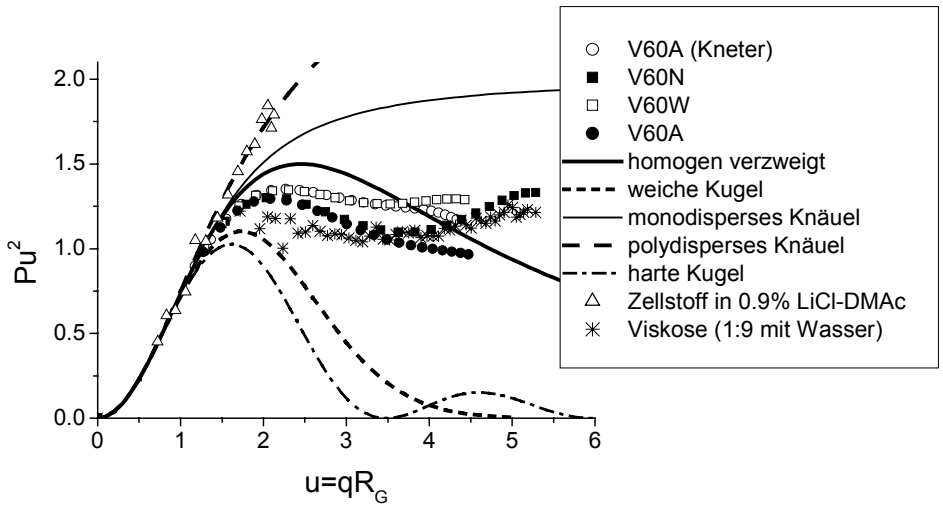

Abbildung 1. Vergleich der Formfaktoren der Proben aus Tab. 1 mit theoretischen Modellen.

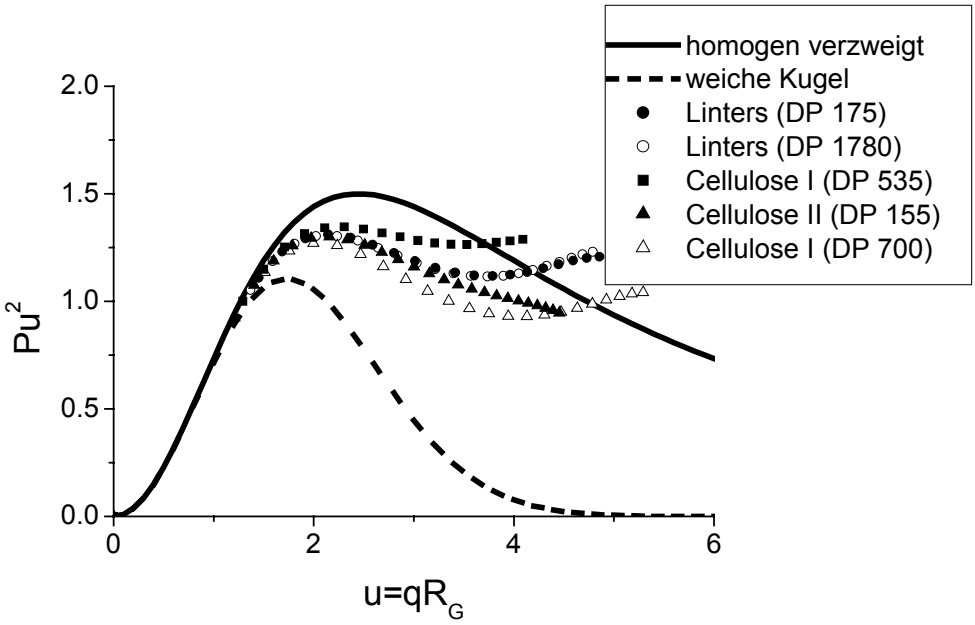

Abbildung 2. Vergleich der Formfaktoren wassergequollener Proben mit theoretischen Modellen.

Wassergequollene Zellstoff- und Lintersproben weisen keine signifikanten Unterschiede der Teilchenform (Abb. 2) auf. Bemerkenswert ist der identische Verlauf der Formfaktorkurven im Fall der Lintersproben, trotz deutlicher Unterschiede beim Polymerisationsgrad. Dieses Verhalten deutet auf vergleichbare kolloidale Strukturen hin. Die Formfaktorkurven der Zellstoffe unterscheiden sich teilweise stark voneinander. Zellstoffe werden aus den unterschiedlichsten Rohstoffen und nach verschiedenen Verfahren hergestellt. Die verschiedenen Rohstoffquellen und die mechanische Belastung, der die Cellulose während des Aufschlußverfahrens ausgesetzt ist, sind für Änderungen in der Cellulosestruktur verantwortlich. Linters sind dagegen chemisch und physikalisch einheitlicher, da kein Aufschluß notwendig ist und die Fasern von der gleichen Pflanze (Baumwolle) stammen. In allen Fällen wurden auch in verdünnten Lösungen Aggregate nachgewiesen. Diese bestehen aus einem mehr oder weniger kompakten Kern mit seitlichen Fransen, wie ein zusammengerollter Igel mit weichen Borsten [13].

Verdünnte Viskoselösungen

Viskosespinnlösungen wurden im Verhältnis 1:9 mit Wasser verdünnt. Die statische Lichtstreuung lieferte M_W = 4,3 Mio g/mol, R_G = 227 nm und $A_2 = 3 \cdot 10^{-6}$ molml/g^2. Bei einem durchschnittlichen Polymerisationsgrad (DP) von 470 und einem angenommenen durchschnittlichen Substitutionsgrad (DS) von 1 bedeutet das, daß 35 Cellulosemoleküle ein Aggregat bilden. Die enorme Größe des Aggregates im Vergleich zu den in NMMO beobachteten, ist durch eine geringere Cellulosedichte und eine lockerere Struktur erklärbar. In ihrer äußeren Form ähneln die Aggregate den in NMMO gefundenen, was durch den Verlauf der Formfaktorkurve in Abb. 1 belegt wird.

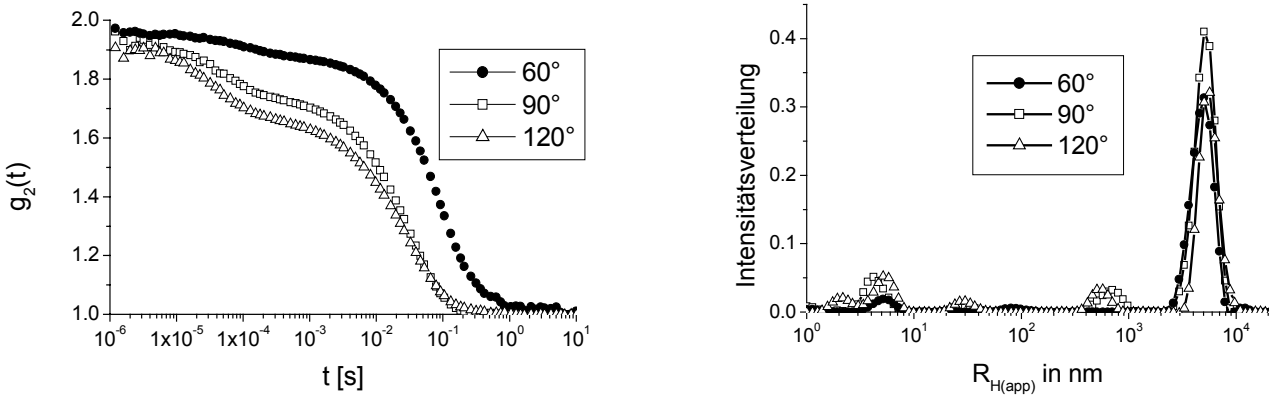

Abbildung 3. Intensitätsautokorrelationsfunktionen und Intensitätsverteilungen der hydrodynamischen Radii für eine Modalviskose mit Wasser 1:9 verdünnt, gemessen bei unterschiedlichen Winkeln.

Die dynamische Lichtstreuung, bei der die Änderung der Streuintensität bei einem festen Winkel gemessen wird, eignet sich nicht für quantitative Auswertungen im System NMMO/Cellulose, da NMMO eine ausgeprägte „Eigenstruktur“ aufweist. Für Viskoselösungen gilt diese Einschränkung nicht. Die Analyse der mittels DLS aufgenommenen Intensitätskorrelationsfunktionen (IKF) von mit Wasser verdünnten Viskoselösungen (Abb. 3) ergab, daß zwei charakteristische Bewegungen auftreten, die von verschiedenen Teilchen herrühren. Die schnelle Bewegung mit Korrelationszeiten zwischen 10^{-5} und 10^{-4}s kann Einzelmolekülen und frei beweglichen Seitenketten von größeren Aggregaten zugeordnet werden. Die mit den SLS-Messungen nachgewiesenen großen Partikel weisen Relaxationszeiten zwischen 10^{-2} und 10^{-1}s auf. Messungen bei verschiedenen Winkeln ergaben keine Änderung bei der Berechnung der Intensitätsverteilung [14], so daß es sich bei den detektierten Bewegungen um diffusive Prozesse handelt.

Durch Filtrieren werden die Aggregate nicht vollständig abgetrennt. Der Vergleich der Intensitätsverteilungen einer unfiltrierten und einer filtrierten verdünnten Viskoselösung in Abb. 4a zeigt, daß die Aggregate durch Filtration kleiner werden. Ihre Größe liegt dennoch oberhalb des Durchmessers der Filterporen. Das läßt darauf schließen, daß entweder die Aggregate verformt werden und hindurchgleiten oder die Aggregate zerteilt werden und sich anschließend neu bilden.

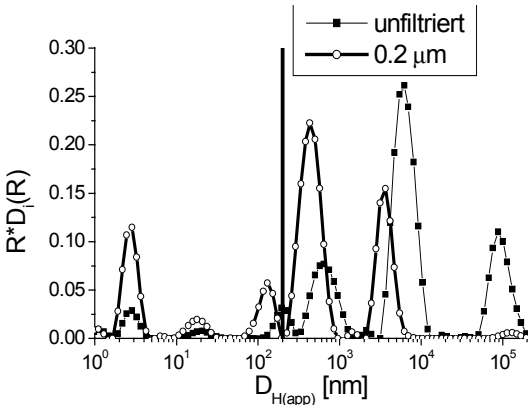

Abbildung 4a. Intensitätsverteilungen der hydrodynamischen Durchmesser für eine Normalviskose mit Wasser 1:9 verdünnt, gemessen bei 130°, unfiltriert und filtriert (0,2 µm).

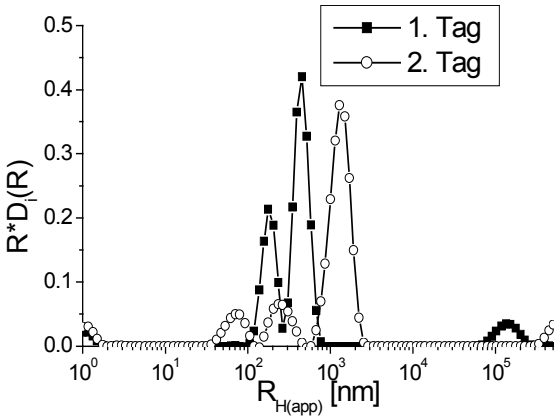

Abbildung 4b. Einfluß der Standzeit auf den scheinbaren hydrodynamischen Radius der Aggregate (Normalviskose, 1:9 mit Wasser verdünnt, 90°)

Mit zunehmender Standzeit zerfällt das Cellulosexanthogenat, die Aggregate werden größer (Abb. 4b). Nach einigen Tagen ist dieser Vorgang auch visuell zu beobachten, die Cellulose fällt aus und bildet einen Gelkörper.

Konzentrierte Lösungen

Konzentrierte NMMO-Lösungen können mit Hilfe von DLS-Messungen qualitativ bewertet werden. Wenn die Zellstoffkonzentration so hoch ist, daß sich die Aggregate teilweise durchdringen, miteinander verhaken und ein Netzwerk bilden, steigt die Viskosität der Lösung stark an. Die Bewegung der Aggregate ist praktisch eingefroren. Es sind nur noch die Bewegungen der Fransen detektierbar (Abb.5).

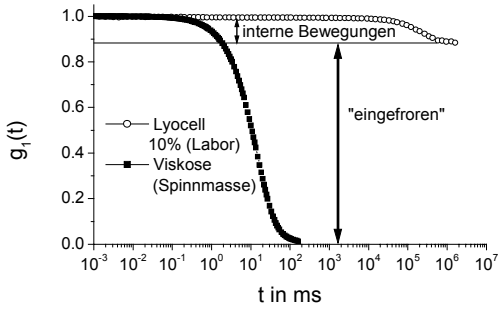

Abbildung 5. Intensitätsautokorrelationsfunktionen konzentrierter Spinnlösungen.

Viskoselösungen zeigen dieses Phänomen nicht und sind durch eine für das System charakteristische Korrelationszeit gekennzeichnet. Die Form der Aggregation ist in diesem System anders. Durch die Derivatisierung sind nicht mehr alle OH-Gruppen der Cellulose für die Bildung von Wasserstoffbrücken verfügbar. Daher weisen Aggregate in Viskoselösungen eine wesentlich lockerere Struktur auf.

Die Cellulosestrukturen in Viskose- und in NMMO-Lösungen sind von ihrer Dimension her zu groß für eine Messung mittels Röntgenkleinwinkelstreuung (SAXS). Aus den SAXS-Daten kann dennoch das Oberflächen-Volumen-Verhältnis (A_O/V) als ein Maß für die Porosität und Lockerheit der Strukturen berechnet werden [15].

Das A_O/V-Verhältnis ist ein Absolutwert und wurde für eine Konzentrationsreihe von 3% bis 13% bei 80°C und 95°C bestimmt (Abb. 6). Es ist ein Maß für die „Zerklüftung“ der Oberfläche und damit der Güte der Lösung. Dabei gilt: je größer A_O/V, desto besser ist der Lösungszustand. Aus Abb. 6 ist ersichtlich, daß der Lösungszustand mit zunehmender Zellstoffkonzentration günstiger ist, was wahrscheinlich auf die Herstellungsbedingungen zurückzuführen ist. Bei der Herstellung der Lösung im Laborkneter sorgt eine hohe Zellstoffkonzentration für hohe Konsistenz und damit für große Scherkräfte. Dadurch werden die großen Aggregate zerteilt.

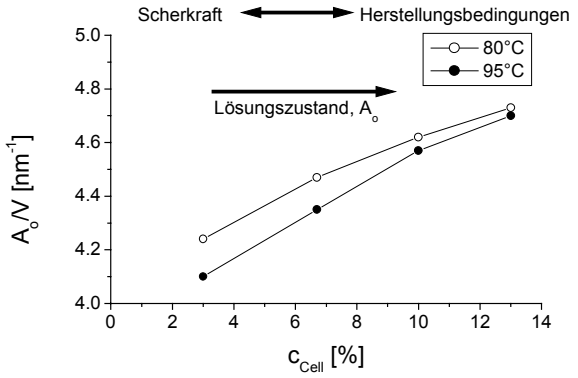

Abbildung 6. A_O/V-Verhältnis (aus SAXS-Messungen) von Lyocell-Lösungen.

Rheologie an Spinnmassen

Um die vergleichsweise niedrige Viskosität und die unterschiedlichen rheologischen Eigenschaften von Viskosen [16] im Vergleich zu Lyocellösungen [17] darzustellen, wurden Oszillationsversuche durchgeführt. Mit Hilfe dieser Versuche lassen sich auch Aussagen über den Lösungszustand und die molekularen Parameter wie mittlere Molmasse und Verteilungsbreite treffen. Die Viskositäten und die dynamischen Moduln sind bei Lyocell (Abb. 7) um das 100- bis 1000-fache größer als bei der Normal-Viskose, trotz deutlich höherer Messtemperatur. Gründe dafür sind zum einen die höhere Cellulosekonzentration bei Lyocell im Vergleich zur Normalviskose, zum anderen die niedrigere Molmasse der beim Viskoseprozess stärker als beim Lyocellverfahren abgebauten Cellulose. Auch die Molmassenverteilung ist unterschiedlich.

Der Zusammenhang zwischen dem Massenmittel der Molmasse Mw und der Nullviskosität h_0 mit einer Steigung von ca. 3 in der log h_0 - log Mw-Darstellung zeigt, daß es sich bei Viskosen um Netzwerklösungen handelt, bei der die einzelnen Cellulosemoleküle ineinander verhakt und verschlauft sind.

Der Verlauf der Moduln über die Frequenz zeigt, daß bei den N-Viskosen in der Lösung auch Assoziate oder Mikrogele vorliegen.

Übermolekulare Strukturen sind bei den dynamischen Moduln daran zu erkennen, daß in einer doppeltlogarithmischen Auftragung bei G" zu kleinen Frequenzen hin die terminale Neigung 1 – daraus ergibt sich η_0 – annähernd erreicht wird, die Neigung dann aber wieder abnimmt. Bei G' wird die terminale Neigung 2 meist gar nicht erreicht, bevor es wiederum zu einer Abnahme der Neigung kommt. Auch der vergleichsweise niedrige Verlustwinkel tan δ, der sich aus dem Quotienten von G" und G' berechnen läßt, deutet auf starre Vernetzungen zwischen den Molekülen oder Anteile an hochmolekularen Verbindungen hin. Sehr große Moleküle oder Aggregate lassen sich besser deformieren und können daher die Deformationsenergie besser speichern.

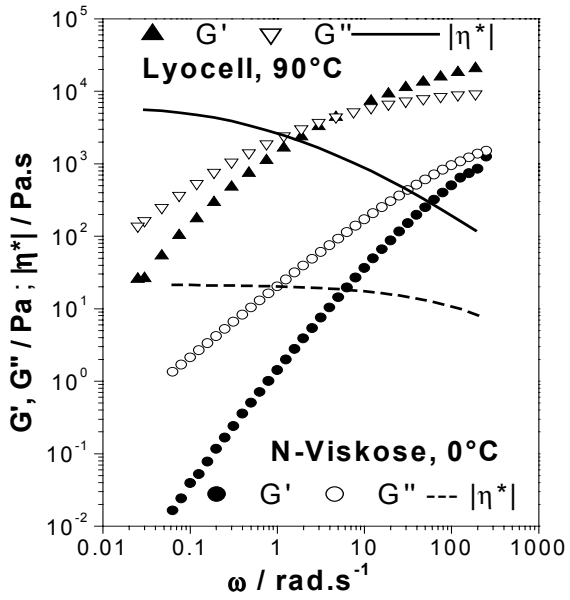

Abbildung 7. Vergleich der dynamischen Moduli und der komplexen Viskosität von Lyocell- und Viskoselösungen.

Bei Lyocell hingegen werden die terminalen Bereiche bei kleinen Frequenzen nicht erreicht, womit die Nullviskosität nur aus dem Verlauf von |η*| berechnet werden kann. Lyocelllösungen zeigen ein stark ausgeprägtes strukturviskoses Verhalten, das dem Verhalten von Kunststoffschmelzen analog ist. Der Crossover-Punkt, an dem Speicher- und Verlustmodulkurven sich kreuzen, liegt im Gegensatz zu den Viskosen im Messbereich.

Lösungen in LiCl-DMAc

Das System LiCl-DMAc wird als Lösungsmittel für die GPC verwendet. Nach der Aktivierung der Cellulose erfolgt das Lösen in 9%igem LiCl-DMAc [7]. Die so hergestellte Stammlösung weist üblicherweise einen Cellulosegehalt von 1% auf.

Für die Injektionslösung zur GPC wird diese Lösung auf einen LiCl-Gehalt von etwa 2,6% verdünnt. Als Laufmittel wird 0,9% LiCl-DMAc verwendet. Unsere Untersuchungen zeigten, daß die Cellulose in 9% LiCl-DMAc aggregiert vorliegt. Bei Verdünnung auf 0,9% LiCl zerfallen diese Aggregate [18]. Der Verlauf der Formfaktorfunktion der Cellulose-teilchen in 0,9% LiCl-DMAc (Abb.1) ähnelt dem eines polydispersen Knäuels. Die Cellulose liegt molekulardispers gelöst vor.
Zur Auflösung von Cellulose in LiCl-DMAc muß die LiCl-Konzentration zwischen 5 und 9% betragen [19]. Auftretende Aggregate könnten Reste von ursprünglich kristallinen Bereichen der Cellulose sein. Um die Struktur dieser Aggregate besser bestimmen zu können, wurden Lösungen unter Bedingungen her-gestellt, die die Aggregation begünstigen (niedriger LiCl-Gehalt, mikrokristalline Cellulose, hohe Cellulosekonzentration). Bereits mit 1% Avicel (mikrokristalline Cellulose, DP = 285) und 6% LiCl wurden in der IKF (Abb. 8) zwei Bewegungen sichtbar. Während der Anteil der schnellen Bewegung mit steigender Cellulosekonzentration stetig abnahm, stieg der Anteil der langsamen Bewegung an.

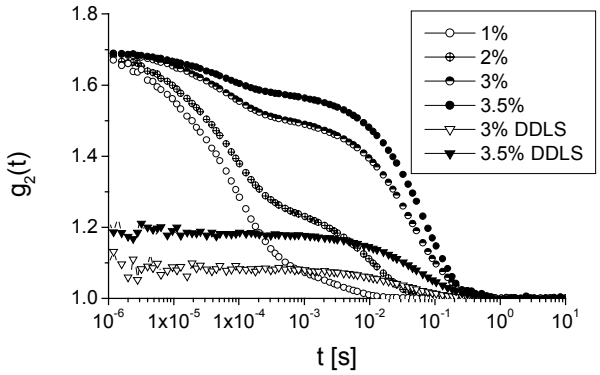

Abbildung 8. Intensitätsautokorrelationsfunktionen (IKF) von Avicel-Lösungen in 6% LiCl-DMAc

Die Kurven verschieben sich zu größeren Zeiten, was konform zur Viskositätsänderung aufgrund erhöhter Cellulosekonzentration ist. Zur Detektion optischer Anisotropien wurde zusätzlich depolarisiert gemessen. Dabei wird der Primärstrahl durch einen auf „vertikal“ gestellten Polarisator geschickt, das gestreute Licht fällt durch einen auf „horizontal“ gestellten Polarisator. Diesen passiert nur das Licht, das beim Durchgang durch die Probe in seiner Polarisierung gedreht wurde. Ab 3% Avicel konnte eine IKF aufgenommen werden. Bei dieser depolarisierten dynamischen Licht-streuung wird nur der relativ kompakte und harte anisotrope Kern der Aggregate be-obachtet. Das ist ein weiteres Indiz für die fransenmicellare Struktur der Aggregate. Die schnelle Bewegung, die im normalen Modus zu beobachten ist und im depolarisierten Modus völlig fehlt, ist daher wahrscheinlich auf die Bewegungen der „Fransen“ zurückzuführen.
Einen weiteren Hinweis für die Richtigkeit dieser Erklärung lieferten Untersuchungen zum Einfluß des Wassergehaltes auf den Lösungs-zustand in GPC-Lösungen mit 0,9% LiCl und weniger als 0,1% Cellulose.
Als Beispiel ist in Abb. 9 die Messung einer Lösung mit 0,05 M Wasser dargestellt. Die Stammlösung wurde mit trockenem DMAc mit 9% LiCl-Gehalt hergestellt. Der Wassergehalt wurde nach der Auflösung der Cellulose eingestellt. Die Verdünnung erfolgte mit DMAc des gleichen Wassergehaltes. Bereits 25 Minuten nach Verdünnung auf GPC-Niveau (0,9% LiCl), verschob sich die Korrelationsfunktion $g_2(t)$ zu größeren Zeitwerten (Abb. 9a).
Die Streuintensität derart verdünnter Lösungen ist sehr gering, was sich in einem kleinen „intercept“ (Wert der $g_2(t)$ für t=0) äußert. Das „intercept“ steigt mit zunehmender Aggregation. Dieser Effekt hat keinen wesentlichen Einfluß auf die Prinzipien der Analyse, nur ein Driftfaktor von 2 in der berechneten Größenverteilung ist möglich.
25 Minuten nach dem Verdünnen bildete sich eine zweite Partikelpopulation mit scheinbaren hydrodynamischen Radien um 100 nm (Abb. 9b). Nach einem Tag betrug der Radius dieser zweiten Fraktion 80-200nm. Bei DDLS-Messungen an der selben Lösung ergab sich eine Korrelationsfunktion, was auf optisch anisotrope Partikel hinweist.

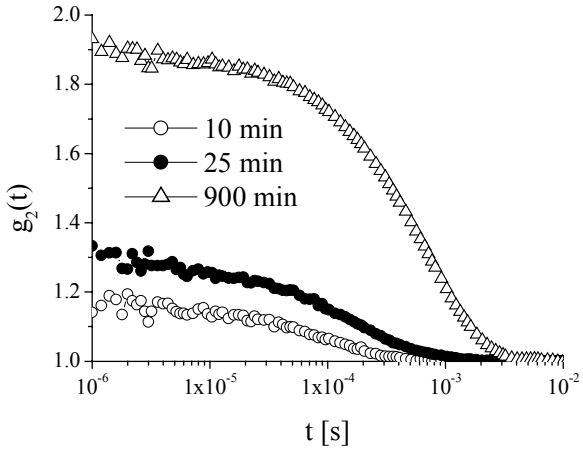

Abbildung 9a. Zeitabhängigkeit der Autokorrelationsfunktion, KZO_3 (0,028%) in 0,9% LiCl-DMAc mit 0,05 M Wasser.

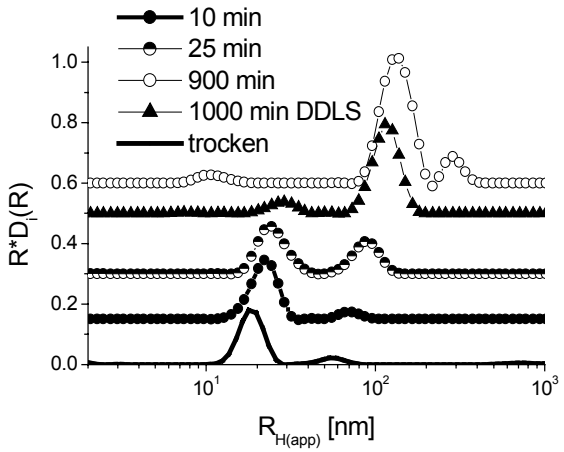

Abbildung 9b. Zeitabhängigkeit der Intensitätsverteilung der gelösten Cellulose als Funktion des scheinbaren Radius (vergl. Abb. 7a).

Der scheinbare hydrodynamische Radius dieser Partikel lag zwischen 70 und 180 nm. Unter der Annahme der Gültigkeit des Modells der Fransenmicelle (relativ harter Kern und gut orientierte gequollene Hülle, vergleichbar einem zusammengerollten Igel mit weichen Borsten) spiegeln die DLS-Messungen das gesamte Partikel wider, während bei DDLS-Messungen nur der Kern sichtbar ist. Eine quantitative Bestimmung der Dimensionen der Partikel scheiterte an der zeitlichen Instabilität der Lösung.

Zusammenfassung

Celluloseaggregate in Lösungen sind ein altbekanntes Phänomen. Viskoselösungen sind gekennzeichnet durch ein Verhakungsnetzwerk mit Gelpartikeln. Auch beim Verdünnen wird kein molekulardisperser Lösungszustand erreicht. In NMMO bildet die Cellulose bereits in verdünnten Lösungen kompakte Aggregate, die einer Fransenmicelle, relativ kompakter Kern mit seitlich herausstehenden Armen, ähneln. Bei höheren Konzentrationen liegt ein Verhakungsnetzwerk dieser hochgequollenen Aggregate vor. In LiCl-DMAc-Lösungen mit hohem LiCl-Gehalt wurden ebenfalls aggregierte Cellulosemoleküle gefunden. Diese Aggregate zerfallen beim Verdünnen mit DMAc. In 0,9% LiCl-DMAc liegt die Cellulose molekulardispers gelöst vor. Die Zugabe von geringen Mengen Wasser induziert die erneute Bildung von Aggregaten, die ähnliche Eigenschaften wie die in NMMO-Lösungen gefundenen aufweisen.

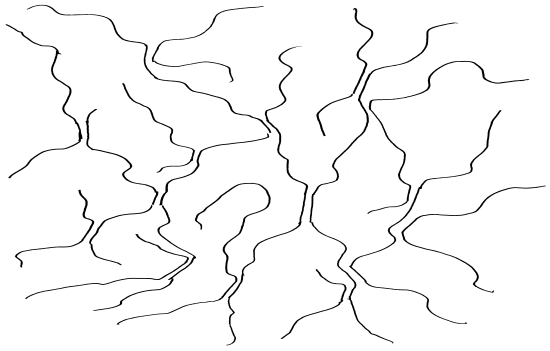

Abbildung 10a. Strukturvorschlag Viskose

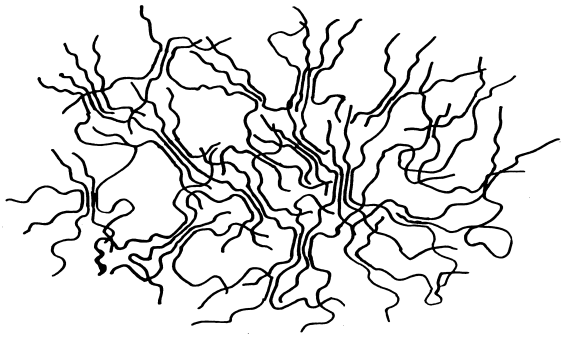

Abbildung 10b. Strukturvorschlag Lyocell

Danksagung

Unser besonderer Dank gilt Herrn Prof. Dr. W. Burchard (Freiburg, Germany) und Herrn Univ.-Doz. Dr. H. Sixta (Lenzing AG) für die vielen anregenden Diskussionen.
Wir danken Frau Dr. A. Potthast (CD-Labor, BOKU Wien), Herrn G. Ebner (CD-Labor, BOKU Wien) und Herrn W. Milacher (Lenzing AG) für die Bereitstellung der LiCl-DMAc- und der Viskoselösungen. Der Christian-Doppler-Forschungsgesellschaft, der Lenzing AG und dem Freistaat Sachsen danken wir für die Finanzierung.

Literatur

[1] Cross, C.F., Bevan, B.T., Beadle, C., Ber. Dtsch. Chem. Ges. 26 (1893) 1096 und 2520
[2] Schurz, J., Paperi ja Puu 7 (1960) 401
[3] Seger, B., Dissertation 1996, Freiburg, Germany
[4] Gränacher, C., Sallmann, R., US Patent 2.179.181 (1939)
[5] Johnson, D.L., British Patent 1.144.048 (1969)
[6] Turbak, A.F., El-Kafrawy, A., Snyder, F.W., Auerbach, A.B., US Patent 4.302.252 (1981)
[7] Schelosky, N., Röder, T., Baldinger, T., Das Papier (Darmstadt) 53 (1999) 728
[8] Ekmanis, J.L., Pol. Notes, Waters 1 (1986)
[9] Morgenstern, B., Kammer, H.-W., Trends Polym. Sci. (TRIP) 4 (1969) 87
[10] Burchard, W., Adv. in Colloid and Interface Sci. 64 (1996) 45
[11] Röder, T., Morgenstern, B., Polymer 40 (1999) 4143
[12] Burchard, W., Adv. Pol. Sci. 48 (1983) 1
[13] Röder, T., Dissertation 1998, Dresden, Germany
[14] Schnablegger, H., Glatter, O., J. Applied Optics 30:33 (1991) 4889
[15] Glatter, O., Kratky, O., „Small Angle X-Ray Scattering" Academic Press London (1982)
[16] Schausberger, A., Möslinger, R., Das Papier (Darmstadt) 53 (1999) 715
[17] Schrempf, C., Schild, G., Rüf, H., Das Papier (Darmstadt) 49 (1995) 748
[18] Röder, T., Morgenstern, B., Glatter, O., Polymer 42 (2001) 6765
[19] Dawsey, T.R., McCormick, C.L., J. Macromol. Sci., Rev. Macromol. Chem. Phys. C30 (1990) 405

Lenzinger Berichte, 82 (2003) 128-135

Contribution to dissolution state of cellulose in aqueous amine oxide characterized by optical and rheological methods

Ch. Michels und B. Kosan

Thüringisches Institut für Textil- und Kunststoff-Forschung,
Breitscheidstrasse 97, D-07407 Rudolstadt-Schwarza,
Tel.: (0 36 72) 37 92 20, Fax: (0 36 72) 37 93 79, e-mail: michels@titk.de and kosan@titk.de

Abstract

The dissolution of cellulose in aqueous amine oxides to isotropic, completely solvated cross-linked solutions is a multiple stage process in microscopic, submicroscopic and molecular ranges. In a suspension of cellulose, water and NMMO at 85°C and with decreasing water content the cellulose undergoes a growing swelling accompanied by an increased flexibility of the chain leading to a heterogeneous phase for the 1,5 hydrate (81,3 % NMMO) to an irreversible transfer of cellulose I into cellulose II and for the 1,2 hydrate (84,4 % NMMO) to a homogeneous, partly solvated gel phase. Discrete inhomogeneities with equivalent spherical diameters greater than 0,5 µm and a concentration greater than 1 µl/l can be analyzed by microscopy and laser diffraction. Rheological parameters and in particular recording of deformation graphs and calculating relaxation time spectra were proven to be efficient for characterization of the solvation occurring during dissolution.

Keywords

Cellulose / cellulose solution / solution state / particle analysis / shear rheology

Introduction

Swelling and dissolution of cellulose in non-derivating solvents and the description of the achieved dissolution state is an important task and is a matter both of scientific and technical interest.

Diluted solutions of cellulose in metal complexes of copper, iron, zinc, nickel etc. with ammonia , tartaric acid , ethylene diamine and Bis- respectively Tris(2-amino-ethyl)amine have superficial analytic importance and are repeatedly described in literature [1-3]. Taking in account technical as well as commercial aspects, concentrated solutions of cellulose became important, as for example solutions of cellulose in copper-ammonia, since the dissolution and coagulation of shaped cellulose should be performed by changing, as far as possible, only one parameter.

With the aqueous amine oxides and in particular with the N-methyl morpholine-N-oxide-hydrate (NMMO) there was discovered already in 1936 a solvent system, which can take up cellulose up to 20 wt % whereas its dissolution state undergoes significant changes when slightly changing the water content [4–7].

Highly diluted solutions of one and the same cellulose in NMMO , " Cuoxam " or " Cuen " exhibit similar behavior and contain comparable intrinsic viscosity numbers with about 340 [ml/g] at 75 °C respectively 290 or 400 [ml/g] at 23 °C. That means assuming free swelling behavior 1 mol of cellulose takes up 480 mol of NMMO. With increasing molecular weight and/or cellulose concentration a transition of the particle solution to a network solution takes place, approaching the so-called critical molecular weight range, where lyotropic mesophases are formed with exceeding cellulose concentration $\geq$ 20 %.

Technical dissolving and shaping processes favor solutions with 10 – 15 wt % of cellulose, that means one has to deal with isotropic network solutions. These isotropic network solu-

tions are the objective of the following reflections.

Contrary to the described direction the experimental dissolution process, starting from native cellulose, undergoes a dilution from the highly concentrated network solution to the diluted particle solution. Polymer chains of native cellulose are stiffened alongside the chain via intramolecular hydrogen bridge bonds and they are cross-linked each other via existing intermolecular hydrogen bridge bonds between the chains.

Feeding of cellulose into the aqueous NMMO under applied shear forces will cause a simultaneous swelling of the amorphous ranges of cellulose fibers and thereby generate a suspension. With increased evaporation of water in vacuum and rise in temperature and shear force, the swelling increases spontaneously with a mol ratio NMMO: water ~ 1 : 1,5 – 1,2, the differences of the refractive indices of the individual components disappear to a large extent and the remaining gel appears to be largely homogeneously based on corresponding microscopic investigations.

Based on the appearance one could be apt to consider this suspension as a solution. However when paying much closer attention, several facts are contrary to this assumption. The following figures 1 – 4 should make evident the transition of a multiple phase suspension to a microscopically homogeneous gel phase of a solution with 12,5 wt % cellulose, having a Cuoxam DP of about 563 of the dissolved cellulose .

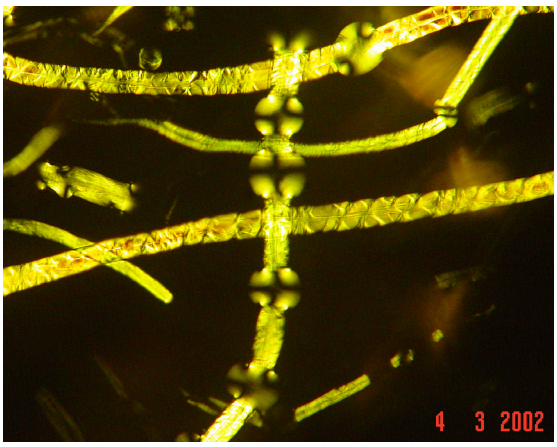

Figure 1. suspension - gel – solution

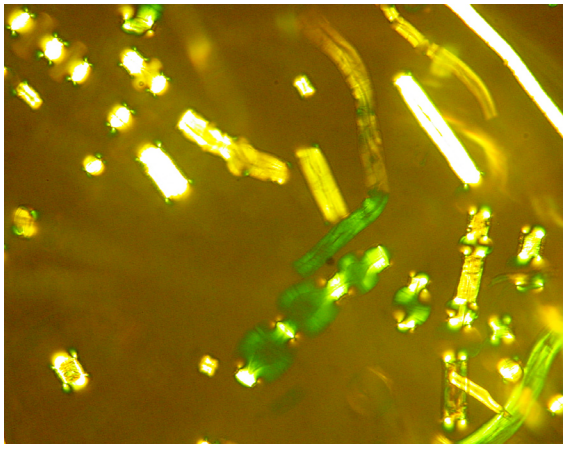

Figure 2. suspension - gel - solution

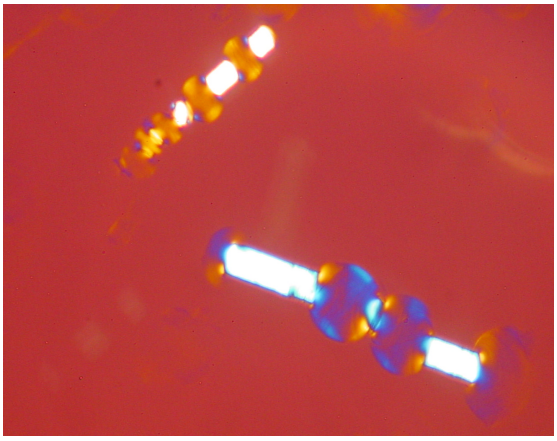

Figure 3. gel – solution

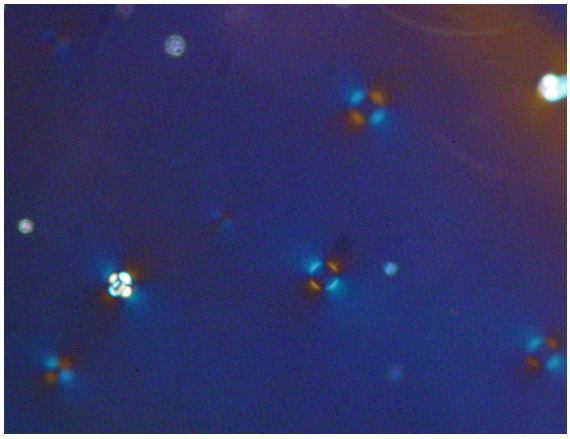

Figure 4. gel - solution

At this state the measurable viscosity will reach a maximum value, one part of the hydrogen bridge bonds is solvated and the chain mobility is increased to such an extent that a non-reversible transition from cellulose I into cellulose II takes place. Wide angle X-Ray spectros-

copy measurements (WAXS) made from samples being swollen in solutions of different NMMO-concentrations, washed and dried, or coagulated and dried after dissolving, have confirmed this transition.

Figure 5 shows the spectra in the range of 4 – 40 °, for medium chain orientation of the untreated starting sample- Kraft cellulose pulp on the on the side, and of such samples being swollen or dissolved within 5 hours at 80 °C with different NMMO concentrations on the other side.

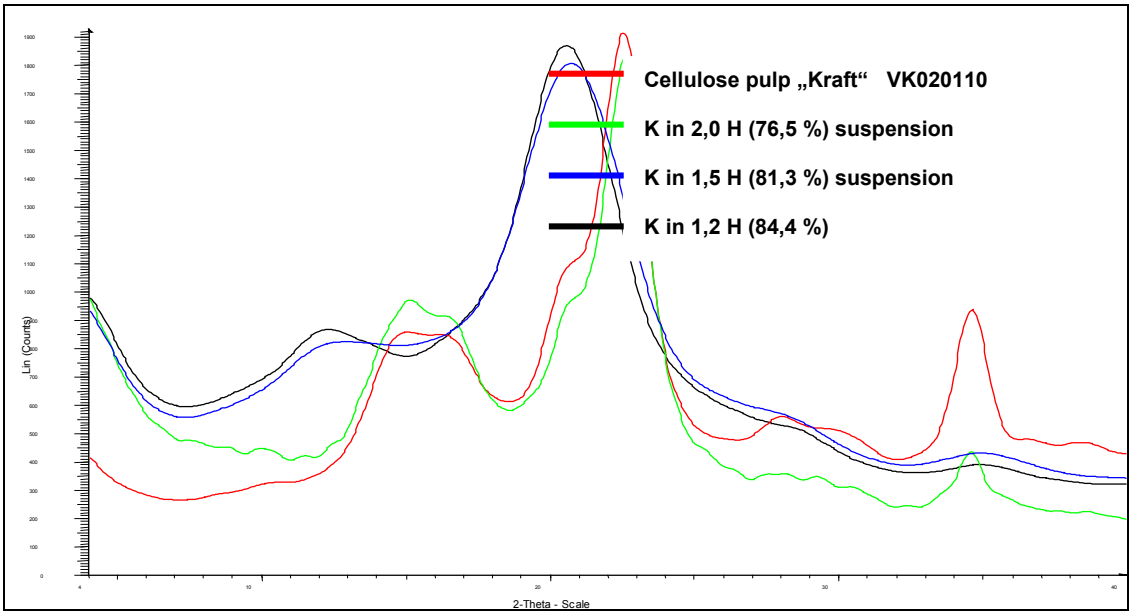

Figure 5. Wide angle X-ray 4 - 40° - transition of cellulose I / II

One can see clearly, that the peaks of the cellulose pulp and of the sample, being swollen in dihydrate (76,5 % NMMO) at the one hand and those of the samples being either swollen in 1,5 hydrate (81,3 % NMMO) or dissolved in 1,2 hydrate (84,4 % NMMO) on the other side show a good analogy. That means, the chain mobility in heterogeneous phase (1,5 hydrate) has already reached such an extent, causing a non-reversible transition of cellulose I into cellulose II. Furthermore it can be derived that the transition to the one phase gel does not cause further apparent changes in structure.

Based on the ZERO-shear viscosities at 85 °C and their corresponding standard deviations, measured at various points of a larger sample, one can conclude the existence of an inhomogeneous solution state. With increased shearing, and where necessary, further removal of water, the ZERO-shear viscosity changes in relatively short time in the order of one magnitude and the reproducibility of all measurements is within the limit of errors for this method. Since the molecular weight and the concentration are almost unchanged, the decrease in viscosity should be caused by an increased cleavage of hydrogen bridge bonds, that implies increasing solvation.

At this point, at the latest, there should be posed the question regarding the realized dissolution state and the method for its characterization as well.

We have postulated the ideal dissolution state as follows: Both in microscopic (>5 µm) as well as in sub-microscopic (>0,5 µm) ranges no gel particles can be detected and all hydrogen bridge bonds alongside and between the cellulose chains are completely solvated.

Measuring methods and results

For the investigation of the dissolution state in microscopic range a binocular microscope type “Axiolab®” was used, with polarization, λ -

compensation, phase contrast, various filters and a magnification up to 500 : 1 made from Carl Zeiss Jena. With a high degree of certainty, the microscopic viewing enables the unambiguous detection or exclusion of all particles >5 µm if their refractive index is sufficiently different from that of the ambient solvent phase .

The figures 1 – 4 should demonstrate the application limits of the microscopy method. A typical feature of the dissolutions process accompanied with the water / NMMO exchange is the attack in transverse direction to the fiber length axis with a simultaneous forming of spherical gel ranges. When dissolving dry cellulose pulp in monohydrate , however, one can find always an ablation of layers from only the surface.

Laser diffraction method with the HELOS® measuring instrument type BF (Sympatec GmbH Clausthal is well proven for the investigation of the dissolution state in sub-micron range [8]. The He-Ne-laser with the wave length of 633 nm lights through a specific measuring cell containing the sample of defined thickness (4 mm and 2 mm) and maintained at a temperature of 85 °C. A Detector measures the optical concentration, classifies the laser light diffraction into 31 particle classes within the range from 0,5 – 175 µm and calculates by use of corresponding software the particle size distribution spectrum. By calibration the optical concentration allows conclusions regarding the particle content as well.

In case of deep colored solutions a certain correction for the optical concentration becomes necessary. The Laser diffraction method even enables the detection of such inhomogeneities, that, exhibit very small differences in refractive indices comparison with the ambient solvent and for that reason cannot be detected by light microscopy.

In figure 6 is given the summary and density distribution of particles in a solution containing 12,3 wt % eucalyptus pulp with a Cuoxam DP of 563 for the dissolved cellulose.

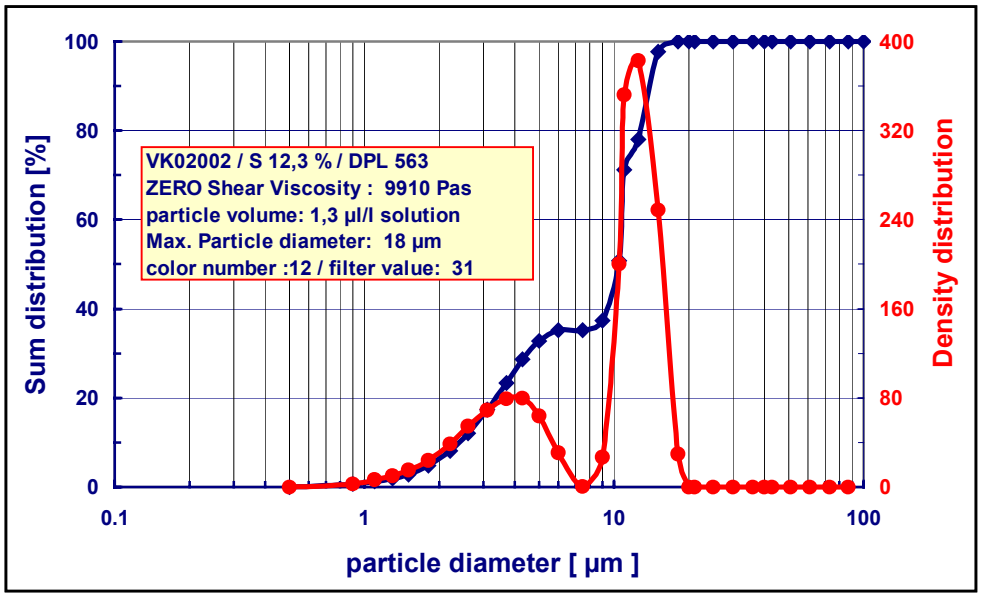

Figure 6. particle analysis by Laser Diffraction at 633 nm

The measured particle volume amounts to 1,3 µl/l of solution with a maximum particle diameter of 18 µm. However, the question remains unanswered whether the "residual particles" have to be considered as cellulosic material itself or as other impurities of cellulose. By suitable choice of dissolution conditions – particularly shear forces and temperature – a relative huge number of diverse cellulose pulps with different sources of consistency can be processed to more or less particle free solutions. Considering the aspect of solution shaping for getting anisotropic shaped bodies we have subdivided the term of solution state and we speak about the solution quality when evaluating the microscopic and submicroscopic ranges, that

means in case of the existence of discrete inhomogeneities.

In molecular range the solution state should differ only by the degree of solvation achieved. That means the network consists of more or less large units crosslinked by hydrogen bonds, which completely dissolve in ideal case. The solution state describes this limited range. In searching for suitable methods, rheological measuring methods were found to promise the best chances of success, since smallest variations in molecular weight, molecular weight distribution and chain branching cause a significant change in rheological parameters like ZERO-shear viscosity, loss and storage modulus, relaxation time etc. For measuring these parameters a Rheometer was used, with temperature controllable cone/plate and plate/plate-sensor of different size (THERMOHAAKE® Karlsruhe) which enabled sample shearing both in rotational as well as oscil-
Whilst one can find an exponential increase of the ZERO shear viscosity in case of cellulose slightly crosslinked via real chemical bonds, for example with glyoxal, the essential weaker and more flexible hydrogen bridge bonding causes a slight change in order of only one magnitude, during transition from swollen cellulose pulp to completely solvated solution. Indeed, the measurement of the viscosity decrease versus time allows a coarse differentiation; however, it is not suitable for making unambiguous classification of slight differences. The recording of the deformation graphs, that means change of loss (G') and storage (G'') modulus versus shear rate (ω) yields the necessary data like plateau modulus (G_0), complex viscosity ($\eta^{*\#}$) and shear rate ($\omega^{\#}$) at the "cross over" for calculation of the critical DP,

lating operating modes and permitting by use of the corresponding software (Rheowin® , Rheosoft®) readouts of discrete measuring parameters, master curves and calculated spectra.

For evaluation of the solution state in molecular range we applied the ZERO-shear viscosity (η_0^{ϑ}) , the molecular unevenness U_η as obtained by rheology, the critical average polymerization degree ($DP_{crit.}$) and the relaxation time spectra ($H = f(\lambda)$).

More Details of these methods are described in literature [9, 10].

The ZERO shear viscosity changes exponentially in dependence on the molecular weight.

$$\eta_{0,\vartheta} = K_\eta \cdot M^a$$

$$DP_{crit.} = 123{,}5 \cdot \frac{R \cdot T \cdot \rho_L \cdot c_{Cell.}}{G_0}$$

unevenness

$$U_\eta = \frac{\eta_0^{\vartheta}}{\eta_{\vartheta}^{*\#}} - 1 = \frac{\omega^{\#} \cdot \eta_0^{\vartheta}}{\sqrt{2} \cdot G'^{\#}} - 1$$

and relaxation time spectra. The response of relaxation times corresponding to the respective molecular weights should be much more sensitive, as the summary parameter ZERO shear viscosity ever can do.

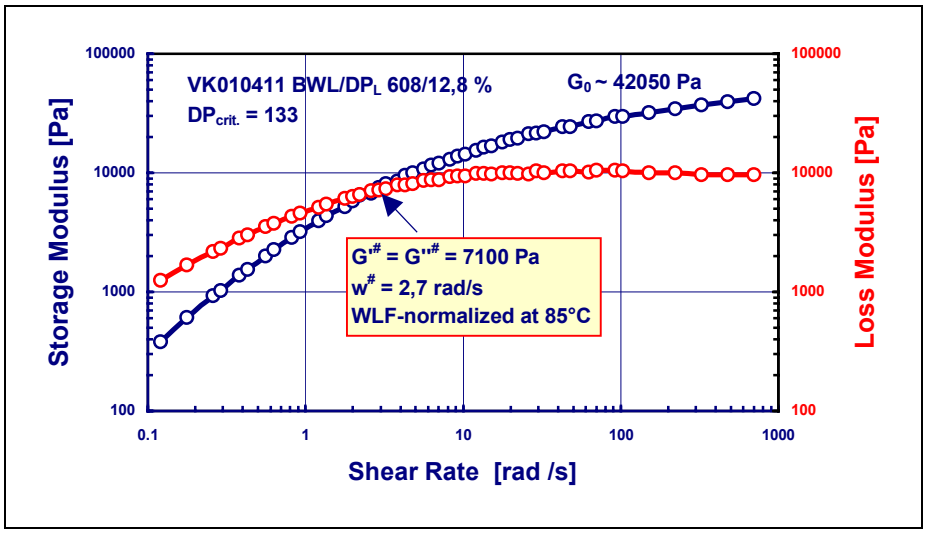

Figure 7. deformation master curves for loss and storage moduli

In figure 7 is shown the normalized master curve at 85°C for the deformation of a solution containing 12,8 wt % cotton linters (BWL) pulp after 1,5 h dissolving time. The Cuoxam DP of the dissolved cellulose pulp was 608. Storage – and loss modulus were measured with 7100 Pa at a shear rate of 2,7 rad/s and the plateau modulus was 42050 Pa. From these parameters a DP$_{crit.}$ of 133 and an unevenness of about 2,5 is obtained.

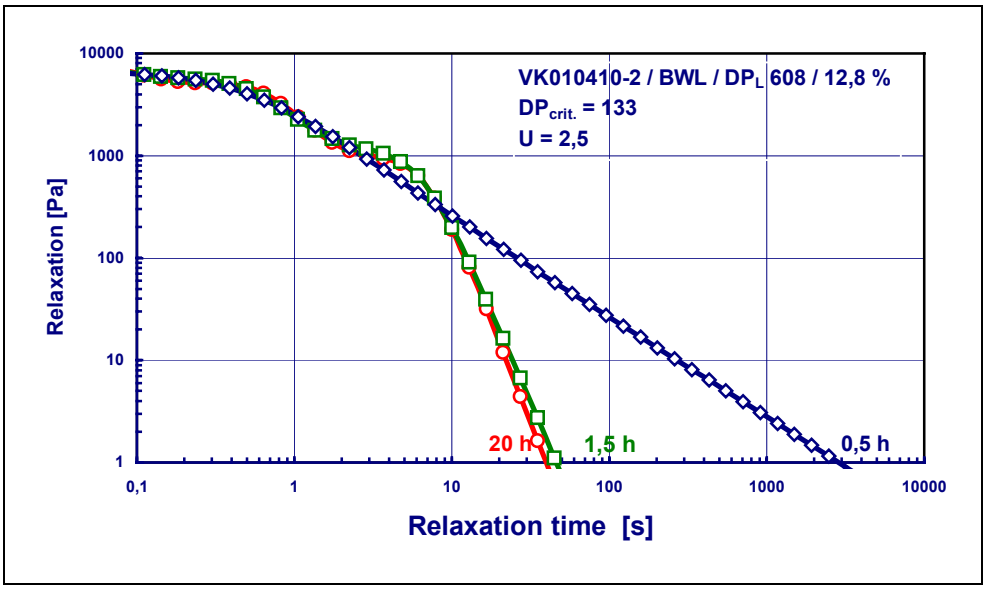

Figure 8. relaxation time spectrum for cotton linters pulp

Figure 8 presents a relaxation time spectrum of this solution after 0,5 and 1,5 hours of dissolving time and a subsequent hold-up time of 20 hours at 80°C. Whilst still observing a remarkable decrease in the relaxation times during dissolution, after further 20 hours hold-up time relaxation time keeps virtually constant.

In figure 9 is given the relaxation time spectrum of a solution of 12,3 wt % eucalyptus pulp (Cuoxam DP$_L$: 530) and in figure 10 the relaxation time spectrum of a 12 wt % softwood pulp solution each after 1,5 hours of dissolving time and further 20 respectively 45 hours hold-up time at 80 °C.

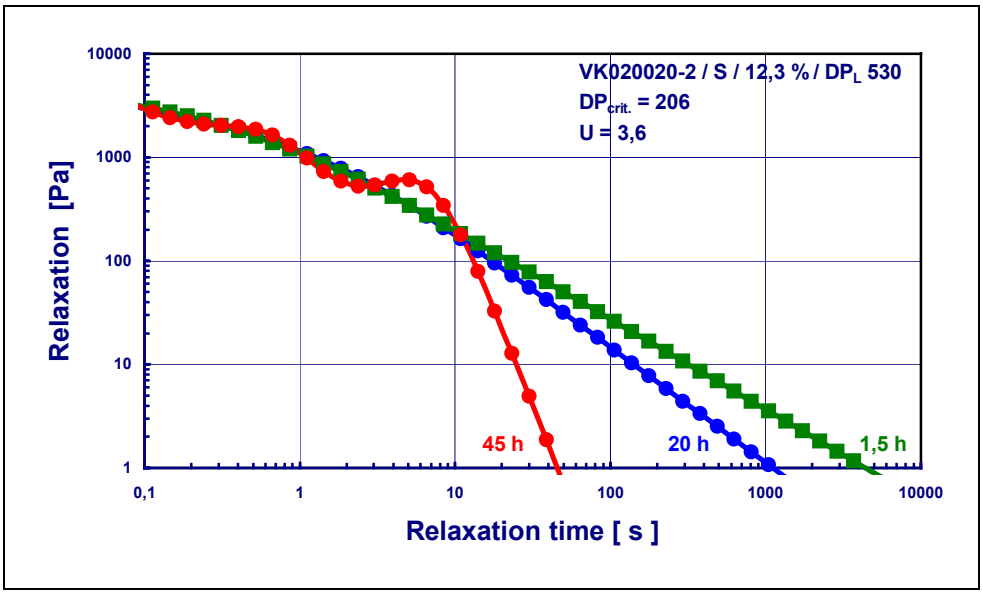

Figure 9. relaxation time spectrum for eucalyptus sulphite pulp

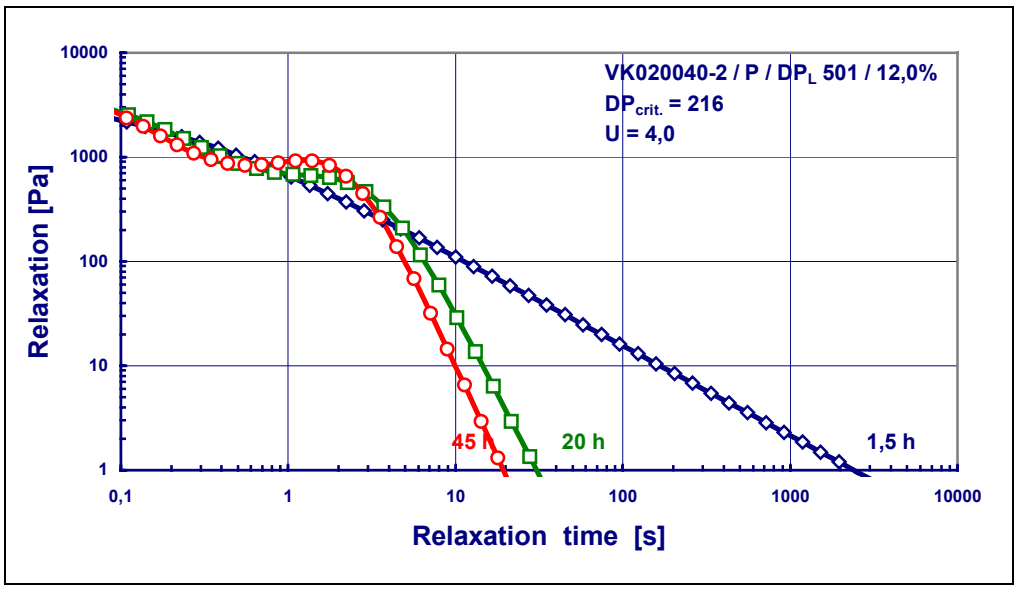

Figure 10. relaxation time spectrum Kraft-pulp – pine tree

From these spectra it can be observed that this method enables a highly differentiated detection of differences in solution state and on the other side, the solution state within the molecular range is less effected by the shear field, but more by the parameters like temperature and time.

In dependence on the molecular weight distribution a completely solvated solution, that means a stable state, can be achieved after more or less hold-up times , only.

However, the completely solvated solution is a prerequisite for reproducible measurements. In particular this is imperative for weighted relaxation time spectra where predictions concerning the molecular weight distribution should be derived from. In figure 11 are given the relaxation time spectra of solutions of cotton linters (BWL) cellulose pulp with a Cuoxam DP 1528 and 606 for the dissolved cellulose.

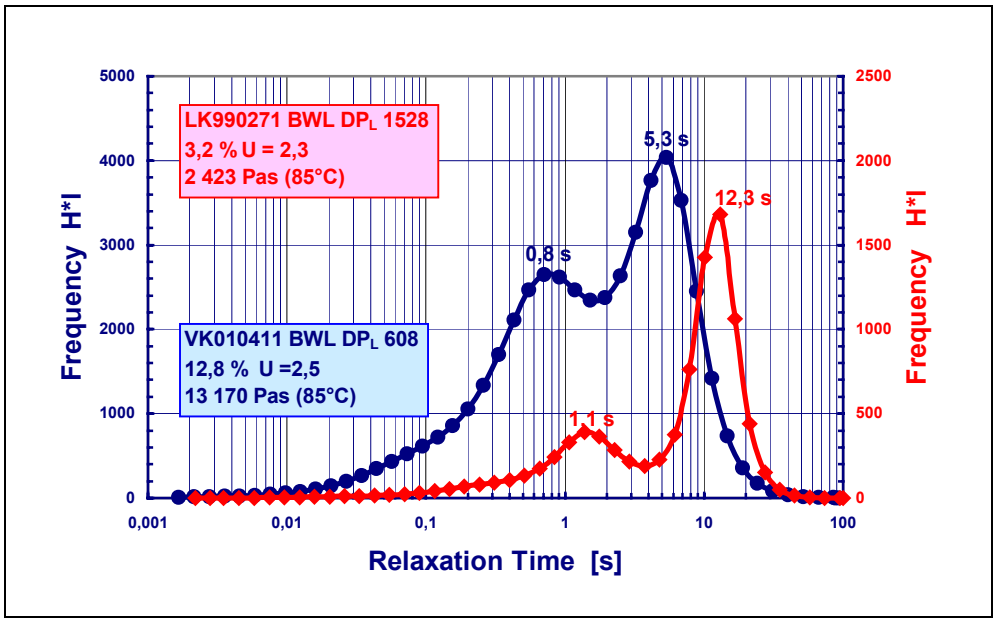

Figure 11. relaxation time spectra (weighted) for cotton linters cellulose pulps with different molecular weight and molecular weight distribution

Both spectra indicate bimodal distributions of different width according to the measured unevenness of 2,3 and 2,5 respectively with maximum values for the relaxation time of 12,3/1,1 and 5,3 / 0,8 s respectively, and according to the measured average polymerization degree of 1528 respectively 606 . Using a corresponding calibration of the abscissa ($\lambda = K_\lambda \cdot M^a$) predictions regarding the molecular weight distribution should be possible.

Literature

1 Götze, K.: Chemiefasern nach dem Viskoseverfahren. Berlin/Heidelberg/ New York:, Springer-Verlag 1967

2 Klüfers, P.: Lösungsgleichgewichte und Strukturprinzipien in Cellulose-Metall-Netzwerken. Vortrag DFG-Kolloquium 03.06.1997 in Bad Herrenalb

3 Klüfers, P.: Welche Metalle bilden Komplexe mit Cellulosedianionen. Vortrag; DFG-Kolloquium 16.03 1999 in Bad Herrenalb

4 Gränacher, Ch.; Sallmann, R.: Ver fahren zur Herstellung von Cellulose-lösungen. DRP 713486 07.10.1936

5 Johnson, D.L.: Method of preparing Polymers from a mixture of cyclic amine oxides and Polymers USP 5 508 941 02.09.1966

6 Mc Corsley, C.C.: Geformter Zellu losegegenstand DE 29 13 589 02.03.1979

7 Wachsmann, U.; Diamantoglou, M.: Potential des NMMO-Verfahrens für Fasern und Membranen Das Papier 12 (1997) 660 - 664

8 Kosan, B. ; Michels, Ch.: Particle analysis by laser diffraction – application and restrictions in the lyocell process Chemical Fibers Int. 49 (1999) 3 50 - 54

9 Michels, Ch.: Beitrag zur Bestimmung von Molmasseverteilungen in Cellulosen aus rheologischen Daten Das Papier 52 (1998) 1 3 - 8

10 Michels, Ch.; Kosan, B.: Lyocell proc ess - material and technological restrictions Chemical Fibers International 50 (2000) 12 556 – 561